This electronic thesis or dissertation has been downloaded from the King's Research Portal at https://kclpure.kcl.ac.uk/portal/

The Unfolded Protein Response
A potential link between heterozygous mutations in GBA1 and Lewy body dementia?

Clarke, Emily Jayne

Awarding institution:
King's College London

The copyright of this thesis rests with the author and no quotation from it or information derived from it may be published without proper acknowledgement.

END USER LICENCE AGREEMENT

Unless another licence is stated on the immediately following page this work is licensed

under a Creative Commons Attribution-NonCommercial-NoDerivatives 4.0 International

licence. https://creativecommons.org/licenses/by-nc-nd/4.0/

You are free to copy, distribute and transmit the work

Under the following conditions:

- Attribution: You must attribute the work in the manner specified by the author (but not in any way that suggests that they endorse you or your use of the work).
- Non Commercial: You may not use this work for commercial purposes.
- No Derivative Works - You may not alter, transform, or build upon this work.

Any of these conditions can be waived if you receive permission from the author. Your fair dealings and other rights are in no way affected by the above.

Take down policy

If you believe that this document breaches copyright please contact librarypure@kcl.ac.uk providing details, and we will remove access to the work immediately and investigate your claim.

Download date: 05. May. 2023

The Unfolded Protein Response – a potential link between heterozygous mutations in *GBA1* and Lewy body dementia?

Submitted for the degree of Doctor of Philosophy

Emily Jayne Clarke

Wolfson Centre for Age-Related Disease, Guy's Campus,
King's College London. SE1 1UL

i. Abstract

Lewy body dementia (LBD) is characterised by the deposition of α-synuclein containing Lewy bodies throughout cortical brain regions. Pathology is confounded by the co-occurrence of pathological Aβ and tau deposition. LBD comprises dementia with Lewy bodies (DLB) and Parkinson's disease dementia (PDD), distinguished by the timing of onset of classical symptoms: cognitive impairment occurs at least one year prior to motor impairment in DLB and *vice versa* in PDD. Currently, there are no disease modifying therapeutic agents for LBD.

Heterozygous mutations in *GBA1* have become established as the most common genetic risk factor for Parkinson's disease and dementia with Lewy bodies. *GBA1* encodes the lysosomal enzyme glucocerebrosidase. Deficient glucocerebrosidase activity causes accumulation of α-synuclein. Homozygous *GBA1* mutation causes the lysosomal storage disorder Gaucher's disease. In this thesis, a possible mechanism underlying the link between *GBA1* mutation and LBD is investigated - the unfolded protein response (UPR). We hypothesise that the UPR is activated in response to mutant *GBA1* but is unable to serve a protective function under increasing levels of stress. We also characterise the impact of heterozygous *GBA1* mutation (D427V) on mice to establish whether a cognitive impairment phenotype is displayed which may be translational for the study of LBD.

The results presented in this thesis support the activation of both IRE1α and PERK mediated UPR responses since we show increased expression of spliced XBP1 and CHOP in a L444P mutant *GBA1* SH-SY5Y cell model. We also demonstrate spliced XBP1 ceases to be expressed under increasing cellular stress whilst CHOP expression continues. Since CHOP is associated with detrimental cell outcomes, predominantly initiation of apoptosis, we suggest that the imbalance of UPR responses towards CHOP mediated effects may potentially underlie pathological consequences associated with *GBA1* mutation. Results presented in this thesis also reveal a previously unreported progressive cognitive decline in D427V/WT *GBA1* mice.

In conclusion, preventing the withdrawal of protective spliced XBP1 mediated effects and continued expression CHOP may be a therapeutic avenue for further investigation in D427V/WT *GBA1* mice which show promising signs of being a translational model for LBD.

ii. Acknowledgements

I would firstly like to thank my supervisors' Dr Martin Broadstock and Professor Paul Francis for making the completion of this thesis possible. Their help and support has been greatly appreciated. I would especially like to thank Martin for continuing to help and assist with my thesis after leaving King's. I am hugely grateful that you continued to support me in your own time. Working together has been an absolute blast and I'm glad I managed to see those green cells before you left! I owe you many a beer for your support, *positivity* and *kind words*!

The past few years working at the Wolfson CARD have been some of the best of my life. I have embarked upon a career pathway that I genuinely love and made some wonderful friends who are not only supremely smart and intelligent but are also kind, funny and incredibly supportive. There is nothing that a good cup of tea/beers and cake cannot fix. Lizzie- you've been my partner in crime throughout this whole experience and have been invaluable for my mental health! I promise never to make you drink Jager again as a mark of my gratitude. Ariana, Sotiris, Lizzie, Ed and Book – so many good times! You guys have made it an absolute pleasure to come to work (and to the pub). More than that, your help and support has been appreciated immensely. The good times will continue for sure!

My gratitude also extends to everyone I have worked with and has helped me over the time of my PhD - David Howlett, Dave Whitfield, Caroline, Cigdem and Mai as part of the Francis lab. Dr Susan Duty, thank your encouraging and kind words as well as allowing me to be a surrogate member of your lab! I would also like to thank Professors Pat Doherty and Dag Aarsland for kindly extending my PhD and collaborating on some exciting future proposals.

I would like to thank my friends and family. Phil and Linda, your constant encouragement has been truly appreciated. The Bell's as always have been the antidote to any self-doubt. The London family – Rach, Chris, James, Lizzie, Brett, Tom and Sarah – and friends from the motherland particularly Chaz and the Kaighan three, thanks for putting up with me! Sorry for becoming a recluse whilst writing!

Finally, the last and biggest thank you goes to my husband Simon. You encouraged me right from the beginning to follow my goal of doing a PhD and have never doubted that I would be able to do this. You have been absolutely invaluable in keeping me going at times when things became difficult – predominantly by interspersed *'treats'* of gigs and holidays to keep me sane! I would not have been able to do this without you. Thank you also for not judging me during those writing days when I wouldn't change out of my pyjamas for days on end and chain eat biscuits! '*You're rarer than a can of dandelion and burdock. And those other girls are just postmix lemonade'*

iii. Abbreviations

4-MU	4-Methylumbelliferone
4-MUG	4-Methylumbelliferyl-β-D-galactopyranoside
4-MUP	4-Methylumbelliferyl phosphate
4-MAP	4-Methylumbelliferyl-2-acetoamindo-2-deoxy-β-D-glucopyranoside
6-OHDA	6-hydroxydopamine
AD	Alzheimer's disease
ANOVA	Analysis of variance
ATF6	Activating transcription factor 6
BCA	Bicinchoninic acid
BCL-2	B-cell lymphoma 2 protein
BiP	Binding immunoglobulin protein
cDNA	Complementary DNA
ChAT	Choline acetyltransferase
CHOP	CCAAT-enhancer-binding protein homologous protein
CSF	Cerebrospinal fluid
CβE	Conduritol-β-epoxide
DAPI	4',6-diamidino-2-phenylindole
DAT	Dopamine transporter
dATP	Deoxyadenosine triphosphate
DLB	Dementia with Lewy bodies
DMSO	Dimethyl sulfoxide
DNA	Deoxyribonucleic acid
EDTA	Ethylenediaminetetraacetic acid
Endo H	Endoglycosidase H
ER	Endoplasmic reticulum
ERAD	Endoplasmic reticulum associated degradation
ERT	Enzyme replacement therapy
FACS	Fluorescence assisted cell sorting
FBA	Foetal bovine serum

FTD	Frontotemporal dementia
GalCer	Galactosylceramide
GCase	Glucocerebrosidase
GCS	Glucosylceramide synthase
GD	Gaucher's disease
GFAP	Glial fibrillary acidic protein
GFP	Green fluorescent protein
GluCer	Glucosylceramide
GluSph	Glucosylsphingosine
GM2A	GM2 ganglioside activator
GSL	Glycosphingolipid
GWAS	Genome wide association study
HPRT1	Hypoxanthine phosphoribosyltransferase 1
HSA	Human serum albumin
iPSC	Induced pluripotent stem cell
IPTG	Isopropyl-β-D-1-thiopyranoside
IRE1α	Inositol-requiring enzyme 1 subunit α
LacCer	Lactosylceramide
LB	Lewy body
LBD	Lewy body dementia
LN	Lewy neurite
LNL	loxP-neo-loxP
MCS	Multiple cloning site
MIBG	metaiodobenzylguanidine
MMSE	Mini mental state examination
MoCA	Montreal cognitive assessment
MRI	Magnetic resonance imaging
MTT	3-(4,5-dimethylthiazol-2-yl)-2,5-diphenyltetrazolium bromide
NaCl	Sodium Chloride
NFT	Neurofibrillary tangle
NIA-RI	National institute on aging-Reagan institute

ORF	Open reading frame
PBS	Phosphate buffered saline
PBST	Phosphate buffered saline - tween 20
PCR	Polymerase chain reaction
PD	Parkinson's disease
PDD	Parkinson's disease dementia
PERK	Protein kinase RNA like endoplasmic reticulum kinase
PET	Positron emission tomography
PPN	Pedunculopontine nucleus
pSER129	Serine 129 phosphorylated α-synuclein
PSG	Polysomnography
qPCR	Quantitative polymerase chain reaction
REM	Rapid eye movement
RIDD	Regulated IRE1 dependent decay
RNA	Ribonucleic acid
SAP	Spontaneous arm performance
SapC	Saposin C
scAAV	Self-complementary adeno-associated virus
sDLB	Sporadic dementia with Lewy bodies
SDS	Sodium dodecyl sulphate
SEM	Standard error of the mean
shRNA	Short hairpin RNA
SNP	Single nucleotide polymorphism
SNpc	Substantia nigra pars compacta
sPD	Sporadic Parkinson's disease
SPECT	Single photon emission computed tomography
SRT	Substrate replacement therapy
TCS	Transcranial sonography
TrisHCl	Tris hydrochloride
TUNEL	Terminal deoxynucleotidyl transferase dUTP nick-end labelling
UPDRS	Unified Parkinson's disease rating scale
UPR	Unfolded protein response

X-Gal	5-bromo-4-chloro-2-indolyl-D-galactoside
XBP1	X-box binding protein 1
XBP1u	X-box binding protein 1 un-spliced

iv. List of tables

v. Table of figures

vi. Table of contents

1. General Introduction

1.1. Lewy body dementia

Dementia is defined as a progressive cognitive decline of sufficient magnitude to interfere with normal social or occupational functions, or with usual daily activities (Costa et al., 2017). Worldwide, according to the World Health Organisation, more than 47 million people have dementia with approximately 9.9 million new cases being diagnosed annually http://www.who.int/mediacentre/factsheets/fs362/en/ . The total number of people with dementia is projected to triple by 2050 to 132 million http://www.who.int/mediacentre/factsheets/fs362/en/ . These startling figures have led the World Health Organisation to designate dementia as a public health priority.

Lewy body dementia (LBD) is a term used to collectively describe a subset of dementias characterised by proteinaceous deposition of α-synuclein containing Lewy bodies throughout the brain (Galasko, 2017). LBD includes Parkinson's disease dementia (PDD) and dementia with Lewy bodies (DLB) (Galasko, 2017). Despite being the second most common progressive dementia in people over the age of 65 behind Alzheimer's disease (AD), LBD is chronically misdiagnosed and under researched predominantly due to clinically heterogeneous overlapping symptoms and neuropathology with Alzheimer's and Parkinson's disease (Walker et al., 2015). Alzheimer's disease is characterised predominantly by the proteinaceous deposition of Aβ containing plaques and neurofibrillary tangles comprised of tau.

Lewy bodies were first described in Parkinson's disease (PD) brain by Friederich H. Lewy in 1912 as abnormal inclusions in nerve cell bodies (Goedert et al., 2013). Classically, Lewy bodies are eosinophilic cytoplasmic inclusions within neurons consisting of a dense core surrounded by a halo of 10nm wide radiating fibrils (Goedert et al., 2013). It was not until 1997, when a rare missense mutation in *SNCA* (A53T) was shown to cause a dominantly inherited form of PD that α-synuclein was established as the predominant component of Lewy bodies based upon the subsequent identification of α-synuclein immunoreactivity in the brain of sporadic PD cases (Spillantini et al., 1997). α-synuclein is a 140 residue natively unfolded protein encoded by *SNCA* gene which exists in a dynamic equilibrium between a soluble and membrane bound state, with its secondary structure dependent upon the environment (Jakes et al., 1994; Spillantini and

Goedert, 2017). Whilst ubiquitously expressed throughout the brain, α-synuclein is primarily localised to neuronal presynaptic membranes and is thought to have a role in neurotransmitter release (Burre, 2015). Electron microscopy shows that Lewy bodies are composed of unbranched α-synuclein filaments with classical cross β sheet amyloid structure (Spillantini et al., 1998). Hyperphosphorylation of serine129 residue is a classical hallmark of aggregated α-synuclein and α-synuclein filaments become ubiquitinated after assembly (Fujiwara et al., 2002; Goedert et al., 2013).

Lewy body pathology follows a predictable pattern of development throughout the brain which is thought to correspond to the severity of parkinsonism symptoms described by six stages of Lewy body deposition (Braak et al., 2003). The first LB structures in the brain usually occur in the olfactory bulb and/or dorsal motor nucleus of the glossopharyngeal and vagal nerves (stage 1) (Braak et al., 2003). In stage 2, LB pathology proceeds in a caudorostal pattern to the medulla oblongata and the pontine tegmentum before reaching the amygdala and substantia nigra resulting in the characteristic motor symptoms of PD by stage 3 (Braak et al., 2003). As pathology worsens, LBs reach the temporal cortex (stage 4) before inclusions appear in the neocortex during stages 5 and 6 accounting for cognitive impairments associated with advanced PD (Braak et al., 2003).

Previously considered an anomaly, the identification of cortical Lewy bodies outside the brainstem and midbrain was first described in 1976 and associated with pre-senile dementia (Kosaka et al., 1976). The progression of LB pathology to cortical regions continues the caudorostal progression of Lewy pathology and underlies the development of PDD (Braak et al., 2003). It was not until 1996 however that a consensus was reached whereby DLB, pathologically characterised by widespread LB distribution throughout cortical regions, was considered a distinct and separate condition to PDD based primarily upon symptom progression (McKeith et al., 1996; Kosaka, 2014{McKeith, 2017 #317; McKeith et al., 2017).

DLB and PDD have many clinical and pathological similarities. Diagnostically, the two syndromes are arbitrarily differentiated based upon the timing of cognitive decline relative to motor symptoms – 'The one year rule' (McKeith et al., 2005{McKeith, 2017 #317; McKeith et al., 2017). PDD diagnosis depends on the occurrence of a dementia syndrome of insidious onset and slow

progression, that develops in the context of established PD i.e. cognitive decline at least one year after diagnosis of PD (Meissner et al., 2011). Conversely, DLB is diagnosed with dementia as the central feature, emerging at least 1 year before any parkinsonism symptoms are observed (McKeith et al., 2005). However, accurate diagnosis of DLB can be difficult due to initial similarities with Alzheimer's disease (AD) and the heterogeneity of symptoms, discussed below.

1.1.1.Clinical symptoms

Clinically, DLB and PDD are mostly indistinguishable other than the predominant presenting clinical feature – cognitive impairment in DLB and parkinsonism in PDD as per the 'one year rule' discussed above (McKeith et al., 2005). Despite the vast heterogeneity of symptoms, there are some features such as fluctuations in consciousness and alertness particularly in DLB which can aid accurate diagnosis (McKeith et al., 2005). The clinical symptoms of both DLB and PDD are described below.

1.1.1.1. Dementia with Lewy bodies

Typically, DLB patients present with cognitive impairment which develops into dementia (Aarsland, 2016). Although short term memory loss may have been the presenting symptom for diagnosis, cognitive domains other than memory are frequently involved, including attention, executive function and visual-spatial skill (Takemoto et al., 2016). While reminiscent of hippocampal-dependent memory encoding seen in AD, impairment of short term memory in DLB generally reflects a problem of retrieval of stored information which can be improved with cues (Walker et al., 2015). These errors of memory encoding and retrieval can be differentiated by detailed cognitive testing (Walker et al., 2015).

Neuropsychiatric symptoms are a strong feature of DLB (Brodaty et al., 2015). Recurrent, complex visual hallucinations are a key symptom distinguishing DLB from AD (Mosimann et al., 2004; Brodaty et al., 2015). The hallucinations are usually well formed and animate featuring people, children or animals (Walker et al., 2015). Hallucinations are predominantly unimodal, without involvement of sound, smell or touch (Walker et al., 2015). Delusions can also arise, typically later in the disease course and usually have a paranoid quality e.g. delusions of infidelity, house intruders and theft are common (Walker et al., 2015). As cognition continues to deteriorate, patients may believe that their spouse or caregiver has been replaced by an imposter, a phenomenon known as Capgras syndrome (Thaipisuttikul et al., 2013). DLB patients are also significantly more likely to present with symptoms of anxiety early in the disease course compared with AD, increasing the rate of development of more severe neuropsychiatric conditions such as hallucinations and delusion (Shea et al., 2015). Attention and alertness may also fluctuate leading to episodes of staring and perturbed flow of ideas or frequent daytime drowsiness (Gomperts,

2016). DLB fluctuations are typically delirium-like, occurring as spontaneous alterations in cognition, attention and arousal. (Gomperts, 2016).

Spontaneous parkinsonian features are common in DLB, eventually occurring in over 85% of patients (Postuma et al., 2015). Parkinsonism usually presents bilaterally in DLB with more axial rigidity, whereas in PD it typically presents unilaterally and asymmetrically (Gomperts, 2016). Resting tremor is not as common in DLB compared with PD (Takemoto et al., 2016) but bradykinesia and gait impairment are commonly reported (Burn et al., 2006). However, presentation of parkinsonism symptoms varies considerably between individuals (Gomperts, 2016). Furthermore, in contrast to patients with PD, DLB patients have a limited response to medications such as carbidopa/levodopa (Goldman et al., 2014).

REM sleep behaviour disorder is a parasomnia in which the normal paralysis of REM sleep is impaired (Bassetti and Bargiotas, 2018). REM sleep behaviour disorder is experienced as individuals acting out their dreams with behaviours such kicking, punching and yelling (Bassetti and Bargiotas, 2018). REM sleep behaviour disturbance is a known characteristic of synucleinopathies, particularly DLB (Hogl et al., 2018). Symptoms typically begin prior to cognitive impairment, parkinsonism, or autonomic dysfunction (Hogl et al., 2018). The interval between REM sleep behaviour disturbance and the onset of cognitive impairment can typically be around 10 years or even longer making REM sleep behaviour disturbance an important prodromal symptom for DLB diagnosis (Boeve et al., 2013; Hogl et al., 2018).

Autonomic impairment is frequently reported in the prodromal stages of DLB (Gomperts, 2016). However, the severity of autonomic symptoms are not comparable to the synucleinopathy multiple system atrophy (Gomperts, 2016). Constipation is common and problematic as is orthostatic hypotension (Blanc and Verny, 2017). Furthermore, some patients experience neurogenic urinary frequency or incontinence (Gomperts, 2016; Blanc and Verny, 2017).

1.1.1.2. Parkinson's disease dementia

PDD patients first present with the characteristic motor symptoms of PD: resting tremor, rigidity and bradykinesia (Postuma et al., 2015). A diagnosis of PD is a pre-requisite for the development of PDD (Emre et al., 2007).

Executive function represents the most common cognitive domain affected in PDD particularly in the early stages of the dementia syndrome reflecting dopaminergic dysfunction in frontostriatal networks (Goldman et al., 2014). However, impairments in attention which may fluctuate, explicit memory and visuospatial function are also seen in early PDD (Goldman et al., 2014).

The cognitive profile in PDD and DLB overlaps significantly making diagnosis by cognitive clinical symptoms difficult. Visual hallucinations also occur frequently in PDD which like DLB are usually animate and unimodal (Gomperts, 2016). Delusions are less common but can arise. Both hallucinations and delusions can be exacerbated by dopamine replacement medications, particularly dopamine agonists, used to treat the motor symptoms (Gomperts, 2016).

Interestingly, the motor phenotype of PDD differs from PD (Emre et al., 2007; Gomperts, 2016). PDD patients are more likely to have a postural instability gait disorder phenotype compared with PD, which constitutes a risk factor for dementia (Burn et al., 2006). Furthermore, PDD patients have a more rapid motor decline and falls are more frequent (Emre et al., 2007). Levodopa responsiveness and related dyskinesias may also differ in PDD patients, but the evidence is inconclusive as is the relative frequency of autonomic symptoms (Emre et al., 2007).

1.1.2.Diagnosis

1.1.2.1. DLB

Accurate clinical diagnosis of DLB is challenging due to the considerable heterogeneity of symptoms and pathology (McKeith et al., 2017). Detection rates in clinical practice are suboptimal with many cases misdiagnosed, usually as Alzheimer's disease (Vann Jones and O'Brien, 2014). The DLB consortium have composed a set of guidelines to help improve accurate diagnosis and better describe DLB clinically based upon evaluation of research and clinical experience. These guidelines are revised and updated to reflect breakthroughs in the field, with the most recent consensus report of the DLB consortium being published in July 2017 (McKeith et al., 1996; McKeith et al., 2005; McKeith et al., 2017).

Dementia is an essential requirement for DLB diagnosis, dementia defined as a progressive cognitive decline of sufficient magnitude to interfere with normal social or occupational functions or with usual daily activities (McKeith et al., 2017). DLB should be diagnosed when dementia occurs before or concurrently with parkinsonism (McKeith et al., 2005). While there is no DLB specific assessment battery of tests available, composite risk score tools have been developed which consider different aspects of DLB associated dementia, helping to distinguish DLB from AD (Walker et al., 2015). Mini mental state examination (MMSE) and Montreal Cognitive assessment (MoCA) are useful tests to identify global cognitive impairment but cannot distinguish between DLB and AD (Shea et al., 2015). Measures of attention and executive function e.g. Stroop tasks and trail making tasks, can be very useful to differentiate DLB from AD (McKeith et al., 2017). Furthermore, spatial and perceptual difficulties occur earlier in DLB as identified through tasks of figure copying e.g. intersecting pentagons. Also, memory and object naming, assessed through story recall and verbal list learning is less affected in DLB compared with AD (McKeith et al., 2005; McKeith et al., 2017).

The core clinical features of DLB include: fluctuation, visual hallucinations, parkinsonism and REM sleep behaviour disorder (McKeith et al., 2017) **(Table 1).** Fluctuating cognition, attention or arousal can be difficult to ascertain from direct questioning of the individual but the level of daytime drowsiness is a good indicator (Ferman et al., 2004) . At least one measure of fluctuation should be documented to meet DLB diagnostic criteria particularly when presenting early in the disease course since early presence of fluctuations are a reliable differentiating symptom from

Alzheimer's disease (Ferman et al., 2004). Complex recurrent visual hallucinations occur in up to 80% of DLB patients and are a frequent, reliable signpost to diagnosis (Fujishiro et al., 2008; Urwyler et al., 2016). Typically, patients and caregivers are able to report the episodes of hallucination in order to aid diagnosis, but assessment scales are available for characterising and quantifying visual hallucinations (Mosimann et al., 2004). Parkinsonism is typically defined as bradykinesia in combination with resting tremor, rigidity or both (Postuma et al., 2015). Most patients with DLB will not have parkinsonism to the extent seen in Parkinson's disease and so documentation of only one of the defining triad of Parkinson's symptoms is required as a core clinical feature for diagnosis of DLB (McKeith et al., 2017). REM sleep behaviour disorder has been reassigned as a core clinical feature for diagnosis of DLB due to evidence suggesting the frequency may be as high as 76% (Ferman et al., 2011). REM sleep behaviour disorder is screened for by scales allowing for bed partner or patient reports. Confirmation can be sought from specialist sleep clinics or polysomnography (PSG) (McKeith et al., 2017).

A probable diagnosis of DLB can be made if two or more of the core clinical features described above are present (McKeith et al., 2017). However, a probable diagnosis of DLB can also be made if only one of the core clinical features is present but one or more indicative biomarkers are confirmed: reduced dopamine transporter (DAT) uptake in the basal ganglia demonstrated by single-photon emission computed tomography (SPECT) or positron emission tomography (PET) imaging; reduced uptake on metaiodobenzylguanidine (MIBG) myocardial scintigraphy and confirmation of REM sleep without atonia by PSG (McKeith et al., 2017) **(Table 1).** Importantly, guidance suggests that a probable diagnosis of DLB in the absence of any core clinical features should not made from indicative biomarkers alone (McKeith et al., 2017). DAT plays a key role in determining the extracellular concentration of dopamine through facilitating reuptake of dopamine into dopaminergic nerve terminals (Nutt et al., 2004). Expression of DAT is significantly reduced in PD (Nutt et al., 2004). Reduced pre-synaptic DAT uptake in the basal ganglia of DLB brain compared with AD using the specific DAT ligand [^{123}I]-N-(3-fluoropropyl)-2-carbomethoxy-3-(4-iodophenyl) nortropane with SPECT consistently differentiates DLB from AD with over 80% sensitivity and specificity (Brigo et al., 2015; Shimizu et al., 2016; Abbasi et al., 2017). Furthermore, the presence of parkinsonism symptoms is significantly higher in DLB patients who display significantly reduced striatal DAT uptake (Shimizu et al., 2016). MIBG enters the sympathetic synaptic cleft and is taken into presynaptic neurons, accumulating in a similar

manner to norepinephrine (Yoshita et al., 2006). Labelled ^{131}I or ^{123}I MIBG myocardial scintigraphy denotes cardiac sympathetic innervations (Yoshita et al., 2006). Reuptake of MIBG in sympathetic neurons of the heart is defective in PD (Yoshita et al., 2006). The reduced heart to mediastinum (H/M) ratio of MIBG, reflecting reduced sympathetic reuptake of MIBG on myocardial scintigraphy, has approximately 90% sensitivity and specificity for differentiating DLB from AD using either ^{131}I or ^{123}I radioisotopes (Shimizu et al., 2016; Abbasi et al., 2017). DLB patients who demonstrate reduced uptake on MIBG myocardial scintigraphy also demonstrate a significantly higher frequency of REM sleep behaviour disturbance (Shimizu et al., 2016). The confirmation of REM sleep without atonia by PSG is reported in over 80% of DLB patients (Pao et al., 2013). Conversely, Boeve et al report 98% of patients with PSG confirmed REM sleep without atonia have an underlying synucleinopathy, illustrating the power and utility of PSG in aiding the accurate diagnosis of DLB (Boeve et al., 2013) .

2017 DLB Consensus criteria for clinical diagnosis of probable DLB
Essential
DEMENTIA - Progressive cognitive decline of sufficient magnitude to interfere with normal social or occupational functions, or with usual daily activities
Core clinical features
• Fluctuating cognition with pronounced variations in attention and alertness • Recurrent visual hallucinations • REM sleep behaviour (may precede cognitive decline) • 1 or more feature of parkinsonism: bradykinesia, resting tremor or rigidity.
Indicative biomarkers
• Reduced DAT uptake in the basal ganglia demonstrated by SPECT or PET • Low iodine 123/131-MIBG uptake demonstrated by myocardial scintigraphy • PSG confirmation of REM sleep without atonia

Table 1- 2017 DLB consensus criteria for probable diagnosis of DLB. Probable diagnosis of DLB can be made if dementia in addition to 2 or more clinical features are present. Probable diagnosis of DLB can also be made if dementia in addition to 1 core clinical feature and at least 1 indicative biomarker is present. Figure compiled from (McKeith et al., 2017)

1.1.2.2. PDD

Diagnosis of PDD is comparatively straightforward since the disease course of PD and development of dementia is relatively consistent amongst patients (Emre et al., 2007). Consensus diagnostic criteria for PDD were developed in 2007 (Emre et al., 2007). Diagnosis of PDD requires both the diagnosis of PD and presence of a dementia syndrome with insidious onset and slow progression developing in the context of PD (Emre et al., 2007). Associated features for diagnosis of PDD include the presence of a profile of cognitive deficits including impairment in at least 2 of the 4 cognitive domains: attention, executive functions, visuospatial and free recall memory (Emre et al., 2007). While not considered critical for diagnosis, hallucinations, delusions, apathy and mood changes are frequently associated behavioural features of PDD (Emre et al., 2007).

As mentioned previously, the clinical and neuropsychological features of DLB and PDD can be similar and difficult to distinguish between the conditions. Therefore, the relative timing of dementia onset relative to presentation of parkinsonism symptoms defines the clinical distinction between PDD and DLB. PDD is clinically diagnosed when dementia occurs in the context of well-established PD, where the onset of dementia occurs at least one year following the diagnosis of PD (McKeith et al., 2005; McKeith et al., 2017).

1.1.3.Epidemiology

PDD and DLB are age related diseases although onset before the age of 65 is not uncommon (Walker et al., 2015). Both conditions are more common in men than in women (Walker et al., 2015).

The point prevalence of dementia is approximately 30% in patients with PD (Aarsland et al., 2005a). PDD accounts for 3-4% of patients with dementia in the general population while the prevalence of PDD in the general population aged 65 and over is 0.3-0.5% (Aarsland et al., 2005a; Aarsland and Kurz, 2010). According to community based longitudinal studies, 10% of the PD population will develop dementia per year (Aarsland and Kurz, 2010). However, since the risk for developing dementia depends on disease duration, this rises to 30% when monitoring PD patients from the onset diagnosis (Williams-Gray et al., 2007). Since mortality is higher in demented compared to non-demented PD patients (Hely et al., 2008), point prevalence is an underestimate of the true frequency of dementia in PD. Cumulative prevalence studies indicate that 83% of PD patients will develop dementia within 20 years of diagnosis (Hely et al., 2008), but when adjusting for mortality, 78% will develop dementia within 8 years of diagnosis (Aarsland et al., 2003). Adjusting for mortality when looking at cumulative prevalence of PDD is important since once dementia occurs, it indicates a short time to death, irrespective of age or disease duration (Kempster et al., 2010).

There are far fewer epidemiological data relating to DLB, presumably due to the difficulty in diagnosis. Systematic reviews have placed the incidence of DLB between 0.5 and 1.6 cases/1000 person-years in the general population (Zaccai et al., 2005; Hogan et al., 2016). The incidence of DLB in cases of newly diagnosed dementia is between 3.2% and 7.1% and is more common in those aged over 65 years (Zaccai et al., 2005; Hogan et al., 2016). Prevalence of DLB in the general population aged over the age of 65 ranges between 0% and 5% (van Weely et al., 1993; Zaccai et al., 2005; Vann Jones and O'Brien, 2014; Hogan et al., 2016). The prevalence of DLB ranged from 0 to 30% amongst diagnosed cases of dementia (Zaccai et al., 2005; Vann Jones and O'Brien, 2014; Hogan et al., 2016) although when diagnosis involved neurological assessment, the prevalence rises to a consistent 16-24% (Vann Jones and O'Brien, 2014).

1.1.4.Genetics

Genetic factors have been implicated in the development of PDD and DLB. Unsurprisingly, *SNCA* the strongest genetic risk factor for PD, is also strongly associated with both PDD and DLB (Bras et al., 2014). Interestingly however, the haplotype conferring risk is different: PD having an association 3' to the gene and DLB association occurring 5' of the gene (Bras et al., 2014). Some heritable forms of PD involving *SNCA*, most notably triplication of *SNCA*, demonstrate an early onset dementia phenotype (Poulopoulos et al., 2012).

However, not all PD associated genes confer risk for developing PDD or DLB (Irwin et al., 2013). *LRRK2* mutations causes autosomal dominant PD without cognitive impairment and dementia is rare in *PARK2, PARK6* and *PARK7* forms of hereditary PD (Poulopoulos et al., 2012).

Conversely, genes other than those associated with hereditary forms of PD are implicated in PDD. The *APO*ε4 genotype, a well-known and studied AD risk allele, is considered an important predictor of cognitive decline in PD (Mata et al., 2014). Furthermore, the *APO*ε4 allele is predictive of PDD independent from AD or Lewy body related pathology in post mortem studies (Irwin et al., 2012). The *APO*ε4 allele is also associated with DLB, present in approximately 30% of DLB patients compared with 14% of controls free from neurodegenerative and neuropsychiatric disease (Vergouw et al., 2017). Furthermore, *APO*ε4 allele confers a 6-fold increased risk of developing a dementia with Lewy pathology in carriers compared with controls which increases to a 12-fold increased risk of developing dementia with mixed AD and Lewy pathology, characteristic of DLB as discussed in chapter 1.1.5 (Vergouw et al., 2017). The *APOE* locus has also been identified as the strongest genetic risk factor for DLB in the largest genetic association study in DLB published to date (Bras et al., 2014).

The gene that encodes tau, *MAPT* is also implicated in the development of dementia (Irwin et al., 2013). *MAPT* contains two major haplotypes in humans: H1 and H2 (Irwin et al., 2013). Traditionally associated with AD, presence of the H1/H1 haplotype in PD has been suggested as an independent predictor of PDD (Goris et al., 2007). Furthermore, H1 haplotype may influence the degree of AD pathology in PD, consistent with the mixed pathology of PDD discussed in chapter 1.1.5 (Goris et al., 2007). The H1 haplotype is also associated with a higher risk of

developing DLB in a conclusive study comparing both clinically and pathologically diagnosed cases of DLB with non-demented controls (Labbe et al., 2016). Furthermore, the H1 haplotype is associated with enhanced α-synuclein deposition in DLB brain, particularly in the brainstem (Colom-Cadena et al., 2013).

More recently, the largest gene association study in DLB to date has been performed in which three loci were unequivocally associated with DLB: *APOE, SNCA* and *SCARB2* (Bras et al., 2014). The identification of *APOE* and *SNCA* as risk loci for DLB confirm previous findings discussed above. *SCARB2* represents a novel and intriguing risk gene since *SCARB2* encodes the glucocerebrosidase specific receptor for lysosomal transport, LIMP 2 (Bras et al., 2014).

1.1.5.Pathology

The pathology associated with LBDs displays considerable overlap with some debate as to whether PDD and DLB are in fact a continuum of the same disorder (Aarsland et al., 2004). LBDs are neuropathologically characterised primarily by the presence of aggregated α-synuclein in Lewy bodies (LBs) and Lewy neurites (LNs) in the brain (Halliday et al., 2014). However, it is now understood that common pathologies such as those associated with Alzheimer's disease: neurofibrillary tangles (NFTs) composed of tau and neuritic plaques composed of Aβ, are also frequently found in the brains of these patients (Irwin et al., 2013; Halliday et al., 2014; Howlett et al., 2015; Colom-Cadena et al., 2017). Furthermore, extensive cholinergic deficits occur relatively early in the disease course of DLB and have become established as a differentiating factor from AD (Jellinger, 2017). More severe neuronal loss in the nucleus basalis of Meynert and widespread cholinergic cortical losses, predominantly due to loss of choline acetyltransferase (ChAT) activity are not seen in classical AD (Jellinger, 2017).

1.1.5.1. Dementia with Lewy bodies

The 1996 consortium of the DLB international workshop subdivided the neuropathological features of DLB into 3 categories: brainstem predominant, limbic, and diffuse neocortical based upon the progressive propagation of α-synuclein pathology along the caudo-striatal axis according to Braak staging of PD (McKeith et al., 1996; Braak et al., 2003). Braak et al describe a progressive spread of LBs originating in the caudal brainstem, typically involving the dorsal motor nucleus and also the olfactory bulb (Braak et al., 2003). LB pathology continues to spread through the midbrain involving the basal ganglia, most prominently the substantia nigra pars compacta before culminating in widespread cortical pathology at advanced stages of the disease (Braak et al., 2003).

Morphologically DLB involves the co-occurrence of Lewy/α-synuclein pathology predominantly involving cortical and limbic areas consistent with Braak LB stages 3-5 and AD related pathologies (Jellinger, 2017). High cortical LB load in the temporal and parietal regions is a distinguishing feature of DLB accounting for a shorter latency to dementia (Jellinger, 2017). Attentional dysfunction and visual hallucination in DLB can be attributed to neuronal impairment of orbitofrontal and anterior cingulate cortices (Jellinger, 2017). Most DLB cases with cortical LBs

show some degree of AD pathology with concurrent AD pathological findings more common in DLB than PDD (Jellinger, 2017). Furthermore, deposition of extracellular Aβ into plaques is present in over 85% of DLB cases (Gomperts, 2014; Adamowicz et al., 2017) and the presence of amyloid plaques in the striatum has been reported to differentiate DLB from PDD (Kalaitzakis et al., 2011).

There is some debate as to whether high neocortical and limbic LB burden is an independent predictor of dementia in DLB (Schneider et al., 2012) or whether AD pathology is more important (Deramecourt et al., 2006). According to Braak staging, it is assumed that all patients with widespread diffuse α-synuclein pathology, such as those with DLB, will be demented and exhibit extrapyramidal symptoms of PD (Braak et al., 2003). However, this is not case and conversely some individuals with severe α-synuclein pathology at autopsy show no clinical symptoms of DLB (Parkkinen et al., 2008). However, the ability of clinicians to accurately diagnose DLB is positively correlated to the extent of LB pathology and negatively related to the severity of Alzheimer neuritic pathology, while Aβ load has no effect (Tiraboschi et al., 2015).

Large cohort studies of post mortem brain tissue suggest a strong correlation between both cortical Lewy pathology and AD-type pathologies (Compta et al., 2011; Irwin et al., 2012). Indeed, it has suggested that aggregated semi-quantitative scores of Aβ plaques, NFTs and Lewy pathology particularly in the prefrontal and temporal cortex give the best correlate to cognitive decline in DLB (Howlett et al., 2015). It has been suggested that phosphorylated α-synuclein promotes the phosphorylation of tau (Guo et al., 2013). The bidirectional synergistic relationship between AD pathology and α-synuclein by which each protein promotes the synthesis of the other is confirmed in animal models of PDD/DLB (Jellinger, 2017). Transgenic mice overexpressing both Aβ and α-synuclein have higher levels of Lewy body pathology and greater memory deficits compared with α-synuclein transgenic mice alone (Masliah et al., 2001).

Unlike AD pathology, the presence of LBs or LNs in the neocortex is not obviously associated with neuron loss or atrophy; DLB is characterised by preserved whole brain temporal lobe volumes (Nedelska et al., 2015). However, DLB patients with mixed AD pathology show greater atrophy in the whole brain, temporal-parietal cortices, hippocampus and amygdala similar to what

is seen in AD correlating with cognitive decline and progression of motor symptoms (Burton et al., 2004; Nedelska et al., 2015). This finding further implicates AD pathology as an important contributing factor to the severity of clinical symptoms of DLB (Nedelska et al., 2015).

Studies suggest early development of significant Lewy pathology in the hippocampus and surrounding cortical regions, particularly the entorhinal cortex, are crucial for memory impairments seen in DLB (Armstrong and Cairns, 2015). The CA1 subfield of the hippocampus is an important area for memory function and is preferentially affected by amyloid plaque and tangle pathology in AD (Armstrong and Cairns, 2015). Lewy pathology is also found in both CA1 and the entorhinal cortex in DLB often co-existing with AD pathology. (Armstrong and Cairns, 2015). Axon terminals in the CA2 sub-region of the hippocampus and cell bodies of the entorhinal cortex have significantly higher Lewy pathology than any other hippocampal region in either neocortical or limbic subtypes of DLB (Armstrong and Cairns, 2015).

Despite levels of LB pathology being highest in the hippocampal CA2 region and entorhinal cortex, correlation with memory performance is strongest with CA1 Lewy pathology burden, even after accounting for tangles (Adamowicz et al., 2017). This suggests that CA2 pathology is a prerequisite for CA1 pathology since the effects of Lewy pathology on learning and memory are most apparent at a later stage; a critical Lewy pathology burden must be reached across hippocampal circuitry to contribute to memory dysfunction beyond that relating to co-existing AD pathology (Adamowicz et al., 2017).

Accumulation of LBs in the dorsal raphe nucleus, the major serotonergic nucleus projecting to the neocortex has been associated with lowered serotonin levels in the striatum and neocortical areas of DLB brain (Ballard et al., 2013). Increased expression of the serotonin receptor is seen in the parietal cortex of DLB patients while the converse is seen in AD (Ballard et al., 2013).

1.1.5.2. Parkinson's disease dementia

As discussed earlier in this chapter, neuropathological substrates for PDD appear to be heterogeneous including both Lewy/α-synuclein related pathology in cortical, limbic and subcortical brainstem structures and AD-related pathologies (Aβ deposition, diffuse and neuritic plaques and NFTs).

Cognitive impairment in PDD is often correlated with the density of LNs and neuritic degeneration in the hippocampus and periamygdaloid cortex (Mattila et al., 1999). Density of both limbic LBs and neuritic plaques also correlate with dementia severity (Harding and Halliday, 2001). However, increased cognitive decline with increasing pathological LB staging has not universally been confirmed (Weisman et al., 2007; Jellinger, 2008). Autopsy studies demonstrate a picture of mixed pathology in PDD brain with approximately 50% of cases demonstrating diffuse LB deposition in addition to severe AD type pathology (Irwin et al., 2013; Jellinger, 2017). Generally, it is assumed that these pathological substrates co-occur and act synergistically although others suggest a positive relationship between cortical Aβ and NFT deposition respectively and cognitive impairment (Hurtig et al., 2000; Petrou et al., 2015; Biundo et al., 2016). Indeed, AD pathology does appear to be a more specific correlate of dementia in PD than cortical α-synuclein pathology (Compta et al., 2011; Irwin et al., 2012).

Clinicopatholgical study has identified 3 subgroups of PDD based upon mixed pathology: (1) predominant synucleinopathy Braak LB stage 5-6 (38%), (2) synucleinopathy with Aβ deposition but minimal or no tau pathology (59%), (3) synucleinopathy with considerable neocortical tau pathology (3%) (Kotzbauer et al., 2012). Patients in group 2 show significantly reduced survival (Kotzbauer et al., 2012). The additive effect of α-synuclein and AD pathology may influence the clinical features of PDD, such as a shorter duration with more malignant course (Compta et al., 2011; Halliday et al., 2014; Irwin et al., 2017). Regression analysis points towards a combined pathology (Aβ plaques + phosphorylated tau + LB/LN) particularly in the prefrontal cortex and the temporal lobe neocortex as a major determining factor in the development of dementia (Howlett et al., 2015).

Alterations to neurotransmission due to the involvement of subcortical nuclei are also associated with PDD (Jellinger, 2017). Substantial loss of limbic and cortically projecting dopaminergic neurons of the mesocortical limbic system and loss of neurons in the nucleus basalis of Meynert leading to cortical cholinergic denervation contribute to clinical symptoms of PDD (Jellinger, 2017).

Ballard et al describe a correlation between longer duration of parkinsonism prior to dementia and more pronounced cortical deficits, implying that extensive cholinergic deficits may be a feature of PDD (Ballard et al., 2006). Cholinergic deficits are compounded in PDD by significantly reduced neuronal cholinesterase activity when compared with DLB (Klein et al., 2010). Furthermore, pedunculopontine (PPN) cholinergic cell loss occurs in hallucinating PDD but not DLB (Hepp et al., 2013). PPN neurons project and receive inputs from the basal ganglia, with the exception of the substantia nigra pars compacta to which it projects to but does not receive from and the substantia nigra pars reticulata which it receives inputs from but does not project to (Jellinger, 2017). Neuronal loss in the substantia nigra is more severe in PDD compared with DLB potentially underlying changes to PPN cholinergic transmission and the development of attentional deficits and REM sleep disorders (Tsuboi and Dickson, 2005).

Lesion	DLB	PDD
LB/α-synuclein pathology	Both characterised by combination of progressed LB and AD pathology of variable severity and extent	
Amyloid beta	Severe and extended in cortex and striatum	Less severe in cortex and striatum
Tau	High. Particularly in medial temporal lobe	Low in cortex and striatum
Cortical LB load	Higher in temporal and parietal cortex, hippocampus	Diffuse or focal
α-synuclein load in hippocampus	CA2 more severely involved	CA2/3 more frequently involved
Substantia nigra neuronal loss	Less severe	More severe
Pedunculopontine cholinergic cell loss	Negative	Hallucinating PDD patients
Serotonin receptor density in the striatum	High	Low

Table 2 - Pathological overlap and differences between DLB and PDD. Compiled from (Jellinger, 2017)

1.1.6.Current therapeutic options

Currently, there are no disease modifying therapies for either DLB nor PDD (Galasko, 2017). Clinical management is based upon symptomatic treatment of the cognitive, psychiatric, motor and non-motor symptoms that represent the core features of the disease (Galasko, 2017).

1.1.6.1. DLB

Meta analyses support the use of the cholinesterase inhibitors rivastigmine and donepezil in DLB for improving cognition, hallucinations, delusions and activities of daily living without worsening motor symptoms of parkinsonism (Wang et al., 2015). The effectiveness of cholinesterase inhibitors is based upon cholinergic deficits associated with DLB as discussed in chapter 1.1.5. Rivastigmine is associated with greater risk of adverse events compared with donepezil (Stinton et al., 2015; Wang et al., 2015). Since anxiety and hallucinations are sometimes driven by psychosis the cholinesterase inhibitors may have secondary benefits for these symptoms (Wang et al., 2015). Evidence suggests the use of antipsychotics such as olanzapine and quetiapine for the acute treatment of behaviour disturbance, delusions or visual hallucinations should be limited due to high levels of adverse events, in particular the increased risk of mortality specifically in DLB (Ballard et al., 1998; Aarsland et al., 2005b; McKeith et al., 2017). However, this does not preclude their use since quetiapine may be beneficial for the psychiatric symptoms of some patients with DLB but not PDD (Stinton et al., 2015). Evidence is weak or lacking to support the use of the PD therapeutics levodopa, amantadine or selegiline in managing the parkinsonism symptoms of DLB (Stinton et al., 2015). Parkinsonism is often less responsive to dopaminergic agents in DLB than in PD and their use may be associated with an increased risk of psychosis (Galasko, 2017). However, individual patient and disease characteristics may significantly impact the efficacy of treatment. Younger patients with DLB appear to respond better to levodopa for the treatment of parkinsonism symptoms whilst patients with hallucinations show a greater benefit from rivastigmine for global cognition and attention (Stinton et al., 2015).

1.1.6.2. PDD

A Cochrane review of the use of cholinesterase inhibitors in PDD demonstrated a good evidence base with positive impacts on global assessment, cognitive function, behavioural disturbance and activities of daily living scales (Rolinski et al., 2012). To date rivastigmine is the only cholinesterase inhibitor that is licenced for the treatment of PDD in the UK (Rolinski et al., 2012). Parkinsonism symptoms and tremor are reported more frequently in patients taking

cholinesterase inhibitors but they do not impact PD severity rating scales (Rolinski et al., 2012). Further support for cholinesterase inhibitors in PDD has been seen in a more recent meta-analysis where cholinesterase inhibitors significantly attenuate decline in MMSE scores, an indicator of global cognitive ability, without increasing the risk of falls (Pagano et al., 2015). Cholinesterase inhibitors have also shown evidence of improving global psychiatric symptoms in PDD but not in DLB (Pagano et al., 2015). Responsiveness to levodopa is more efficacious for cognitive symptoms in PDD compared with DLB but also when compared with PD (Emre et al., 2014; Stinton et al., 2015). As with DLB, there have been few well designed clinical trials in PDD cohorts with the appropriate control groups to study pharmacological treatments for the wide range of symptoms these patients can experience. Therefore, evidence for several compounds is lacking, limiting therapeutic options in these patients (Stinton et al., 2015).

However, pimavanserin, a selective serotonin 5-HT2A inverse agonist, is a promising new drug showing positive results for the treatment of psychosis in PDD without affecting motor symptoms in successful phase 3 clinical trials (Cummings et al., 2014; Velayudhan et al., 2017). The strategy behind the use of pimavanserin is based upon the reduced amount of 5-HT1A receptor binding in the cortex of PDD patients (Francis and Perry, 2007). Ambroxol is another new compound in clinical trial for the treatment of cognitive impairment and dementia in PD which has been shown to reduce the levels of α-synuclein in both the brainstem and striatum *in vivo* (Migdalska-Richards et al., 2016). Ambroxol functions to enhance activity of the lysosomal enzyme glucocerebrosidase (Migdalska-Richards et al., 2017), the focus of this thesis which will be discussed in further detail herein.

1.2. Glucocerebrosidase

1.2.1. *GBA1*

GBA1 encodes the lysosomal enzyme glucocerebrosidase (GCase) (Ginns et al., 1985). *GBA1* was localised to the genetic loci 1q21 in 1985 (Ginns et al., 1985), a particularly gene rich region of chromosome 1 considered a recombination hotspot (Gregory et al., 2006). *GBA1* spans 7.6kb of genomic DNA divided into 11 exons (Horowitz et al., 1989). A highly homologously transcribed but non-functional pseudogene, *GBAP*, is located 16kb downstream from *GBA1*, containing the same organisation of exons (Sorge et al., 1990). Due to the combination of 96% exonic sequence homology and proximity, recombination events are facilitated contributing to the creation of mutant alleles (Hruska et al., 2008). Currently, the number of mutations reported in *GBA1* has exceeded 300 including: missense, nonsense, frame-shift and splice mutations (Hruska et al., 2008).

1.2.2. *GBA1* mRNA

GBA1 has at least 2 mRNA species of 2.2kB and 2.6kB arising from alterative polyadenylation (Horowitz et al., 1989). *GBA1* mRNA has two in frame methionine start codons located in exons 1 and 2 respectively (Horowitz et al., 1989). Both methionine codons are translated to produce the functional protein (Horowitz et al., 1989). GCase translated from start codon 1 contains a 39-amino acid long signal peptide whereas the signal peptide for GCase from exon 2 is 19-amino acids long (Sorge et al., 1985; Sorge et al., 1987). Both mRNA strands are ultimately translated and processed into 496 amino acid long mature GCase after removal of signal peptides, a common occurrence for secreted peptides (Horowitz et al., 1989).

1.2.3. Glucocerebrosidase enzyme

GCase is a membrane associated lysosomal hydrolase enzyme, the mature form of which is comprised of 496 amino acids and has molecular weight of approximately 60kDa depending upon glycosylation (Horowitz et al., 1989). It is ubiquitously expressed in all types of tissues (Migdalska-Richards and Schapira, 2016). Structurally, GCase is comprised of three non-continuous domains with domains I and II designated as non-catalytic (Kacher et al., 2008). Domain I is comprised of a triple stranded anti-parallel β-sheet containing two disulphide bridges which are likely involved in GCase folding (Kacher et al., 2008). Domain II consists of two β-sheets forming an

immunoglobulin-like domain (Kacher et al., 2008). Although these domains are non-catalytic and the functions are not fully understood, the location of several mutations throughout these domains suggest an important regulatory role. Domain III contains the $(\beta/\alpha)_8$ (TIM) barrel catalytic site (Kacher et al., 2008). Residue Glu235 serves as the acid/base and Glu340 as the nucleophile in the catalytic cycle (Kacher et al., 2008). Human GCase is glycosylated at 4 out of 5 available asparagine residues and glycosylation is required for catalytic function (Migdalska-Richards and Schapira, 2016).

GCase is translated in endoplasmic reticulum (ER) bound polyribosomes into a 56kDa polypeptide, from where it translocated through the ER (Erickson et al., 1985). Passage through the ER is accompanied by cleavage of a leader sequence and N-linked glycosylation of 4 asparagine resides (Erickson et al., 1985). High mannose sugars are modified as GCase moves through the Golgi apparatus (Erickson et al., 1985). GCase is further modified via sugar residues in the Golgi before being trafficked to the lysosome as a mature protein by a mannose 6 phosphate receptor independent pathway utilising the GCase specific receptor, LIMP 2 (Reczek et al., 2007). LIMP 2 a highly abundant type 3 transmembrane protein essential for GCase function since it is crucial for targeting GCase to the lysosome (Reczek et al., 2007). GCase binds to a coiled-coil domain in the luminal domain of LIMP 2 in the neutral pH of the ER, where the complex persists through the Golgi apparatus and endosomes (Reczek et al., 2007). When the LIMP 2-GCase complex reaches the lysosome, dissociation occurs in a pH dependent manner (Reczek et al., 2007; Gruschus et al., 2015) **(Figure 1).** LIMP 2 deficient mice and humans have significantly reduced GCase enzyme activity and associated elevation of serum GCase since GCase does not reach the lysosome, accompanied by accumulation of α-synuclein (Reczek et al., 2007; Rothaug et al., 2014). *SCARB2*, the gene encoding LIMP 2 has been genetically linked to PD and DLB supporting the hypothesis that LIMP 2 is central to α-synuclein homeostasis within the lysosome (Do et al., 2011; Michelakakis et al., 2012; Hopfner et al., 2013; Bras et al., 2014).

Saposin C (SapC) is a requisite enzyme activator molecule for optimal GCase enzymatic activity (Grabowski et al., 1990). Saposins are a set of small glycoproteins generated in the endosome via proteolysis of a 73kDa precursor protein, prosaposin, encoded by *PSAP1* (Tamargo et al., 2012). Each saposin is approximately 80 amino acids with 6 similarly located cysteine residues

that confer heat stability and a characteristic tertiary structure through the formation of three conserved disulphide bridges (Tamargo et al., 2012). Mature saposins A-D assist lysosomal hydrolases in the degradation of sphingolipids (Tamargo et al., 2012). SapC is the specific activator of GCase enzyme (Tamargo et al., 2012). The mechanisms by which SapC promotes lysosomal hydrolysis are unknown but Forster resonance energy transfer studies suggest SapC interacts with both GCase and the phospholipid membrane, bringing them together so GCase can hydrolyse endogenous GluCer (Alattia et al., 2007). Sap C may also help extract and solubilise the lipid substrate from the membrane to facilitate GCase access for GluCer hydrolysis (Alattia et al., 2007). Additionally, SapC is also able to protect GCase from proteolytic degradation, a protective effect not observed with other saposins (Sun et al., 2003).

Evidence suggests that α-synuclein and SapC compete for binding to GluCer and that SapC binding can induce the release of α-synuclein from GCase alleviating an inhibitory effect of α-synuclein on GCase enzyme activity (Yap et al., 2013b). Mutations in SapC result in significantly reduced GCase enzyme activity and accumulation of lipids causing a rare form of the lysosomal storage disorder Gaucher's disease (Vaccaro et al., 2010).

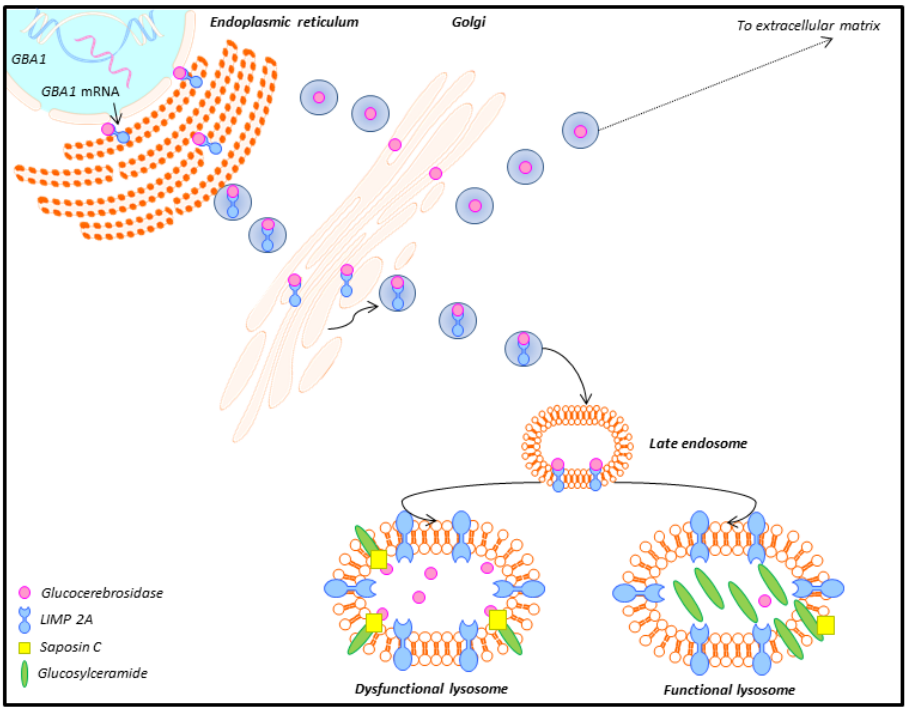

Figure 1 - Trafficking of GCase to the lysosome. Compiled and adapted from (Westbroek et al., 2011)

1.2.4.Glycosphingolipid metabolism

GCase cleaves the glycosidic bond in the glycosphingolipid glucosylceramide (GluCer) to form the constituent parts glucose and ceramide (Brady et al., 1965). Glycosphingolipids (GSLs) are ceramides with linked oligosaccharides of variable composition predominantly found in the plasma membrane of almost all cell types (Kolter and Sandhoff, 2010). The brain has the highest content of complex GSLs with particular abundance in neurons (Massimo et al., 2016). Located asymmetrically in the extracellular leaflet of the plasma membrane specifically within microdomains known as lipid rafts, GSLs have important roles in regulating membrane fluidity (Morad and Cabot, 2013). Additionally, GSLs are bioactive effectors in cellular functions such as apoptosis and proliferation (Morad and Cabot, 2013; Massimo et al., 2016).

GluCer represents a key juncture in glycosphingolipid metabolism (Astudillo et al., 2016). Over 90% of all mammalian glycosphingolipids including complex gangliosides and sulfatides essential for mammalian function are derived from GluCer through a ceramide glucosylation reaction in the lumen of the late Golgi (Astudillo et al., 2016). Unsurprisingly therefore, GluCer is absolutely essential for mammalian development with homozygous mutation within *Ugcg*, the gene encoding GluCer synthase, being embryonically lethal (Astudillo et al., 2016).

Generation of GluCer is dependent upon the transfer of constituent molecules to the cis-Golgi followed by transportation to the late Golgi (Gault et al., 2010). Ceramide can be galactosylated in the ER, to produce galactosylceramide (GalCer) or it can be transported to the Golgi complex, reaching the cis-Golgi through vesicular transport to be glucosylated producing GluCer (Gault et al., 2010). The glucosylation of ceramide is catalysed by the enzyme GluCer synthase (D'Angelo et al., 2013). GluCer is produced on the cytosolic leaflet of the early Golgi membranes and is translocated to the luminal membrane leaflet of the Golgi via vesicular trafficking for further glycosylation (D'Angelo et al., 2013). Alternatively, GluCer can be picked up from the cis-Golgi membranes by the lipid transfer protein FAPP2 for delivery to the trans Golgi network, where it is translocated to the luminal membrane leaflet of the Golgi and trans Golgi network (D'Angelo et al., 2013).

Once in the trans Golgi network, GluCer is galactosylated to produce lactosylceramide (LacCer) which once produced cannot be translocated back to the cytosolic leaflet of Golgi membranes

(D'Angelo et al., 2013). LacCer functions as the branching point for the formation of the different classes of complex GSLs including GA2, GM3, Gb3 and Lc3 which form the precursors for synthesis of GSLs belonging to the asialo, ganglio, globo and laco series respectively (D'Angelo et al., 2013). From the trans Golgi network, GSLs are transported to the plasma membrane in membrane bound transport carriers (D'Angelo et al., 2013). At the plasma membrane, GSLs can undergo partial remodelling through the action of specific glycosidases or can be transported along endocytic routes from the plasma membrane to lysosomes for degradation by specific glycosidases e.g. GCase (Kolter and Sandhoff, 2010). GSLs undergo stepwise dismantling of glycan moieties until ceramide is remaining (Kolter and Sandhoff, 2010). Ceramide in lysosomes is catabolized by acid ceramidase to produce a fatty acid and sphingosine, which can be transported to the ER and used for the synthesis of GSLs – the salvage pathway of ceramide production (Kolter and Sandhoff, 2010) **(Figure 2).**

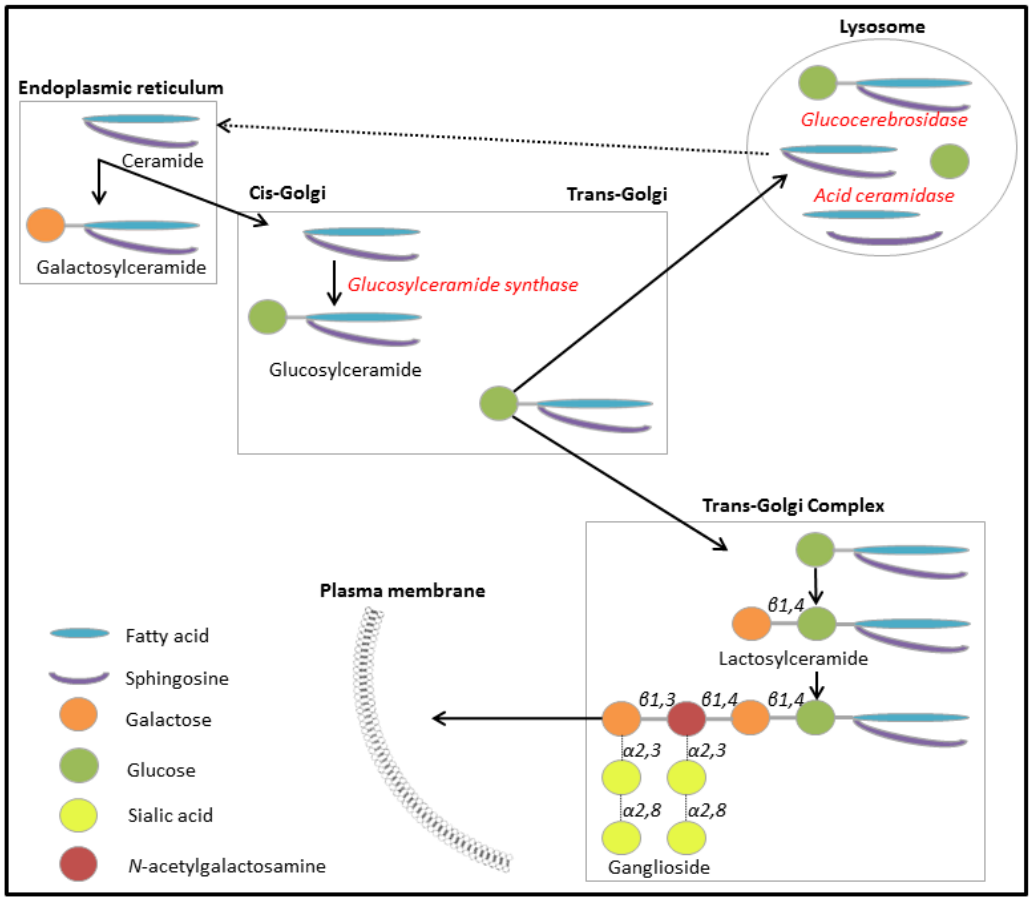

Figure 2 - Summary of glycosphingolipid metabolism. Compiled and adapted from (Kleene and Schachner, 2004)

1.2.5.Non-lysosomal glucocerebrosidase – *GBA2* and *GBA3*

GluCer accumulation characteristic of the lysosomal storage disorder Gaucher's disease (GD) is predominantly seen in tissue macrophages (Stirnemann et al., 2017). Since GluCer is ubiquitously expressed, it raises the question whether another enzyme present in specific tissues could be compensating for GCase enzyme deficiency present in other cells.

GBA2 was first characterised in 1993 where the fundamental properties of the enzyme were described as: strongly membrane bound; not located in lysosomes and not deficient in GD (van Weely et al., 1993). While the GCase enzymes transcribed by *GBA1* and *GBA2* can hydrolyse the same substrate, GluCer, there is no sequence homology and the proteins are encoded by different genes (van Weely et al., 1993). *GBA2* is found on chromosome 9, mapping position 19.3 (Massimo et al., 2016). *GBA2* mRNA is particularly abundant in brain, heart, skeletal muscle and kidney (Massimo et al., 2016). Genetic mutations in *GBA2* can result in hereditary spastic paraplegia and cerebellar ataxia (Massimo et al., 2016).

There is some suggestion that *GBA2* may have a compensatory role in *GBA1* deficient states and could possibly be upregulated to limit substrate accumulation (Aureli et al., 2011). *GBA2* knock out mice demonstrate accumulation of GluCer in several tissues that treatment with recombinant *GBA2* protein is able to reverse (Yildiz et al., 2006). *GBA2* enzyme activity is significantly increased in GCase deficient mice compared with wild type (Burke et al., 2013). However, a recent paper suggests that a negative feedback loop exists between *GBA1* and *GBA2* whereby sphingosine build up due to *GBA1* enzyme deficiency causes inhibition of *GBA2* enzyme through the direct binding between *GBA2* enzyme and sphingosine (Schonauer et al., 2017). Consequently, further accumulation of sphingosine leads to cytotoxicity (Schonauer et al., 2017). Additionally, *GBA2* hydrolyses glucosylsphingosine, an alternative product of GluCer metabolism through the action of acid ceramidase enzyme, producing sphingosine (Ferraz et al., 2016a)

GBA3 has also been identified. *GBA3* enzyme is cytosolic in cells of the kidney, liver, spleen, intestines and lymphocytes (Dekker et al., 2011a). While the function of *GBA3* is unclear, it is known that *GBA3* does not modify GD (Dekker et al., 2011a). Despite this, relatively high GCase enzyme activity attributable to neither *GBA1* nor *GBA2* has been reported in normal and GCase deficient fibroblasts (Dekker et al., 2011a).

1.3. Gaucher's Disease

First described in 1882 by Phillipe Gaucher, Gaucher's disease (GD) is a rare autosomal recessive genetic disorder occurring with an incidence of 1 in 40-60,000 live births, increasing to 1 in 800 within the Ashkenazi Jewish population (Grabowski, 2008). The most common of the sphingolipidosis classification, GD is caused by homozygous mutation in *GBA1,* and very rarely, mutation in *PSAP*; the gene encoding the GCase activator protein Saposin C (Vaccaro et al., 2010; Kang et al., 2018).

1.3.1. Gaucher cells and glucosylceramide

As a consequence of homozygous *GBA1* mutation, residual GCase enzyme deficiency within the lysosome is reduced to between 5 and 20% of normal levels (Aerts et al., 2008). GluCer, the natural substrate of GCase enzyme, accumulates 5-10-fold, principally in tissue macrophages giving rise to characteristic 'Gaucher cells' - swollen macrophages of 20-100μM diameter (Parkin and Brunning, 1982). As seen by light microscopy Gaucher cells have distinctive features: enlargement; eccentric nuclei; condensed chromatin and a cytoplasm with heterogeneous appearance, all related to the presence of GluCer aggregates within the cell (Parkin and Brunning, 1982). Cells of monocyte / macrophage lineage are preferentially affected in GD due to their function in eliminating erythrocytes and leukocytes which contain large amounts of glycosphingolipids (Parkin and Brunning, 1982). Gaucher cells subsequently go on to infiltrate various tissues most commonly the spleen, liver, bone marrow and rarely the lungs (Boven et al., 2004). Massive infiltration of Gaucher cells alone does not explain the multifaceted characteristics of GD (Boven et al., 2004). Gaucher cells can cause secondary activation of macrophages, including activation of the inflammatory cascade and release of lysosomal proteins (Boven et al., 2004). Once such protein, the enzyme chitotriosidase, an enzyme selectively activated in tissue macrophages, is produced in Gaucher cells and is raised up to a 1000-fold compared with healthy individuals, serving as a diagnostic marker for GD (Aerts et al., 2008; Sheth et al., 2010).

1.3.2. Glucosylsphingosine

Glycosphingolipid metabolism is complex. GluCer is a substrate for an alternative pathway in which acid ceramidase can de-acylate GluCer into glucosylsphingosine (GluSph) (Ferraz et al., 2016a) **(Figure 3).** Although GluCer is the primary lipid which accumulates in GD, GluSph is also

significantly elevated, over 100-fold, due to increased availability of GluCer substrate (Nilsson and Svennerholm, 1982; Ferraz et al., 2014; Murugesan et al., 2016). GluSph has reduced hydrophobicity and is able to diffuse out of the lysosome into fluids and tissues, notably the brain, where it is able to affect wide spread consequences implicated in the heterogeneous symptoms of GD (Ferraz et al., 2016a).

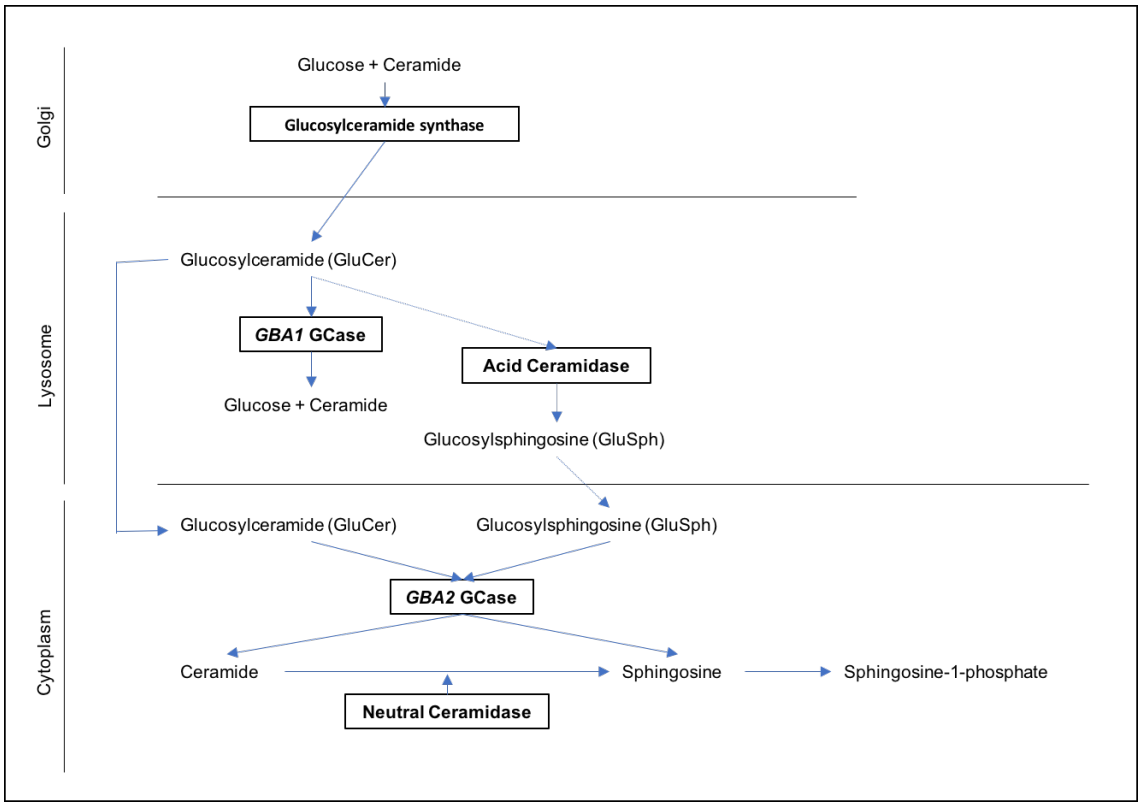

Figure 3 - Production of glucosylsphingosine and metabolites. Compiled and adapted from (Mistry et al., 2014)

In the cytoplasm, GluSph is hydrolysed by an alternative GCase enzyme derived from *GBA2* that is active at neutral pH, producing sphingosine and then sphingosine-1-phosphate which are considered to be toxic metabolites (Dekker et al., 2011b; Mistry et al., 2014; Ferraz et al., 2016b). GluSph is considered to play a key role in neuronal injury accompanying types 2 and 3 GD (Dekker et al., 2011b). Since GluCer turnover in neurons in low, accumulation of GluCer is only significant and available for metabolism by acid ceramidase when residual GCase activity is drastically reduced as seen with types 2 and 3 GD (Orvisky et al., 2002). Accordingly, GluSph is not normally present in the brain, but is present in the brain of GD patients with neurological involvement even in the absence of stereotypical Gaucher cells (Nilsson and Svennerholm, 1982; Stirnemann et al., 2017).

1.3.3.Symptoms

GD varies hugely in clinical presentation with multi organ involvement illustrated by the continuum of phenotypes. There are three distinguishable major phenotypic presentations of GD: type 1 (non-neuronopathic); type 2 (acute neuronopathic); and type 3 (sub-acute neuronopathic).

1.3.3.1. Type 1

Type 1 is by far the most common presentation of GD, accounting for 90-95% of patients in Europe and north America (Stirnemann et al., 2017). It is distinguishable from types 2 and 3 through the absence of neurological involvement and is essentially a macrophage disorder (Stirnemann et al., 2012). Clinical presentation is extremely variable and can even be asymptomatic throughout life (Stirnemann et al., 2012). The characteristic feature of type 1 GD is splenomegaly, which is seen in over 90% of patients, followed by hepatomegaly in 60-80% (Stirnemann et al., 2017). These patients also have a 5 times increased incidence of gallstones and may also suffer from blood disorders, pulmonary involvement and characteristic bone disorders especially in the pelvis and lower limbs (Stirnemann et al., 2017).

1.3.3.2. Type 2

Type 2 GD is the most severe form of GD and accounts for less than 5% of diagnosed cases (Tylki-Szymanska et al., 2010). It is characterised by early and severe neurological involvement first seen in infants between the age of 3-6 months following characteristic hepatosplenomegaly (Tylki-Szymanska et al., 2010). Type 3 GD is usually diagnosed by the presence of a highly suggestive triad of neurological symptoms: rigidity of the neck and trunk (opisthotonos), bulbar signs (severe swallowing disorders) and oculomotor paralysis (bilateral fixed strabismus). Following these suggestive symptoms, trismus and hypertonia can be seen and associated with pyramidal rigidity (Tylki-Szymanska et al., 2010). Apnoea, altered psychomotor development and myoclonic epilepsy can follow (Tylki-Szymanska et al., 2010).

1.3.3.3. Type 3

Type 3 GD accounts for approximately 5% of all diagnosed cases and comprises of the visceral symptoms of type 1 GD combined with neurological involvement (Grabowski et al., 2015). Neurological involvement is far less severe compared to that seen in type 2 and is usually diagnosed before the age of 20 (Grabowski et al., 2015). Type 3 GD is considered a slowly progressing form of neuronopathic GD, in which patients can live in to their 60s (Tylki-Szymanska et al., 2010). As with the other forms of GD, symptoms are highly heterogeneous particularly the

neurological symptoms which can range from mild such as horizontal opthalmoplegia, to more severe including: myoclonus epilepsy, cerebellar ataxia, spasticity and dementia (Grabowski et al., 2015). The type 3 associated D409H mutation is specifically associated with cardiac involvement (Grabowski et al., 2015).

1.3.4.Mutation dosage effect

The wide variability of symptoms amongst individuals with the same genotype and *vice versa*, including between twins, has made it increasingly difficult to categorise *GBA1* mutations into the 3 classic types of GD (Hruska et al., 2008). Compounding the difficulty with the classification approach is the fact that the majority of mutations identified are not found solely in the homozygous form therefore the combination of different mutations on both alleles is the determining factor of phenotype (Grabowski, 2008). It may be more accurate to consider the associated phenotypes as a continuum with the major distinction being the presence or degree of neurological involvement (Sidransky, 2004). However, there are some established genotype-phenotype correlations.

N370S is encountered only in patients with type 1 GD (Huang et al., 2015). However, some individuals homozygous for N370S mutation are asymptomatic. While the homozygous N370S genotype is associated with type 1 GD, the presence of one N370S mutant allele prevents the development of neurological manifestations even in combination with mutations considered severe (Huang et al., 2015). Accordingly, N370S is considered a mild mutation in *GBA1.*

GD patients with neurological involvement, typically those with type 3, predominantly carry: L444P, R463C, N188S, G377S or V394L mutant alleles (Hruska et al., 2008) **(Table 3).** Accordingly, these mutations are classified as severe. However, the presence of one of these alleles in combination with a null allele is more likely to invoke a more severe type 2 phenotype, highlighting the importance of the combination of mutant alleles, presumably on residual GCase enzyme activity (Hruska et al., 2008). However, even residual GCase enzyme activity does not appear to be associated with patient phenotype, implying genetic or environmental modifiers are critical (Hruska et al., 2008).

Genotype-phenotype correlations have been examined in the limited number of cases with pure homozygous genotypes uncovering a clear gene dosage effect with some alleles. Homozygous mutation for K79N, N188S or G377S clearly results in type 1 GD, whilst compound heterozygosity with a null allele leads to type 3 phenotype (Hruska et al., 2008). Similarly, homozygosity for F213I or L444P usually leads to a type 3 phenotype, whilst compound heterozygosity with a null allele leads to a type 2 phenotype (Hruska et al., 2008) **(Table 3)**

Broad classification of mutant *GBA1* alleles		
Mild	Severe	Null
N370S	L444P	RecNciI
	R463C	84GG
	N188S	
	G377S	
	V394L	
Gene dosage effect of mutant *GBA1* alleles based upon homozygous expression		
Type 1 GD	**Type 3 GD**	
K79N	F213I	
N188S	L444P	
G377S		
N370S*		
Compound heterozygosity with null allele causes type 3 phenotype *Presence of one allele prevents neurological involvement	Compound heterozygosity with null allele causes type 2 phenotype	

Table 3- Classification of mutant *GBA1* alleles based upon genotype-phenotype correlations. Compiled from (Sidransky, 2004; Hruska et al., 2008; Huang et al., 2015)

1.3.5.Pharmacological treatment

1.3.5.1. Enzyme replacement therapy (ERT)

The principle behind ERT is simple - to replace deficient GCase enzyme in cells, particularly Gaucher cells, with functioning GCase to reduce accumulation of GluCer substrate thereby improving symptoms (Barton et al., 1991). 26 years following the description of GCase enzyme deficiency characteristic of GD, macrophage targeted GCase, alglucerase, was FDA approved for non-neurological forms of GD (Barton et al., 1991).

The original ERT therapeutic alglucerase was extracted from human placenta and deglycosylated, exposing mannose sugars required for uptake by macrophage receptors and subsequent transport to lysosomes (Bembi et al., 1994). As technology has developed, ERT now uses Chinese hamster ovary cell derived recombinant GCase enzyme (Cerezyme®) (Serratrice et al., 2016). Cerezyme® is the current treatment standard for type 1 GD (Serratrice et al., 2016). Treatment results in a striking and rapid reversal of many aspects of type 1 GD (Serratrice et al., 2016). It is highly effective at reversing characteristic symptoms such as hepatosplenomegaly, cytopenia and osteopenia (Serratrice et al., 2016). Cerezyme® also enhances quality of life and reverses growth retardation (Serratrice et al., 2016). Cerezyme® does not modify neurological manifestations of GD, and so is ineffective for type 2 GD (Bembi et al., 1994). This is partially explained by the inability of the recombinant enzyme to cross the blood brain barrier (Altarescu et al., 2001). However, delivery of recombinant GCase directly infused into the cerebral spinal fluid or directly into the brainstem of infants with type 2 GD does not attenuate neurological symptoms either (Bembi et al., 1994; Lonser et al., 2007). The introduction of ERT has drastically reduced the number of GD patients requiring splenectomy (Mistry et al., 2017). Since treatment generally begins before irreversible complications occur severe manifestations of type 1 GD are now rarely seen in the clinic (Mistry et al., 2017).

1.3.5.2. Substrate reduction therapy (SRT)

Glycosphingolipids are synthesised in the Golgi apparatus by addition of monosaccharides to ceramide through the sequential action of glycotransferase enzymes as discussed in section 1.2.4. SRT is based upon inhibition of one of these enzymes – glucosylceramide synthase (GCS) – responsible for generating GluCer, the natural substrate of GCase enzyme (Coutinho et al.,

2016). The principle behind GCS inhibition is to reduce the amount of GluCer produced that needs metabolising in the lysosome since GCase enzyme activity in GD is deficient (Aerts et al., 2006; Coutinho et al., 2016). Rebalancing the synthesis and catabolism of GluCer may therefore address characteristic symptoms caused by the accumulation of GluCer in macrophages (Coutinho et al., 2016).

*N*B-DNJ, later known as miglustat, was the first SRT compound targeting GCS (Aerts et al., 2006). It was authorised by the European Medicines Agency in 2002 for the treatment of mild to moderate type 1 GD where ERT is not suitable (Aerts et al., 2006). Structurally, a N-alkylated imino sugar, miglustat is a structural mimic of monosaccharides other than the replacement of the ring oxygen for a nitrogen atom (Butters et al., 2005). Miglustat was a known compound, tested previously in HIV patients having acted as an inhibitor of HIV replication *in vitro* but was unsuccessful in clinical trials (Butters et al., 2005). This profile of miglustat aided the repurposing of the drug for use in the Gaucher's clinic. Miglustat is able to demonstrate effective reduction in the size of the liver and spleen, key outcome measures for type 1 GD therapeutics (Aerts et al., 2006). Furthermore, miglustat reduces the expression of the surrogate GD biomarker chitotriosidase significantly compared with placebo (Aerts et al., 2006; Shemesh et al., 2015; Stirnemann et al., 2017). However, efficacy on haematological parameters is limited and despite being able to cross the blood brain barrier, miglustat is unable to attenuate neurological defects (Van Rossum and Holsopple, 2016). Additionally, miglustat is reported to be an inhibitor of non-lysosomal GCase produced by *GBA2* and also exhibits some functionality as a chaperone molecule, facilitating transport of mutant GCase to the lysosome (Butters et al., 2005; Ridley et al., 2013).

A second ERT, eliglustat, achieved market authorisation in 2015 (Sechi et al., 2016). Eliglustat, an analogue of ceramide, is a more specific and potent inhibitor of GCS (Sechi et al., 2016). It has significantly greater efficacy compared to placebo and non-inferiority to Cerezyme® when tested over 2 years (Cox et al., 2015; Sechi et al., 2016). These factors combined mean eliglustat can be considered as a first line treatment for type 1 GD, an oral daily treatment as an alternative to i.v. injection fortnightly with Cerezyme® (Cox et al., 2015). However, eliglustat requires patient specific evaluation of variables (Sechi et al., 2016). Patients also need to be genotyped for

CYP2D6 metabolism status and eliglustat is contraindicated in patients with certain heart conditions (Sechi et al., 2016; Van Rossum and Holsopple, 2016).

1.4. Genetic association between GD and synucleinopathies

Heterozygous mutations in *GBA1* have become established as the most common genetic risk factor for PD (Sidransky et al., 2009a). Furthermore, *GBA1* insufficiency has been strongly linked with an enhanced cognitive impairment phenotype in PD (Neumann et al., 2009). Heterozygous *GBA1* mutation has subsequently been associated with both Parkinson's disease dementia and dementia with Lewy bodies (Sidransky et al., 2009b; Nalls et al., 2013).

1.4.1. Clinic based observations

Unlike the standard methods used to identify risk genes using genome wide associations studies (GWAS) and more recently next generation genome sequencing, *GBA1* heterozygosity was first identified as a genetic risk factor for PD though clinical observations of GD patients and their first-degree relatives (Neudorfer et al., 1996).

The link between mutations in *GBA1* and PD was first postulated in the 1990s following the publication of several striking case studies of GD patients displaying parkinsonism symptoms (Neudorfer et al., 1996). Neudorfer et al described six patients with classical type 1 GD who by the mean age of 49 had developed parkinsonism symptoms and similar reports of L-DOPA refractory parkinsonism manifestations including tremor, bradykinesia, rigidity and often cognitive decline soon followed (Neudorfer et al., 1996; Bembi et al., 2003; Tayebi, 2003; Goker-Alpan et al., 2004). Intriguingly, it was also noted that up to 25% of first degree relatives of GD patients also developed parkinsonism symptoms (Goker-Alpan et al., 2004; Halperin et al., 2006). Collectively, these clinical observations prompted a plethora of genetic association studies in an attempt to establish the mutation frequency of *GBA1* in sporadic PD and the degree to which mutations in *GBA1* increase susceptibility to PD.

1.4.2. Genetic studies

1.4.2.1. PD

The first genetic study looking at the frequency of *GBA1* mutations in PD was reported in 2004 (Aharon-Peretz et al., 2004). Aharon-Peretz et al studied the occurrence of 6 of the most common *GBA1* mutations in idiopathic PD, AD and healthy Ashkenazi Jewish populations (Aharon-Peretz et al., 2004). Mutations in *GBA1* were found in a startling 31.3% of PD patients, compared with

4% of AD patients and 6.2% of healthy controls (Aharon-Peretz et al., 2004). In the same year, Lwin et al sequenced all exons in a small cohort of sporadic PD patients (n=57) and controls (n=44) excluding those of Ashkenazi Jewish heritage (Lwin et al., 2004). *GBA1* mutation frequency was reported at 21% in PD and 0% in the non-demented control cohort (Lwin et al., 2004). Several genetic studies of *GBA1* mutation frequency in PD followed which differed in the ethnicity of cohorts and sequencing of the gene, making comparison and interpretation difficult. *GBA1* mutation frequencies in all studies excluding Ashkenazi Jewish populations are summarised in **Table 4.** When categorised by ethnicity, the mutation frequency in European PD patients was between 2.3% and 10.24% (Toft et al., 2006; Moraitou et al., 2011), 1.8% and 8.7% in Asian PD patients ((Hu et al., 2010; Yu et al., 2015) and between 2.9% and 12% in north and south American PD patients (Eblan et al., 2005; Mata et al., 2008).

Owing to the variations in study methods and cohorts, a large multicentre meta-analysis was performed to give a definitive *GBA1* mutation frequency in PD (Sidransky et al., 2009b). 5491 patients with sporadic PD and 4898 controls were included across the 16 participating centres (Sidransky et al., 2009b). When the whole gene was sequenced in non-Ashkenazi Jewish PD patients, *GBA1* mutation frequency was 6.9% compared with less than 1% in controls (Sidransky et al., 2009b). When genotyping specifically for N370S and L444P, mutation frequency was 3% in PD patients compared with less than 1% in controls (Sidransky et al., 2009b). The presence of any *GBA1* mutation was associated with an odds ratio of 5.43 across all centres: PD subjects are 5.43 times more likely to harbour a *GBA1* mutation than controls (Sidransky et al., 2009b).

Studies of relative risk have found that *GBA1* homozygotes have a 20-fold increased risk for developing PD in their lifetime (Bultron et al., 2010), while *GBA1* heterozygotes are at 30-fold increased risk of developing PD (McNeill et al., 2012). Not all carriers of *GBA1* mutations go on to develop PD. The penetrance (age specific cumulative PD risk) of PD in *GBA1* mutation carriers has been reported at 29.7%, 15% and 10.9% respectively by the age of 80 (Anheim et al., 2012; McNeill et al., 2012; Rana et al., 2013). Confirmation of *GBA1* as a strong risk loci for PD has come from a meta-analysis of GWAS studies in PD (Nalls et al., 2014). Having examined 13,708 sporadic PD cases and 95,282 controls, *GBA1* was one of 4 risk loci following conditional analyses to contain a secondary independent risk variant (Nalls et al., 2013). While the effect of

the individual *GBA1* loci may be small, risk profiles show a substantial cumulative risk (Nalls et al., 2014).

1.4.2.2. DLB

Far fewer genetic association studies looking at *GBA1* mutation frequency and relative risk in DLB have been carried out, predominantly due to the difficulties surrounding accurate diagnosis of DLB in the clinic, limiting most studies to pathologically confirmed cases of DLB as discussed in section 1.1.2.

GBA1 mutation frequency appears to be even higher in DLB compared with PD. Studies which sequenced the entire gene or coding sequences reported relatively consistent mutation frequencies of 8.50%, 12.61% and 8.80% respectively compared with less than 1% in controls (Tsuang et al., 2012; Gamez-Valero et al., 2016; Geiger et al., 2016). Variation between 13.8% and 3.50% was seen in cases which had exons 8 and 9 sequenced and the SNPs N370S and L444P genotyped, respectively (Mata et al., 2008; Asselta et al., 2014) **(Table 5).**

Following the example of the large collaborative study of *GBA1* mutations in PD (Sidransky et al., 2009b), a large multicentre meta-analysis of *GBA1* mutations in DLB was performed in 2013 (Nalls et al., 2013). The study included 721 DLB cases and 1962 controls. Overall, *GBA1* mutation frequency in DLB was 7.49% compared with less than 1% in controls (Nalls et al., 2013). When stratified by samples which had the entire gene sequence, *GBA1* mutation frequency in DLB was 7.57% compared with 1.48% in controls (Nalls et al., 2013). This robust finding supports independent studies reporting *GBA1* mutation frequency in DLB at approximately 8% (Tsuang et al., 2012; Gamez-Valero et al., 2016). The presence of any *GBA1* mutation was associated with an odds ratio of 8.28 across all centres: DLB subjects are 8.28 times more likely to harbour a *GBA1* mutation than controls (Nalls et al., 2013). A genetic study including relative risk reported than *GBA1* heterozygotes have a 20-fold increased risk of developing DLB in their lifetime (Asselta et al., 2014). Interestingly, while *GBA1* was not a hit in a large scale GWAS, *SCARB2* was identified as the 3rd strongest risk factor for DLB (Bras et al., 2014). Since *SCARB2* encodes LIMP 2, the specific GCase receptor necessary for lysosomal trafficking, accumulated evidence suggests that GCase is strongly implicated in DLB. Furthermore, heterozygous *GBA1* mutations

appear to strongly associate with sex; 90% of *GBA1* mutation carriers in a DLB cohort being male (Gamez-Valero et al., 2016).

1.4.2.3. PDD

Very few studies have investigated the genetic association between *GBA1* mutations and PDD specifically. As with DLB, this is because of the difficulties in accurate diagnosis, coupled with the consideration of PDD as a continuum of PD. Despite these problems, a significant study involving 151 PDD cases and 1962 controls found *GBA1* mutation frequency overall to be 5.96% compared with less than 1% in controls (Nalls et al., 2013). When stratified by samples which underwent whole gene sequencing, mutation frequency in PDD was 8% and 1.48% in controls, almost identical to DLB (Nalls et al., 2013). The presence of any *GBA1* mutation was associated with an odds ratio of 6.48 across all centres: PDD subjects are 6.48 times more likely to harbour a *GBA1* mutation compared to controls (Nalls et al., 2013).

Table 4 - *GBA1* mutation frequency in PD

Reference	PD Cases	Control Cases	Method	Ethnicity	Mutation frequency PD	Mutation frequency control	Significant	Odds Ratio
(Torok et al., 2016)	124	122	N370S,L444P,R120W	Hungarian	2.40%	0%	yes	
(Asselta et al., 2014)	2350	1111	Exons 8 and 9	Italian	4.50%	0.63%	yes	
(Wang et al., 2012)	208	298	N370S,L444P,R120W	Chinese	3.40%	0%	yes	10.2
(Moraitou et al., 2011)	205	206	8 mutations	Greek	10.24%	3.40%	yes	3.24
(Dos Santos et al., 2010)	110	155	5 mutations	Brazilian	5.40%	0%	yes	
(Hu et al., 2010)	328	300	N370S	Han Chinese	1.80%	0.29%	no	
(Sun et al., 2010)	402	413	4 mutations	Chinese	2.74%	0%	yes	
(Mao et al., 2010)	616	411	L444P	Chinese	3.20%	0.20%	yes	13.76
(Mata et al., 2008)	721	554	N370S and L444P	USA	2.90%	0.40%	yes	
(De Marco et al., 2008)	395	483	N370S and L444P	Italian	2.80%	0.20%	yes	13.8
(Spitz et al., 2008)	65	267	N370S, L444P, G377S	Brazilian	3.00%	0%	yes	21.06
(Wu et al., 2007)	518	339	L444P, RecNcil, R120W	Taiwanese	2.10%	1.20%	no	
(Toft et al., 2006)	331	472	N370S and L444P	Norwegian	2.30%	1.70%	no	
(Han et al., 2016)	225	110	All exons	Canadian	4.40%	0.90%	yes	
(Pulkes et al., 2014; Yu et al., 2015)	184	130	All exons	Chinese	8.70%	1.54%	yes	6.09
(Pulkes et al., 2014)	480	395	All exons	Thai	4.98%	0.50%	yes	
(Choi et al., 2012)	227	291	All exons	Korean	3.20%	0%	yes	20.6
(Bras et al., 2009)	230	430	All exons	Portuguese	6.10%	0.70%	yes	9.2
(Neumann et al., 2009)	790	257	All exons	British	4.18%	1.17%	yes	3.7
(Clark et al., 2007)	278	179	All exons	Mixed	13.70%	4.50%	yes	3.4
(Ziegler et al., 2007)	92	92	All exons	Taiwanese	4.30%	1.10%	yes	
(Lwin et al., 2004)	57	44	All exons	Unknown	21%	0%	yes	
(Sidransky et al., 2009b)	1682	1674	All exons	Mixed	6.90%	<1%	yes	5.43

Table 5 - *GBA1* mutation frequency in DLB

Reference	DLB Cases	Control Cases	Method	Ethnicity	Mutation frequency DLB	Mutation frequency control	Significant	Odds Ratio
(Asselta et al., 2014)	29	1111	Exons 8 and 9	Italian	13.80%	0.63%	yes	
(Mata et al., 2008)	57	554	N370S and L444P	USA	3.50%	0.40%	yes	
(Tsuang et al., 2012)	80	391	All exons	Caucasian	8.80%	1%	yes	7.6
(Geiger et al., 2016)	111	222	All exons	Caucasian USA	12.61%	Not reported	Not reported	
(Gamez-Valero et al., 2016)	47	131	All exons	Spanish	8.50%	0%	no	
(Nalls et al., 2013)	721	1962	All exons	Mixed	7.49%	0.97%	yes	8.28

1.5. *GBA1* associated synucleinopathy

Owing to the strong association between *GBA1* mutations and both PD and DLB, it may be expected that the presence of a mutant *GBA1* allele may impact the clinical presentation and pathology of both conditions when compared with sporadic forms. The impact of *GBA1* mutation on PD and DLB is summarised below.

1.5.1.GBA-PD

1.5.1.1. Clinical presentation

Clinically, GBA-PD is indistinguishable from sporadic PD (sPD). Both forms of PD exhibit the classical triad of symptoms: bradykinesia, rigidity and tremor with asymmetric onset (Clark et al., 2007; Goker-Alpan et al., 2008; Seto-Salvia et al., 2012). However, *GBA1* variants affect the age of onset, disease progression and presentation of non-motor symptoms.

1.5.1.2. Age of onset

GBA-PD frequently presents at a significantly earlier age of onset compared with sPD (Goker-Alpan et al., 2004; Clark et al., 2007; Tan et al., 2007; Gan-Or et al., 2008; Neumann et al., 2009; Nichols et al., 2009; Sidransky et al., 2009a; Brockmann et al., 2011; Chahine et al., 2013; Davis et al., 2016a; Jesus et al., 2016). Variation in the age of onset reported can be attributed to the different clinical tests used to diagnose PD, but on average the age of onset in GBA-PD is between 49 and 59 years old compared with between 56 and 64 years old in sPD (Neumann et al., 2009; Jesus et al., 2016). The proportion of patients presenting with symptoms before the age of 50 is significantly higher in GBA-PD (Neumann et al., 2009; Nichols et al., 2009). Linear regression models predict the age of onset in the presence of *GBA1* variants is 6.04 years earlier than sPD (Nichols et al., 2009).

1.5.1.3. Progression of motor symptoms

Progression of parkinsonism motor symptoms is significantly greater in GBA-PD as measured by progression to Hoehn & Yahr scale (H&Y) level 3 and UPDRS III scoring (Winder-Rhodes et al., 2013; Beavan et al., 2015; Davis et al., 2016b). While there is no difference in response to L-DOPA (Neumann et al., 2009), dyskinesia is more common in GBA-PD which could be related to higher doses and longer duration of L-DOPA therapy in GBA-PD patients as a consequence of

progression to more severe PD (Clark et al., 2007; Davis et al., 2016b; Jesus et al., 2016). Motor fluctuations have also been reported in 80% of GBA-PD patients compared with 52% in sPD (Jesus et al., 2016). Although there is no difference in combined motor symptoms, one study indicates that GBA-PD patients are more likely to present with tremor as the first symptom (Clark et al., 2007) although Davis et al did not find any difference in the progression of tremor scores (Davis et al., 2016b).

1.5.1.4. Cognitive impairment

GBA-PD patients have repeatedly been reported to be significantly more likely to develop cognitive impairment and dementia compared with sPD (Goker-Alpan et al., 2008; Neumann et al., 2009; Sidransky et al., 2009a; Brockmann et al., 2011; McNeill et al., 2012; Seto-Salvia et al., 2012; Chahine et al., 2013; Beavan et al., 2015; Jesus et al., 2016). On average, the proportion of GBA-PD patients who develop cognitive impairment is approximately 50% compared with 20-30% of sPD. Cognitive impairment is also seen at an earlier age of onset in GBA-PD, with one study reporting 40% of GBA-PD patients under the age of 50 showing signs of cognitive impairment (Neumann et al., 2009). Unsurprisingly therefore, *GBA1* mutation is also a significant predictor of progression of dementia (Neumann et al., 2009; Winder-Rhodes et al., 2013; Jesus et al., 2016). The risk of progression to dementia is increased five-fold when comparing GBA-PD to non-mutant PD patients (Winder-Rhodes et al., 2013). Combined, the clinical findings strongly implicate *GBA1* mutations in the development and severity of PDD.

1.5.1.5. Non-motor symptoms

GBA-PD appears to be associated with a stronger non-motor phenotype of PD compared with sPD. Visual hallucinations occur more frequently in GBA-PD (Neumann et al., 2009; Jesus et al., 2016) in addition to symptoms of depression including anxiety and apathy (Brockmann et al., 2011; McNeill et al., 2012; Beavan et al., 2015). Other non-motor symptoms such as fatigue, unexplained pain and constipation also occur more frequently in GBA-PD (McNeill et al., 2012; Jesus et al., 2016). Furthermore, the severity of autonomic disturbances such as orthostatic symptoms, urinary function, sexual function and bowel function also appear to be more prominent in GBA-PD (Brockmann et al., 2011). Additionally, REM sleep disorders are reported in greater frequency in GBA-PD patients (McNeill et al., 2012; Jesus et al., 2016) with greater deterioration in scores over 2 years (Beavan et al., 2015). Olfactory dysfunction, an early symptom considered

a biomarker for PD, is also implicated in GBA-PD, being present in carriers of *GBA1* mutation without PD symptoms and also deteriorating significantly over 2 years (McNeill et al., 2012; Beavan et al., 2015). GBA-PD patients also exhibit increased incidence of retinal thinning as determined by optical coherence tomography (McNeill et al., 2013).

1.5.1.6. Imaging

Transcranial sonography (TCS) shows a comparable degree of substantia nigra hyperechogenicity and similar size of the basal ganglia and ventricular system between GBA-PD and sPD (Brockmann et al., 2012; Barrett et al., 2013). However, almost 70% of GBA-PD patients demonstrate interrupted brainstem raphe nuclei compared with 21% of sPD patients demonstrated by reduced echogenicity as assessed by TCS (Brockmann et al., 2011). Disruption to the raphe nuclei may potentially explain the increased incidence of depression due to disruption of serotonergic transmission (Brockmann et al., 2011). Nigrostriatal imaging with fluorodopa positron emission spectroscopy or single photon emission spectroscopy with dopamine sensitive ligands demonstrates an asymmetric pattern of abnormality indistinguishable from sPD (Goker-Alpan et al., 2012; Barrett et al., 2013). Fludeoxyglucose-PET imaging comparing GBA-PD patients with asymptomatic *GBA1* mutation carriers shows comparable hypometabolism in the supplementary motor area (Kono et al., 2010). However, only GBA-PD patients show parietal-occipital hypometabolism, consistent with greater incidence of cognitive impairment (Kono et al., 2010; Barrett et al., 2013). Age adjusted analysis of perfusion SPECT shows a significant reduction in activity of the posterior parietal and occipital regions in GBA-PD patients compared with sPD which was more pronounced in association with the presence of severe mutations such as L444P (Cilia et al., 2016). White matter changes are also implicated in GBA-PD (Agosta et al., 2013). As illustrated by MRI, sPD is not associated with any white matter changes whereas GBA-PD shows a distributed pattern of white matter abnormalities involving the interhemispheric, frontal corticocortical and parahippocampal tracts (Agosta et al., 2013). These abnormalities may impact clinical changes, most notable cognitive impairment (Agosta et al., 2013).

1.5.1.7. Neuropathology

Neuropathologically examined cases of GBA-PD can be considered within the spectrum of classical sPD with characteristic nigral dopamine neuronal loss and the deposition of brain stem LBs and LNs (Westbroek et al., 2011). In addition to subcortical α-synuclein inclusions, cortical

areas corresponding to Braak stages 5 and 6 are routinely present in GBA-PD cases, consistent with increased incidence of cognitive impairment (Goker-Alpan et al., 2010). GCase is present in α-synuclein containing LB inclusions (Goker-Alpan et al., 2010). While there may not be a statistical difference in Braak staging between GBA-PD and sPD, approximately 75% of cases fulfil McKeith criteria for diffuse neocortical Lewy body pathology compared with 38% of sPD (Neumann et al., 2009). However, when compared by McKeith protocol to give an indication of cortical LB burden, there is no statistical difference (Neumann et al., 2009). Increased incidence of cortical LBs in GBA-PD has been reported by Clark et al: 82% in GBA-PD compared with 43% sPD (Clark et al., 2009). Application of logistic models to adjust for age, sex, *APOE4* and clinical diagnosis of dementia does not affect the significant association between *GBA1* mutation status and cortical LB burden (Neumann et al., 2009). However, a more recent study using the outcome measure of cortical density of LBs (count/mm^2) did not find a statistical association between *GBA1* mutation status and total cortical LB load nor LB load in specific cortical areas (Parkkinen et al., 2011).

GBA-PD cases are statistically less likely to meet the NIA-RI pathological criteria for AD compared with sPD (38% v 63%) (Clark et al., 2009). When assessing cortical density of amyloid plaques as an outcome measure, there is no significant difference in total Aβ nor Aβ in any specific brain region (Parkkinen et al., 2011).

Astrogliosis and neuronal cell loss specifically targeted to the hippocampal pyramidal cell layers of sub regions CA2-CA4 are seen in GD at post mortem (Wong et al., 2004). LBs are found in these same specific sub regions of the hippocampus in GD-PD (Tayebi, 2003). This is particularly interesting since these regions have especially high constitutive levels of *GBA1* expression (Dopeso-Reyes et al., 2017). Furthermore, one of the few disorders that selectively targets the neuronal population of CA2-CA4 is DLB, suggesting the association between LBs in these regions and GD-PD more than a statistical coincidence (Tayebi, 2003; Wong et al., 2004). Investigation of CSF has found that levels of total tau, phosphorylated tau and amyloid beta 1-42 are similar between GBA-PD and healthy controls (Lerche et al., 2017). In contrast, lower levels of Aβ 1-42 and higher levels of total tau and phosphorylated tau are associated with worse cognitive impairment in sPD patients when compared with healthy controls (Lerche et al., 2017).

1.5.1.8. Gene dosage effect

A gene dosage effect in PD and DLB depending upon the severity of *GBA1* mutation (chapter 1.3.4) has been demonstrated. GBA-PD patients carrying the null mutation 84GG have an odds ratio of 14 whilst carriers of the null mutation IVS2+1 have an odds ratio of 42 (Gan-Or et al., 2008). This compares to an odds ratio of 2.2 associated with the mild mutation N370S implying carriers of more severe *GBA1* mutations are at increased risk of developing synucleinopathies when compared to mild mutation carriers (Gan-Or et al., 2008). Furthermore, severe *GBA1* mutation carriers have a significantly earlier age of motor symptom onset in PD compared to mild mutation carriers (Gan-Or et al., 2008; Bultron et al., 2010). Individuals carrying a severe mutation in *GBA1* are at significantly greater risk for developing dementia (Cilia et al., 2016). Multivariate analysis describes a 3-fold increased risk of developing dementia in severe mutation carriers (L444P) compared with mild mutation carriers (N370S) (Cilia et al., 2016). Whilst the difference in various non-motor and motor symptoms is not significantly different when comparing L444P and N370S GBA-PD patients, comparison with sPD patients reveals L444P *GBA1* mutation results in significantly more severe motor symptoms off medication, more frequent psychotic symptoms, apathy and orthostatic hypotension (Cilia et al., 2016). There is no significant difference in mortality rate between L444P GBA-PD and N370S GBA-PD patients although severe mutation carriers do show a significantly increased mortality risk compared with sPD (Cilia et al., 2016).

1.5.2.GBA-DLB

1.5.2.1. Clinical presentation

There are very few studies evaluating the effect of *GBA1* mutation on the clinical presentation of DLB. As with GBA-PD, gross presentation of GBA-DLB and non-mutant DLB is indistinguishable with the classical hallmarks of DLB also defining GBA-DLB. However, there are some features which indicate a more aggressive disease course reflected by an earlier age of onset, more frequent hallucinations and poorer performance in cognitive and motor tests, discussed below.

1.5.2.2. Age of onset

A significantly reduced age of onset associated with heterozygous *GBA1* mutation in DLB has been reported by three independent studies involving both clinically diagnosed DLB patients and neuropathologically confirmed cases (Nalls et al., 2013; Gamez-Valero et al., 2016; Shiner et al., 2016). Age of onset is consistent between studies, ranging from 63.5 years to 65.7 years in *GBA1* heterozygotes and 68.9 years to 72.1 years in non-mutant DLB controls. This approximate 6-year earlier onset of symptoms is consistent with findings in GBA-PD (Nalls et al., 2013; Gamez-Valero et al., 2016; Shiner et al., 2016). Interestingly, the non-GD causing E326K polymorphism has the opposite effect in PDD, increasing the age of onset to 69 years compared with 55 years in sPDD (Gamez-Valero et al., 2016). Heterozygous *GBA1* mutations are also associated with an earlier age of death, although the age from diagnosis to death is similar (Nalls et al., 2013).

1.5.2.3. Cognitive impairment, hallucinations and REM sleep behaviour disorder

GBA-DLB is associated with a worsening of global cognitive function as assessed by MoCA (Shiner et al., 2016). Specifically, GBA-DLB patients perform worse than non-mutant DLB controls in phonemic verbal fluency tests and Hooper visual organisation tests (Shiner et al., 2016). This suggests poorer executive and visuospatial function implicating the dorsolateral prefrontal cortex and visual association areas respectively, both known areas implicated in the pathology of DLB (Shiner et al., 2016). Hallucinations are reported with increased frequency in GBA-DLB: 82% compared to 55% in non-mutant DLB (Nalls et al., 2013; Shiner et al., 2016). This finding is supported by the increased prescribing of antipsychotics in this cohort (Nalls et al., 2013). Additionally, REM sleep behaviour disorder has been reported with increased frequency in GBA-

DLB cohorts (Shiner et al., 2016). Furthermore, REM sleep disorder symptoms are more severe as assessed by standard questionnaire-based tools (Shiner et al., 2016).

1.5.2.4. Motor impairment

GBA-DLB patients have significantly higher motor scores than non-mutant DLB patients assessed by both Hoehn and Yahr staging and UPDR stage III scoring, with marked extrapyramidal signs more prevalent (Nalls et al., 2013; Shiner et al., 2016).

Across the synucleinopathy spectrum, heterozygous *GBA1* mutations confer an earlier age of onset of symptoms with a more progressive and severe disease course. Most notably, there is a strong evidence base emerging for *GBA1* mutations particularly being associated with the development of earlier and more severe cognitive impairment (Malec-Litwinowicz et al., 2014; Mata et al., 2016; Mata et al., 2017).While there is no overt difference in the neuropathology between *GBA1* mutation carriers and non-carries, the differences in clinical presentation may be accounted for by alterations in and effected by mutant GCase biochemistry.

1.6. Mutant GCase biochemistry

The biochemistry associated with GCase enzyme and mutations in *GBA1* has been investigated since the role of the enzyme in GluCer metabolism and the subsequent consequences for Gaucher's disease were first described by Dr Roscoe Brady in 1965 (Futerman and Platt, 2017). Accordingly, most studies have investigated biochemistry associated with homozygous mutations in *GBA1* and Gaucher's disease. Since the link between GD and PD was first described in 1996, the consequence of heterozygous *GBA1* mutations have become increasingly relevant since explorations of mutant GCase biochemistry may hold some clues to common pathogenic mechanisms.

1.6.1. GCase enzyme activity

1.6.1.1. Human samples

GCase enzyme activity is significantly reduced in GBA-PD human post mortem brain tissue compared with controls; the largest reductions are observed in the substantia nigra (58%) but significant reductions are also seen in the cerebellum (47%), amygdala (40%) and putamen (48%) (Gegg et al., 2012). GCase enzyme activity is also significantly reduced in the prefrontal cortex, primary motor cortex and cerebellum of human post mortem Lewy body disease tissue when comparing *GBA1* mutant heterozygotes with non-carriers (Clark et al., 2015). The reduction in GCase enzyme activity is mutation dependent following the gene-dosage effect (described in section 1.5.1.8.) with a significant difference in the reduction of GCase enzyme activity between severe and mild mutation carriers when compared with non-demented controls (Clark et al., 2015). Furthermore, GCase enzyme activity is significantly reduced in Lewy body disease cases with the diagnosis of dementia (Clark et al., 2015). The pattern of association between *GBA1* mutation status and GCase enzyme activity is comparable between cases indicating that the presence of dementia and diagnosis of Lewy body disease drive the association (Clark et al., 2015). *GBA1* heterozygote individuals have also shown significantly reduced GCase enzyme activity in the frontal cortex irrespective of disease state (Kurzawa-Akanbi et al., 2012). This reduction in GCase activity is modest, approximately 25% for both cases of PD and DLB compared with age-matched controls, suggesting a small decrease in GCase enzyme could impart a substantial effect (Kurzawa-Akanbi et al., 2012). The presence of reduced GCase enzyme activity in the frontal cortex of healthy controls is an unexpected and interesting finding

which requires further investigation (Kurzawa-Akanbi et al., 2012). It may be that this finding represents the gradual age-related decrease in GCase enzymatic activity (Rocha et al., 2015a), which in turn may underpin parkinsonian neurodegenerative diseases. This intriguing possibility is further discussed below.

A key finding has been the significant reduction of GCase enzyme activity in sPD brain (Gegg et al., 2012; Murphy and Halliday, 2014; Rocha et al., 2015a). GCase activity is significantly reduced by 24% reduction in the cerebellum and 33% in the substantia nigra (Gegg et al., 2012). GCase activity is also significantly decreased in the hippocampus of sPD patients between the age of 70 and 80 (Rocha et al., 2015a). Reduced GCase enzyme activity in the cerebellum indicates reduced GCase enzyme activity is not a direct consequence of neurodegeneration since this brain area is not affected in PD. This is further supported by the absence of any reduction in GCase enzyme activity in the amygdala of AD patients, an area associated with marked neuronal loss (Gegg et al., 2012; Rocha et al., 2015a). Furthermore, significant reduction in GCase enzyme activity is seen also seen in the anterior cingulate cortex in early stage sPD, but not in the occipital cortex, an area not usually associated with α-synuclein accumulation in sPD (Murphy et al., 2014). Correlation analysis indicates that increased α-synuclein deposition observed in early stage sPD corresponds to reduced GCase enzyme activity (Murphy et al., 2014). Taking into account neuronal death indirectly through measurement of NeuN levels, GCase enzyme activity continues to decrease in the anterior cingulate cortex of late stage sPD brain in the absence of further GCase protein decline (Murphy et al., 2014). Intriguingly, GCase enzyme activity has become implicated in normal aging, the biggest risk factor for dementia and all neurodegenerative diseases (Rocha et al., 2015a). GCase activity progressively declines in the substantia nigra of healthy control subjects, eventually becoming comparable to sPD patients by the seventh decade of life; when most individuals with sPD are diagnosed (Rocha et al., 2015a). Similarly, GCase activity also progressively declines in the putamen (Rocha et al., 2015a), an area of the brain inextricably linked with sPD.

GCase enzyme activity measured from dried blood spots is also significantly reduced in heterozygous *GBA1* mutation carriers compared with sPD and age-matched controls, although the ranges of activity do overlap (Alcalay et al., 2015). Interestingly, mutations considered as

'mild' had similar if not lower GCase activity than 'severe' mutations, opposed to the gene dosage effect described in GD. The *GBA1* polymorphic variants E326K and T369M had the lowest GCase enzyme activity (Alcalay et al., 2015). Furthermore, sPD with higher GCase activity were associated with longer disease duration and worse performance on MoCA, suggestive of more advanced PD (Alcalay et al., 2015). This finding in dried blood is unexpected and opposes findings from post mortem tissue. It may be that longer disease duration in association with *GBA1* mutation enhanced GCase activity compared with controls is an indicator of a more benign form of PD, where those with the potentially protective effect of high GCase enzyme activity are more likely to survive and progress to dementia. Overall, lower enzyme activity was observed in samples from PD patients, even after adjustment for age, gender and *GBA1* mutation status, indicating that reduced GCase enzyme activity is independently associated with PD corroborating observations from post-mortem human studies (Alcalay et al., 2015). Interestingly sPD G2019S mutation carriers on the PD related gene *LRRK2* have higher levels of GCase enzyme activity as tested from dried blood spots when compared to non-carriers and controls without PD (Alcalay et al., 2015). This finding further implicates *GBA1* and GCase enzyme activity in the pathogenesis of PD and other synucleinopathies.

CSF from GBA-PD patients exhibit significantly reduced GCase enzyme activity in addition to reduced activity of *GBA2* GCase enzyme activity and β-galactosidase (Schondorf et al., 2014). However, CSF from sPD patients in the same study did not exhibit any alterations in GCase enzyme activity (Schondorf et al., 2014). The study by Schondorf et al contradicts the earlier findings of 35% and 59% reduced GCase enzyme activity in the CSF of sPD patients and sDLB patients respectively when compared with healthy controls (Parnetti et al., 2009; Parnetti et al., 2014). GCase enzyme activity is also significantly reduced in sPD compared with CSF from AD patients (Parnetti et al., 2009; Schondorf et al., 2014). A more recent and conclusive study has established a significant 25% decrease in GCase enzyme activity in CSF of a sporadic PD cohort, complementing earlier findings (Parnetti et al., 2017). Interestingly, reduced GCase activity in the CSF of these patients correlates with worse cognitive impairment as measured by MoCA and more advanced motor symptoms (Parnetti et al., 2017). GCase enzyme activity was found to be significantly lower in GBA-PD compared to sPD but the reduction in CSF GCase enzyme activity regardless of *GBA1* mutation status suggests the reduction in enzyme activity is independent of *GBA1* mutation and implicates other mechanisms (Parnetti et al., 2017). Taken together, these

studies strongly implicate a reduction in CSF GCase activity is specifically linked to synucleinopathies, rather than a marker of overt neurodegenerative diseases.

1.6.1.2. In vitro

Early *in vitro* experiments investigating the impact of *GBA1* mutations used overexpression cell models (Cullen et al., 2011). Reduced GCase enzyme activity is not universally reported in association with *GBA1* mutation in these models (Cullen et al., 2011). Transient expression of various *GBA1* mutant plasmids in both MES23.6 and PC12 cells expressing human WT α-synuclein did not change GCase enzyme activity despite accumulation of α-synuclein (Cullen et al., 2011). These data provide evidence to support a 'gain of function' hypothesis rather than loss of enzyme activity underlining pathogenic mechanisms relating the *GBA1* mutation, although the impact of endogenous wild type GCase protein does need to be taken into consideration.

More elegant cellular models do provide evidence for alterations in GCase enzyme activity (McNeill et al., 2014). Cultured fibroblasts from *GBA1* heterozygote carriers demonstrate significantly reduced GCase enzyme activity both in those with and without PD (McNeill et al., 2014). However, GCase enzyme activity is unaffected in fibroblasts generated from sPD patients (McNeill et al., 2014). Once again, these findings need to be considered in the context of the cell type tested. Fibroblasts only express *SNCA* at very low levels (Auburger et al., 2012) and so α-synuclein, the key pathological protein of PD and DLB is not accurately represented and the likely impact of α-synuclein in conjunction with heterozygous *GBA1* mutation can therefore not be represented accurately.

A significant reduction in GCase enzyme activity in the presence of heterozygous *GBA1* mutations is further evidenced by studies using iPSC derived dopaminergic neurons (Schondorf et al., 2014; Fernandes et al., 2016). GCase enzyme activity is reduced by approximately 50% in cells generated from *GBA1* heterozygous PD patients; activity of GCase generated from *GBA2* is also reduced (Schondorf et al., 2014; Fernandes et al., 2016). A similar degree of reduction in GCase activity has also been reported in cells generated from *GBA1* heterozygous monozygotic twins discordant for PD (Woodard et al., 2014).

Looking at GCase enzyme activity using a cellular model of PD involving α-synuclein overexpression, a novel experimental set up involving transfection of rat primary cortical neurons with human α-synuclein demonstrated reduced GCase enzyme activity levels (Wang et al., 2016). The complex interplay between α-synuclein and GCase activity is described more fully in section 1.6.6. Upon addition of plasma from sPD patients to these cultures, GCase enzyme activity is further reduced, and is significantly lower than GCase activity in cells treated with plasma from healthy controls (Wang et al., 2016).

1.6.1.3. In vivo

Heterozygous D409V *GBA1* (D409V/WT) mice show an approximate 40% reduction in GCase enzyme activity compared with wild type mice (Sardi et al., 2011). This degree of enzyme activity loss is comparable to a heterozygous *GBA1* knockout mouse (GBA1 +/-) (Sardi et al., 2011). L444P/WT mice also show a significant reduction in GCase enzyme activity corresponding to a 32% reduction compared with age-matched wild type controls (Fishbein et al., 2014).

Looking at GCase enzyme activity in models of PD, transgenic human A53T α-synuclein mice exhibit significantly lower lysosomal GCase enzyme activity compared to WT animals (Sardi et al., 2013). This effect was dependent upon the levels of α-synuclein since homozygous A53T α-synuclein mice show greater reduction in GCase enzymatic activity compared to heterozygote mice (Sardi et al., 2013). Furthermore, the reduction in enzyme activity is GCase specific since the activities of hexosaminidase and β-galactosidase remain unaffected (Sardi et al., 2013). However, the same result was not observed in mice expressing human A53T α-synuclein or human wild type α-synuclein in a *SNCA* null background; GCase enzyme activity was similar to wild type animals (Fishbein et al., 2014). Interestingly, knock out of murine *SNCA* alone causes a significant 35% increase in GCase enzyme activity (Fishbein et al., 2014), implicating α-synuclein as a repressor of endogenous GCase enzymatic activity.

1.6.2. GCase protein levels

An important factor when considering the impact of heterozygous mutations in *GBA1* is the protein expression level of GCase enzyme since protein levels may indicate whether reduced GCase enzyme activity is solely due to a global reduction in the amount of GCase enzyme. Altered levels

of GCase protein expression may also implicate changes to degradation or transcription/translation of the enzyme which may in turn impede function.

GCase protein levels were significantly reduced in the substantia nigra, putamen and cerebellum of *GBA1* heterozygous PD brain (Gegg et al., 2012). Furthermore, GCase protein levels were significantly reduced in the cerebellum and substantia nigra of sporadic PD brain, following the same pattern as GCase enzyme activity (Gegg et al., 2012). SDS-soluble GCase was also selectively significantly reduced in the anterior cingulate cortex from subjects with early stage sPD (Murphy and Halliday, 2014). GCase protein levels were not reduced in the occipital cortex in early stage sPD, a brain region not associated with α-synuclein accumulation in PD (Murphy et al., 2014). GCase protein levels were also significantly reduced by approximately 20% in the frontal cortex of a combined cohort of *GBA1* heterozygous PD and DLB cases as well as *GBA1* mutation carrier 'healthy' controls, irrespective of disease state (Kurzawa-Akanbi et al., 2012). This reduction was confirmed as not being a consequence of cell loss or gliosis by assessment of NeuN and GFAP levels (Kurzawa-Akanbi et al., 2012). Reduction of GCase protein in *GBA1* carrier 'healthy' controls suggests that reduction in GCase protein may need to reach a critical point before related pathogenic changes occur to cause symptoms to be detectable (Kurzawa-Akanbi et al., 2012). Post-mortem studies therefore appear to suggest that the overall levels of GCase protein mirror the decline in GCase enzymatic activity, implicating the loss of GCase protein as the cause of deficient GCase enzyme activity.

At the cellular level, GCase protein was also significantly reduced in cultured fibroblasts from heterozygous mutation carriers with and without PD (McNeill et al., 2014). iPSC derived midbrain dopaminergic neurons from *GBA1* heterozygous PD patients also display a significant reduction in GCase protein, including cells derived from a set of monozygotic twins discordant for PD (Schondorf et al., 2014; Woodard et al., 2014).

An interesting finding from GBA-PD iPSC derived dopaminergic neurons was the presence of an extra isoform of GCase at a higher molecular weight which is sensitive to the recombinant glycosidase enzyme, Endoglycosidase H (Endo H) (Fernandes et al., 2016). This Endo H sensitive isoform of GCase is significantly increased in GBA-PD dopaminergic neurons and represents 20% of the total GCase suggesting a significant proportion of ER retained GCase in

this population of susceptible cells (Fernandes et al., 2016). Retention of mutant GCase protein in the ER could therefore account for reduced enzymatic activity of GCase since it requires the acidic environment of the lysosome to function.

1.6.2.1. *GBA1* mRNA

GBA1 mRNA was not altered in human brain regions showing reduced GCase enzyme activity and GCase protein levels in both GBA-PD and sPD at either at early or late stages of the disease (Gegg et al., 2012; Murphy et al., 2014). Consistent *GBA1* mRNA levels imply the reduction and redistribution of GCase is not due to altered transcription and is therefore more likely associated with mechanisms relating to trafficking, degradation and possible interactions with α-synuclein.

At the cellular level and *in vivo*, generally *GBA1* mRNA levels also do not alter in association with *GBA1* mutations (Xu et al., 2003; Garcia-Sanz et al., 2017). However, cultured fibroblasts from patients with GD or GBA-PD show a mixed picture of *GBA1* transcript changes. Fibroblasts from GD patients show a significant reduction in *GBA1* mRNA except in the case of N370S homozygosity (McNeill et al., 2014). Furthermore, PD patients with the severe mutations L444P or RecNcil also demonstrate an approximate 50% reduction in *GBA1* mRNA (McNeill et al., 2014).These findings suggest that a reduction in transcription underlies GCase deficiency in cases with severe mutations but not those with milder mutations.

1.6.3.Lipid accumulation

Lipid accumulation, specifically the GCase substrate GluCer is characteristic of cells associated with the symptoms of GD (Brady et al., 1965). Investigation of GluCer and other components of the glycosphingolipid pathway is important in the context of *GBA1* heterozygosity as well as PD and DLB, since alterations in this critical pathway may provide some clues to potential pathological mechanisms underpinning these diseases.

1.6.3.1. Human Tissue

Lysates from human post mortem GBA-PD and sPD brain tissue do not appear to show GluCer accumulation as perhaps would be expected in association with GCase deficiency (Gegg et al., 2015). When tested, neither the putamen or cerebellum, regions previously identified as having significant reductions in GCase enzyme activity show any GCase substrate accumulation, GluCer

or GluSph, compared with age-matched controls (Gegg et al., 2015). However, the ganglioside GM3 does show a strong increasing trend (Gegg et al., 2015). Lipidomic analysis from the primary motor cortex of post mortem sDLB cases follows the same trend: non-significant accumulation of GluCer and enrichment of GM3 (Clark et al., 2015).Lipidomic analyses of plasma derived from sPD patients has also identified a significant increase in the ganglioside GM3, supporting the function of altered glycosphingolipid metabolism in PD which is not necessarily identified by alterations in GluCer (Chan et al., 2017; Zhang et al., 2017). Increased levels of GM3 gangliosides may have direct pathogenic consequences. Vesicles composed from lipids characterised by relatively high solubility in water, such as GM3 gangliosides, are able to initiate amyloid formation (Galvagnion, 2017). Therefore, enhanced GM3 gangliosides may be able to initiate the aggregation of α-synuclein (Galvagnion, 2017).

A significant increase of GluSph in the hippocampus of sPD patients between the age of 70 and 80 years has been reported (Rocha et al., 2015a). Interestingly, brain samples from GD-PD patients do not show accumulation of GluSph compared with controls (Tayebi, 2003; Gegg et al., 2015) contradicting the finding of increased GluSph in the brains of neuronopathic GD patients (Orvisky et al., 2002). Significantly enhanced glysphingosine (GalSph + GluSph) has also been demonstrated in plasma from GBA-PD patients when compared with sPD (Guedes et al., 2017). These findings imply that GluSph may prove useful as a biomarker for *GBA1* mutations and reflects disrupted glycosphingolipid metabolism. Indeed, emerging evidence suggests that GluSph accumulates in the brain of GCase deficient mice at an earlier age, with the accumulation of GluCer occurring at a later stage (Dai et al., 2016; Taguchi et al., 2017).

The anterior cingulate cortex, an area significantly affected by Lewy body pathology in PD and DLB, shows a significant 53% reduction in total ceramide and 42% reduction in sphingomyelin in sPD human brain compared with age-matched controls (Abbott et al., 2014). Ceramide levels do not appear to change in the occipital cortex, an area normally spared in PD (Abbott et al., 2014). The ceramide species in the anterior cingulate cortex of PD patients shifts towards shorter acyl chain compositions and ceramide synthase I mRNA increases (Abbott et al., 2014). A selective reduction in ceramide is also reported in the anterior cingulate cortex of sPD brain by Murphy et al, specifically in early PD (Murphy et al., 2014). There is no overall difference in ceramide levels between early and later stage sPD (Murphy et al., 2014). Reduction in several ceramide species

(d18:0/22:0, d18:0/26:0, d18:1/20:1, d18:1/22:1) are also demonstrated in lipidomic analysis of plasma from sPD patients (Zhang et al., 2017). It should be highlighted that reductions in total ceramide levels are not reported in GD which predominantly involves GluCer accumulation in tissue macrophages (Murphy et al., 2014). This suggests that neurons selectively rely on the salvage pathway of ceramide synthesis, rendering neurons exquisitely vulnerable to lysosomal perturbations (Murphy et al., 2014). However, alternative lipidomic analyses report increased ceramide species measured in peripheral blood plasma when comparing sPD with healthy controls and sPD with GBA-PD respectively (Mielke et al., 2013; Guedes et al., 2017). Additionally, higher ceramide plasma levels are associated with worse cognition (Mielke et al., 2013).

1.6.3.2. In Vitro

A significant 4-fold accumulation of GluCer is seen in primary cortical neurons treated with siRNA against *GBA1* to reduce the enzyme activity to approximately 50% in order to mirror *GBA1* heterozygosity (Mazzulli et al., 2011). No changes in ceramide or other sphingolipids are observed (Mazzulli et al., 2011). Lentiviral sh-RNA mediated knockdown of *GBA1* to produce a 60% reduction in GCase protein level in differentiated SH-SY5Y cells also causes accumulation of GluCer (Kong et al., 2013).

Conversely, iPSC derived dopaminergic neurons from GBA-PD patients do not show GluCer accumulation (Fernandes et al., 2016). Nevertheless, a difference in the distribution of GluCer species is present. A 30% decrease in C20:0 and a 65% decrease in C16:0 and C24:0 is demonstrated (Fernandes et al., 2016). However, the converse is seen in iPSC derived dopaminergic neurons from GBA-PD patients by Schondorf et al who report a significant increase in GluCer in GBA-PD neurons (Schondorf et al., 2014). Fibroblasts and iPSCs from GBA-PD patients mainly contain GM3 gangliosides, with small amounts of other ganglioside types such as GM1, GM2 and GD3 (Schondorf et al., 2014). Differentiation into dopaminergic neurons and neuronal enrichment reduces the proportion of GM3 and GD3 in relation to total gangliosides (Schondorf et al., 2014). The ratios of GM1, GD1a, GD1b and GT1b in cultured neurons resemble normal human brain distribution (Schondorf et al., 2014). This apparent reduction in GM3 species opposes to what is seen in human post mortem brain tissue and patient plasma (Clark et al., 2015). It may be that post mortem tissue is capturing the lipid profile at an advanced stage of

disease which does not correlate to the lipid profile seen in relatively 'young' cultured dopaminergic neurons. Alternatively, the difference in GM3 species distribution may reflect an artefact of using iPSCs to derive dopaminergic neurons. Regardless, careful consideration needs to be given to the species of fibroblasts and iPSC derived cells when interpreting glycosphingolipid distribution since the relative distribution of species changes between cell type and maturation status (Schondorf et al., 2014).

Approaching glycosphingolipid metabolism from cellular models of PD and mirroring changes reported above in relation to GCase, ceramide levels are reduced in rat primary cortical cultures treated with extracellular α-synuclein (Wang et al., 2016). Upon addition of plasma from sPD patients to the culture, ceramide levels are further reduced, and are significantly lower than ceramide levels in cells treated with plasma from healthy controls (Wang et al., 2016). Furthermore, PP2A, the ceramide activated enzyme responsible for de-phosphorylation of the characteristic pathogenic ser129 phosphorylated species of α-synuclein is significantly reduced in primary cortical neurons treated with extracellular α-synuclein (Wang et al., 2016). PP2A enzyme is further reduced when plasma from PD patients is subsequently added to the culture media (Wang et al., 2016).

1.6.3.3. In Vivo

Interestingly, a homozygous D409V *GBA1* mouse model exhibiting 25% GCase enzyme activity compared to WT animals did not show GluCer accumulation in the hippocampus, cerebral cortex or cerebellum but a significant progressive accumulation of GluSph starting at 2 months of age (Sardi et al., 2011). Neither D409V/WT or *GBA1* +/- heterozygous mice exhibit GluSph accumulation suggesting one WT allele is sufficient to prevent build-up of toxic substrate (Sardi et al., 2011). Bilateral hippocampal administration of scAAV1-*GBA1* to D409V *GBA1* homozygous mice significantly reduces GluSph accumulation (Sardi et al., 2011).

	Result	Model	Reference
GluCer	No change n.s. increase Increase Increase Increase No change No change	Post-mortem: GBA-PD, sPD Post-mortem: primary motor cortex sDLB Primary cortical neurons 50% GCase activity SH-SY5Y 50% GCase activity iPSC derived dopaminergic neurons: GBA-PD iPSC derived dopaminergic neurons: GBA-PD D427V/D427V *GBA1* mouse	Gegg et al 2015 Clark et al 2015 Mazzuli et al 2011 Kong et al 2013 Schondorf et al 2014 Fernandes et al 2106 Sardi et al 2011
GluSph	No change No change Increased Increased Increased	Post-mortem: GBA-PD, sPD Post mortem GD-PD Hippocampus post-mortem D427V/D427V *GBA1* mouse Plasma: GBA-PD c.f. sPD	Gegg et all 2015 Tayebi et al 2003;Gegg et al 2015 Rocha et al 2015 Sardi et al 2011 Guedes et al 2017
Ceramide	Decreased Decreased Decreased Decreased Decreased Increased No change	Post-mortem: anterior cingulate sPD Post-mortem: anterior cingulate sPD Plasma: sPD iPSC derived dopaminergic neurons Primary cortical neurons + *SNCA* Plasma: sPD, GBA-PD c.f. sPD Primary cortical neurons 50% GCase activity	Abbot et al 2014 Murphy et al 2014 Zhang et al 2017 Fernandes et al 2016 Wang et al 2016 Mielke et al 2013;Guedes et al 2017 Mazzuli et al 2011
GM3 Gangliosides	n.s. increase Increase Increase	Post-mortem: GBA-PD, GD Post-mortem: primary motor cortex sDLB Plasma: sPD	Gegg et al 2015 Clarke et al 2015 Chan et al 2017; Zhang et al 2017

Table 6 - Summary of glycosphingolipid related changes to lipid profiles in PD/DLB

1.6.4.LIMP 2

LIMP 2 protein levels are unaffected in the substantia nigra of GBA-PD and sPD brain (Gegg et al., 2012). LIMP 2 protein levels also do not change between GD, GBA-PD, GBA-controls or healthy controls in cultured fibroblasts (McNeill et al., 2014) or in a SH-SH5Y cell model expressing high levels of exogenous α-synuclein (Gegg et al., 2012). Despite significant inter-individual variability, iPSC derived dopaminergic neurons from GBA-PD patients demonstrate significantly enhanced LIMP 2 protein expression compared with controls (Fernandes et al., 2016). Furthermore, significantly increased expression of LIMP 2 in the frontal cortex of a human post mortem age matched control cohort expressing heterozygous mutation in *GBA1* has also been reported (Kurzawa-Akanbi et al., 2012). An increase was also seen in GBA-PD/DLB in the same study but the difference did not reach statistical significance (Kurzawa-Akanbi et al., 2012).

Regardless of the expression levels of LIMP 2, the increase in α-synuclein associated with GCase deficiency does alter the binding between GCase and LIMP 2 in the ER (Gegg et al., 2012). Immunoprecipitation of GCase and LIMP 2 in a SH-SY5Y cell model overexpressing high levels of α-synuclein shows that GCase is not associated with LIMP 2 (Gegg et al., 2012). Additionally, LIMP 2 is not associated with α-synuclein (Gegg et al., 2012). This indicates that increased α-synuclein does reduce the amount of GCase delivered to the lysosome by LIMP 2 but not through a direct interaction between LIMP 2 and α-synuclein (Gegg et al., 2012).

LIMP 2 and GCase trafficking is further implicated in sporadic PD and DLB as two intronic *SCARB2* polymorphisms have been associated with PD in Greek and North American/European cohorts (Maniwang et al., 2013). However, neither polymorphism affects the levels of LIMP 2 protein nor RNA expression complementing the theory of altered binding between LIMP 2 and GCase (Maniwang et al., 2013). Furthermore, a comprehensive genetic association study identified the *SCARB2* loci as one of three, the others being *APOE* and *SNCA,* as being strongly associated with DLB (Bras et al., 2014).

1.6.5.Lysosomes

Lysosomal number and integrity are critical factors when considering *GBA1* heterozygosity since GCase is a lysosomal enzyme (Brady et al., 1965). Lysosomes are the major site of α-synuclein

degradation in the cell (Blanz and Saftig, 2016). Furthermore, it has previously been reported that GCase and α-synuclein interact within the lysosome (discussed in chapter 1.6.6). Therefore, lysosomes are an important factor for consideration in the pathogenesis of synucleinopathies

Analysis of the anterior cingulate cortex of early and late stage sPD post mortem cases, taking into account neuronal loss, does not show any overt loss of lysosomes as seen through comparable expression of LAMP 1, LAMP 3 and LIMP 2 with age-matched controls (Murphy et al., 2014). This finding suggests that loss of lysosomes is not an underlying cause of reduced GCase enzyme activity (Murphy et al., 2014). Furthermore, Gegg et al report that reduced GCase protein expression is not associated with a decrease in lysosomal content since the lysosomal enzymes Cathepsin D and β-hexosaminidase activity are unaffected in GBA-PD and sPD (Gegg et al., 2012). Murphy et al similarly did not report any correlation between cathepsin A or D with GCase or α-synuclein levels despite increases in early stage sPD (Murphy et al., 2014). At a cellular level, no difference in lysosomal mass as measured by Lyso ID, LAMP 1 protein expression and β-galactosidase activity has been seen in fibroblasts generated from GD, GBA-PD and GBA-'healthy' controls despite significant increases in Cathepsin D and β-hexosaminidase activity associated with *GBA1* mutation (McNeill et al., 2014). Despite these findings, there is a body of evidence to suggest a perturbation of lysosomal properties, particularly in cellular models contradicting finding in post mortem brain tissue. This could reflect the limitations of post-mortem tissue in documenting end stage disease or conversely limitations of cellular models not fully recapitulating all details of a complex biological system.

shRNA mediated knockdown of *GBA1* in primary cortical neurons resulting in 50% reduced GCase protein expression causes accumulation and enlargement of LAMP1 positive puncta (Mazzulli et al., 2011). SH-SY5Y cells harbouring a nonsense mutation in *GBA1* due to zinc finger nuclease direction also have increased LysoTracker signal (Bae et al., 2015). iPSC derived dopaminergic neurons from GBA-PD patients show significantly increased expression of LAMP 1 and LAMP 2 in addition to increased expression of cathepsin D (Fernandes et al., 2016). Furthermore, electron microscopy shows a 2-fold increase in the number of lysosomes and a 2.5-fold increase in the area occupied by lysosomes specifically in dopaminergic tyrosine hydroxylase positive iPSC derived dopaminergic neurons (Schondorf et al., 2014; Fernandes et al., 2016).

Studies in the frontal cortex of a combined cohort of PD and DLB post mortem cases demonstrate a significant increase in LAMP 1 expression associated with *GBA1* mutation (Kurzawa-Akanbi et al., 2012). LAMP 2 is also significantly increased by 10-15% in association with *GBA1* mutation (Kurzawa-Akanbi et al., 2012). Cathepsin D expression is significantly reduced by 15% in GBA-PD/DLB cases and 16% in PD/DLB cases without *GBA1* mutations, implying that reduced Cathepsin D expression could be a PD/DLB effect (Kurzawa-Akanbi et al., 2012). Mice treated with conduritol-β-epoxide (CβE), a pharmacological inhibitor of GCase also demonstrate significantly enhanced expression of LAMP 2 in the substantia nigra, striatum and motor cortex (Rocha et al., 2015b) although there is no change in D409V *GBA1* homozygous mice (Sardi et al., 2011).

1.6.6.α-synuclein

The relationship between α-synuclein and GCase is central to understanding the role of GCase in LBD. Accordingly, a strong link has been established between GCase deficiency and the deposition of aggregated α-synuclein (Stojkovska et al., 2017). Whether this relationship is consequence of a loss or gain of function of GCase due to heterozygous *GBA1* mutation remains a matter of debate.

1.6.6.1. Direct interaction between GCase and α-synuclein

There is strong evidence suggesting a direct interaction between GCase and α-synuclein. Strikingly, 75% of Lewy bodies and Lewy neurites in PD and DLB post mortem brain carrying heterozygous mutations in *GBA1* are positive for GCase compared with 4% of age-matched non-mutant disease controls by immunohistochemical analysis (Goker-Alpan et al., 2010). The distribution of GCase positive Lewy bodies correlates with neuropathological diagnosis (Goker-Alpan et al., 2010). A physical non-covalent interaction between wild type GCase and the C-terminal amino acids 118-137 of α-synuclein has been demonstrated using nuclear magnetic resonance spectroscopy and verified by both immunoprecipitation and immunofluorescence studies in human tissue and neuronal cultures (Yap et al., 2011). Interaction between α-synuclein and GCase is only seen under acidic (pH5.5) conditions, indicating the interaction takes place in the lysosome (Yap et al., 2011; Yap et al., 2013b). The presence of CβE or N370S mutant GCase reduces the affinity of GCase for α-synuclein with a Kd of 49 and 45μM respectively compared to a Kd of 22μM for wild type GCase (Yap et al., 2011). This may contribute to less effective lysosomal degradation of α-synuclein (Yap et al., 2011). In follow up studies, it was discovered that only vesicular membrane bound α-synuclein in the helical conformation is a potent inhibitor of GCase activity by way of shifting GCase away from the membrane thereby impeding substrate availability (Yap et al., 2015). α-synuclein acts as a mixed inhibitor of GCase, impeding substrate availability and steric hindrance as a consequence of binding near the active site of the enzyme (Yap et al., 2013a). Binding of GCase to α-synuclein could additionally cause structural perturbation of the membrane causing changes to local lipid organisation affecting enzyme activity and interfering with lysosomal degradation of α-synuclein (Yap et al., 2013a; Yap et al., 2015).

1.6.6.2. Loss of function

The direct effect of reduced GCase enzyme activity on α-synuclein and cellular processes can be directly assessed in cell and animal models treated with the GCase pharmacological inhibitor conduritol-β-epoxide (CβE). Manning-Bog et al reported accumulated α-synuclein in CβE treated differentiated SH-SY5Y cells and also a 20% increase in the monomeric form of α-synuclein in the ventral mesencephalon of CβE treated mice in the absence of any change in *SNCA* mRNA expression (Manning-Bog et al., 2009). These mice specifically demonstrate robust immunoreactivity in cell bodies within the substantia nigra pars compacta and A9 neurons (Manning-Bog et al., 2009). Striatal and substantia nigral α-synuclein accumulation is also seen in a sub chronic CβE mouse model where the inhibitor was administered at 100mg/Kg daily for 9 consecutive days and also more robustly in a 28-day model (Ginns et al., 2014; Rocha et al., 2015b). Reduced GCase enzyme activity may be able to augment α-synuclein toxicity. CβE treatment in α-synuclein overexpressing LUHMES cells, a human dopaminergic neuronal cell line, significantly enhances α-synuclein accumulation and toxicity (Noelker et al., 2015). Control iPSC derived dopaminergic neurons treated with CβE also show accumulated α-synuclein as do dopaminergic neurons derived from GBA-PD and GD patients (Schondorf et al., 2014). The degree of α-synuclein accumulation varies greatly between specific mutations with the greatest increase associated with L444P, mirroring the mutation dosage effect described previously with GCase enzyme activity (Schondorf et al., 2014). Furthermore, α-synuclein levels are significantly reduced in GBA-PD derived neurons which undergo gene correction compared with non-treated GBA-PD cells (Schondorf et al., 2014).

Knock down of *GBA1* using lentiviral administration of shRNA in differentiated SH-SY5Y cells results in a significant increase of α-synuclein protein corresponding to a 1.8-fold increase compared with controls (Kong et al., 2013). This protein increase is unaccompanied by any change in *SNCA* mRNA expression (Kong et al., 2013). shRNA mediated knockdown of *GBA1* in primary neurons causing a 50% reduction of GCase protein also results in a 1.8-fold increase in steady state α-synuclein levels without any change in *SNCA* mRNA expression (Mazzulli et al., 2011). SH-SY5Y cells harbouring a nonsense mutation in *GBA1* due to zinc finger nuclease direction does not alter monomeric α-synuclein but does cause accumulation of insoluble α-synuclein oligomers (Bae et al., 2015). Additionally, secretion of α-synuclein aggregates is also

significantly increased (Bae et al., 2015). Mixed midbrain primary cultures from GBA1$^{-/-}$ mice also have significantly increased oligomeric species of α-synuclein (Osellame et al., 2013).

Reduced GCase enzyme activity may also be implicated in the increased neuronal cell-to-cell transmission of endogenous α-synuclein (Bae et al., 2014). Transplantation of WT and *GBA1*-/- cells into the hippocampus of transgenic mice expressing human α-synuclein shows increased α-synuclein transmission in grafted cells lacking GCase (Bae et al., 2014). Ectopic expression of WT GCase but not an activity deficient mutant GCase ameliorates propagation of α-synuclein aggregates (Bae et al., 2014)

A novel *in vivo* G*BA1* knock down model in *Oryzias latipes* shows abundant α-synuclein accumulation in the brains of these fish at 3 months of age with α-synuclein detected in axonal swellings containing autophagosomes (Uemura et al., 2015). However, knockdown of *SNCA* in *GBA1* deficient *O. latipes* is insufficient to prolong life span or rescue dopaminergic and noradrenergic cell loss, suggesting that α-synuclein is not involved in the pathological characteristics of this *in vivo* model of GCase deficiency (Uemura et al., 2015).

In vivo models of PD also demonstrate the impact of GCase enzyme activity on α-synuclein accumulation (Sardi et al., 2013). Heterozygous A53T human α-synuclein transgenic mice unilaterally injected with AAV-*GBA1* into the striatum have significantly lower striatal levels of cytosolic α-synuclein and a modest but significant reduction in membrane associated α-synuclein (Sardi et al., 2013). However, the level of insoluble α-synuclein remains unchanged by striatal expression of GCase (Sardi et al., 2013). Similarly, levels of soluble α-synuclein in the spinal cord of A53T mice is significantly reduced by AAV-*GBA1* injection into both cerebral lateral ventricles and the upper lumbar spinal cord (Sardi et al., 2013).

Primary cortical neurons overexpressing either WT or A53T mutant *SNCA* alone causing synaptic α-synuclein enrichment does not cause overt toxicity (Mazzulli et al., 2011). Knockdown of *GBA1* alone in these cells also does not cause toxicity (Mazzulli et al., 2011). However, primary cortical neurons overexpressing WT *SNC*A which have also undergone *GBA1* knockdown show a 25% decrease in viability as measured by neurofilament intensity and neuronal volume (Mazzulli et al.,

2011). This raises the question whether α-synuclein accumulation and associated toxicity due to GCase depletion is due to lysosomal inhibition or alterations in GluCer metabolism.

Mazzulli et al propose a bidirectional loop relationship between GCase deficiency and α-synuclein accumulation (Mazzulli et al., 2011). This relationship is based upon the loss of GCase enzyme activity and the interaction between increased GluCer and α-synuclein as seen in *GBA1* knockdown neurons and iPSC derived dopaminergic neurons from GD patients (Mazzulli et al., 2011). GluCer is able to selectively stabilise the formation of soluble α-synuclein oligomer intermediates on the pathway towards the formation of amyloid fibrils (Mazzulli et al., 2011). Oligomeric α-synuclein is able to inhibit the lysosomal activity of wild type GCase enzyme in neurons and sPD brain (Mazzulli et al., 2011). This bidirectional effect forms a positive feedback loop leading to a self-propagating disease: reduced GCase enzyme activity causes accumulation of GluCer which stabilises the formation and accumulation of α-synuclein which in turn further reduces WT GCase enzyme activity (Mazzulli et al., 2011). Consolidating the bidirectional loop hypothesis, reversible conformational conversion of α-synuclein into toxic oligomeric species and fibrils in iPSC derived dopaminergic neurons has recently been demonstrated (Zunke et al., 2017). More recently, GluSph and sphingosine have also been associated with accelerating the aggregation of oligomeric α-synuclein *in vitro* (Taguchi et al., 2017)

1.6.6.3. Gain of function

Early *in vitro* experiments overexpressing mutant GCase in neural MES23.6 cells suggest a gain of function mechanism of α-synuclein accumulation, albeit it to varying degrees: 21% N370S, 72% L444P and 148% D409H (Cullen et al., 2011). This increase in α-synuclein is associated with reduced GCase enzyme activity, a finding also confirmed in PC12 cells stably expressing WT α-synuclein (Cullen et al., 2011). An interesting study including iPSC derived dopaminergic neurons from a set of N370S/WT monozygotic twins discordant for PD found that α-synuclein accumulated in *GBA1* mutation carriers compared with control neurons regardless of disease state in the absence of any change in *SNCA* mRNA expression (Woodard et al., 2014).

Interestingly, pharmacological inhibition of GCase enzyme activity using CβE does not universally result in α-synuclein accumulation as described in section 1.6.6.2. Indeed, differentiated human cortical neural stem cells treated with CβE do not show any difference in monomeric α-synuclein protein expression or lysosomal proteins (Kurzawa-Akanbi et al., 2012). PC-12 cells expressing WT human α-synuclein also do not demonstrate accumulation of α-synuclein upon treatment with CβE neither do differentiated SH-SY5Y cells nor CβE treated rat primary cortical neurons (Cullen et al., 2011; Dermentzaki et al., 2013). *In vivo*, no evidence of increased α-synuclein accumulation is seen in a study of CβE treated wild type mice (Xu et al., 2011). This implies that the presence of mutant GCase protein is required for pathology and not solely reduced GCase enzyme activity, illustrated by a study in *PSAP* mice (Xu et al., 2011). *PSAP* hydromorphic mutant mice in which GCase enzyme activity is significantly reduced only show small amounts of α-synuclein staining in the cortex (Xu et al., 2011). However, the α-synuclein signal is much stronger in *PSAP* mice with either V394L/V394L or D409H/D409H mutations (Xu et al., 2011).

The homozygous D409V/D409V *GBA1* mutation in mice causes a progressive accumulation of ubiquitin positive α-synuclein aggregates predominantly in the hippocampus although positive α-synuclein-ubiquitin immunoreactivity is also seen to a lesser extent in the cerebral cortex and cerebellum, recapitulating some pathological features of PD and DLB (Sardi et al., 2011). Bilateral hippocampal injection of scAAV-*GBA1* significantly reduces α-synuclein and ubiquitin aggregates (Sardi et al., 2011). Interestingly, despite having similar GCase enzyme activity, D409V/WT but not *GBA1* +/- mice exhibit α-synuclein/ubiquitin aggregates although the degree of α-synuclein

aggregation is approximately 50% less when compared with D409V *GBA1* homozygotes (Sardi et al., 2011). This is further evidence suggesting that reduction in GCase enzyme activity alone is insufficient to cause α-synuclein accumulation and pathology, implicating a gain of function of mutant GCase enzyme.

The glycosylation pattern of GCase protein is altered in response to increased α-synuclein expression (Stojkovska et al., 2017). A reduction of overexpressed α-synuclein significantly increases the proportion of post-ER mature GCase enzyme (Mazzulli et al., 2011). Overexpression of α-synuclein causes accumulation of endoglycosidase H sensitive immature GCase (Mazzulli et al., 2011; Mazzulli et al., 2016a). Retention of immature GCase in the ER reduces the amount of mature GCase reaching the lysosome which in turn causes a reduction of cellular GCase enzyme activity (Mazzulli et al., 2011; Chung et al., 2013; Mazzulli et al., 2016a). An interesting study using control human brain tissue with natural varying degrees of non-symptomatic α-synuclein accumulation identified that while there was no change in the lysosomal GCase enzyme activity between 'high' and 'low' α-synuclein cases, those with 'low" α-synuclein burden had less ER retained GCase enzyme (Mazzulli et al., 2011). This implies that even natural variation of α-synuclein protein levels, let alone accumulated α-synuclein associated with GCase deficiency, modulates lysosomal maturation and therefore lysosomal activity of GCase *in vivo* (Mazzulli et al., 2011).

α-synuclein degradation is significantly impaired in L444P/WT background mice expressing human α-synuclein (Fishbein et al., 2014). The half-life of the human α-synuclein species increases by 77% in neuronal cultures (Fishbein et al., 2014). Neuronal cultures taken from heterozygous L444P mice demonstrate that the presence of L444P mutant GCase is able to exacerbate α-synuclein steady state protein levels by 57% compared with cultures expressing human WT α-synuclein alone (Fishbein et al., 2014). Despite there being no classical Lewy body pathology in the brain of these mice, hippocampal (mainly CA1) human phosphorylated serine 129 (pSer129) α-synuclein, typical of pathologically aggregated α-synuclein, was observed in association in heterozygous mutation by 15 months of age (Fishbein et al., 2014). However, by 19 months of age pSer129 staining was also evident in the hippocampus of A53T α-synuclein mice in the absence of L444P suggesting that the presence of L444P causes an earlier onset of

the pathological α-synuclein process and causes a 70% increase in hippocampal pSer129 α-synuclein load (Fishbein et al., 2014). It is worth pointing out that L444P does not change the staining pattern of α-synuclein using alternative antibodies nor the absolute levels of α-synuclein as measured by western blot in brain homogenates (Fishbein et al., 2014).

Biochemical investigations into the impact of *GBA1* mutation in PD and DLB have thus far uncovered a strong relationship between *GBA1* mutation and α-synuclein accumulation and aggregation. Whilst this goes some way towards explaining pathological processes underlying these conditions, there is still no clear consensus as to whether *GBA1* mutations causes a gain or loss of function of mutant GCase enzyme. With this debate ongoing, the impact of mutant GCase enzyme itself should be considered in more detail to establish whether mutant GCase is able to activate or interact with cellular pathways which may explain the symptoms of PDD and DLB. Accordingly, this thesis will investigate whether mutant GCase enzyme is able to activate the specific cellular stress pathway, the unfolded protein response.

2. Aims and hypothesis

The genetic link between heterozygous mutations in *GBA1* and increased susceptibly for developing PD and DLB has become well established over the last 20 years (Sidransky et al., 2009b; Nalls et al., 2013). Furthermore, the impact of *GBA1* mutations on the presentation and development of PD is well understood: *GBA1* mutations cause a more aggressive disease course particularly associated with earlier and more severe development of cognitive impairment (Neumann et al., 2009; Winder-Rhodes et al., 2013). Whilst it is known that reduced GCase enzyme activity, whether in sPD or GBA-PD, results in accumulation of α-synuclein aggregates (Mazzulli et al., 2011), the role of GCase in pathological mechanisms which underlie LBD are not understood. Furthermore, there is no consensus on whether *GBA1* mutation causes a gain or loss of function effect on mutant GCase enzyme. LBDs are heterogeneous disorders involving diverse pathogenic substrates, exhibiting an array of different symptoms which are unlikely to be solely explained by reduced GCase enzyme activity causing accumulation of α-synuclein (discussed in detail in chapter 1.6.6). Proposed pathological mechanisms include mitochondrial dysfunction, autophagic impairment and ER stress (Migdalska-Richards and Schapira, 2016).

Whilst reduced GCase activity and *GBA1* mutations are associated with reductions in mitochondrial membrane potential and oxygen consumption (Cleeter et al., 2013; Osellame et al., 2013; Xu et al., 2014), suggestions to explain how GCase is implicated are lacking. Similarly, autophagic dysfunction has been proposed as a potential pathogenic consequence of *GBA1* mutation due to the impact of accumulated glycosphingolipids on the reduction of autophagosome clearance (Migdalska-Richards and Schapira, 2016). This chain of events is likely only applicable to GD and not the heterozygous *GBA1* mutations associated with PD, which are not necessarily associated with accumulation of glycosphingolipids in the brain (Gegg et al., 2015). Accordingly, we decided to investigate ER stress, specifically the unfolded protein response (UPR), based upon early positive associations reported in literature. Briefly, evidence suggests that mutant GCase protein and α-synuclein aggregates accumulate in the ER, causing ER stress (Ron and Horowitz, 2005; Bendikov-Bar et al., 2011; Bendikov-Bar and Horowitz, 2012). Furthermore, evidence from human post mortem brain tissue reveals ER stress induced activation of the UPR

in DLB and PD both with and without *GBA1* mutations (Gegg et al., 2012; Baek et al., 2016). Perhaps not unsurprisingly, models involving CβE or *GBA1* knock out models have not demonstrated activation of the UPR (Farfel-Becker et al., 2009). These models are not translatable to the biochemical environment associated with heterozygous *GBA1* mutations. Accordingly, there is a need to better characterise UPR responses in more appropriate models. The unfolded protein response and the association with *GBA1* mutations in both PD and DLB will be discussed in more detail in chapters 5 and 6.

2.1. Overall aim

The aim of this thesis is to investigate whether mutations in *GBA1* confer a gain of function to mutant GCase enzyme which is demonstrated through activation of the cellular stress response, the unfolded protein response (UPR) in cells and human post mortem tissue. It is known that mutant GCase becomes trapped in the ER and subsequently can cause ER stress (Ron and Horowitz, 2005). We wish to establish whether mutant GCase is able to activate and trigger production of specific downstream effectors of the UPR which can initiate pathogenic consequences such as inflammation or cell death. These investigations could therefore implicate pathogenic pathways involved in the development of LBD other than the effect of reduced GCase enzyme activity on α-synuclein accumulation. A series of individual aims for each results chapter are described below.

2.1.1. Individual results chapter aims

2.1.1.1. Chapter 4 –Creation and evaluation of a stable SH-SY5Y cell line overexpressing wild type or L444P mutant *GBA1*

The aim of this chapter was to create a reproducible and consistent SH-SY5Y cell overexpression model of a pathogenic *GBA1* mutation (L444P) and evaluate the associated biochemical characteristics. The biochemical characteristics of the cell lines were investigated to determine if the cells accurately reflect the biochemical environment which is characterised by heterozygous *GBA1* mutation carriers. Establishing the cell lines created as viable models of *GBA1* mutation will facilitate their use in probing the molecular mechanisms linking GCase deficiency to LBD, namely the UPR.

2.1.1.2. Chapter 5 -Investigating the Unfolded Protein Response (UPR) in wild type and L444P *GBA1* overexpressing SH-SY5Y cells – XBP1

The aim of chapter 5 is to establish if L444P mutant GCase enzyme activates the UPR in the *GBA1* SH-SH5Y cell lines created. Specifically, the ability of L444P mutant GCase to evoke a protective UPR response through activation of the IRE1α pathway and production of spliced XBP1 with be investigated. Furthermore, this chapter will try to ascertain the influence of accumulated α-synuclein on the production of spliced XBP1.

2.1.1.3. Chapter 6 -Investigating the Unfolded Protein Response (UPR) in wild type and L444P *GBA1* overexpressing SH-SY5Y cells – CHOP

The aim of chapter 6 is to determine whether the PERK pathway of the UPR is activated in response to *GBA1* mutation in the *GBA1* SH-SY5Y cell lines created. Specifically, the ability of L444P mutant GCase to evoke a response detrimental to cell survival through the enhanced expression of CHOP will be assessed. The relative contribution of accumulated α-synuclein on the expression of CHOP will also be investigated in these cells. Furthermore, the aim of chapter 6 is to also evaluate the expression of CHOP and linked effectors of the apoptotic cascade in human post mortem DLB tissue with and without *GBA1* mutation.

2.1.1.4. Chapter 7 – Behavioural characterisation of D427V/WT transgenic mice

The aim of chapter 7 is to characterise the behavioural phenotype of D427V/WT *GBA1* mice over a 12-month period to establish whether D427V/WT mice are a suitable translational model for the study of LBD. Previously, heterozygous mice had only been tested until the age of 6 months.

2.2. Hypothesis

We hypothesise that mutant GCase protein activates the UPR. As the degree of ER stress increases over time, impacted by accumulating α-synuclein and other pathological proteins associated with LBD, production of protective downstream effectors such as spliced XBP1 will cease. At this point the predominant impact of the UPR response will be production of the apoptosis initiating protein, CHOP, with the consequence of decreased cell viability and development of the symptoms of LBD. We hypothesise that *GBA1* mutation causes a gain of function effect which causes the imbalance of UPR responses in favour of detrimental cellular outcomes, contributing to the hitherto unknown pathological mechanisms linking *GBA1* and LBD.

3. Materials and methods

3.1. Creation of stable *GBA1* SH-SY5Y cell lines

3.1.1. Cell culture

SH-SY5Y cells were grown in incubators maintained at 37°C in 5% CO_2 in T75 flasks containing complete growth media consisting of: DMEM AQMedia™ (D0819, Sigma-Aldrich, USA), 10% foetal bovine serum (FBS)(Gibco, USA) and 1% penicillin (100IU/mL) / streptomycin (100μg/mL)(Gibco, USA). When at approximately 80-90% confluency, cells were sub-cultured. Media was removed, and cells washed twice with PBS. 1mL of trypsin/EDTA 0.25% (Gibco, USA) was added to the flask and cells returned to the incubator for 5 minutes. The flask was gently tapped to aid dissociation of the cells from the flask and 9mL of fresh growth media added. The cell suspension was transferred to a falcon tube and centrifuged at 1000 rpm for 5 minutes. Supernatant was aspirated, and the cell pellet re-suspended in 6mL of complete media. 1mL of the re-suspended cells were transferred to a fresh T75 flask containing 10mL of fresh complete growth media. This 1:6 split of SH-SY5Y cells was performed twice a week. All cells were kept and used below passage number 20.

3.1.2. Polymerase chain reaction (PCR) amplification of *GBA1* open reading frame (ORF)

GBA1 plasmid (NM_000157) was purchased from OriGene technologies (Rockville, USA) and primers designed to amplify the ORF: Forward primer 5'-CTATAGGGCATGGAGTTTTCAAGTCCTTCCAGAG-3' and reverse primer 5'-GGCGACGCCACAGGTAGGTGTGA-3' (Sigma-Aldrich, USA). Q5® High-Fidelity DNA polymerase (New England Biolabs®, USA) was used to ensure accurate replication of nucleotide sequence. The PCR reaction and thermal cycling conditions are outlined in **Table 7**. PCR products were separated by electrophoresis on a 1% agarose gel and visualised under UV light. Fragments corresponding to the right size, 1600 base pairs (bp), were excised and purified using Wizard® SV Gel and PCR clean up kit (Promega,USA) according to manufacturer's instructions. In preparation for TOPO TA cloning, the *GBA1* ORF was subject to adenosine tailing following the New England Biolabs® protocol. This involved incubating the *GBA1* fragment with

deoxyadenosine triphosphate (dATP) and Taq DNA polymerase in Taq DNA polymerase buffer (Sigma-Aldrich, USA) at 72°C for 20 minutes.

DNA Template	2μg
5 X Reaction buffer	10μL
10mM dNTPs	1μL
10μM Forward Primer	2.5μL
10μM Reverse Primer	2.5μL
5X High GC Enhancer	10μL
ddH_2O	Up to 50μL
Q5® High-Fidelity DNA Polymerase	0.5μL

Initial Denaturation	98°C	30 Seconds
Amplification – 35 Cycles	98°C 70°C 72°C	10 Seconds 30 Seconds 60 Seconds
Final Extension	72°C	15 minutes

Table 7 -PCR mastermix and thermal cycling conditions for amplification of *GBA1* ORF

3.1.3.TOPO TA cloning

GFP fusion TOPO® TA expression kit (K4820-01) was purchased from Invitrogen™ life technologies. According to manufacturer's instructions, fresh *GBA1* PCR product was added to 1μL of salt solution and 1μL of TOPO-GFP® vector with ddH_2O making the final volume to 5μL. The reaction mixture was incubated at room temperature for 5 minutes before being placed on ice. The *GBA1*-TOPO-GFP® cloning reaction mix was chemically transformed into One Shot® TOP10 chemically competent *E.Coli* (Life Technologies, USA) according to manufacturer's instructions. DNA was extracted and purified from *E.Coli* colonies using PureYield™ Plasmid Miniprep kit (Promega, USA). Plasmid DNA was subject to diagnostic restriction enzyme digest using *Apa*I (New England Biolabs®, USA) to linearize and check the size of the *GBA1*-GFP plasmid – 7770bp. Plasmid DNA was sent for Sanger sequencing (Source BioScience, UK) to confirm correct integration and orientation of the *GBA1* ORF into the TOPO-TA GFP vector.

3.1.4.Site directed mutagenesis

Site directed mutagenesis was performed using QuikChange® II Site-Directed Mutagenesis Kit (Agilent, USA) according to manufacturer's instructions. In summary, primers were designed complementary to the target sequence of *GBA1* except for the single nucleotide change required to create the L444P mutation in the middle of each primer. The primers used were: forward 5'-TCAGAAGAACGACC**C**GGACGCAGTGG-3' and reverse 5'-GTGCCACTGCGTCC**G**GGTCGTTCTTCTGA-3' (Sigma-Aldrich, USA). Two complimentary nucleotides containing the L444P mutation were synthesized by PCR using *PfuUltra* HF DNA polymerase against the *GBA1*-GFP plasmid DNA template. The PCR reaction and thermal cycling conditions are shown in **Table 8.**

10 X Reaction Buffer	5μL
DNA template	10ng
Forward Primer	125ng
Reverse Primer	125ng
dNTPs	1μL
ddH_2O	Up to 50μL
PfuUltra HF DNA polymerase	1μL

Initial Denaturation	95°C	30 Seconds
Extension (12 Cycles)	95°C 55°C 68°C	30 Seconds 60 Seconds 8 Minutes

Table 8 -PCR reaction mix and thermal cycling conditions for site directed mutagenesis of *GBA1*-GFP plasmid.

Following thermal cycling, the reaction mix was placed on ice prior to digestion with *Dpn*I restriction enzyme at 37°C for 1 hour to preferentially digest template hemi-methylated DNA. The resultant mutant plasmid was chemically transformed into XL1 blue supercompetent cells as per Manufacturer's protocol. Colony growth was subject to a blue/white screen in order to identify bacteria which had successfully taken up the mutant plasmid and repaired the nicks. This was performed by adding 80μg/mL of X-Gal (Sigma-Aldrich, USA) and 20mM IPTG (Sigma-Aldrich, USA) to ampicillin (Sigma-Aldrich, USA) containing agar plates. DNA was extracted and purified

from bacteria using the PureYield™ Plasmid Miniprep kit (Promega, Wisconsin, USA) before being sent for Sanger sequencing to confirm the single nucleotide base change (Source BioScience, UK).

3.1.5.Nucleofection

Amaxa®cell line nucleofector™ kit V (VCA-1003, Amaxa®, Germany) was purchased and the optimised SH-SY5Y protocol followed. SH-SY5Y cells were seeded at a density of $2x10^5$cells per well in a 6 well plate and left to reach confluency of approximately 80%. Cells were harvested by addition of 0.25% trypsin/EDTA (Gibco, USA) and centrifugation at 1000 rpm to create a cell pellet. The cell pellet was re-suspended in 100μL of the nucleofector solution provided before addition of 2μg of either wild type *GBA1*-GFP or L444P *GBA1*-GFP plasmid DNA. The re-suspended cells and plasmid DNA were transferred to a specialised cuvette provided and subject to electroporation by the Nucleofector™ 2b device (Amaxa®, Germany) using the designated SH-SY5Y compatible programme G-004. Nucleofected cells were re-plated in fresh media in a 6 well plate and cultured as normal thereafter. GFP fluorescence was periodically visualised under an inverted fluorescent microscope.

3.1.6.Fluorescence-activated cell sorting (FACS)

Nucleofected cells were harvested and re-suspended in 1mL of FACS buffer consisting of: 2% FBS (Gibco®, USA), 1mM EDTA (Sigma-Aldrich, USA) and PBS (Invitrogen™ life sciences, USA). FACS was performed at a specialised flow cytometry facility at KCL by a flow cytometry technician using the BD FACS Aria™ II cell sorter. Cells were sorted into a 96 well plate, single cell per well in 100μL of complete growth media. Media was refreshed periodically and surviving cells allowed to grow until confluent enough to be transferred to a T25 flask.

3.2. Evaluation of *GBA1* SH-SY5Y cell line biochemistry

3.2.1. Immunocytochemistry

Autoclaved coverslips were coated with poly-D-lysine (Sigma, USA) for 5 minutes at room temperature. Coverslips were washed 3 times with phosphate buffered saline (PBS) prior to being placed in the incubator for at least 2 hours to dry. Cells were seeded at $0.1x10^6$ cells/mL in 12 well plates and left 24 hours to adhere to the coverslips. Media was removed, and the coverslips washed 3 times in PBS. Cells were fixed by addition of 100% methanol, previously chilled to -20°C, for 5 minutes at room temperature. Methanol was aspirated, and coverslips washed 3 times with PBS. Cells were permeabilized by incubation with PBS containing 0.1% Triton X-100 (Sigma, USA) for 10 minutes at room temperature followed by 3 PBS washes. Cells were incubated with blocking solution consisting of 1% bovine serum albumin (BSA) and 22.52mg/mL glycine in PBST (PBS + 0.1% Tween® 20) for 30 minutes at room temperature to block non-specific binding of antibodies. Primary antibodies were prepared at the correct dilution in 1% BSA (Sigma, USA) **(Table 9)** and added to the cells for incubation overnight at 4°C. Antibody solution was decanted, and cells washed 3 times in PBS for 5 minutes each time. Secondary antibody was prepared at the correct dilution in 1% BSA **(Table 9)** and added to the cells for incubation in the dark at room temperature for 1 hour. Following incubation, antibody solution was removed, and cells washed 3 times in PBS for 5 minutes each time whilst keeping cells in the dark. Cells were counterstained with 4',6'-Diamidine-2'-phenylindole dihydrochloride (DAPI)(Sigma, USA) for 1 minute at room temperature and rinsed with PBS before mounting the coverslip with a drop of VectaMount™ AQ mounting medium (Vector Laboratories, California). Slides were stored in the fridge prior to imaging.

Manufacturer	Antibody	Dilution
Abcam	Ab55080 Mouse monoclonal anti-GBA	10μg/mL
Abcam	Ab22595 Rabbit polyclonal anti-Calnexin	1:100
Abcam	Ab37152 Rabbit polyclonal anti-XBP1	10μg/mL
Millipore	ABC955 Rabbit polyclonal anti-CHOP	1:2500
Thermo Fisher	A-11008 Alexa Fluor® goat anti rabbit 488	1:500
Thermo Fisher	A-11004 Alexa Fluor® goat anti mouse 568	1:1000

Table 9 -Antibodies and dilutions used in immunocytochemistry

3.2.2.Western Blot

3.2.2.1. Cell lysis

In preparation for western blot, cells were grown in T75 flasks until confluent. Media was aspirated, and cells washed 3 times in ice cold PBS. Cells were scraped on ice in 1mL of lysis buffer consisting of: 50mM TrisHCl pH8.0 (Sigma, USA), 150mM NaCl (Sigma, USA), 1% NP-40 (Sigma, USA), 0.1% SDS (Thermo Fisher, USA), 0.5% sodium deoxycholate (Sigma, USA) and 0.1mM EDTA (Sigma, USA). Lysates were kept on ice for 30 minutes with regular agitation. Lysates were centrifuged at 12,000 rpm for 20 minutes at 4°C before the supernatant containing the cellular contents was collected and transferred to a fresh tube and stored at -20°C.

3.2.2.2. Protein quantification

Total protein concentration in each lysate was determined using the Thermo Scientific™ Pierce™ BCA assay kit according to manufacturer's instructions. Firstly, a set of standards were prepared using BSA serially diluted in lysis buffer to give the following concentrations to generate a standard curve: 2, 1.5, 1, 0.75, 0.5, 0.25, 0.125, 0.025mg/mL. Preliminary experiments indicated that lysates could be used without further dilution. 5μL of BSA standard or cell lysate was added per well of a 96 well plate (Nunc A/S, Denmark) in triplicate. BCA reagents A and B were prepared at a ratio of 50:1 and mixed thoroughly before pipetting 100μL per well. The plate was covered and incubated at 37°C for 30 minutes before the absorbance was measured at 562nm using a plate reader (Molecular Devices, Spectramax 340PC). The absorbance values from the predetermined standard concentrations were used to generate a standard curve from which linear regression was performed to determine the protein concentration of the unknown cell lysate samples based upon their given absorbance values.

3.2.2.3. Western blotting

Western blotting was carried out as previously described (Broadstock et al., 2012). Samples were normalised to the same protein concentration using ddH_2O and boiled at 95°C for 5 minutes in 5x Laemmli sample buffer (GenScript, USA). Once cooled, the samples were stored at -20°C until required.

15-well 10% SDS-polyacrylamide gels were prepared to run samples. 10μg of sample protein was loaded per lane. 2.5μL of full-range molecular weight marker (Amersham, UK) was loaded in the first lane of every gel for reference. Gels were run at 100 volts until the samples has passed through the separating gel and subsequently at 140 volts until the molecular weight ladder and samples had reached the bottom of the gel. Proteins were subsequently transferred from the gel onto a nitrocellulose membrane (Amersham, UK) in a procedure involving sandwiching the gel between the nitrocellulose membrane, blotting paper and fibre pads and transferring at 60 volts for 90 minutes. Post transfer, nitrocellulose membranes were blocked with 5% powdered milk in PBST at room temperature for 1 hour to minimise non-specific antibody binding. Nitrocellulose membranes were then incubated with primary antibody diluted in 5% powdered milk in PBST overnight at 4°C **(Table 10).** Following primary antibody incubation, 3 x 5-minute washes with PBST were performed to remove excess antibody from the nitrocellulose membrane before secondary antibody prepared in 5% powdered milk in PBST **(Table 10)** was added and incubated at room temperature for 1 hour in the dark. 3 x 5-minute washes with PBST were performed to remove excess antibody and clean the membrane prior to imaging.

Nitrocellulose membranes were imaged using the Odyssey infrared scanner (Li-cor, version 3.0.16). Wavelength selection, size of scan and scan intensity were tailored to the antibodies used for the specific western blot. The integral of band density corresponding to the protein of interest was generated and expressed as a ratio to that of a housekeeping protein in the same sample, serving the purpose of a loading control.

Manufacturer	Antibody	Dilution
Abcam	Ab55080 Mouse monoclonal anti-GBA	1:1000
Abcam	Ab6556 Rabbit polyclonal anti-GFP	1:1000
Abcam	Ab9485 Rabbit polyclonal anti-GAPDH loading control	1:2500
Abcam	Ab21685 Rabbit polyclonal anti-BiP	1:2000
Abcam	Ab37152 Rabbit polyclonal anti-XBP1	1:500
Abcam	Ab7291 Mouse monoclonal anti-αTubulin	1:10,000
Millipore	ABC955 Rabbit polyclonal anti-CHOP	1:1:2500

Novus Biologicals	NBP 2-34444 Mouse monoclonal anti-BCL-2	1:1000
Millipore	AB3623 Rabbit polyclonal anti-Caspase 3 (cleaved,active)	1:200
Abcam	Ab62484 Rabbit polyclonal anti-Caspase 12	1:1000
Thermo Fisher	A-21057 Alexa Fluor® goat anti mouse 680	1:5000
Thermo Fisher	A-32735 Alexa Fluor® goat anti rabbit 800	1:5000

Table 10 - Antibodies and dilutions used in western blotting

3.2.3. Quantitative PCR (qPCR)

qPCR was performed as previously described (Medhurst et al., 2000).RNA was extracted from cells grown in T75 flasks until confluent using the Qiagen RNeasy® kit (Qiagen, Germany) according to manufacturer's instructions. RNA concentration and quality were measured using the Nanodrop™ 1000 spectrophotometer (Thermo scientific, USA) prior to conversion to complementary DNA (cDNA). cDNA conversion was performed using Applied Biosystems™ high capacity RNA-to-cDNA™ kit (Applied Biosystems™, USA) as per manufacturer's instructions. Pre-designed housekeeping and gene of interest primers and fluorescent probes in the form of TaqMan® Gene Expression Assays (Applied Biosystems, USA)**(Table 11)** were purchased and the qPCR mastermix prepared following the manufacturer's instructions based upon 4 repeats of each sample: 5μL 20x TaqMan® expression assay (Applied Biosystems, USA), 50μL TaqMan® Universal Mastermix (Applied Biosystems, USA) and 41μL nuclease free H_2O. 19μL of mastermix was pipetted per well in a 384 well plate (Roche, Switzerland) with 1μL of sample cDNA added per well. Pooled cDNA was serially diluted to create standard curves to monitor the efficiency of the primer sets in each assay. Thermal cycling conditions were set at 95°C for 10 minutes followed by 45 cycles of 95°C for 10 seconds and 60°C for 30 seconds before starting the PCR reaction (Roche LightCycler® 480, Switzerland).

Data, specifically the threshold values (C_t), were analysed by relative quantification to give an indication of the relative expression of the gene of interest compared to *HPRT1* housekeeping

mRNA (Roche®LightCycler 480 Software Version 1.5) C_t values were compared using the published $\Delta\Delta^{CT}$ method to give a value of relative gene expression (Livak and Schmittgen, 2001).

Assay ID	Gene
Hs00986836_g1	*GBA1*
Hs02800695_m1	*HPRT1*
Hs00231936_m1	*XBP1*
Hs00358796_g1	*CHOP*

Table 11 - TaqMan® gene expression assays

3.2.4.Lysosomal enzyme activity assays

Lysosomal enzyme activity assays, specifically GCase, β-galactosidase and β-hexosaminidase were optimised and validated in both leucocytes and SH-SY5Y cells by Dr Derek Burke who kindly shared his protocol for these experiments (Burke, 2017).

3.2.4.1. GCase enzyme activity assay

Cells were grown in T75 flasks until confluent prior to harvesting in 1mL of sterile ddH_2O. Cells were lysed by sonication for 10 seconds and protein quantification performed by BCA assay as described in chapter 3.2.2.2. Cell lysates were normalised to 1mg/mL.

GCase enzyme activity in sample lysates was determined as previously described (Burke et al., 2013) by the hydrolysis of 5mM 4-methylumbelliferyl-β-D-glucopyranoside (4-MUP) (Sigma, USA) in McIlvaine buffer pH5.4 in the presence of 22mM sodium taurocholate (Sigma, USA) at 37°C for 1 hour. The same reaction mixture was prepared concurrently in the absence of sodium taurocholate to account for the potential contribution of *GBA2* GCase (Peters et al., 1976). Furthermore, both reaction mixes were prepared in the absence of any test sample to constitute negative controls. Reactions were stopped by the addition of 0.25M glycine (Sigma, USA) pH10.4. 1nmol 4-methylumbelliferone (4-MU) (Sigma, USA) standard, the product of 4-MUP hydrolysis by GCase enzyme, in 0.25M glycine pH10.4 was prepared as a positive control. 4-MU fluorescence was determined at excitation 365nm, emission 450nm (FlexStation II, Molecular Devices). GCase enzyme activity was calculated using the following equation:

$$\frac{(sample - blank)}{standard} \times \frac{60}{incubation\ time} \times \frac{1000}{protein\ concentration\ \times\ volume} = nmol/hr/mg\ protein$$

3.2.4.2. β-Galactosidase enzyme activity assay

β-galactosidase enzyme activity was calculated in cell lysates added to a solution of 0.4% human serum albumin (HSA) (Sigma, USA) and 0.4M sodium chloride (Sigma, USA) as previously described (Burke et al., 2013), A reaction was produced in parallel without cell lysate to act as a negative control. 1mM of enzyme substrate 4-methylumbelliferyl-β-D-galactopyranoside (4-MUG) (Sigma, USA) in McIlvaine buffer pH 4.1 was prepared and added to the reaction solution containing the cell lysates/blanks and incubated at 37°C for 15 minutes. The reaction was stopped by addition of 0.25M glycine pH10.4. A standard of 1nM 4-MU in 0.25M glycine pH 10.4 was prepared as a positive control. Fluorescence was measured at excitation 365nm, emission 450nm (FlexStation II, Molecular Devices). β-galactosidase enzyme activity was calculated using the same equation used for GCase enzyme activity.

3.2.4.3. β-Hexosaminidase enzyme activity assay

β-hexosaminidase enzyme activity was measured in cell lysates added to 0.2% HSA in McIlvaine buffer pH4.5 as previously described (Burke et al., 2013). 0.2% HSA in McIlvaine buffer pH5.4 without any cell lysate was prepared as a negative control. 3mM of the enzyme substrate, 4-methylumbelliferyl-2-acetoamido-2-deoxy-β-D-glucopyranoside (4-MAP) (Sigma, USA) in McIlvaine buffer pH4.5 was prepared and added to the cell lysates/blanks and incubated at 37°C for 10 minutes. The reaction was stopped by the addition of 0.25M glycine pH 10.4. A standard of 1nM 4-MU in 0.25M glycine pH 10.4 was prepared as a positive control. Fluorescence was measured at excitation 365nm, emission 450nm (FlexStation II, Molecular Devices). β-hexosaminidase enzyme activity was calculated using the following equation:

$$\frac{(sample - blank)}{standard} \times \frac{60}{incubation\ time} \times \frac{1000}{protein\ concentration\ \times\ volume} \times \frac{1}{1000} = \mu mol/hr/mg\ protein$$

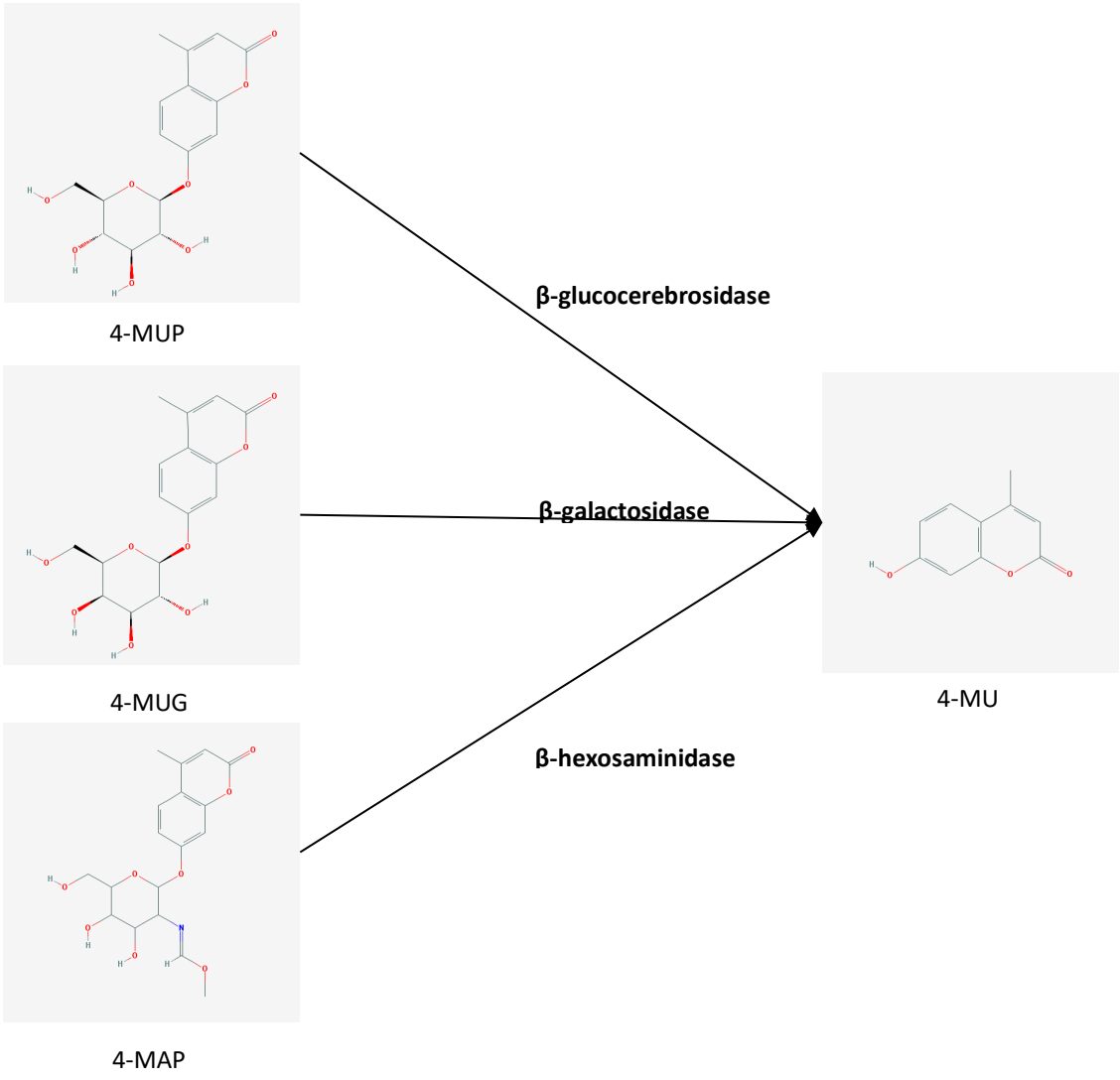

Figure 4 – Substrates and fluorescent product of lysosomal enzyme activity assays

3.2.5.Cell viability assays

3.2.5.1. PrestoBlue®

PrestoBlue® assay was performed as previously described (Puangmalai et al., 2015). PrestoBlue is a resazurin based solution which, when added to cells, is modified by the reducing environment of viable cells, turning red in colour and becoming highly fluorescent (Lall et al., 2013).

Cells were plated in a 96 well plate at a density of $3x10^5$ per well in 100μL of media. Once confluent, 10μL of PrestoBlue® reagent (ThermoFisher Scientific, USA) was added per well and the plate returned to the incubator for 1 hour. Wells were prepared containing media and PrestoBlue® reagent to calculate background. Cell viability was determined at excitation 550nm, emission 590nm (FlexStation II, Molecular Devices).

3.2.5.2. MTT assay

MTT (3-(4,5-dimethylthiazol-2-yl)-2,5-diphenyltetrazolium bromide) assay was performed as previously described (Mosmann, 1983). The assay is based upon the ability of cells to convert water soluble MTT to insoluble formazan. Formazan is subsequently solubilised and the concentration determined by optical density (Mosmann, 1983).

Cells were plated in a 96 well plate at a density of 100 cells per well in 100μL of media. Once confluent, 12mM Vybrant® MTT stock solution (ThermoFisher Scientific, USA) was prepared and 10μl added per well. Wells containing media and MTT stock solution were also prepared to calculate background. The plate was returned to the incubator for 4 hours. 85μL of media was removed per well leaving cells in 25μL of media. Product was solubilised by adding 50μL of dimethyl sulfoxide (DMSO) per well and mixing thoroughly. The plate was returned to the incubator for a further 10 minutes before the solubilised product was mixed thoroughly. Cell proliferation was determined by reading absorbance at 540nm (FlexStation II, Molecular Devices).

3.2.6.Transfection of α-synuclein

SNCA-GFP plasmid (RG210606) was purchased from OriGene Technologies (Rockville, USA). Empty vector-GFP plasmid was a generous gift from Professor Diane Hanger. Plasmids were

transfected into SH-SY5Y cells using the Nucleofector™ 2b device (Amaxa®, Germany) as described in section 3.1.5. Successful transfection was confirmed and expression of *SNCA*-GFP or empty vector-GFP validated by visualisation of GFP fluorescence under an inverted fluorescent microscope. Unfortunately, the accompanying camera was unavailable and images were unable to be taken for presentation in this thesis.

Amaxa®cell line nucleofector™ kit V (VCA-1003, Amaxa®, Germany) was purchased and the optimised SH-SY5Y protocol followed. SH-SY5Y cells were seeded at a density of $2x10^5$cells per well in a 6 well plate and left to reach confluency of approximately 80%. Cells were harvested by addition of 0.25% trypsin/EDTA (Gibco, USA) and centrifugation at 1000 rpm to create a cell pellet. The cell pellet was re-suspended in 100μL of the nucleofector solution provided before addition of 2μg of either wild type *GBA1*-GFP or L444P *GBA1*-GFP plasmid DNA. The re-suspended cells and plasmid DNA were transferred to a specialised cuvette provided and subject to electroporation by the Nucleofector™ 2b device (Amaxa®, Germany) using the designated SH-SY5Y compatible programme G-004. Nucleofected cells were re-plated in fresh media in a 6 well plate and cultured as normal thereafter. GFP fluorescence was periodically visualised under an inverted fluorescent microscope.

3.3. Human post mortem brain tissue

3.3.1. Case details

Post mortem brain tissue from N370S *GBA1* heterozygous DLB, sporadic DLB and non-demented control cases was obtained from South West Brain Bank University of Bristol and Queen Square brain bank, University College London. Diagnosis was made by the respective brain banks based upon standardised post mortem diagnostic criteria. A 500mg sample of frozen tissue was taken from the dorsolateral prefrontal cortex (BA9), temporal cortex (BA21) anterior cingulate gyrus (BA24) and parietal cortex (BA40). Due to the pathological overlap between PDD and DLB in addition to the variable of using two different brain banks, the decision was made to combine PDD and DLB cases to form a LBD cohort for comparison. Cases were matched for mean age at death and mean post mortem delay and confirmed using Levene's test for equality of variances and independent t-test for equality of means using IBM SPSS statistical software programme version 22 (IBM, USA) **(Table 12).** There was a significantly higher number of male cases across all study cohorts which does need to be given consideration when interpreting results. pH data was not available for all the cases; a limitation of this study. Since pH, specifically more acidic environments, contributes to the degradation of proteins within the brain, ideally pH would be controlled for across study groups. The impact of post mortem delay on the representation of protein expression by western blot was considered. Post-mortem delay in non-demented control cases did not correlate with expression of any protein of interest when tested by Pearson correlation.

Diagnosis	n	Male	Female	Mean age at death (years)	Mean post mortem delay (hours)
Non-demented control	11	9	2	86.09 (±3.081)	56.19 (±0.929)
N370S *GBA1* -DLB	4	4	0	77.75 (±8.221)	56.04 (±40.643)
LBD	10	9	1	83.70 (±6.430)	44.75 (±27.315)

Table 12 - Summary of post mortem cases included in the study

3.3.2.Preparation of human tissue for western blot

Tissue was prepared following standard protocols developed in our lab (Whitfield et al., 2014). For each tissue sample, the cortical grey matter was dissected from the white matter and meninges on dry ice. Approximately 300mg of cortical grey matter was homogenised in 6mL of ice-cold homogenisation buffer at pH 7.4 using an Ultra-Turrax tissue homogeniser (KIA Werke, Germany) resulting in a crude homogenate. The homogenisation buffer contained: 50mM Tris-HCl, 5mM EGTA, 10mM EDTA, Roche® 'complete protease inhibitor cocktail tablets' (Roche, Switzerland) and 2µg/mL pepstatin A (Sigma-Aldrich, USA). Crude homogenates were immediately frozen on dry ice and stored at -70 for protein assay and western blot.

3.3.3.Protein quantification of human tissue homogenate

The total protein concentration of the crude homogenate was determined using the Bradford protein assay method (Bradford, 1976) . Bovine serum albumin (BSA) (Thermo Scientific, USA) standards were prepared in homogenisation buffer resulting in the following concentrations: 0.2, 0.4, 0.6, 0.8, 1.0, 1.2, 1.4, 1.6, 1.8 and 2.0 mg/mL. Serial dilutions of crude homogenate were prepared also using homogenisation buffer.

5 µL of crude homogenate, diluted homogenate or standard were added per well of a 96 well plate (Nunc A/S, Denmark) in triplicate. Then, 250µL of Coomassie Reagent (Thermo Scientific, USA) was added per well and the plate incubated at room temperature for 10 minutes. After ensuring there were no bubbles which could interfere with absorbance, absorbance was read at 595nm using Flexstation II (Molecular devices, USA). Samples were normalised to 1µg/mL of protein and boiled at 95°C for 5 minutes in 5x Laemmli sample buffer (GenScript, USA). Once cooled, the samples were stored at -20°C until required. Western blotting was performed as described earlier in chapter 3.2.2.3.

3.4. D427V/WT *GBA1* mouse

3.4.1. Animal husbandry and colony maintenance

Homozygous *GBA1* D427V/D427V mice were purchased from Jackson laboratories (Charles River, UK) and used for breeding with female wild-type C57BL/6 mice (Charles River, UK) to produce animals for breeding. Mixed gender mice were maintained in a 12-hour light dark cycle at ambient temperature and humidity with *ad libitum* access to water and food. After weaning, mice were ear clipped for identification purposes and for DNA extraction. DNA was extracted from ear clips using the Qiagen DNeasy® extraction kit (Qiagen, Germany) according to the manufactures instructions. Genotyping was performed using the following primers: Forward 5'-CAG TTC ACA CAG TGT TGG AGC-3' and reverse 5'-AGG TGA TCG TAT TTC AGT GGC-3' (Sigma-Aldrich, USA) following the genotyping protocol and thermal cycling conditions from Jackson Laboratory (USA) https://www2.jax.org/protocolsdb/f?p=116:5:0::NO:5:P5_MASTER_PROTOCOL_ID,P5_JRS_CODE:9353,019106.

3.4.2. Behavioural testing

All behavioural testing was performed at the same time each day (beginning at 9:30am) and under the same light conditions. Furthermore, all testing was remotely reordered by video camera in a cordoned off area of the room where the mice were unable to see any researchers. This experimental set up reduced the potential for researchers becoming a cue and as such affecting the behavioural performance. Open field and Morris water maze videos were analysed using the behavioural software Ethovision XT version 11 (Nodlus, Netherlands) as discussed below, preventing researcher bias. Y-maze videos were manually scored for open arm entry since the software did not perform this function.

3.4.2.1. Open field behavioural testing

Open field testing was carried out according to previously described (Seibenhener and Wooten, 2015). Mice were habituated to the testing room for 30 minutes prior to testing before being placed in a 45cm^2 open field area for 20 minutes and allowed to explore. Lighting across the arena was even and the arena cleaned with ethanol between trials. Trials were recorded by video camera and the recording analysed using EthoVision XT version 11 software (Noldus, Netherlands). The

arena was calibrated using the EthoVision software to reflect the dimensions and additionally the presence of a 11.25cm^2 square border. The following parameters were measured per mouse over the 20-minute trial: distance moved (cm); velocity (cm/s) and time spent in the 11.25cm^2 border to the centre (s).

3.4.2.2. Y-Maze behavioural testing

Mice were placed in the centre of a Y-maze and allowed to explore the arms of the maze for 8 minutes. The arms of the maze measured 35cm in length and 4cm in diameter. The maze was cleaned with ethanol between trials and lightning was even across the maze. The recording of each trial was manually scored for the number of spontaneous arm entries – the total number of correct triad arm entries attempted within 8 minutes. The % of spontaneous arm performance was calculated. The protocol for Y-maze testing and spontaneous arm performance was based upon the paradigms described by Deacon et al and Hughes et al (Hughes, 2004; Deacon and Rawlins, 2006)

3.4.2.3. Morris water maze behavioural testing

A circular water maze measuring 1 meter in diameter was filled with water and opacifier added the day prior to testing to allow the water to reach ambient temperature. A platform was placed in the centre of a designated quadrant for the entirety of testing for each age cohort, submerged 2cm below the surface of the water. Large visual cues were placed at the north, south, east and west point of the arena. Mice were placed in the water maze at randomly generating starting points and given 90 seconds to find the submerged platform. If the mouse failed to find the platform, it was placed on the platform for 10 seconds before being returned to its cage. Each mouse underwent 4 trials per day from randomly generated starting points with a 30-minute interval between each trial. Average values were calculated using EthoVision measures for the time taken to find the platform (s), distance to platform (cm) and the velocity (cm/s). Mice underwent 5 consecutive days of trials to generate learning curves. On day 6 a probe trial was performed to validate the learning curve findings by extinguishing the learning curves. The platform was removed from the water maze and the time mice spent in the correct quadrant which previously contained the platform was measured over 60 seconds. The same protocol was employed for testing across different age groups. The protocol employed for Morris water maze

testing was based upon the widely adopted paradigm described by Vorhees et al (Vorhees and Williams, 2006)

3.5. Statistical Analyses

All statistical analyses for cell line and *in vivo* studies were conducted using GraphPad Prism 7 software, following the recommended tests suggested by the software. All statistical analyses pertaining human post mortem tissue were performed using SPSS version 24 software (IBM analytics). The statistical tests used are descried within figure legends. GraphPad Prism 7 software was used to plot all graphs. All data are presented as mean ± SEM.

3.5.1. Cell lines

One-way ANOVA followed by Tukey's HSD post hoc test was used for comparison between cell lines: SH-SY5Y, WT *GBA1* SH-SY5Y, L444P *GBA1* SH-SY5Y. Upon transfection of α-synuclein, two-way ANOVA followed by Bonferroni post hoc test was used for comparison between cell lines either expressing α-synuclein or empty vector. Prior to comparison of means, Levene's test for equality of variances was performed on all data to check for normal distribution of data allowing for the application of parametric statistical tests.

3.5.2. Human post mortem tissue

Non-demented control cases were selected to match both DLB and N370S-DLB cases for age as described in chapter 3.3.1. All data from western blots was Log10 transformed to normalise distribution which was subsequently confirmed using Levene's test. Outliers were identified in SPSS by generating boxplots and subsequently excluded. Excluded data points are highlighted in scatter graphs. One-way ANOVA followed by Tukey's HSD post hoc test was used for comparison between non-demented controls, sporadic DLB and N370S *GBA1* DLB cases.

3.5.3. D427V/WT *GBA1* mouse model

Data was analysed between D427V/WT *GBA1* and WT mice across 4 different age ranges using repeated measures ANOVA followed by Sidak's post hoc test. Learning curves at individual age points for the Morris water maze were compared by two-way ANOVA followed by Bonferroni post-hoc test.

4. Creation and evaluation of a stable SH-SY5Y cell line overexpressing wild type or L444P mutant *GBA1*

4.1. Introduction

Several cell models have been created for the study of GCase and *GBA1* mutations to better understand the relationship between mutant GCase and mechanisms underlying GD and more recently synucleinopathies. Each model has their advantages and disadvantages pertaining their biochemical characteristics and ability to accurately reflect the biochemical environment associated with heterozygous *GBA1* mutation carriers, the focus of this thesis. These factors need to be considered when interpreting findings.

4.1.1.Cell models

4.1.1.1. Conduritol beta epoxide (CβE)

CβE is an irreversible pharmacological inhibitor of glucocerebrosidase (GCase) enzyme activity (Grabowski et al., 1986). Administration of CβE is a simple method of investigating the effect of reduced GCase enzyme and as such has been utilised by many studies both in cells and in mice (Enquist et al., 2007; Dermentzaki et al., 2013). However, the degree of GCase enzyme activity varies considerably in association with *GBA1* mutations and the degree of GCase inhibition by CβE needs to be taken into account, especially if trying to recapitulate the effect of heterozygous mutations in *GBA1* or the reduced GCase enzyme activity seen in sporadic PD brain (Gegg et al., 2012).

CβE is also able to inhibit non-lysosomal GCase produced by *GBA2* (Ridley et al., 2013). Whilst CβE inhibits *GBA2* related GCase less efficiently than lysosomal *GBA1* GCase, CβE still produces a non-specific effect on overall glycosphingolipid metabolism within cells. The contribution and significance of diminished *GBA2* GCase enzyme activity should be factored into interpretations from these models.

The appropriateness of cell types treated with CβE also needs to be taken into consideration. Since GCase is being investigated in the context of PD and DLB, cells should be ‘neuronal like’,

if not actual neurons, or cells which overexpress α-synuclein. Accordingly, many CβE studies have been performed in SH-SY5Y cells, an immortal human neuroblastoma cell line which can be differentiated using retinoic acid into dopaminergic 'neuron like' cells (Manning-Bog et al., 2009; Dermentzaki et al., 2013). Whilst SH-SY5Y cells are 'neuron like', they are not neurons. Furthermore, SH-SY5Y cells only express low levels of α-synuclein whilst pre-synaptic α-synuclein is abundant in neurons (Hunya et al., 2008). Appropriate representation of α-synuclein in any model used for GCase investigations is important since GCase and α-synuclein physically interact (Yap et al., 2011) and GCase deficiency is strongly associated with α-synuclein accumulation (Mazzulli et al., 2011)(chapter 1.6.6). These factors are strongly implicated in the pathogenic mechanisms of LBD and so the absence of a GCase/α-synuclein relationship may question the validity of experimental results. Taking these factors into consideration, SH-SY5Y cells are still widely used and are a valuable model due to their ease of culture compared with primary cultures. Primary neuronal cultures whether cortical or mesencephalic have the advantage of being actual neurons and so are directly translational. However, in order to prevent damage of the neuronal tissue during dissociation, primary rodent cultures are generated at embryonic days 11-17 for cortical neurons and embryonic day 13.5 for mesencephalic neurons (Pozzi et al., 2017). These neurons are not mature and certainly do not reflect the mature neurons of the aging brain. Furthermore, accuracy in dissection can also affect the phenotype of neuronal subpopulations present in the culture. However, both SH-SY5Y and primary neuronal cultures represent a pragmatic approach to the study of *GBA1* mutations as long as the limitations are acknowledged.

4.1.1.2. Overexpression of *GBA1*

Simple models involving the overexpression of *GBA1* plasmids are relatively easy and cheap to produce. This approach has been taken in MES 23.5 (rodent mesencephalic), PC12 (rat neuroendocrine tumour) and primary cortical neurons in a key paper implicating mutant GCase in α-synuclein accumulation (Cullen et al., 2011). In this case, mutations were generated by site-directed mutagenesis of *GBA1* plasmids with the resultant mutant plasmids transiently transfected into cells. Mutant plasmids generated include: N370S, D409H, L444P, E235A and E350A (Cullen et al., 2011). The key consideration of this approach is background endogenous expression of wild-type (WT) GCase protein. Since cells do not reflect the impact of mutant

GCase alone, the contribution of endogenous GCase must always be taken into account when interpreting results. One way of addressing this issue is to make comparison to cells transfected with WT *GBA1,* generating values of relative change to WT overexpressing cells. Furthermore, the cell type used as the basis for the model also needs to be evaluated for suitability as discussed earlier.

4.1.1.3. *GBA1* Knockdown

An alternative approach to studying GCase *in vitro* is knockdown of *GBA1.* Knockdown of *GBA1* has been performed by lentiviral administration of shRNA to differentiated SH-SY5Y cells (Kong et al., 2013) and also primary neurons resulting in a 50% reduction in GCase protein (Mazzulli et al., 2011). The degree of knockdown and resultant GCase protein level and enzyme activity are critical factors when interpreting results and considering the translational impact for LBD. Although not strictly *GBA1* knockdown, zinc finger nuclease direction has also been used to cause a knock-out of GCase enzyme activity to residual levels attributable only to *GBA2* derived GCase (Bae et al., 2015). This was achieved by targeting a zinc finger directed frame shift causing translation of a termination stop signal in exon 3 (Bae et al., 2015). Since GCase enzyme activity is attributable to exons 5 through to 10 (Hruska et al., 2008), *GBA1* translated GCase enzyme activity is knocked out.

4.1.1.4. Fibroblasts

Skin fibroblasts taken from living LBD patients represent a model of primary human cells, which comprise chronological and biological ageing according to individual polygenic predisposition and environmental factors (Alcalay et al., 2014). Skin fibroblasts are easily isolated from 2mm punch skin biopsies and the ensuing culture is initially a mix of fibroblasts and keratinocytes until a pure culture of fibroblasts is achieved through passage (Auburger et al., 2012). However, fibroblast cultures contain a mixture of mitotic and post-mitotic cells contributing to a heterogeneous cell population (Auburger et al., 2012). Furthermore, clonal selection and drift in culture are inherent features of fibroblasts and so appropriate matching to controls can be challenging (Auburger et al., 2012). Fibroblasts generated from PD and DLB patients both with and without *GBA1* mutation as well as from patients with GD have proved a popular model for interrogation since the direct effect of either the disease or *GBA1* mutation on the human cell can be examined (McNeill et al., 2014). However, as a model system translational to LBD, human fibroblasts have a major flaw

since they only express *SNCA* at very low levels unlike neurons and so the interaction between α-synuclein and GCase is not accurately represented (Auburger et al., 2012).

4.1.1.5. iPSC derived neurons

Takahashi and Yamanka first demonstrated in 1996 that retroviral transduction of a cocktail of transcription factors highly enriched in embryonic stem cells can reprogram fibroblasts into embryonic stem cell like cells named induced pluripotent stem cells (iPSCs) (Takahashi and Yamanaka, 2016). These iPSCs can be differentiated into cells of interest, specifically dopaminergic neurons for the study of PD (Zhao et al., 2014).

Human iPSCs are considered excellent models to study the molecular mechanisms underlying LBD *in vitro* because they are derived directly from patient somatic cells and so comprise the specific genetic predisposition and biochemical features of the individual (Zhao et al., 2014). Application of iPSC technology to study disease mechanisms has coined the phrase 'disease in a dish'. The biochemical features of LBD neurons with or without *GBA1* mutation can now be realistically reflected *in vitro* and as such iPSCs have become increasingly utilised (Schondorf et al., 2014; Woodard et al., 2014; Fernandes et al., 2016; Mazzulli et al., 2016b).

The major limitation to this technology is the variability between iPSC lines (Zhao et al., 2014). This is addressed by robust quality control measures such as verification of transgene silencing and karyotype analysis (Zhao et al., 2014). Variability between lines may reduce the ability to perceive meaningful phenotypes, especially when a limited number of cell lines are used in a study (Zhao et al., 2014).

When interpreting data from iPSCs used to study PD and DLB, the relative maturity of the derived dopaminergic neurons needs to be considered. Typically, these neurons are relatively immature and do not accurately reflect mature and aged neurons present in PD or DLB, conditions where age remains the biggest risk factor (Hindle, 2010). The maturity of neurons is an important factor since many biochemical pathways become less efficient with age (Hindle, 2010). The content and pattern of gangliosides markedly changes during brain development, a feature which is particularly relevant to *GBA1* mutant iPSC studies (Svennerholm et al., 1989). The total brain ganglioside content is very low at embryonic and foetal stages before increasing several fold with

a shift from gangliosides of the Lac series: GM3 and GD3, to monosialo-species during development and polysialo-species in the adult brain (Svennerholm et al., 1989). The ganglioside pattern of fibroblasts is characterised by the presence of GM3 which remains the main ganglioside represented in iPSC cultures (Schondorf et al., 2014). However, differentiated dopaminergic neurons contain all the polysialogangliosides found in the CNS, even though high levels of GM3 and GD3 are still present (Schondorf et al., 2014). iPSC derived dopaminergic neurons do recapitulate key glycosphingolipid pathways related to GCase enzyme activity although not completely (Schondorf et al., 2014). Nevertheless, dopaminergic neurons do not reflect the neuronal species most affected in LBD. Glutamatergic and cholinergic neurons are extensively implicated and therefore investigating the impact of *GBA1* mutations on these cell types may prove to be more informative.

In vitro models for study of *GBA1*

CβE

Pharmacological inhibitor of GCase used in various cell types resulting in <10% GCase enzyme activity

ADVANTAGES

- Cheap and easy to administer
- Gives neuronogenic GD phenotype i*n vivo*

DISADVANTAGES

- Does not affect the structure of GCase.
- GCase activity reduced to non-translational level for PD/DLB

Knock down

siRNA directed against *GBA1* or
zinc finger directed knock down in a variety of cell types

ADVANTAGES

- Easy and fast results
- Good for mechanistic studies

DISADVANTAGES

- Knockdown tends to cause reduction in GCase enzyme activity not translational for PD/DLB

Overexpression

Overexpression of wild type or mutant *GBA1* in a variety of cell types

ADVANTAGES

- Simple to perform
- Expression of human mutant *GBA1* mirroring patients
- Good for pathway studies

DISADVANTAGES

- Need to consider impact of endogenous GCase

Fibroblasts

Derived from heterozygous *GBA1* mutant or sporadic PD/DLB patients

ADVANTAGES

- Human cell model expressing mutant GBA1 to a translational extent
- Good for drug testing

DISADVANTAGES

- Low expression of α-synuclein
- Not neurons

iPSC derived dopaminergic neurons

Derived from heterozygous *GBA1* mutant or sporadic PD/DLB patients

ADVANTAGES

- Neurons reflecting the *GBA1* deficient environment
- 'Gold star' translational model

DISADVANTAGES

- Time consuming, expensive and difficult to produce
- Immature neurons
- Variability between iPSC lines

Table 13 – Summary of *in vitro* models studying *GBA1* mutation

4.1.2.Biochemistry of *GBA1* cell models

As already discussed, the biochemical environment of any cell model used to study *GBA1* mutations and GCase activity in LBD should reflect as accurately as possible the biochemical conditions in living individuals, predominantly to make experimental findings using these models easily translatable into humans. The key biochemical parameter which needs to be assessed in any model of *GBA1* mutation or LBD is the level of GCase enzyme activity which should be considered in the context *GBA1* gene expression and GCase protein levels.

4.1.2.1. GCase enzyme activity

Immortal cell lines such as PC12 and MES23.5-SNCA have been engineered to overexpress *GBA1* plasmids with varying common mutations in the gene as discussed in chapter 4.1.1.2 (Cullen et al., 2011). Whilst overexpression of WT *GBA1* into MES23.1-SNCA cells results in increased GCase enzyme activity to 167% compared with non-transfected cells, no significant reduction in GCase activity was seen when mutant *GBA1* plasmids were overexpressed (Cullen et al., 2011). The same effect was seen in PC12 cells when either D409V or D409H *GBA1* plasmids were overexpressed (Cullen et al., 2011). Since it is known that GCase enzyme activity is significantly reduced in the cerebellum, substantia nigra, anterior cingulate gyrus and frontal cortex of sporadic PD and DLB patients (Gegg et al., 2012; Murphy and Halliday, 2014; Rocha et al., 2015a), cellular models which do not show comparable reductions in GCase enzyme activity may not be suitable for pathway interrogation. However, one immortal cell line used to model PD does show a reduction in GCase enzyme activity. Mouse neuroblastoma cells overexpressing human WT α-synuclein show a significant reduction in GCase enzyme activity of over 50% (Yang et al., 2016).

The use of CβE in immortal cell lines or primary cultures pharmacologically inhibits GCase enzyme activity (Grabowski et al., 1986). The degree of reduced GCase enzyme activity conferred by CβE depends upon the concentration used. 50μM of CβE in SH-SY5Y cells reduces GCase activity to less than 5% of untreated cells (Cleeter et al., 2013; Dermentzaki et al., 2013). Higher concentrations, 200μM of CβE, are required to achieve a similar degree of impaired GCase enzyme activity in primary cortical neurons (Dermentzaki et al., 2013). The extent of

reduced GCase enzyme activity needs to be considered since these reductions are more comparable with severe forms of GD and not heterozygous mutations associated with LBD.

Patient derived fibroblasts would be expected to give a representative picture of GCase enzyme activity and indeed GBA-PD and non-disease manifesting *GBA1* heterozygotes show an approximate 50% reduction in GCase activity (McNeill et al., 2014). A lower magnitude of reduced GCase activity has been reported in alternative studies: 35% reduction in L444P-PD fibroblasts; 32% reduction in N370S-PD fibroblasts (Sanchez-Martinez et al., 2016; Garcia-Sanz et al., 2017). Interestingly, fibroblasts from sporadic PD patients do not show a significant reduction in GCase enzyme activity (McNeill et al., 2014; Sanchez-Martinez et al., 2016; Garcia-Sanz et al., 2017).

iPSC derived dopaminergic neurons from GBA-PD patients shows an approximate 50% reduction in GCase enzyme activity (Schondorf et al., 2014; Fernandes et al., 2016). A similar degree of GCase enzyme activity is seen in dopaminergic neurons generated from *GBA1* heterozygous monozygotic twins discordant for PD (Woodard et al., 2014). iPSC derived dopaminergic neurons from healthy individuals infected with lentiviral particles to express human WT α-synuclein also show a significant reduction in GCase enzyme activity specifically in the lysosomal compartment (Mazzulli et al., 2016a).

In conclusion, the cell line created in chapter 4 should demonstrate a significant reduction in GCase enzyme activity to be considered a suitable model to investigate the UPR response which may contribute to LBD pathology.

4.1.2.2. Other lysosomal enzymes

The effect of *GBA1* mutation should be considered in the context of activity of other lysosomal enzymes. Since GCase is located at a critical juncture in the glycosphingolipid pathway, alteration in GCase activity may influence the activity of other enzymes in the pathway but also other enzymes which function within the lysosome indirectly through a toxic gain of function effect on the lysosome. The activity of other lysosomal enzymes can determine whether pathological effects noted in association with *GBA1* mutation are GCase specific or due to global lysosomal dysfunction in which case non-specific lysosomal enzyme activity will be affected.

4.1.2.2.1. β-Galactosidase

β-galactosidase enzyme cleaves the terminal β-galactosyl residues from GM1 gangliosides, glycoproteins, oligosaccharides and the glycoaminoglycan keratan sulfate (Sandhoff and Harzer, 2013). Within lysosomes, β-galactosidase is complexed with two other hydrolases: serine peptidase protective protein / Cathepsin A (PPCA) and neuramidiase (Sandhoff and Harzer, 2013). This multi-enzyme complex is critical for enzyme stability and function within lysosomes (Sandhoff and Harzer, 2013).

In relation to cell models of *GBA1* mutation the activity of β-galactosidase is increased in fibroblasts with *GBA1* mutations but is significantly reduced in the corresponding iPSC derived dopaminergic neurons (Schondorf et al., 2014). However, a significant reduction in GBA-PD fibroblasts has been reported by Garcia-Sanz et al (Garcia-Sanz et al., 2017) whilst McNeill et al reports no alteration in β-galactosidase activity in *GBA1* heterozygotes either with or without PD (McNeill et al., 2014). iPSC derived dopaminergic neurons from healthy individuals infected with lentiviral particles to express human WT α-synuclein show a significant reduction in β-galactosidase enzyme activity specifically in the lysosomal compartment (Mazzulli et al., 2016a). However, there is no change in β-galactosidase activity, despite significant reduction in GCase activity in a murine model of α-synuclein accumulation due to transgenic overexpression of human A53T SNCA (Sardi et al., 2013). Furthermore, β-galactosidase activity and gene expression is unaffected in GD mouse models (Vitner et al., 2010; Sardi et al., 2013).

Interestingly, β-galactosidase enzyme activity is unchanged in lumbar CSF from sporadic PD and AD patients compared with controls but is significantly reduced in DLB (Balducci et al., 2007; Parnetti et al., 2009). These findings potentially implicate more extensive disruption to glycosphingolipid metabolism in DLB which could underlie the symptoms of dementia.

4.1.2.2.2. β-Hexosaminidase

β-hexosaminidase catalyses the degradation of GM2 gangliosides and other molecules containing N-acetyl hexosamines (Kolter and Sandhoff, 2006). Functional lysosomal β-hexosaminidase enzyme exists as a dimer through the combination of α and β subunits to form one of three isoenzymes: A, B or S (Kolter and Sandhoff, 2006). Only isoenzyme A, composed

of both α and β subunits, can hydrolyse GM2 gangliosides *in vivo*. Enzymatic hydrolysis by β-hexosaminidase requires the enzyme to be complexed to the specific GM2 activator protein within the lysosome (Kolter and Sandhoff, 2006) (**Figure 5**).

GM2 gangliosidosis are a group of autosomal recessive inherited neurodegenerative disorders caused by excessive intra-lysosomal neuronal accumulation of ganglioside GM2 related glycolipids (Sandhoff and Harzer, 2013). Genetic defect in either the gene encoding the α or β subunits (*HEXA* or *HEXB*) or the GM2 activator protein (*GM2A*) can result in accumulation of GM2 in neural tissue leading to three forms of GM2 gangliosidosis: Tays-Sachs disease, Sandhoff disease and GM2 activator protein deficiency respectively (Sandhoff and Harzer, 2013).

The influence of *GBA1* mutations on β-hexosaminidase activity is debated. Increased activity is seen in GBA-PD fibroblasts by McNeill et al (McNeill et al., 2014) but was not replicated by Schondorf et al or Garcia-Sanz et al in fibroblasts or by Chiasserini et al in human brain tissue (Schondorf et al., 2014; Chiasserini et al., 2015; Garcia-Sanz et al., 2017).

There is no change in β-hexosaminidase activity, despite significant reduction in GCase activity seen in a murine model of α-synuclein accumulation due to transgenic overexpression of human A53T SNCA (Sardi et al., 2013). Furthermore, β-hexosaminidase activity is unaffected in D409V/D409V *GBA1* homozygous mice (Sardi et al., 2013). Additionally, neuronopathic GD mice do not exhibit any alteration in β-hexosaminidase mRNA expression (Vitner et al., 2010). Interestingly, as with β-galactosidase enzyme activity in humans, whilst β-hexosaminidase activity remains unchanged in CSF from PD patients, enzyme activity is significantly reduced in DLB patients indicating DLB may involve more extensive lysosomal pathology (Balducci et al., 2007; Parnetti et al., 2009).

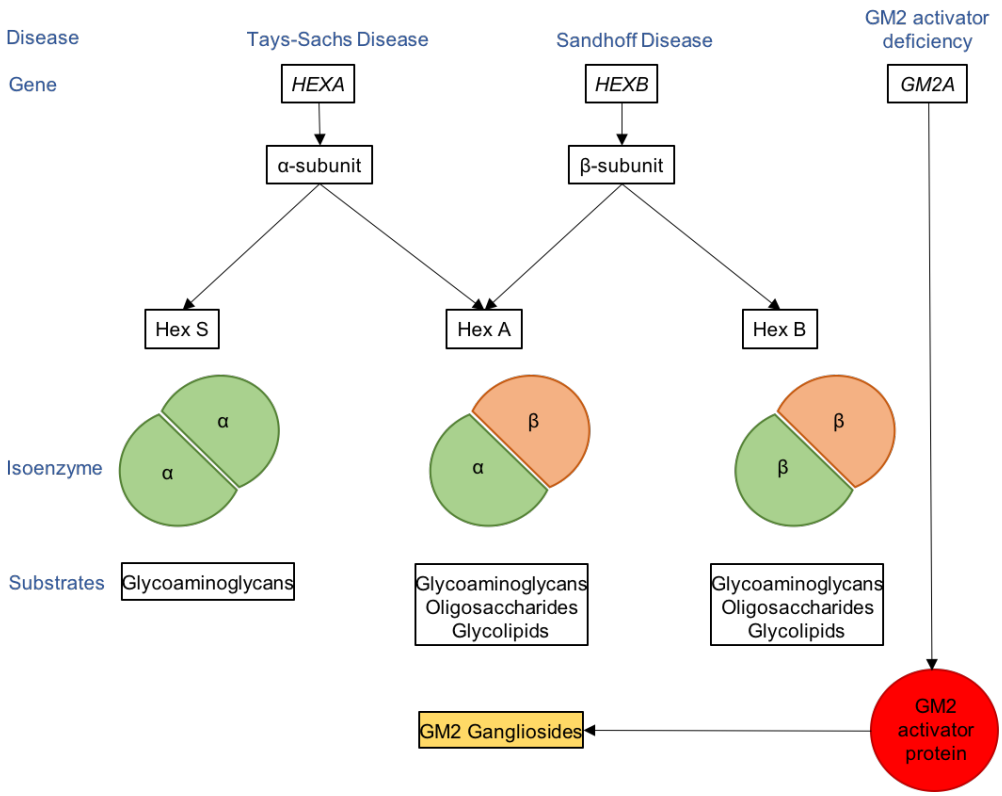

Figure 5 - Composition of β-hexosaminidase enzyme and substrates.

4.1.3.GCase protein levels

The expression levels of GCase enzyme are an important consideration in any model. A reduction in GCase suggests two possibilities: reduced transcription of *GBA1* or increased degradation of GCase protein. GCase protein levels are significantly decreased in the substantia nigra and cerebellum of sporadic PD brain along with the putamen and frontal cortex in GBA-PD/DLB patients (Gegg et al., 2012; Kurzawa-Akanbi et al., 2012). However, not all brain regions show reduced GCase protein expression suggesting some regions are more susceptible than others. To model these brain regions accurately, a corresponding level of GCase protein expression should be reflected in the cell model created.

GCase protein expression is significantly reduced in a mouse neuroblastoma cell line overexpressing human WT α-synuclein (Yang et al., 2016). GCase protein expression is also significantly reduced in cultured fibroblasts from *GBA1* heterozygotes both with and without PD (McNeill et al., 2014; Garcia-Sanz et al., 2017). Furthermore, GCase protein expression is also significantly reduced in iPSC derived dopaminergic neurons from GBA-PD patients (Garcia-Sanz et al., 2017).

Therefore, GCase protein expression should ideally be reduced in L444P *GBA1* SH-SY5Y cells compared with WT *GBA1* SH-SY5Y cells to mirror what is reported in literature.

4.1.4. *GBA1* mRNA expression

As indicated in chapter 1.6.2.1, changes associated with *GBA1* mutation and in sporadic PD and DLB do not appear to be associated with any significant reduction in *GBA1* mRNA expression as evidenced in human tissue and animal or cell models (Gegg et al., 2012; Garcia-Sanz et al., 2017). However, overexpression of α-synuclein in SH-SY5Y cells does cause a reduction in *GBA1* mRNA expression (Gegg et al., 2012). Taking this into consideration, the cell model created for this study should not demonstrate any significant change in *GBA1* mRNA expression under basal levels of α-synuclein expression.

Taking into consideration the different approaches for modelling *GBA1* mutation *in vitro* and the associated advantages and disadvantages discussed in this chapter, we decided to use an overexpression model for this project. The overexpression of *GBA1* in SH-SY5Y cells provides a technically straightforward approach which is suitable for the study of UPR responses in the presence of *GBA1* mutation. This cell model is ideal for 'proof of concept' experiments which can identify new targets and test novel hypotheses before subsequent testing in a more translational model.

4.2. Aims and objectives

4.2.1. Aims

The aim of this chapter was to create a reproducible and consistent SH-SY5Y cell overexpression model of a pathogenic *GBA1* mutation (L444P) and evaluate the associated biochemical characteristics. The biochemical characteristics of the cell lines were investigated to determine if the cells accurately reflect the biochemical environment which is characterised by heterozygous *GBA1* mutation carriers. Establishing the cell lines created as viable models of *GBA1* mutation will facilitate their use in probing the molecular mechanisms linking GCase deficiency to LBD, namely the UPR.

4.2.2. Objectives

- Establish a method to identify cells expressing *GBA1* plasmids by cloning the *GBA1* open reading frame into a GFP tagged plasmid.
- Generate a mutant L444P *GBA1*-GFP plasmid by site directed mutagenesis
- Electroporate WT and L444P *GBA1* plasmids into SH-SY5Y cells
- Separate SH-SY5Y cells by expression of *GBA1*-GFP plasmids using fluorescence assisted cell sorting (FACS)
- Generate SH-SY5Y cells stably expressing *GBA1* plasmids by clonal selection
- Determine the effect of WT and L444P *GBA1* overexpression on the expression of GCase protein in SH-SY5Y cells by immunocytochemistry and western blot.
- Establish the cellular location of overexpressed WT and L444P GCase protein within SH-SY5Y cells by immunocytochemistry.
- Determine the effect of WT and L444P *GBA1* overexpression on *GBA1* gene expression globally in SH-SY5Y cells by quantitative PCR.
- Quantify GCase enzyme activity in WT and L444P *GBA1* overexpressing SH-SY5Y cells by performing GCase enzyme activity assays.
- Quantify the enzyme activity of other lysosomal enzymes: β-galactosidase and β-hexosaminidase to determine if L444P mutation causes a GCase specific or a general lysosomal effect. This will be achieved by performing enzyme activity assays.

- Establish whether *GBA1* mutation affects the cell viability of SH-SY5Y cells by performing PrestoBlue® and MTT assays.

4.3. Results

4.3.1. Creation of a GFP tagged *GBA1* plasmid

4.3.1.1. PCR amplification of *GBA1* ORF

Primers were successfully designed to amplify the *GBA1* ORF from the existing *GBA1* plasmid by PCR. **Figure 6** clearly shows bands at approximately 1600bp, the size of the ORF of *GBA1* according to OriGene technologies, the manufacturers of the *GBA1* containing plasmid used as the template.

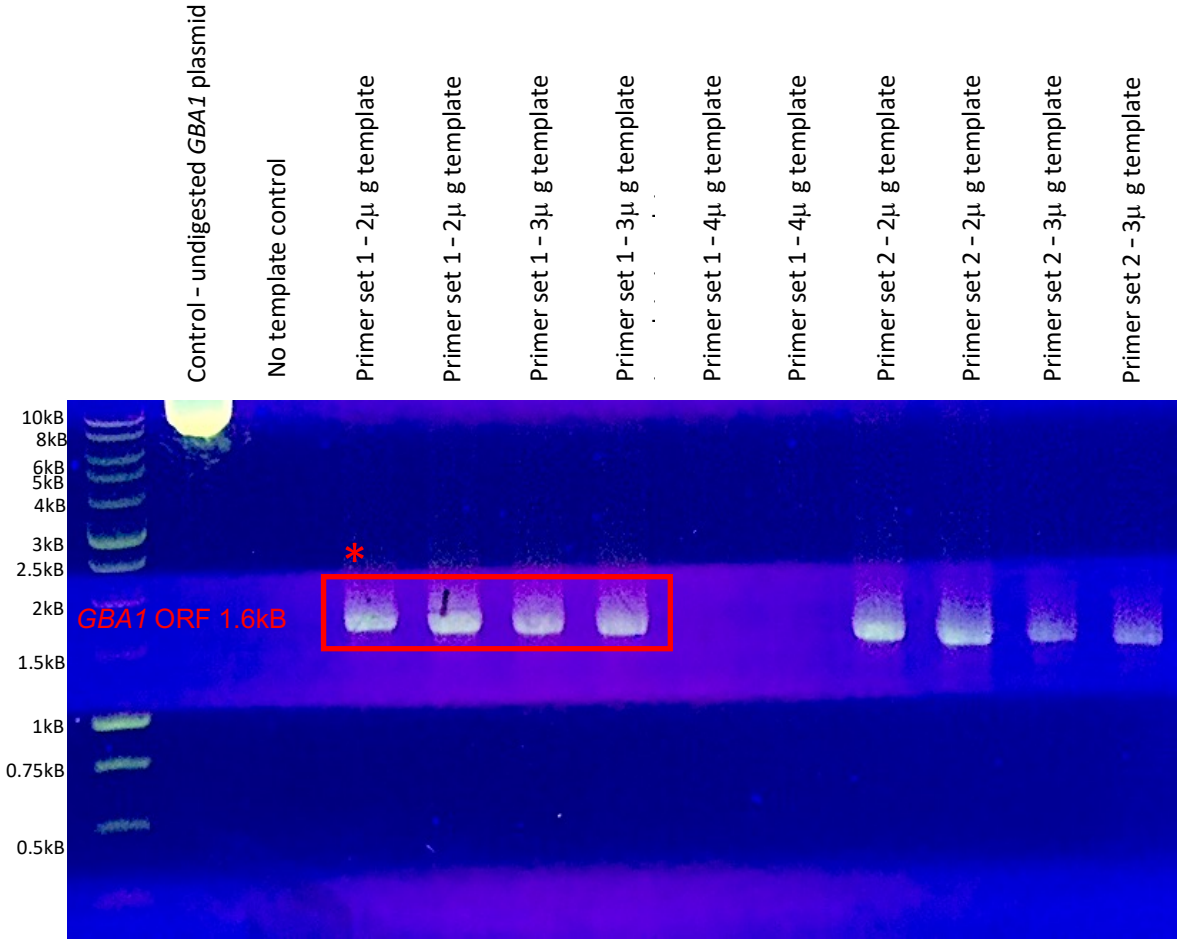

Figure 6 - Generation of *GBA1* ORF PCR products in preparation for TOPO TA cloning. * denotes PCR products taken forward for cloning.

Bands were excised and purified using the Wizard® SV Gel and PCR clean up kit (Promega, Wisconsin USA) according to manufacturer's instructions. PCR products from reaction number one were taken forward for cloning since the DNA had the most favourite characteristics: concentration 275.5 ng/µg and 260/280 value 1.67.

4.3.1.2. TOPO TA Cloning

GBA1 PCR products were subject to adenosine-tailing- addition of adenosine residues to the 3' end of PCR products in preparation for thymidine-adenosine (TA) assisted cloning. The TOPO® TA vector containing GFP is supplied linearized with topoisomerase enzyme covalently attached to phosphate molecules on the 3' terminal thymidine base of each stand. *GBA1* PCR products were successfully ligated to the TOPO GFP containing vector utilising topoisomerase enzyme, assisted by TA binding. Ligated plasmids were transformed into chemically competent Top10 *E.coli* for purification. Bacteria which had taken up the plasmid were selected by ampicillin challenge and plasmid DNA extracted. Plasmids from different colonies were subject to diagnostic restriction enzyme digest with *Apa*I to linearize the plasmid and determine if cloning had been successful **(Figure 7).**

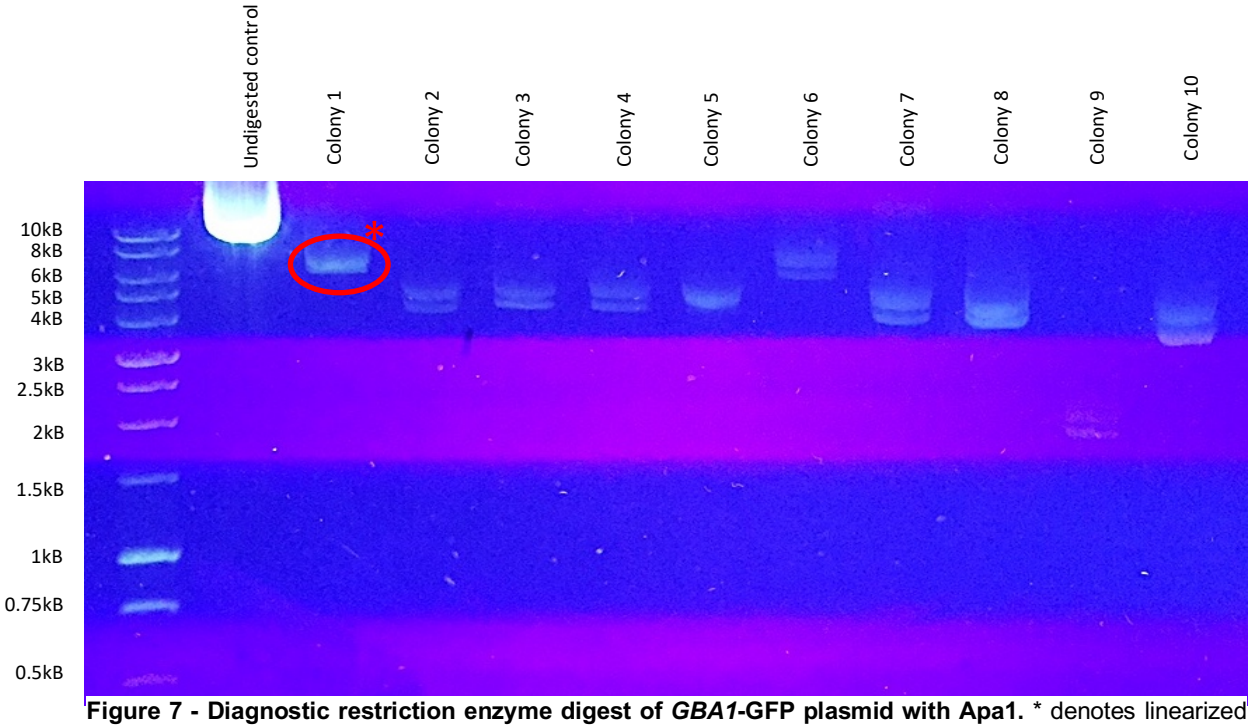

Figure 7 - Diagnostic restriction enzyme digest of *GBA1*-GFP plasmid with Apa1. * denotes linearized plasmid of the correct size, approximately 7770bp.

Figure 7 shows TOPO TA cloning has been successful in colony number one since the linearized plasmid is of the correct size – approximately 7770bp (6157bp GFP containing TOPO® vector + 1611bp *GBA1* ORF). Consequently, plasmids from this bacterial colony were sent for Sanger sequencing to confirm insertion of the *GBA1* ORF and to check correct orientation of the insert **(Figure 8).**

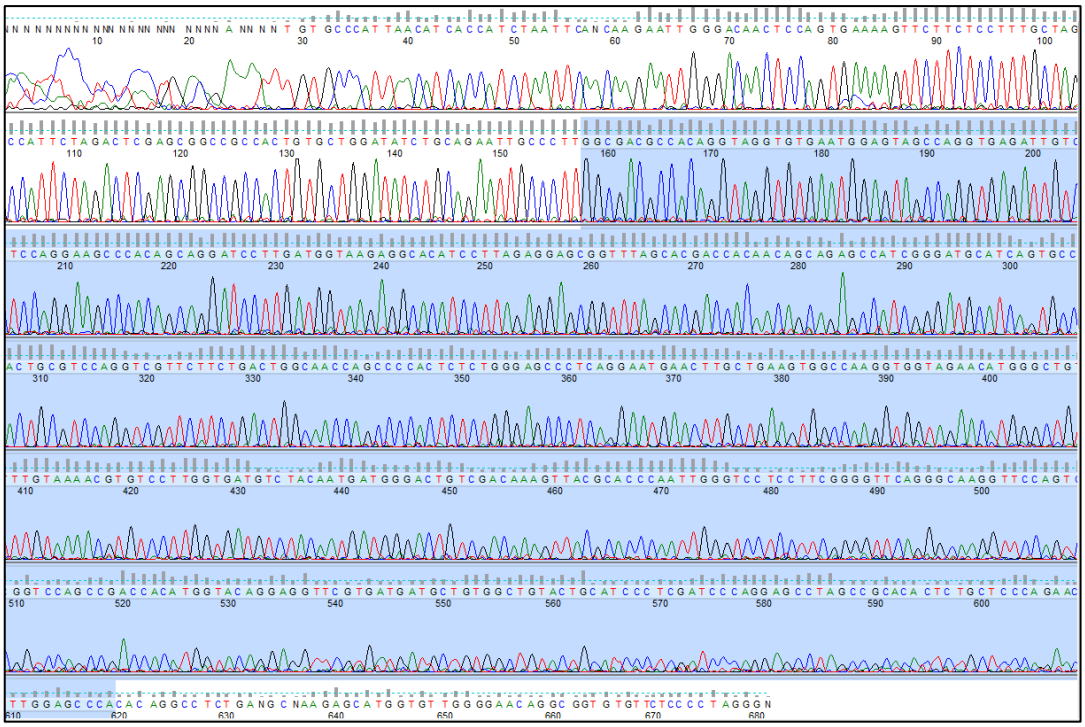

Figure 8 - Sanger sequencing of *GBA1* ORF in TOPO® TA GFP vector. Highlighted region shows the correct insertion of *GBA1* ORF nucleotide sequence flanked by the expected TOPO nucleotide sequence

4.3.2.Site directed mutagenesis of *GBA1*-GFP plasmid to create L444P *GBA1*-GFP

Primers were designed according to guidelines in the QuikChange® II Site-Directed Mutagenesis Kit (Agilent, Santa Clara, USA) protocol. These primers were complementary and encompassed the region of sequence containing the nucleotide which would be changed. Primers were complementary to the parent sequence i.e. the *GBA1* GFP plasmid, other than the insertion of the single nucleotide required to generate L444P mutation. The mutant plasmid was synthesised by PCR using the designed primers against the 'parent' *GBA1*-GFP plasmid template utilising *PfuUltra* High Fidelity DNA polymerase (Agilent, Santa Clara, USA). Mutant plasmids were separated from the 'parent' template by digestion with the restriction enzyme *Dpn1*, which only recognises hemi-methylated DNA, and as such selectively digests the 'parent template'. The mutant plasmids were transformed into XL1-blue supercompetent cells to repair 'nicks' in the DNA and to purify the plasmids. *E.coli* which had successfully taken up a plasmid were identified by ampicillin selection. Of these, bacteria which had taken up the mutant plasmid were identified by a blue white screen based upon functional recombination of the *lacZ* gene between a sequence in the synthesised plasmid found in the multiple cloning site (MCS) and a sequence in XL1-blue supercompetent *E.coli*. Functional β-galactosidase enzyme is produced which is able to cleave the artificial substrate X-Gal to form an insoluble blue pigment, 5,5'-dibromo-4,4'-dichloro-indigo.

Usually, the MCS has been altered to insert a gene of interest, and so recombination of *lacZ* does not occur, X-Gal is not cleaved, and colonies appear white, forming the basis of the screen. However, in this case, the plasmid component of *LacZ* has not been affected, and so bacteria of interest are able to produce functional β-galactosidase and subsequently the colonies are blue **(Figure 9).**

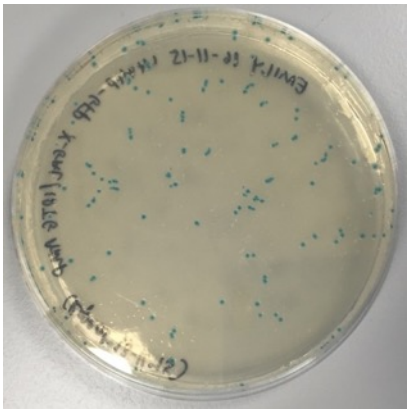

Figure 9 - Blue/White screen of *E.coli* for L444P *GBA1*-GFP plasmid

Plasmid DNA was extracted from bacterial colonies and sent for sanger sequencing to confirm the single nucleotide change within the *GBA1* ORF of thymidine to cytosine, in turn changing the amino acid from leucine (CTG) to proline (CCG) **(Figure 10).**

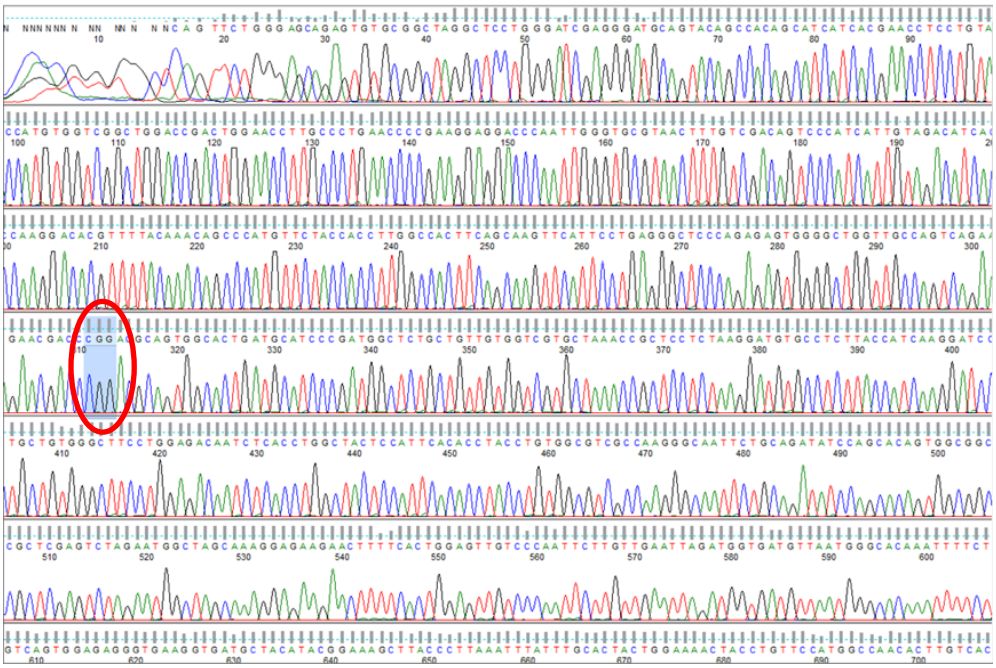

Figure 10 - Sanger sequencing confirming single nucleotide change to create L444P mutant *GBA1*-GFP plasmid. Chromatogram shows sequencing from the reverse primer. Highlighted area shows the change from CAG (leucine) to CGG (proline) on the anti-strand.

4.3.3.Amaxa® Nucleofection™ of wild type and L444P *GBA1*-GFP plasmids into SH-SY5Y cells

Previous attempts at transfection of the *GBA1*-GFP plasmid constructs into SH-SY5Y cells using calcium phosphate and Lipofectamine® proved to be unsuccessful. A new approach was taken using Amaxa® Nucleofection™, a form of electroporation. An optimised Nucleofection™ solution for SH-SY5Y was supplied and optimised Nucleofection™ parameters used according to the manufacturers protocol. Nucleofection™ of both the wild type and L444P *GBA1*-GFP plasmids was successful, with green fluorescence from the GFP tag visible under an inverted fluorescent microscope. Cells were subsequently checked for cell viability visually using Trypan Blue staining. 10μL of cell suspension was added to 10μL of Trypan Blue and the resultant solution visualised on a haemocytometer. The number of dead cells stained blue was calculated as a percentage of non-stained viable cells.

4.3.4.FACS of *GBA1*-GFP containing SH-SY5Y cells to create stable cell lines

Cells which had successfully undergone Nucleofection™ were prepared in a FACS buffer at the requisite cell density, alongside control cells – non-transfected SH-SY5Y and empty vector GFP plasmid transfected SH-SY5Y cells, in order to create the gating parameters. FACS was performed at a specialist FACS facility by a technician who determined the gating strategy. Cells with GFP fluorescence (wild type *GBA1*-GFP and L444P *GBA1*-GFP cells) were individually separated into separate wells of a 96-well plate in order to generate monoclonal cell lines **(Figure 11).** The transfection efficiency of both the wild type and L444P *GBA1*-GFP plasmid were relatively low but similar in both cases: approximately 0.1% of the total cell population screened by FACS. However, this was sufficient to fill a 96 well plate with individual cells to generate clones. These cells were maintained under normal conditions until they were confluent enough to be scaled up into flasks. As expected from literature, over 90% of the individual cells died, predominantly due to the combination of the physical effect of the FACS process and being grown from a single cell. Despite this, a stable monoclonal cell line was successfully generated for overexpressing wild type *GBA1* and overexpressing L444P *GBA1.*

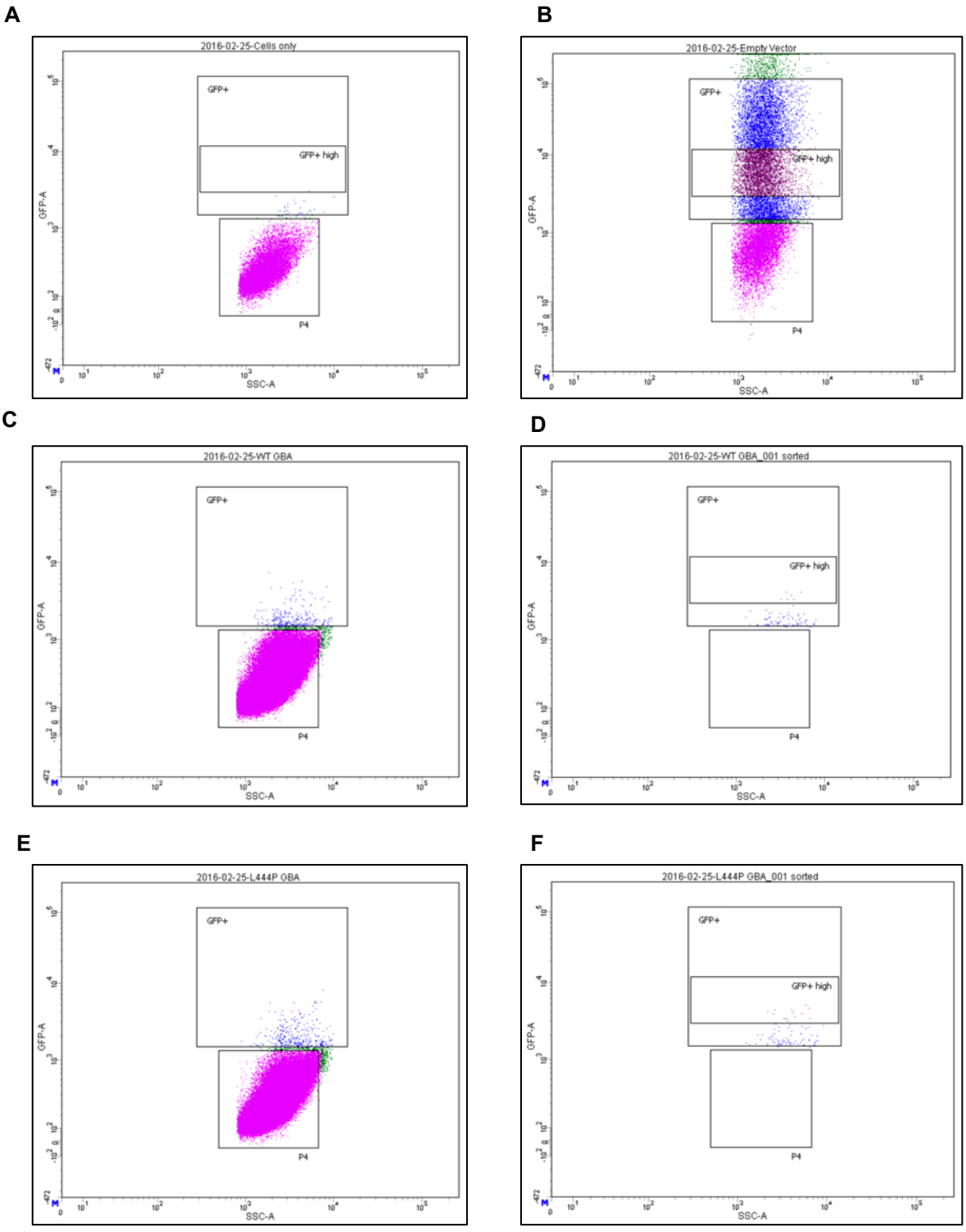

Figure 11 – FACS to separate cells based upon GFP fluorescence. (a) Cells only and (b) empty vector GFP transfected cell controls for gating strategy, (c) Wild type *GBA1* SH-SHSY cell population and (d) wild type *GBA1* SH-SY5Y sorted cells by GFP fluorescence, (e) L444P *GBA1* SH-SY5Y cell population and (f) L444P SH-SY5Y cells sorted by GFP fluorescence.

4.3.5.Evaluation of SH-SY5Y cell lines overexpressing wild type or L444P *GBA1*

4.3.5.1. GCase Protein

Control SH-SY5Y cells demonstrated endogenous levels of GCase protein which was further increased in both wild type *GBA1* and L444P *GBA1* overexpressing SH-SY5Y cell lines. This was visually demonstrated by immunocytochemistry **(Figure 12).**

A

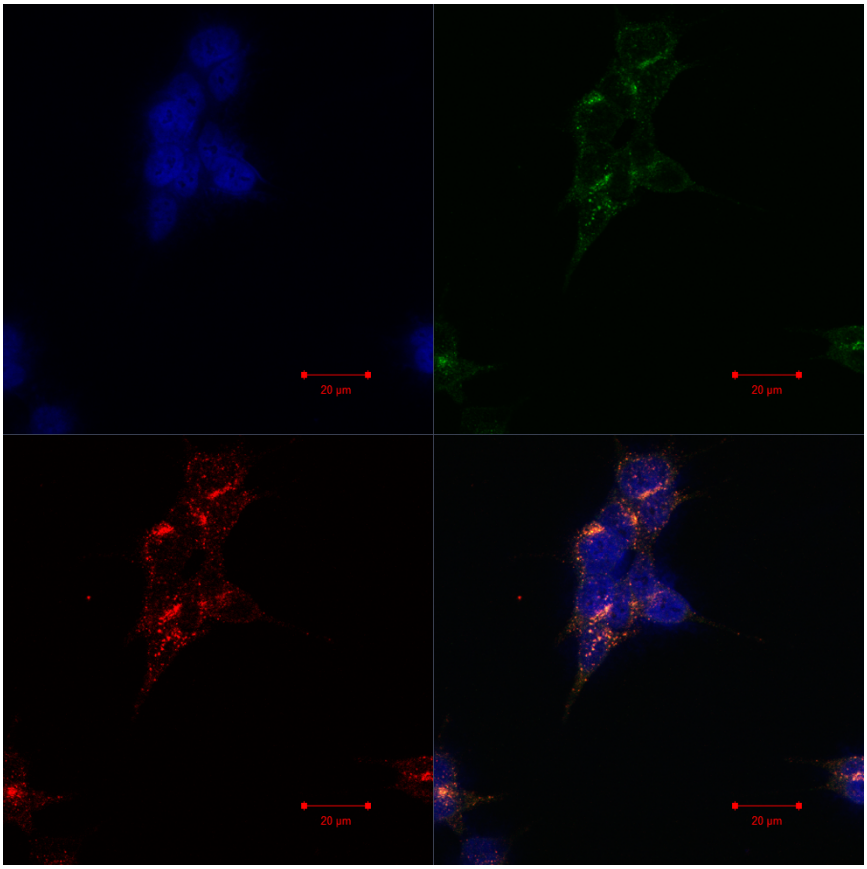

B

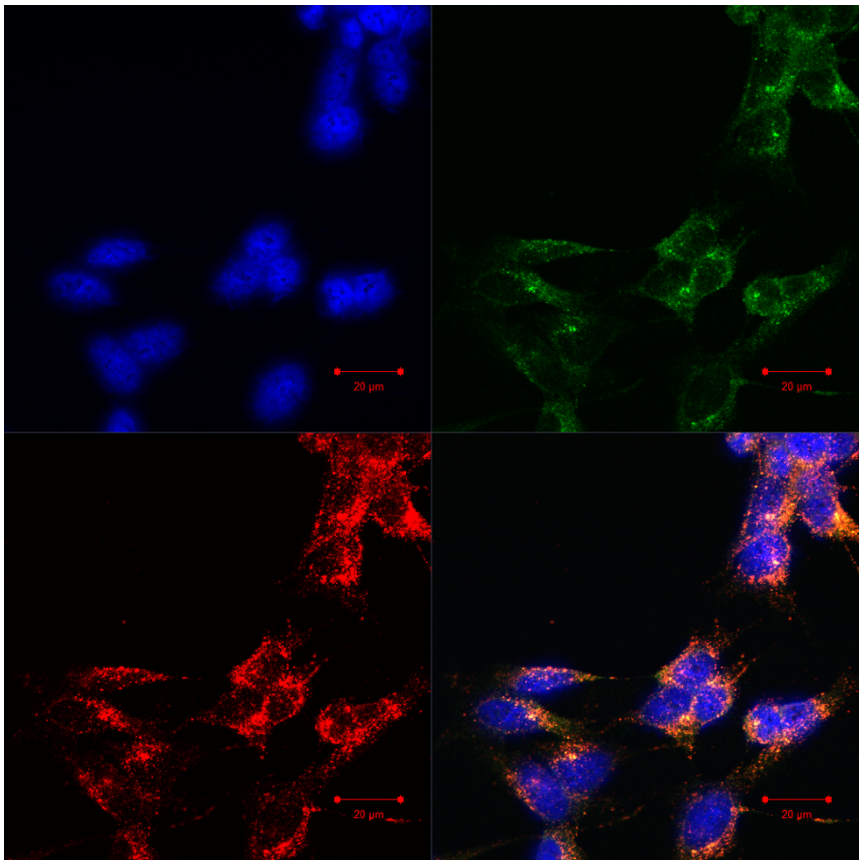

C

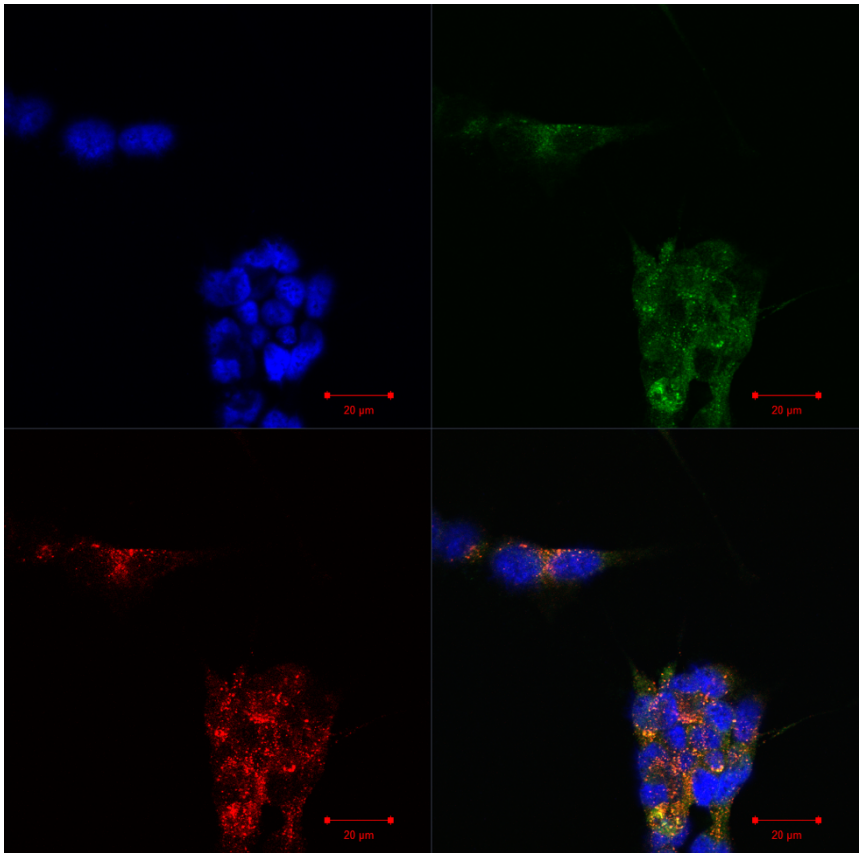

Figure 12 - Immunocytochemistry of (a) SH-SY5Y (b) WT *GBA1* SH-SY5Y (c) L444P *GBA1* SH-SY5Y cells. GCase protein is shown in red, calnexin green and DAPI in blue. Images were taken at x63 magnificantion with oil immersion. Scale bars shown at 20µM.

Cells were probed with calnexin antibody to try and ascertain the cellular location of GCase protein. Calnexin is a commonly used marker of endoplasmic reticulum membrane and the cis-Golgi (Lynes and Simmen, 2011). **Figure 12** shows a similar co-localisation pattern between GCase and calnexin in control SH-SY5Y and wild type *GBA1* SH-SY5Y cells. However, L444P *GBA1* overexpressing cells show a more diffuse staining pattern with isolated intense points of co-localisation with calnexin. This suggests the location of GCase is less well defined in the L444P *GBA1* mutant cells, implicating trafficking of GCase as an area for further investigation.

To quantify increased GCase protein expression in the overexpressing cell lines, semi quantitative western blotting was performed **(Figure 13)**. There was no statistical difference in GCase protein level between control SH-SY5Y cells and the overexpressing *GBA1* cell lines **(Figure 13).**

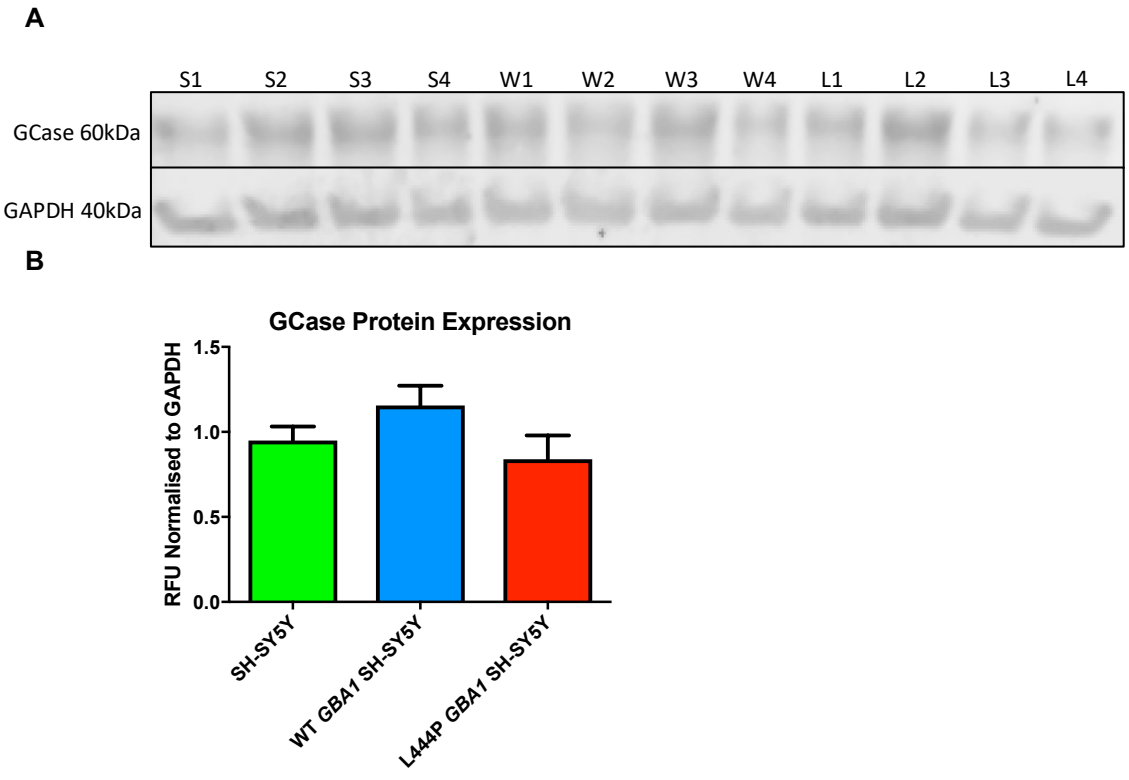

Figure 13 – GCase protein expression in *GBA1* cell lines (a) Representative western blot of GCase protein expression in SH-SY5Y cell lines. S=SH-SY5Y, W= WT *GBA1* SH-SY5Y, L= L444P *GBA1* SH-SY5Y (b) Quantitation and statistical analysis of western blot. Bars are mean ±SEM, one-way ANOVA, p=0.199, n=4 biological replicates

Since GFP tagged *GBA1* plasmids were used to transfect SH-SY5Y cells in order to create the stably overexpressing cell lines, western blot for GFP was performed to confirm overexpression of GCase as a consequence of *GBA1* plasmid transfection, as illustrated by immunocytochemistry **(Figure 12). Figure 14** shows strong bands in wild type and L444P *GBA1* mutant overexpressing cell lines at approximately 90kDa. This corresponds to the combined size of GCase protein (60kDa) and GFP (30kDa). This confirms that excess GCase in the overexpressing cell line is due to transfection with the GFP tagged *GBA1* plasmids and not an indirect consequence of the transfection process or conditions of stress.

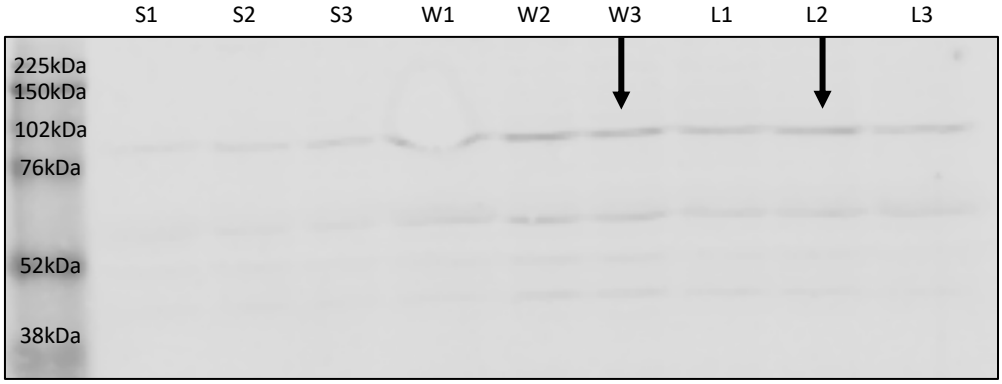

Figure 14 - Representative western blot for GFP as an indirect marker of transfected GCase protein. S=SH-SY5Y, W= WT *GBA1* SH-SY5Y, L=L444P *GBA1* SH-SY5Y

4.3.5.2. *GBA1* Gene Expression

Gene expression of *GBA1* was investigated in each of the cell lines using quantitative PCR **(Figure 15).** There is an indication of a trend suggesting *GBA1* gene expression is increased in wild type *GBA1* overexpressing cells compared with SH-SY5Y cells alone, as would be expected. Interestingly, these results suggest a reduction in *GBA1* gene expression in L444P *GBA1* mutant cells compared with wild type *GBA1* overexpressing cells, with the relative mRNA level similar to that seen in the control SH-SY5Y cells. This apparent reduction in gene expression between wild type and L444P *GBA1* overexpressing cells reaches statistical significance if a t-test is performed between the two groups (student's t-test, $p=0.0318$).

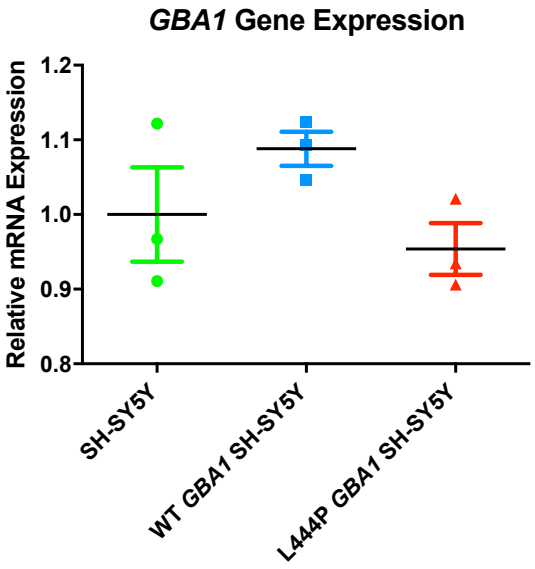

Figure 15 - Relative *GBA1* gene expression in overexpressing *GBA1* cell lines. Relative expression calculated by the $\Delta\Delta^{CT}$ method using *HPRT1* housekeeping gene. Data shown as mean ±SEM, one-way ANOVA, p=0.1672, n=3 biological repeats and 3 technical repeats

4.3.5.3. GCase Enzyme Activity

GCase enzyme activity assays were performed to establish the effect of L444P *GBA1* mutation on GCase enzyme activity of SH-SY5Y cells **(Figure 16)**.

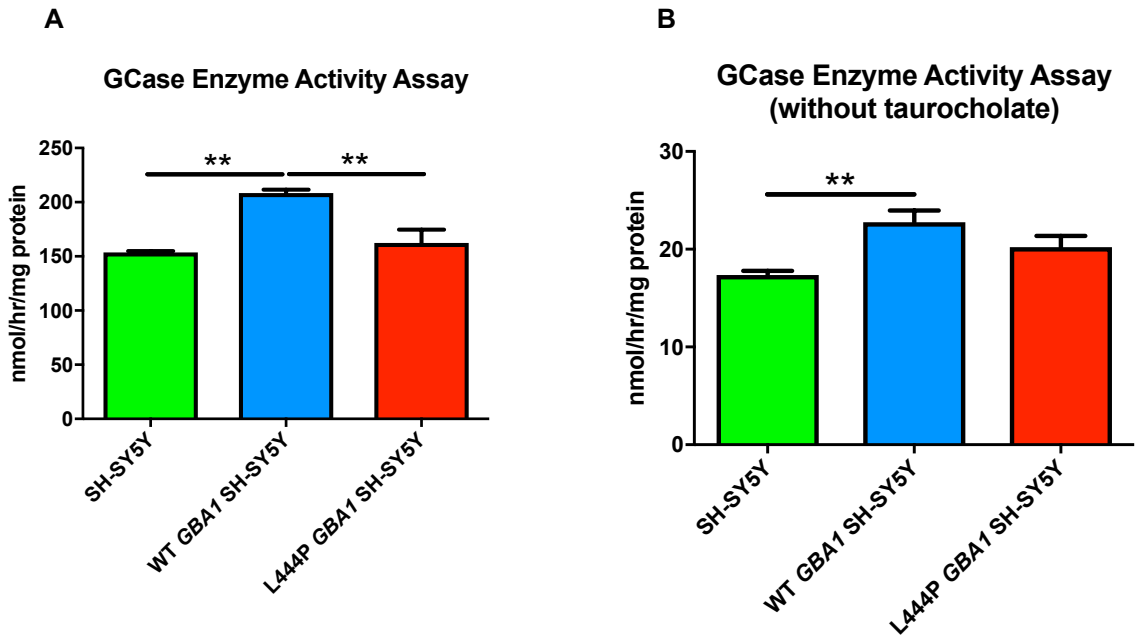

Figure 16 - GCase enzyme activity assay (a) assay performed in the presence of sodium taurocholate or (b) in the absence of sodium taurocholate. Data expressed as mean ±SEM, one-way ANOVA, Tukey's HSD, n=4 biological repeats and 3 technical repeats, **p=<0.01

In the presence of sodium taurocholate, an inhibitor of non-lysosomal glucocerebrosidase (Peters et al., 1976), GCase enzyme activity was significantly increased in wild type *GBA1* overexpressing cells when compared with control SH-SY5Y cells (one-way ANOVA, Tukey's HSD, p=0.0015), representing an increase of 35.7%. GCase enzyme activity was significantly reduced in L444P *GBA1* overexpressing cells when compared with wild type *GBA1* overexpressing cells (one-way ANOVA, Tukey's HSD, p=0.0046), with the enzyme activity at a similar level to control SH-SY5Y cells, representing a decrease of 28.4% **(Figure 16a)**. This suggests that L444P *GBA1* mutation reduces GCase enzyme activity.

In the absence of sodium taurocholate, GCase enzyme activity was significantly increased in wild type *GBA1* overexpressing cells when compared with control SH-SY5Y cells (one-way ANOVA, Tukey's HSD, p=0.0093). However, unlike in the presence of sodium taurocholate, enzyme activity remains at a similar level in L444P *GBA1* overexpressing cells compared with wild type

GBA1 overexpressing cells implying compensatory increase in non-lysosomal GCase activity **(Figure 16b).**

4.3.5.4. β-Galactosidase and β-Hexosaminidase Enzyme Activity

The activity of two related enzymes in the glycosphingolipid metabolism pathway were also examined in the cells; β-galactosidase and β-Hexosaminidase **(Figure 17).**

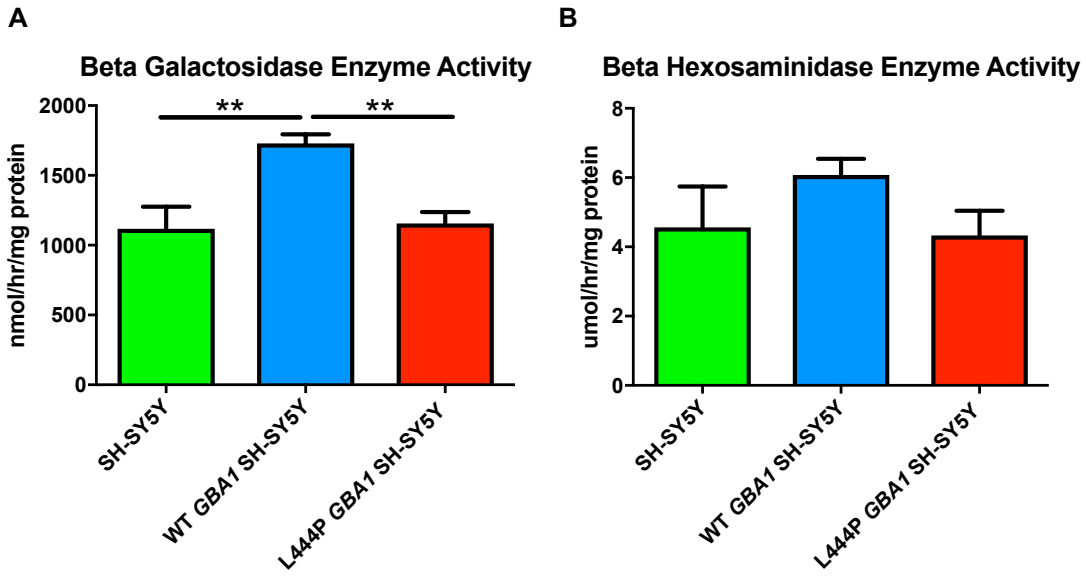

Figure 17 -Enzyme activity of (a) β-galactosidase and (b) β-hexosaminidase. Data expressed as mean ± SEM, one-way ANOVA, Tukey's HSD, n=6 biological repeats and 3 technical repeats, **p=<0.01

Overexpression of wild type *GBA1* caused a significant increase in β-galactosidase activity compared with control SH-SY5Y cells (one-way ANOVA, Tukey's HSD, p=0.007). β-galactosidase enzyme activity was significantly decreased in L444P *GBA1* overexpressing cells compared with wild type *GBA1* overexpressing cells (one-way ANOVA, Tukey's HSD, p=0.0065), with β-galactosidase enzyme activity resembling levels seen in control SH-SY5Y cells. This pattern mirrors GCase enzyme activity as seen in **Figure 16a.** There was no significant difference in the enzyme activity of β-hexosaminidase between the different cell lines.

4.3.5.5. Cell viability

4.3.5.5.1. PrestoBlue® assay

Cell viability was measured indirectly by PrestoBlue® assay. L444P *GBA1* overexpressing cells have significantly reduced cell viability when compared with wild type *GBA1* overexpressing cells (one-way ANOVA, Tukey's HSD, p=0.022). Interestingly, cell viability is significantly increased in wild type *GBA1* overexpressing cells compared to control SH-SH5Y cells (one-way ANOVA, Tukey's HSD, p=0.026) **(Figure 18).**

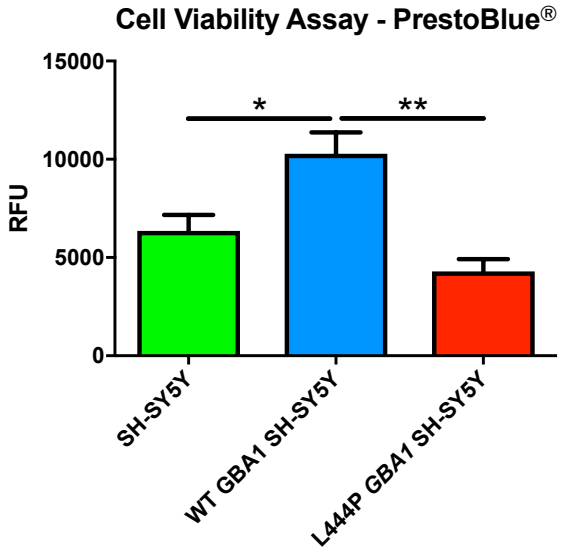

Figure 18 - PrestoBlue® cell viability assay. Data expressed as mean ±SEM, One-way ANOVA, Tukey's HSD, n=4 biological repeats and 3 technical repeats, *p=<0.05, **p=<0.01

4.3.5.5.2. MTT assay

Cell viability was also indirectly measured by MTT assay to corroborate findings in the PrestoBlue® assay. As with PrestoBlue®, a significant reduction in cell viability was seen in L444P *GBA1* overexpressing cells when compared with wild type *GBA1* overexpressing cells (one-way ANOVA, Tukey's HSD, p=0.010). Cell viability is also significantly reduced in L444P *GBA1* overexpressing cells when compared with control SH-SY5Y cells, which is not seen in the PrestoBlue® assay (one-way ANOVA, Tukey's HSD, (p=<0.001). Interestingly, cell viability is also significantly reduced in wild type *GBA1* overexpressing cells when compared with control SH-SY5Y cells alone (one-way ANOVA, Tukey's HSD, p=<0.001) **(Figure 19).**

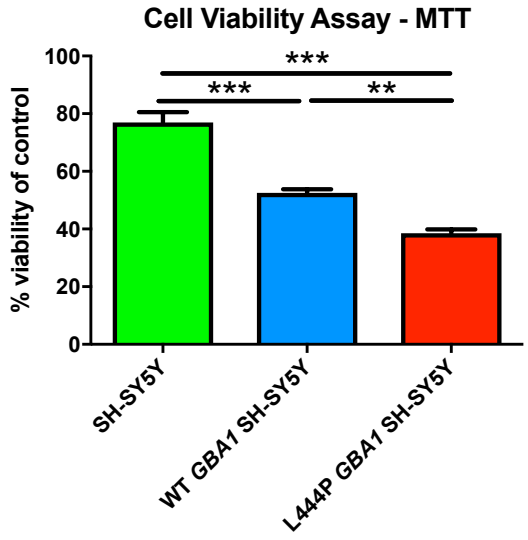

Figure 19 - MTT cell viability assay. Data expressed as mean ± SEM, One-way ANOVA, Tukey's HSD, n=4 biological repeats and 3 technical repeats, **p=<0.01, ***p=<0.001

4.3.5.6. Summary of biochemical characteristics of L444P *GBA1* SH-SY5Y cells compared with WT *GBA1* SH-SY5Y cells.

Biochemical characteristic	L444P *GBA1* SH-SY5Y
GCase enzyme activity	↓
GCase protein expression	No change
GBA1 mRNA	Ambiguous
β-Galactosidase enzyme activity	↓
β-Hexosaminidase enzyme activity	No change
PrestoBlue cell viability	↓
MTT cell viability	↓

Table 14 - Summary of biochemical characteristics tested in L444P *GBA1* SH-SY5Y cells compared with WT *GBA1* SH-SY5Y cells.

4.4. Discussion

4.4.1. Creation of stable SH-SY5Y cell lines overexpressing WT or L444P *GBA1*

SH-SY5Y cell lines stably expressing WT or L444P *GBA1* have been generated successfully. These cells provide a robust and reproducible system for testing the biochemistry and pathogenic pathways associated with *GBA1* mutations and LBD, specifically the unfolded protein response. The rational for creating monoclonal *GBA1* cell lines rather than using SH-SY5Y cells transiently transfected with *GBA1* plasmids was to reduce the effect of inter-cell variability when it came to the expression of *GBA1* and other cellular factors. Accordingly, the monoclonal cell lines generated reflect the homogenous characteristics of the clone selected, allowing for accurate contextual comparison of results between experiments.

Transfection efficiency of *GBA1*-GFP plasmids into SH-SY5Y cells was low. Several attempts were made at transfecting the SH-SY5Y cells with no success, including: calcium phosphate, Lipofectamine® 2000 (ThermoFisher, Massachusetts, USA) and Viromer® Red (Lipocalyx, Halle, Germany). A different approach, using electroporation utilising the Amaxa® Nucelofector™ system was successful to a degree. Since the experimental design was to separate cells individually by expression of the *GBA1*-GFP constructs, the low transfection efficiency was not necessarily a concern. At least 96 GFP positive cells for both the WT and L444P *GBA1* constructs were successfully transfected and separated by FACS. The reason behind the low transfection efficiency is not fully understood although SH-SY5Y are reported to be difficult to transfect cells (Martin-Montanez et al., 2010).

Cell survival following FACS assisted sorting into individual cells was extremely low. This result was not unexpected since this method of cell sorting is notoriously harsh on cells (Foo, 2013). Shear forces on individual cells as they pass through the nozzle can be extreme and particularly detrimental to fragile cells. Shear pressure can be adjusted, for example to 40 from 70 psi, however good separation of cells is more difficult at lower pressure. Despite the extent of cell death, a small number of cells did survive the process and went on to multiply, forming the new *GBA1* cell lines. Given the difficulties encountered in creating the cell lines, to date, cells lines have only been created from one clone for both the WT and L444P *GBA1* cells. Going forward,

experimental procedures will be repeated, and monoclonal cell lines created from at least two additional separate clones in order to confirm findings reported in this thesis.

Overexpression of *GBA1* as an experimental model has been used by other groups. L444P *GBA1* overexpression specifically has been performed in Sf9 cells (Montfort et al., 2004) and MES23.5 cells expressing human WT *SNCA* (Cullen et al., 2011). Overexpression of other *GBA1* mutations has also performed in MES23.5 and PC12 cells (Cullen et al., 2011). Whilst a relatively simple model, the *GBA1* SH-SY5Y cell lines generated in this study are suitable for biochemical pathway analysis, an objective of this project. Crucially, observations purposed to be related to L444P mutation need to be considered both against naïve SH-SY5Y cells and WT overexpressing SH-SY5Y cells. Although not in the scope of this current project, these cells could also be suitable for a simple *in vitro* screen of compounds for LBD based on GCase enzyme activity and ability to reverse biochemical changes assessed in this project and future projects utilising these cells.

4.4.2. Evaluation of stable SH-SY5Y cell lines overexpressing WT or L444P *GBA1*

The cell lines created in this chapter appear to reflect the necessary characteristics to confirm expression of *GBA1* plasmid constructs was successful. Immunocytochemistry clearly shows increased expression of GCase protein as reflected in the increased intensity of staining in the wild type and L444P *GBA1* cells compared with control SH-SY5Y cells **(Figure 12).** However, western blotting to quantify the increase in GCase protein did not indicate any significant difference **(Figure 13).** Western blotting using anti-GBA primary antibody produces a band at approximately 60kDa. Since the *GBA1* plasmid was constructed with the addition of GFP at the C-terminal, encoded GCase should be a fusion protein of GCase-GFP. Accordingly, overexpressed GCase protein in these cells should be approximately 90kDa. Western blotting using anti-GBA primary antibody reflects the levels of endogenous GCase protein in SH-SY5Y cells, explaining why these is no significant difference in the supposed GCase overexpressing cell lines. There were no bands visible at 90kDa when probing the nitrocellulose membrane with anti-GBA primary antibody, suggesting that the GFP tag on the overexpressed GCase protein may be shielding the epitope and preventing anti-GBA antibody binding. In order to confirm the overexpression of GCase protein, western blotting was performed using anti-GFP primary antibody. Strong bands for both the wild type and L444P *GBA1* overexpressing SH-SY5Y cells were seen at approximately 90kDa, corresponding specifically to the overexpressed GCase

fusion protein complete with GFP tag. However, feint bands were seen with control SH-SY5Y cells although not comparable in intensity. This may suggest the anti-GFP antibody lacks specificity. Western blot also indicates GFP reactivity at approximately 60kDa and 40kDa possibly reflecting trafficking and subsequent cleavage of the GCase-GFP fusion protein.

Further evidence to confirm successful expression of *GBA1* plasmid constructs in the cell lines created is demonstrated by the illustration of increased GCase enzyme activity in wild type *GBA1* cells compared with control SH-SY5Y reflecting the overexpression of GCase protein (35.7%, one-way ANOVA, Tukey's HSD, p=0.0015) **(Figure 16)**. However, overexpression of *GBA1* by qPCR was not statistically confirmed in wild type *GBA1* cells compared with SH-SY5Y cells although a trend was demonstrated **(Figure 15).** The small number of samples used for this analysis presumably underlies the variability in results preventing statistical significance.

4.4.3.Impact of L444P *GBA1* mutation on cell characteristics

Overexpressing L444P *GBA1* SH-SY5Y cells demonstrate similar characteristics as described in models of GCase deficiency and in GBA-PD patients (Sanchez-Martinez et al., 2016; Garcia-Sanz et al., 2017). Most notably, in the presence of sodium taurocholate, L444P *GBA1* cells show significantly reduced GCase enzyme activity when compared with wild type *GBA1* cells (28.4%, one-way ANOVA, Tukey's HSD, p=0.0046). A significant reduction was not seen in GCase enzyme activity when comparing control SH-SY5Y cells with L444P *GBA1* cells, indicating the observed reduction is due to defective GCase enzyme which has been overexpressed in the cells and not due to changes in endogenous GCase enzyme activity **(Figure 16).** In order to determine the GCase enzyme activity attributable specifically to *GBA1*, GCase enzyme activity assays were performed both in the presence and absence of sodium taurocholate, an inhibitor of non-lysosomal GCase (Peters et al., 1976). Interestingly, in the absence of sodium taurocholate, no difference is seen in GCase enzyme activity between wild type *GBA1* and L444P *GBA1* cells implicating a compensatory mechanism by which *GBA2* and *GBA3* derived GCase enzyme boosts total GCase enzyme activity within mutant cells. Compensatory increases in *GBA2* related GCase enzyme activity in response to *GBA1* mutation has been suggested previously (Yildiz et al., 2006; Burke et al., 2013).

The significant reduction in *GBA1* GCase enzyme activity (28.4%) seen in the L444P *GBA1* overexpressing SH-SY5Y cells compared with wild type *GBA1* cells is similar to that reported in fibroblasts derived from PD patients harbouring heterozygous L444P (35%) and N370S (32%) mutation in *GBA1* (Sanchez-Martinez et al., 2016; Garcia-Sanz et al., 2017). The reduction in enzyme activity seen here does fall short of the 50% reported in iPSC derived dopaminergic neurons from GBA-PD patients (Schondorf et al., 2014; Fernandes et al., 2016) and post mortem brain (Gegg et al., 2012) but does reflect more subtle reductions in GCase enzyme activity seen in the substantia nigra of post mortem sporadic PD brain (33%) (Gegg et al., 2012). It is interesting that in a study which uses overexpression of mutant *GBA1* plasmids into MES23.5 and PC12 cells, the same approach taken in this study, no difference was seen in GCase enzyme activity (Cullen et al., 2011). The impact of the background in different cells lines needs to be taken into account when generating cell models of GCase deficiency. Taking into consideration the variation of GCase enzyme activity associated with different model systems and in patients, the SH-SY5Y overexpression model created for this study appears to be a good representation of the predominant biochemical defect of reduced GCase enzyme activity which is fundamental to associated pathology.

In addition to a significant reduction in GCase enzyme activity, L444P *GBA1* mutant cells also demonstrate a significant reduction in β-galactosidase enzyme activity compared with wild type *GBA1* overexpressing cells (66.8%, one-way ANOVA, Tukey's HSD, p=0.0065) **(Figure 17).** Overexpression of WT *GBA1* also causes a significant increase in β-galactosidase enzyme activity compared with control SH-SY5Y cells (64%, one-way ANOVA, Tukey's HSD, p=0.007). Situated directly upstream of the GCase substrate GluCer, reduced activity of β-galactosidase suggests *GBA1* mutations impact other elements of the glycosphingolipid metabolism pathway perhaps either directly through alterations to the lipid composition of cells or indirectly due to pathological changes to the lysosome. However, total β-hexosaminidase activity, situated further upstream from GCase and β-galactosidase activity is not significantly altered in response to overexpression of either wild type or L444P mutant *GBA1* **(Figure 17).** This could be a consequence of assaying total β-hexosaminidase activity rather than considering α and β hexosaminidase activity independently. The observation of unaltered β-hexosaminidase is however consistent with reports in GBA-PD fibroblasts (Schondorf et al., 2014; Garcia-Sanz et

al., 2017), human post mortem brain tissue (Chiasserini et al., 2015) and GD mouse models (Sardi et al., 2013).

Immunocytochemistry indicates that L444P GCase protein is differentially located from wild type GCase protein whether overexpressed or endogenous **(Figure 12).** GCase staining appears to be more diffuse throughout L444P *GBA1* mutant cells whilst staining is more focussed in endogenous and wild type overexpressing *GBA1* cells. Furthermore, co-localisation with calnexin is different in L444P *GBA1* cells. The literature indicates that approximately 50% of L444P mutant GCase protein is retained within the endoplasmic reticulum (ER) (Bendikov-Bar et al., 2011) and so the diffuse expression of mutant L444P GCase in this cell model may be a reflection of retention in the diffuse and widespread ER, compared with more compact lysosomes. Whilst co-localisation with calnexin is different with L444P GCase the specific localisation of mutant GCase in this specific cell model remains inconclusive.

The overexpression of both wild type and L444P *GBA1* had a significant impact upon cell viability indirectly measured through PrestoBlue® and MTT assay. PrestoBlue® assay showed a significant increase in cell viability in wild type *GBA1* overexpressing cells compared to SH-SY5Y controls **(Figure 18)**. This implies that overexpression of wild type *GBA1* may provide a protective function. However, MTT assay shows a significant decrease in cell viability upon overexpression of wild type *GBA1* **(Figure 19)**. The difference in response may be due to the nature of the assays used. PrestoBlue® is a resazurin based assay that measures cell proliferation through the reduction ability of cells. MTT assay on the other hand measures the metabolic activity of NAD(P)H dependent cellular oxidoreductase enzymes capable of reducing the tetrazolium dye MTT into insoluble formazan. Enhanced cell viability as seen in the PrestoBlue® assay may be reflecting the protective impact of GCase against cell stresses, whilst the MTT assay is reflecting increased stress and energy involved in the overexpression of protein regardless of mutation status. Interestingly, L444P *GBA1* mutant cells had significantly reduced cell viability compared with wild type *GBA1* overexpressing cells in both PrestoBlue® and MTT assays suggesting that L444P *GBA1* mutation is detrimental to cell survival.

4.4.4.Limitations and further study

Whilst a reduction in GCase enzyme activity is illustrated in L444P *GBA1* cells, the method used does not definitively describe the reduction of GCase enzyme activity specifically within the lysosome. This is an important consideration since *GBA1* derived GCase is lysosomal specific. Additionally, some studies suggest non-lysosomal GCase derived from *GBA2* and *GBA3* may compensate for reduced activity of lysosomal GCase in order to limit substrate accumulation (Burke et al., 2013). Whilst the addition of sodium taurocholate to the GCase enzyme activity does account for *GBA2* derived GCase enzyme activity to an extent, the findings of this study could be complemented by fractionating cell lysates to isolate lysosomes for the testing of GCase enzyme activity.

Localisation of L444P GCase in this cell model remains inconclusive. Co-localisation of GCase with calnexin did not definitively show retention of L444P GCase in the ER. Despite calnexin being widely used as a marker of the ER, it may not have been the best choice for co localisation with a potentially misfolded protein since calnexin protein can shuttle between the ER membrane, specifically the mitochondrial associated membrane, to the peri-nuclear ER quality control compartment upon ER stress caused by unfolded proteins (Myhill et al., 2008; Lynes and Simmen, 2011)**(Figure 20).** This ability of calnexin to translocate within the ER and early Golgi adds another variable to the precise location of any co-localised proteins.

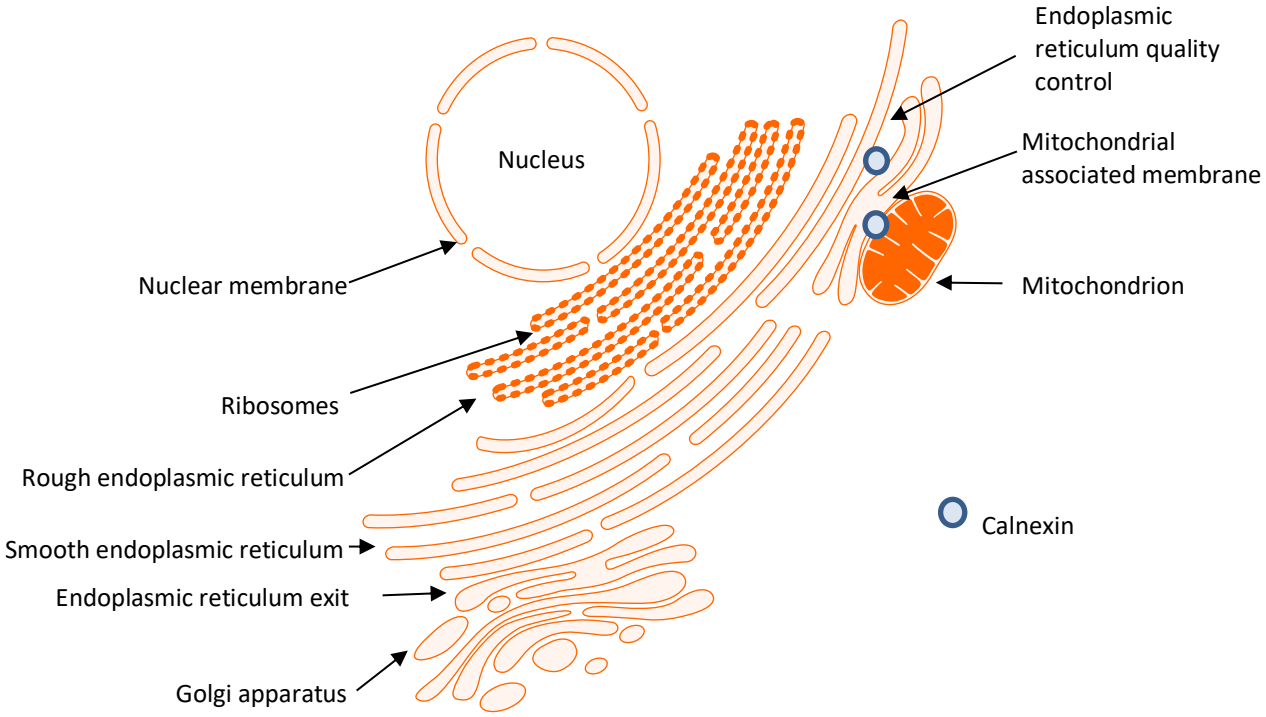

Figure 20 - Localisation of calnexin

Further studies to elucidate the precise location of L444P GCase should include co-localisation with a lysosomal marker such as LAMP. Furthermore, endoH digestion of cell lysates should be performed. Endo-H is a specific endoglycosidase that can distinguish between high mannose sugars and a mature *N*-glycan complex (Koide and Muramatsu, 1974). As GCase matures and is trafficked through the ER and Golgi, Golgi mannosidase II removes two mannose residues in the mid-Golgi (Erickson et al., 1985). Therefore, endo-H distinguishes between glycoproteins that have not reached the mid-Golgi and are most likely retained in the ER and mature glycoproteins.

Further investigation of the impact of overexpressed *GBA1* on cell viability would be an interesting expansion of this work to establish definitively whether L444P *GBA1* does impact cell viability. The repercussions of confirming reduced cell viability in association with L444P *GBA1* mutation could be significant since factors such as apoptosis and necrosis could be implicated. Assays such as lactose dehydrogenase and TUNEL (terminal deoxynucleotidyl transferase dUTP nick-end labelling assay) are options to help explore this area further. Furthermore, it would be interesting to investigate mitochondrial function within the cell lines created to establish whether overexpression of wild type *GBA1* does in fact boost mitochondrial function and whether L444P

GBA1 mutant cells have dysfunctional mitochondria. Since the initiation of mitochondrial apoptosis can be signalled by the UPR, reduced cell viability in *GBA1* mutant cells is further justification for the investigation of UPR responses described in this thesis.

5. Investigating the Unfolded Protein Response (UPR) in wild type and L444P *GBA1* overexpressing SH-SY5Y cells – XBP1

5.1. Introduction

The endoplasmic reticulum (ER) is a key cellular organelle which coordinates the synthesis, folding and structural maturation of at least a third of all cellular proteins (Hetz et al., 2015). Evidence suggests that upwards of 30% of all polypeptides translocated into the ER fail quality control mechanisms that ensure proper folding (Schubert et al., 2000). Misfolded proteins which fail ER quality control are removed to the cytosol for ubiquitination and degradation by the 26S proteasome, a process known as ER associated degradation (ERAD) (Vembar and Brodsky, 2008).

However, ER stress can also trigger an adaptive signal transduction pathway called the unfolded protein response (UPR). The UPR allows cells to manage protein misfolding by temporarily reducing *de novo* protein synthesis and improving the folding and clearance capacity of the ER (Ron and Walter, 2007). However, if these responses do not adequately reduce ER stress, the UPR can signal to initiate apoptosis (Tabas and Ron, 2011).

5.1.1. The unfolded protein response

Misfolded proteins within the ER are detected by three transmembrane UPR sensors which have luminal domains that sense the protein folding environment in the ER, and cytoplasmic effector domains which interact with transcriptional or translational apparatus (Ron and Walter, 2007). These are: double stranded RNA-activated protein kinase-like endoplasmic reticulum kinase (PERK); activating transcription factor 6 (ATF6); and inositol-requiring kinase 1α (IRE1α) (Ron and Walter, 2007).

Under basal conditions, the ER chaperone BiP constitutively binds to the luminal domains of the ER sensors, preventing activation (Bertolotti et al., 2000). However, changes to protein folding and ER stress promote a reversible dissociation of BiP from the luminal domains of PERK and IRE1α triggering signal transduction (Bertolotti et al., 2000). The dissociation of BiP, analogous

to ER stress signals, selectively activates downstream cascades **(Figure 21).** Activation of the first discovered UPR sensor, IRE1α (Hetz et al., 2015) and the corresponding signal cascade is discussed further in this chapter.

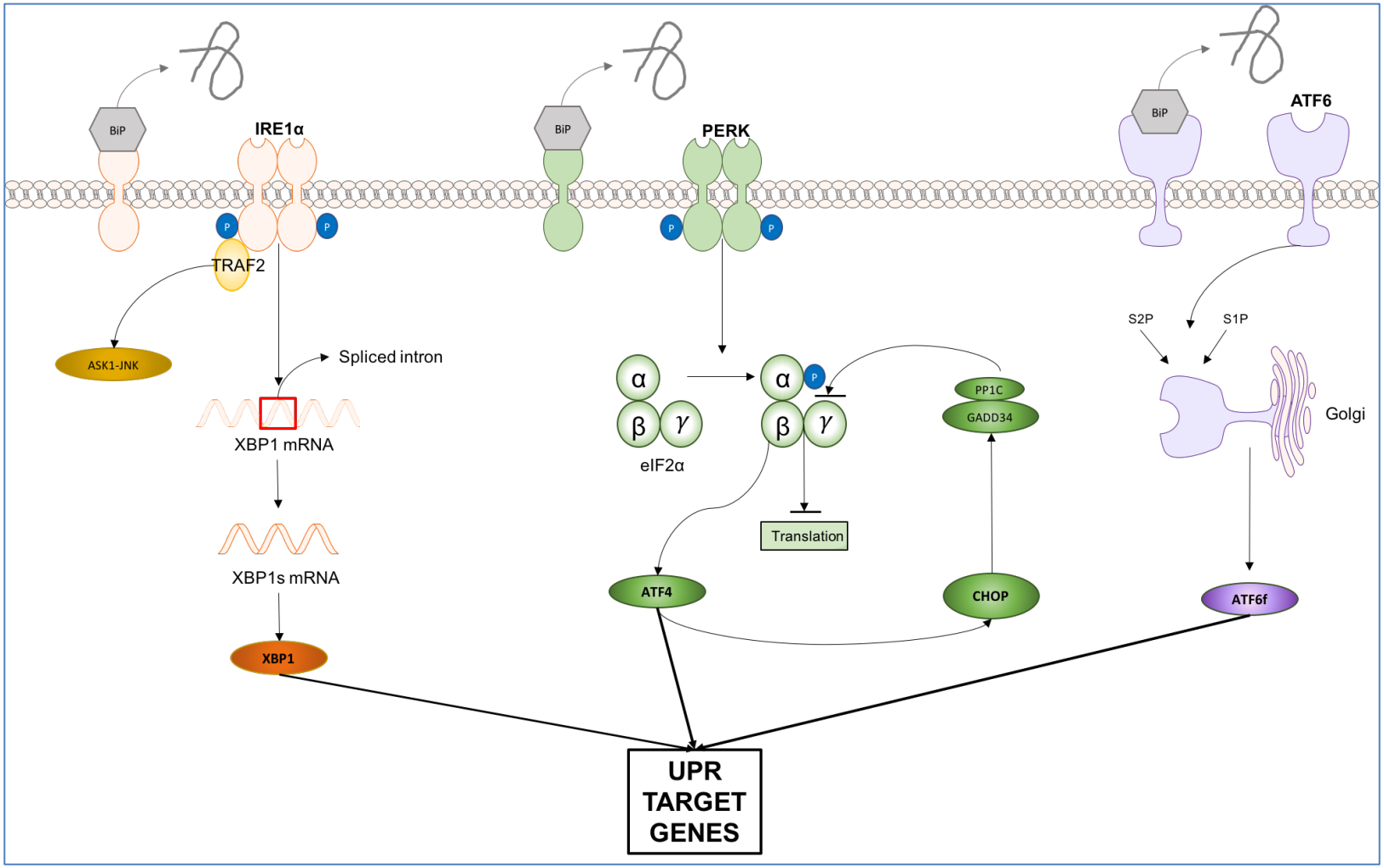

Figure 21 - The unfolded protein response signalling pathways. Adapted from (Hetz et al., 2013)

5.1.2.IRE1α pathway

IRE1α is an ER resident type 1 transmembrane protein; a bifunctional enzyme with both Ser/Thr protein kinase and site-specific endoribonuclease activities associated with the cytoplasmic domain, both regulated by an intrinsic kinase module (Korennykh et al., 2009). IRE1α senses ER stress through the luminal domain causing oligomerization in the plane of the membrane allowing for trans-autophosphorylation of juxtaposed kinase domains (Credle et al., 2005; Korennykh et al., 2009). Oligomerisation can be triggered directly by the binding of unfolded proteins to the IRE1α luminal domain, which bears resemblance to the peptide binding domains of major histocompatibility complex, or through the release of oligomerization repressing chaperones including BiP(Ron and Walter, 2007). Trans-autophosphorylation of the kinase domain of IRE1α causes activation of the endoribonuclease domain resulting in cleavage of the only known IRE1α substrate: XBP1 mRNA (Calfon et al., 2002).

Endoribonuclease activity of activated IRE1α catalyses the excision of a 26-nucleotide intron within XBP1 mRNA, causing a shift in the codon reading frame, generating a stable and active transcription factor known as XBP1s (Calfon et al., 2002). XBP1s controls the upregulation of a pool of UPR related genes involved in processes including: protein folding, protein entry to the ER, ERAD and secretion (Lee et al., 2003). Furthermore, XBP1s also indirectly regulates the biosynthesis of the ER and Golgi by enhancing activity of enzymes related to phospholipid biosynthesis (Sriburi et al., 2004). Additioanlly, XBP1s can heterodimerize with other transcription factors to mediate widespread gene expression, most notably in conjunction with ATF6 (Lee et al., 2003; Acosta-Alvear et al., 2007). Un-spliced nascent XBP1, XBP1u, also contributes to the functioning of the IRE1α pathway since it has a regulatory function involved in translational pausing and efficient targeting and splicing of *XBP1*u mRNA (Yanagitani et al., 2011).

IRE1α activity is also associated with the degradation of RNA known as regulated IRE1-dependent decay (RIDD) (Hollien and Weissman, 2006). RIDD is sequence specific and targets mRNA encoding proteins that are localised in the cytosol, nucleus, ER or secreted, (Maurel et al., 2014). However, ER localised mRNA is preferentially targeted by IRE1α activation (Hollien and Weissman, 2006; Maurel et al., 2014). Basal RIDD is required to maintain ER homeostasis although RIDD activity increases under ER stress (Maurel et al., 2014). During adaptive UPR

responses, IRE1α conducts RIDD on mRNAs encoding ER-translocating proteins to prevent further increases in protein folding demand within the ER (Han et al., 2009; Chen and Brandizzi, 2013). However, persistent and unresolved ER stress causes oligomerization of IRE1α which surpasses a threshold resulting in activation of apoptosis through RIDD, specifically the repression of anti-apoptotic mRNAs (Ghosh et al., 2014) and degradation of adaptive UPR target genes, including BiP (Han et al., 2009)

5.1.3.ER retention of mutant GCase

Mutant GCase species undergo variable levels of ER retention due to misfolding and undergoes ERAD (Ron and Horowitz, 2005; Bendikov-Bar et al., 2011; Bendikov-Bar and Horowitz, 2012). The degree of ER retention and ERAD is considered one of the predominant factors which determines GCase enzyme activity and severity of GD symptoms (Bendikov-Bar and Horowitz, 2012).

Pharmacological chaperones, small molecules which bind misfolded proteins in the ER, assisting folding and trafficking have proven to be effective in improving stability and subsequent delivery of mutant GCase to lysosomes thereby enhancing GCase enzyme activity (Bendikov-Bar and Horowitz, 2012; Migdalska-Richards and Schapira, 2016). Ambroxol, a mucolytic drug identified as a GCase chaperone through a screen of a FDA approved chemical library (Maegawa et al., 2009), significantly increases brain GCase enzyme activity in wild type, L444P/WT *GBA1* and α-synuclein overexpressing mice (Migdalska-Richards et al., 2016). Furthermore, Ambroxol reduces α-synuclein accumulation in an α-synuclein overexpressing mice (Migdalska-Richards and Schapira, 2016). More recently, the ability of oral Ambroxol to cross the blood brain barrier and significantly enhance GCase enzyme activity in the brain of healthy non-human primates has also been reported (Migdalska-Richards et al., 2017). The *in vivo* success of Ambroxol in enhancing brain GCase enzymatic activity and reducing α-synuclein accumulation (Sriburi et al., 2004; Migdalska-Richards et al., 2016) has highlighted the retention of mutant GCase enzyme in the ER as a key pathological event. An indirect consequence of mutant GCase retention could conceivably be ER stress and therefore UPR activation (Bendikov-Bar and Horowitz, 2012), the focus of both this and the following chapter.

5.1.4. Activation of the UPR in association with *GBA1* mutation and synucleinopathy – BiP expression.

Upregulation of BiP protein expression is an indirect measure of global UPR activation (Bertolotti et al., 2000) Expression of BiP is significantly increased in the putamen of GBA-PD human post mortem brain tissue by 26% and in sPD by 28% (Gegg et al., 2012). This implies that mutant GCase is implicated in the activation of UPR responses. However, BiP protein expression is also significantly increased in the cingulate gyrus and parietal cortex of PDD and DLB human post mortem tissue without *GBA1* mutation when compared with controls (Baek et al., 2016). The finding of enhanced BiP protein expression independent from *GBA1* mutation could suggest activation of the UPR is not a direct effect of *GBA1* mutation, rather a consequence of α-synuclein accumulation and neurodegeneration. Conversely, BiP protein expression has been reported to significantly decrease in the frontal cortex of a cohort of PD and DLB patients regardless of *GBA1* mutation status (Kurzawa-Akanbi et al., 2012). 'Healthy' control patients carrying a heterozygous mutation in *GBA1* also show similar reduction in BiP expression to PD/DLB patients in the frontal cortex (Kurzawa-Akanbi et al., 2012).

Cultured fibroblasts generated from GD patients exhibit significantly increased expression of BiP mRNA and protein (Maor et al., 2013; McNeill et al., 2014; Braunstein et al., 2018). A significant increase in BiP expression is also reported in fibroblasts generated from *GBA1* heterozygous PD patients, an increase which is significantly reduced upon treatment with the pharmacological chaperone Ambroxol (Maor et al., 2013; McNeill et al., 2014; Sanchez-Martinez et al., 2016; Garcia-Sanz et al., 2017). Intriguingly, BiP expression is also significantly increased in fibroblasts from 'healthy' *GBA1* mutation carriers (McNeill et al., 2014). Since α-synuclein is predominantly a neuronal protein, fibroblasts have very low expression of α-synuclein, implying the impact of mutant GCase on ER stress and activation of the UPR is independent from α-synuclein mediated effects (McNeill et al., 2014). Confirming the importance of the presence of misfolded GCase, UPR activation is not witnessed in association with CβE treatment nor in the absence of GCase protein (Farfel-Becker et al., 2009; Maor et al., 2013).

Further *in vitro* evidence of activated UPR comes from iPSC derived dopaminergic neuronal cultures from GBA(N370S)-PD patients which also demonstrate significant upregulation of BiP

(Fernandes et al., 2016). However, evidence of UPR activation is not universal in association with *GBA1* mutation. Transient transfection of WT human α-synuclein into MES23.5 cells expressing mutant *GBA1* does not result in activation of the UPR as assessed by BiP expression (Cullen et al., 2011).

In vivo, BiP protein expression is significantly enhanced by 320% in the substantia nigra of a mouse model of α-synuclein overexpression targeted specifically to the nigrostriatal pathway (Bellucci et al., 2011). Furthermore, BiP immunoreactivity is co-localised with α-synuclein immuno-positive inclusions (Bellucci et al., 2011). Overexpression of BiP protects dopaminergic neurons and improves motor performance in rat models of PD induced by direct injection of AAVs encoding human α-synuclein into the SNpc (Gorbatyuk et al., 2012). It is also documented that age-related decline in BiP expression makes dopaminergic neurons more vulnerable to α-synuclein, presumably due to reduced availability of BiP to act as a hold on UPR activation (Salganik et al., 2015). *Drosophila* generated with double heterozygous *GBA1* mutation resulting in 30% GCase enzyme activity, mirroring carriers of *GBA1* mutation, also exhibit a significant increase in the expression of BiP (Maor et al., 2013). Ubiquitous ectopic expression of human N370S or L444P mutant GCase in *Drosophila* also significantly increases mRNA expression of BiP (Maor et al., 2013).

5.1.5. Activation of the IRE1α pathway in association with *GBA1* mutation and synucleinopathy

Activation of the IRE1α pathway of the UPR is predominantly confirmed through the expression of the downstream effector sXBP1(Calfon et al., 2002). Splicing of XBP1 is not universally seen in human post mortem brain tissue from GBA-PD or sPD patients when compared with control brains (Gegg et al., 2012). Transient transfection of WT human α-synuclein into MES23.5 cells expressing mutant *GBA1* also does not exhibit activation of the UPR as monitored by XBP1 splicing (Cullen et al., 2011). However, fibroblasts generated from GD patients do exhibit significantly increased expression of spliced XBP1 as do fibroblasts generated from heterozygous *GBA1* mutation carriers (Maor et al., 2013; Braunstein et al., 2018). Furthermore, iPSC derived dopaminergic neuronal cultures from GBA-PD patients demonstrate upregulation of IRE1α although splicing of XBP1 mRNA was not observed (Fernandes et al., 2016).

Transgenic *Drosophila* expressing human N370S or L444P mutant *GBA1* exhibit significantly increased expression of the ER stress reporter transgene Xbp1-eGFP in the developing eye tissue which is significantly reduced upon treatment with the pharmacological chaperone Ambroxol (Sanchez-Martinez et al., 2016). *Drosophila* generated with double heterozygous *GBA1* mutation resulting in 30% activity, mirroring carriers of *GBA1* mutation, also exhibit significant XBP1 splicing (Maor et al., 2013).

Activation of the adaptive UPR responses through the generation of active XBP1s is associated with neuroprotection of dopaminergic neurons in 6-OHDA models of PD (Mercado et al., 2016). Down regulation of XBP1 specifically in the SNpc of adult mice is associated with chronic ER stress and induction of the pro-apoptotic protein CHOP causing spontaneous neuronal degeneration (Valdes et al., 2014). Additionally, delivery of active XBP1s to the SNpc of adult mice using AAV delivery confers neuroprotection against 6-OHDA (Valdes et al., 2014).

The body of evidence from literature strongly suggests activation of the UPR both in association with *GBA1* mutation and with synucleinopathies (chapter 5.1.4). However, it is important to establish whether adaptive responses of the UPR are mediated through the generation of XBP1s. Whilst evidence does suggest that XBP1s is upregulated there are few dedicated studies investigating UPR responses in association with *GBA1* mutations. It is important to unequivocally determine whether UPR activation is contributing to pathology or has a protective function in an already comprised cellular condition and as such, this results chapter aims to contribute to this area of research.

Table 15 - Summary of BiP expression in relation to *GBA1* mutation and synucleinopathies.

Model	Effector	Result	Reference
GBA-PD putamen human tissue	BiP protein	↑ (126%)	(Gegg et al., 2012)
sPD putamen human tissue	BiP protein	↑(128%)	(Gegg et al., 2012)
sPD and sDLB frontal cortex human tissue	BiP protein	↓	(Kurzawa-Akanbi et al., 2012)
sPDD and sDLB cingulate gyrus human tissue	BiP protein	↑	(Baek et al., 2016)
sPDD and sDLB parietal cortex human tissue	BiP protein	↑	(Baek et al., 2016)
GBA non-demented control frontal cortex human tissue	BiP protein	↓	(Kurzawa-Akanbi et al., 2012)
GD fibroblasts	BiP protein *L444P/WT only	↑ (153%)	(Sanchez-Martinez et al., 2016)
GD fibroblasts	BiP mRNA	↑	(Maor et al., 2013)
GD fibroblasts	BiP protein	↑ (15%)	(McNeill et al., 2014)
GBA-non-demented control fibroblasts	BiP protein	↑ (15%)	(McNeill et al., 2014)
Primary hippocampal neurons +CβE	BiP protein	No change	(Farfel-Becker et al., 2009)
N370S GBA-PD iPSC derived dopaminergic neurons	BiP protein	↑	(Fernandes et al., 2016)
MES23.5 GBA1 + human SNCA	BiP protein	No change	(Cullen et al., 2011)
SNCA overexpressing mouse model targeted to nigrostriatal pathway	BiP protein	↑ (320%)	(Bellucci et al., 2011)
Drosophila double heterozygous *GBA1* mutation	BiP protein	↑	(Maor et al., 2013)
Human N370S/L444P GBA *Drosophila* model	BiP mRNA	↑	(Maor et al., 2013)

Table 16 – Summary of IRE1α pathway activation

Model	Effector	Result	Reference
GBA-PD human post mortem tissue	sXBP1 mRNA	Inconclusive	(Gegg et al., 2012)
sPD human post mortem tissue	sXBP1 mRNA	Inconclusive	(Gegg et al., 2012)
MES23.5 GBA + SNCA	sXBP1 mRNA	No change	(Cullen et al., 2011)
GD fibroblasts	sXBP1 mRNA	↑	(Maor et al., 2013)
GBA-PD fibroblasts	sXBP1 mRNA	↑	(Braunstein et al., 2018)
(N370S) GBA-PD iPSC derived dopaminergic neurons	sXBP1 mRNA	No change	(Fernandes et al., 2016)
(N370S) GBA-PD iPSC derived dopaminergic neurons	IRE1α protein	↑	(Fernandes et al., 2016)
Drosophila double heterozygous *GBA1* mutation	sXBP1 mRNA	↑	(Maor et al., 2013)
Human N370S/L444P GBA *Drosophila* model	sXBP1-eGFP protein	↑	(Sanchez-Martinez et al., 2016)

5.2. Aims and objectives

5.2.1. Aim

The aim of this chapter is to establish whether mutant GCase enzyme activates the UPR in the GBA1 SH-SY5Y cell lines created. Specifically, the ability of L444P mutant GCase to evoke a protective UPR response through the IRE1α pathway and production of spliced XBP1 will be investigated. Furthermore, this chapter will try to ascertain the influence of α-synuclein on the production of spliced XBP1.

5.2.2. Objectives

- Establish if the UPR is activated by evaluating BiP protein expression in SH-SH5Y cell lines stably expressing L444P *GBA1* by western blot.
- Establish XBP1, specifically XBP1s, protein and gene expression in SH-SH5Y cell lines stably expressing L444P *GBA1* by western blot and quantitative PCR.
- Investigate the impact of α-synuclein on XBP1 gene and protein expression in SH-SH5Y cell lines stably expressing L444P *GBA1* by western blot and quantitative PCR.

5.3. Results

5.3.1.BiP

5.3.1.1. BiP protein expression in *GBA1* SH-SY5Y cell lines

BiP protein expression is significantly increased in WT *GBA1* overexpressing SH-SY5Y cells when compared with control SH-SY5Y cells (one-way ANOVA, Tukey's HSD, p=0.0171) However, BiP protein expression is significantly reduced in L444P *GBA1* SH-SY5Y cells compared with WT *GBA1* cells (one-way ANOVA, Tukey's HSD, p=0.0415). BiP protein expression appears to be similar in both SH-SY5Y control and L444P *GBA1* cells **(Figure 22).**

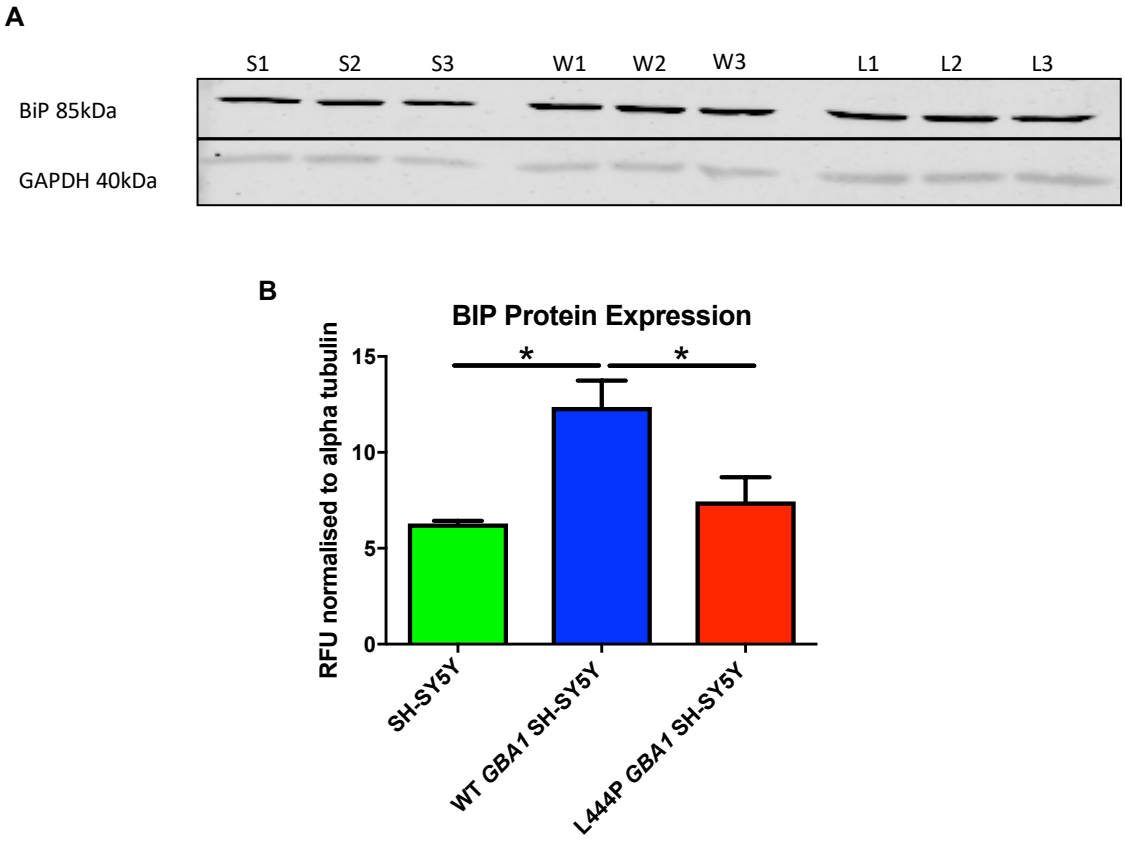

Figure 22 - BiP protein expression in SH-SY5Y cell lines. (a) Representative western blot of BiP protein expression (b) Quantification and statistical analysis of BiP protein expression. Bars are mean ± SEM. One-way ANOVA, Tukey's HSD, n=3, *p=<0.05. S=SH-SY5Y, W= WT *GBA1* SH-SY5Y, L=L444P *GBA1* SH-SY5Y

5.3.2.XBP1

5.3.2.1. *XBP1* gene expression in *GBA1* SH-SY5Y cell lines

The mRNA expression of *XBP1* was measured relative to the housekeeping gene *HPRT1*. There was no significant difference in *XBP1* gene expression between SH-SY5Y control cells, wild type *GBA1* overexpressing or L444P *GBA1* overexpressing cells. Interestingly, *XBP1* gene expression appears similar between SH-SY5Y control cells and L444P *GBA1* overexpressing cells, which is greater than seen in wild type *GBA1* overexpressing cells **(Figure 23).**

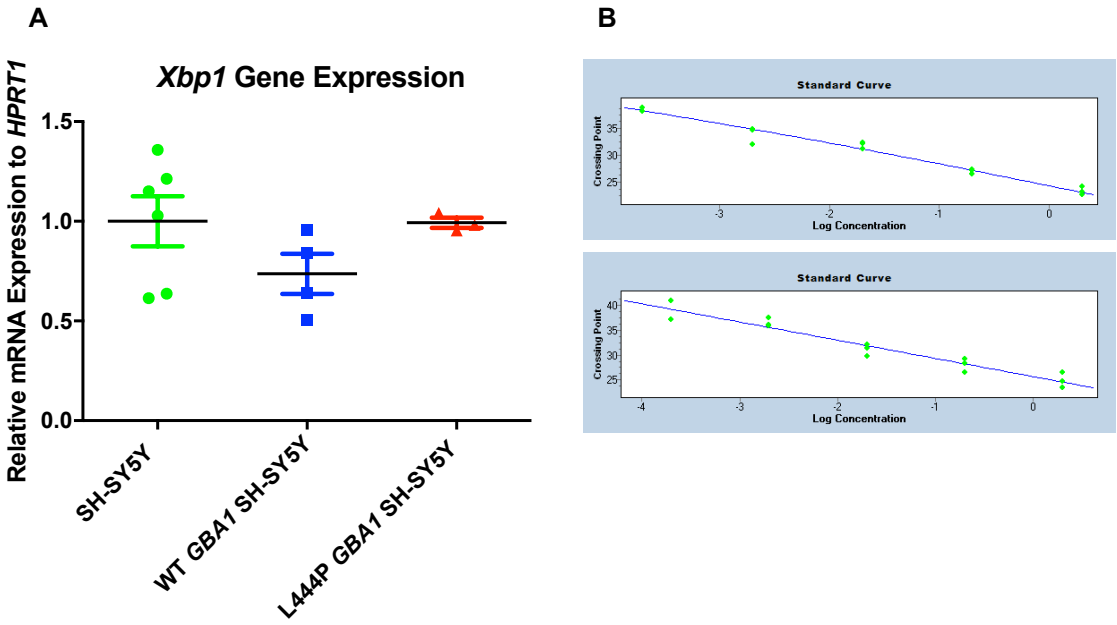

Figure 23 –Relative *XBP1* gene expression in overexpressing *GBA1* cell lines. (a) Relative expression calculated by the $\Delta\Delta^{CT}$ method using *HPRT1* housekeeping gene. Data shown as mean +/- SEM, one-way ANOVA, p=0.2566, n=3-6. (b) Standard curves to measure primer efficiency. *XBP1* primer efficiency = 1.847, *HPRT1* primer efficiency = 1.885. Standard curves show primers successfully target the gene of interest resulting in exponential amplification of the mRNA of interest, validating the gene expression assay.

5.3.2.2. XBP1 protein expression *GBA1* SH-SY5Y cell lines – Immunocytochemistry

Immunocytochemistry clearly shows increased XBP1 protein expression in both the wild type and L444P *GBA1* overexpressing cells when compared with control SH-SY5Y cells. Furthermore, L444P *GBA1* overexpressing cells clearly show increased XBP1 protein when compared with wild type *GBA1* overexpressing cells, with a particular increase in what appears to be nuclear XBP1, consistent with the role XBP1s as a transcription factor **(Figure 24).**

A

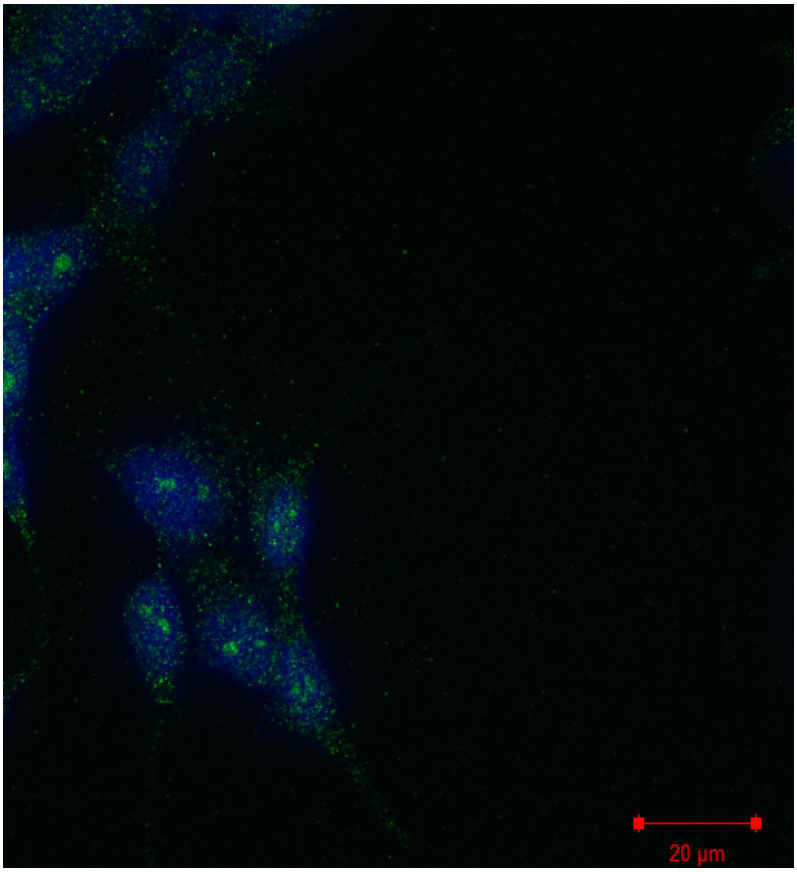

B

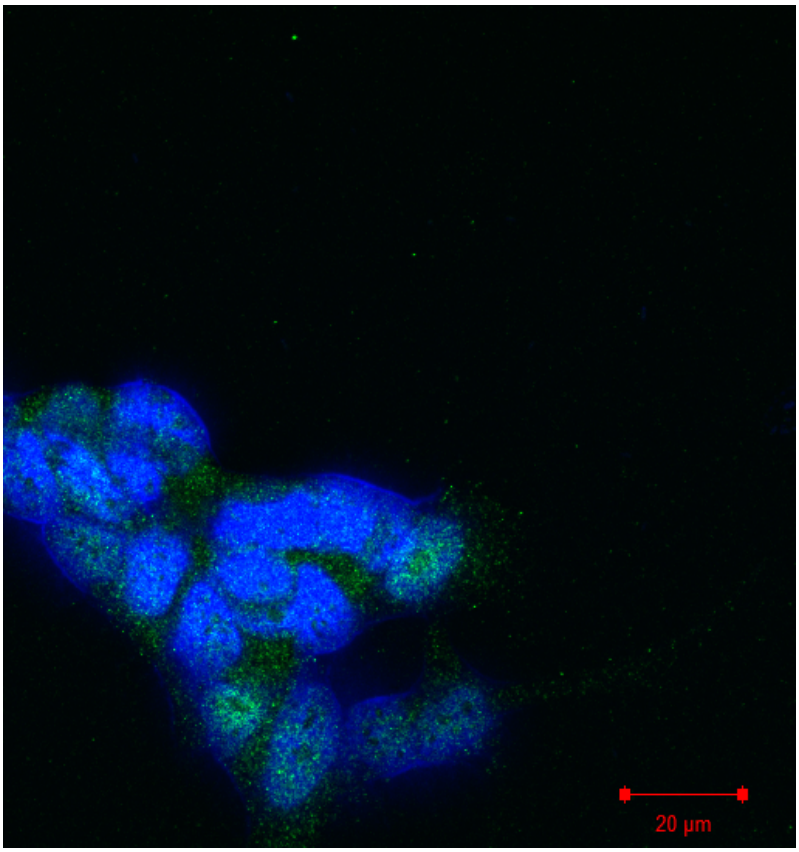

C

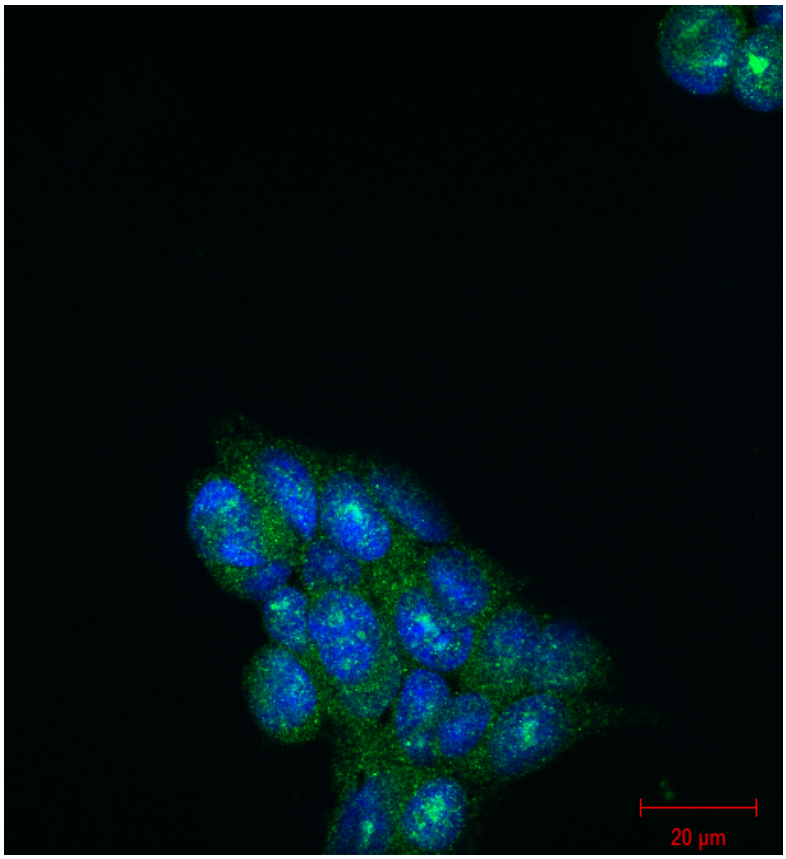

Figure 24 –Immunocytochemistry of (a) SH-SY5Y (b) WT *GBA1* SH-SY5Y (c) L444P *GBA1* SH-SY5Y cells. XBP1 protein shown in green, DAPI in blue. Images were taken at x63 magnificantion with oil immersion. Scale bars shown at 20µM.

5.3.2.3. XBP1 protein expression – Western blot

In a bid to further examine the apparent increase in XBP1 protein expression between wild type and mutant *GBA1* expressing cells, western blotting was used to complement the immunocytochemical findings. Spliced XBP1 protein is comprised of 376 amino acids and is approximately 40kDa in size, whereas un-spliced XBP1 protein is comprised of 261 amino acids and is approximately 29kDa in size (Yoshida et al., 2009).

L444P *GBA1* overexpressing cells have significantly more spliced XBP1 of 37kDa size compared with wild type *GBA1* overexpressing (one-way ANOVA, Tukey's HSD, p=0.0182) and control SH-SY5Y cells (one-way ANOVA, Tukey's HSD, p=0.0365). Interestingly, the level of 37kDa XBP1 protein expression appears to be very similar between control SH-SY5Y and wild type *GBA1* overexpressing cells.

Despite a strong trend showing increased protein expression of 20kDa XBP1 in L444P *GBA1* overexpressing cells compared with both wild type *GBA1* overexpressing and control SH-SY5Y cells, there was no statistically significant difference. Again, 20kDa XBP1 protein expression seems to be very similar in control SH-SY5Y and wild type *GBA1* overexpressing cells **(Figure 25)**. However, while the ratio of spliced to un-spliced XBP1 protein indicates a strong trend towards activation of the IRE1α UPR pathway in response to L444P mutant GCase, no statistical significance was obtained by one-way ANOVA.

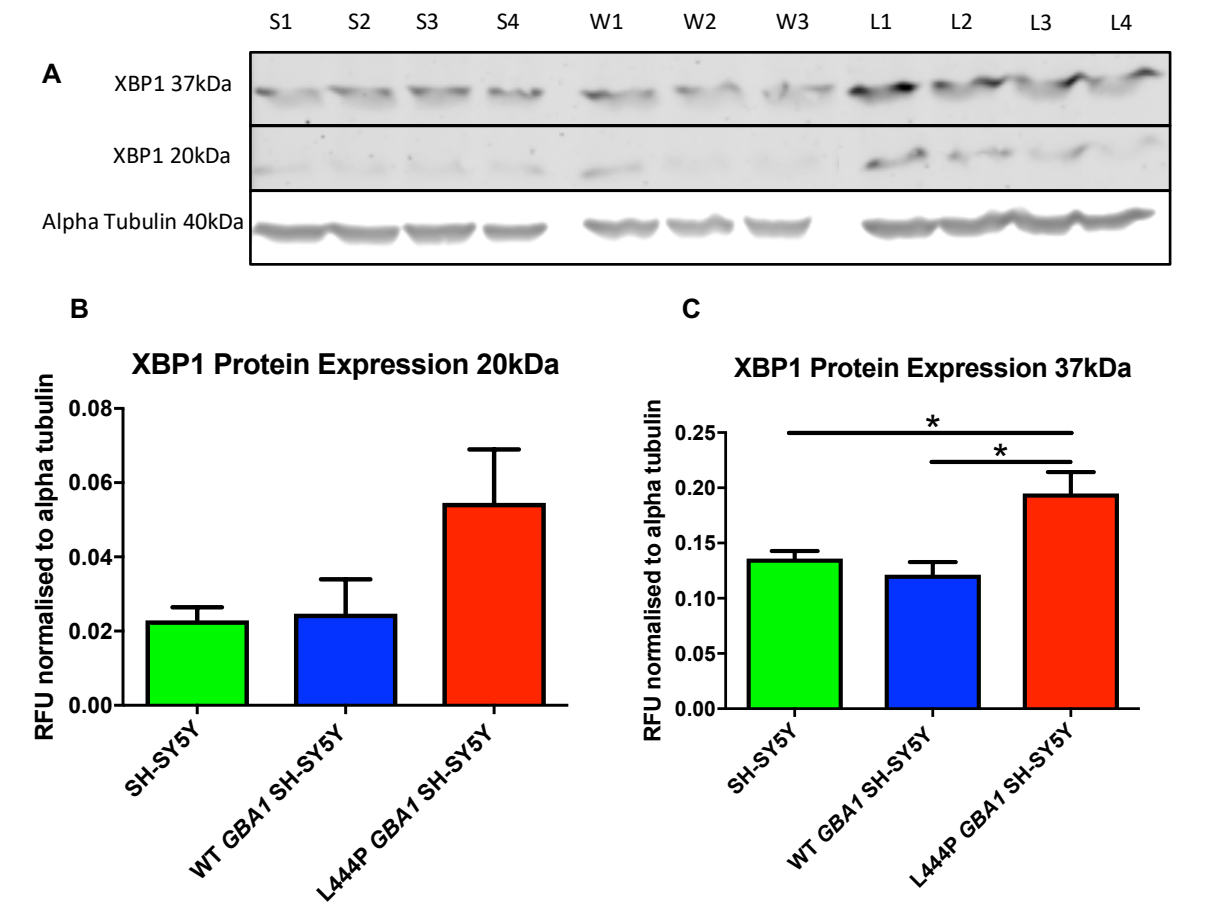

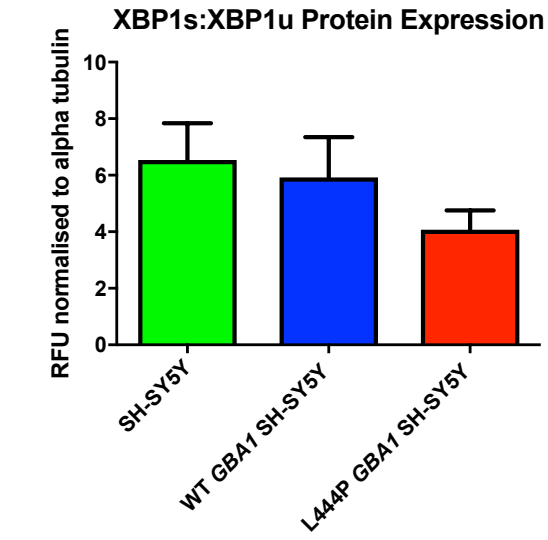

Figure 25 – XBP1 protein expression in SH-SY5Y cells (a) Representative western blot of XBP1 protein expression in SH-SY5Y cell lines (b) Quantification and statistical analysis of XBP1 20kDa western blot (c) Quantitation and statistical analysis of XBP1 37kDa western blot (d) Quantification and statistical analysis of XBP1s:XBP1u. Bars are mean+/- SEM, one way ANOVA, p=0.1017, n=3-4 Bars are mean +/- SEM, one-way ANOVA, Tukey's HSD, n=3-4, *p=<0.05. S=SH-SY5Y, W= WT *GBA1* SH-SY5Y, L=L444P *GBA1* SH-SY5Y

5.3.3.XBP1 in α-synuclein transiently transfected cells

5.3.3.1. *XBP1* gene expression

XBP1 gene expression is highly significantly increased (Two-way ANOVA, Bonferroni post hoc, p=0.0003) in wild type *GBA1* overexpressing cells when transiently transfected with GFP tagged α-synuclein when compared with an empty GFP tagged plasmid This is not seen in either the SH-SY5Y controls or wild type *GBA1* overexpressing cells. Furthermore, when comparing the cell lines transfected with α-synuclein, *XBP1* gene expression is highly significantly increased in both wild type *GBA1* overexpressing cells compared with L444P *GBA1* overexpressing (Two-way ANOVA, Bonferroni post hoc, p=0.0007) and control SH-SY5Y cells (Two-way ANOVA, Bonferroni post hoc, p=0.0015) respectively **(Figure 26).**

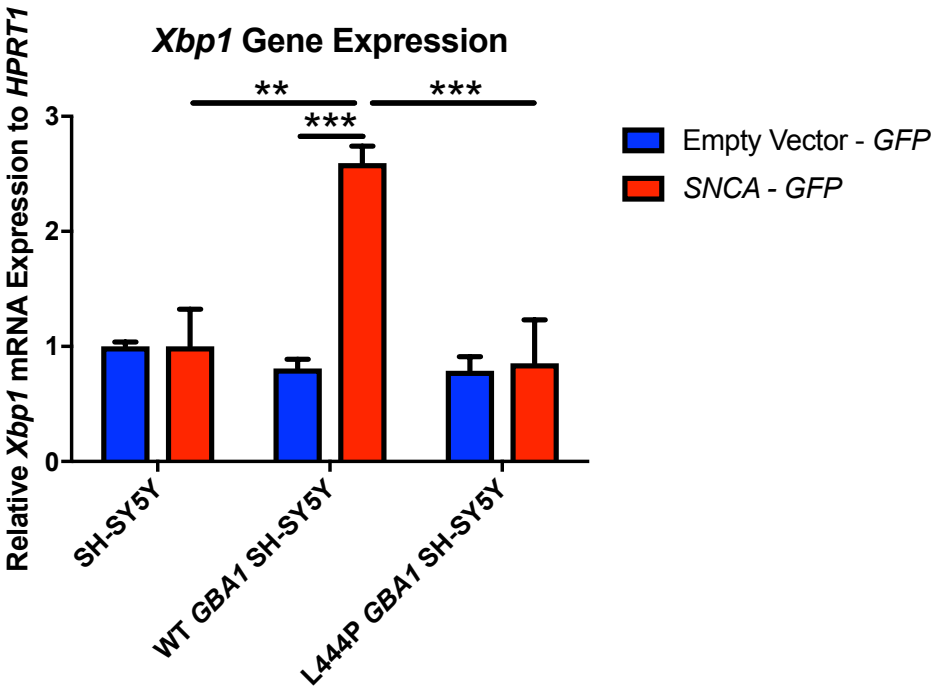

Figure 26 - Relative *XBP1* gene expression in cells transiently transfected with α-synuclein. Relative expression calculated by the $\Delta\Delta^{CT}$ method using *HPRT1* housekeeping gene. Data shown as mean +/- SEM, Two-way ANOVA, Bonferroni post hoc, n=3, **p=<0.01, ***p=<0.001

5.3.3.2. XBP1 protein expression

Transient transfection with α-synuclein did not cause any change in spliced XBP1 protein expression in control SH-SY5Y cells, mirroring the picture seen with *XBP1* gene expression. In WT *GBA1* overexpressing cells, as with gene expression, spliced XBP1 protein expression is increased, although in this case, not to a significant level. Interestingly, L444P *GBA1* overexpressing cells exhibit reduced spliced XBP1 protein expression in response to α-synuclein,

a response not seen with *XBP1* gene expression. The degree of spliced XBP1 protein expression in similar to basal levels associated with control and WT *GBA1* cells. This reduction is response to α-synuclein accumulation is significant when performing a student's t-test between the empty vector and α-synuclein data in this cell line alone (Two-Way ANOVA, without post hoc, p=0.0194) but significance is lost following two-way ANOVA with correction for multiple comparisons **(Figure 27).**

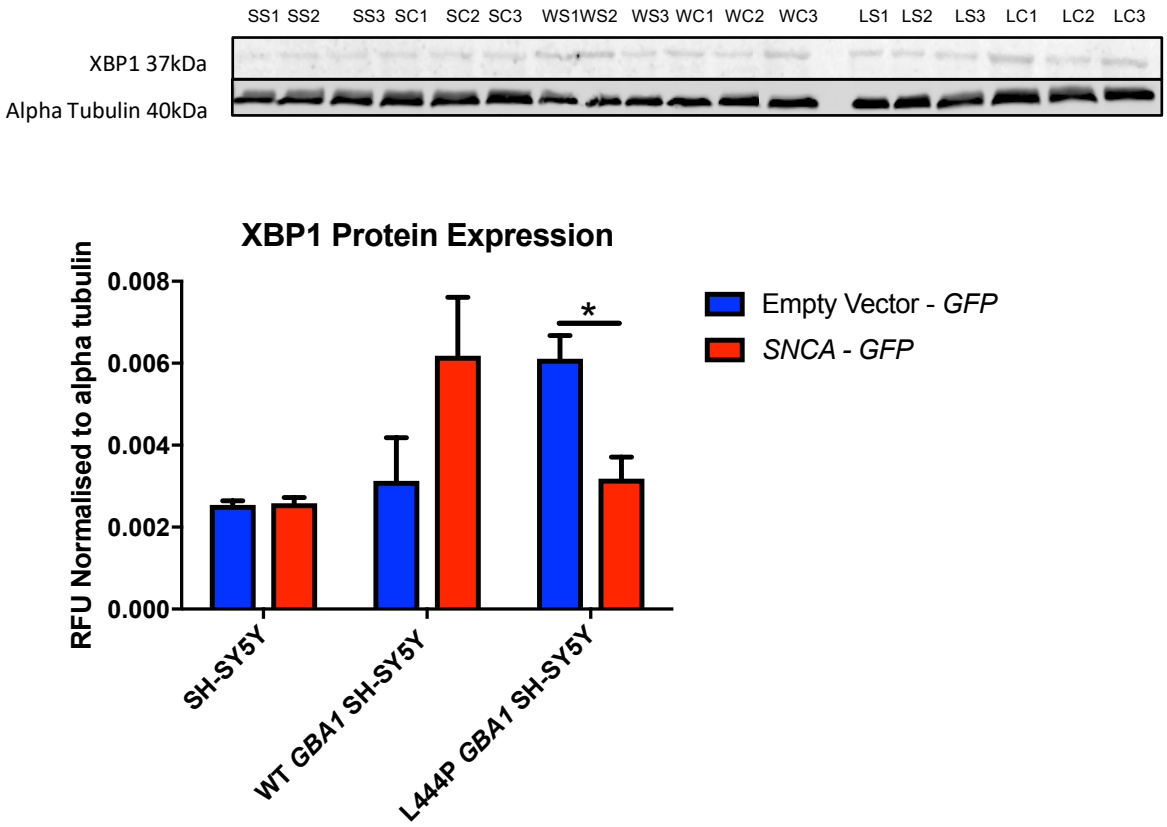

Figure 27 – XBP1s protein expression in SH-SY5Y cells transiently transfected with α-synuclein (a) Representative western blot (b) Quantitation and statistical analysis of XBP1 37kDa western blot. Bars are mean+/- SEM. Two-way ANOVA, (p=0.0194), n.s. following Bonferroni post hoc. Exploratory individual student t-tests per cell line, n=3, *p=<0.05. SS=SH-SY5Y + α-synuclein, SC=SH-SY5Y + empty vector, WS=WT *GBA1* SH-SY5Y + α-synuclein, WC= WT *GBA1* SH-SY5Y + emptor vector, LS=L444P *GBA1* SH-SY5Y + α-synuclein, LC= L444P *GBA1* SH-SY5Y + empty vector.

5.4. Discussion

These results suggest activation of the IRE1α pathway of the UPR occurs in response to misfolded L444P mutant GCase enzyme causing the production of spliced XBP1.

Expression of BiP protein is significantly increased when wild type GCase protein is overexpressed in SH-SY5Y cells due to the increased requirement for protein folding and quality control **(Figure 22).** Despite the implication of increased BiP protein expression, overexpression of *GBA1* does not cause increased gene expression of XBP1 **(Figure 23).** Furthermore, overexpression of *GBA1* does not affect either spliced or non-spliced XBP1 protein expression **(Figure 25).** This could imply that ER stress, although sufficient enough to cause dissociation of BiP, is not sufficient to fully activate the IRE1α pathway to generate downstream effectors. Consequently, this finding suggests that overexpression of wild type GCase protein, potentially as a therapeutic in the future, is not detrimental to the cell in terms of significantly increasing ER stress. Additionally, this result infers that another factor in addition to increased ER load/stress is required to activate the IRE1α pathway of the UPR, nominally the presence of misfolded proteins.

Surprisingly, SH-SH5Y cells overexpressing L444P *GBA1* did not show increased expression of BiP as expected and reported in fibroblasts from 'healthy' *GBA1* mutation carriers and GBA-PD patients (Maor et al., 2013; McNeill et al., 2014; Sanchez-Martinez et al., 2016; Garcia-Sanz et al., 2017) **(Figure 22).** However, the converse has been suggested to explain the role of BiP in the activation of the UPR whereby evidence suggests that loss of BiP correlates with the formation of active IRE1α and PERK while overexpression of BiP attenuates their action (Bertolotti et al., 2000). In this context, these results suggest overexpression of wild type *GBA1* prevents activation of the UPR which can be seen both as protective and detrimental. L444P *GBA*1 overexpressing cells showing a significant reduction in BiP protein expression compared with wild type *GBA1* overexpressing cells could alternatively therefore be indicating activation of the UPR.

Further considerations need to be made when interpreting these results. The model system used in this study does not accurately reflect the conditions and stresses experienced in a complex network of different cells as seen *in vivo* and which underlie cellular signalling. Furthermore, SH-SY5Y cells are a neuroblastoma cell line and as such may have endogenous protective

mechanisms to prevent activation of any pathways which may prevent proliferation. Moreover, these experiments should be repeated in differentiated SH-SY5Y cells.

Whilst L444P *GBA1* expression did not alter XBP1 gene expression **(Figure 23)**, the presence of mutant GCase protein did cause an increase in XBP1 protein expression as seen by immunocytochemistry **(Figure 24).** Specifically, L444P *GBA1* cells showed a significant increase in the expression of spliced, active XBP1 illustrated by western blot **(Figure 25).** This finding is confirmed by the increased nuclear expression of XBP1 seen by immunocytochemistry in L444P *GBA1* cells consistent the function of spliced XBP1 as a transcription factor. Gene expression assays performed using predesigned TaqMan® gene expression assays were performed with primers designed against XBP1, not specifically spliced XBP1 mRNA. It would be interesting to repeat the gene expression assay for XBP1 specifically to see whether there is an increase in spliced, active XBP1 mRNA. However, an increase in total XBP1 gene expression was still expected in order to accommodate any potential increased requirement of splicing to provide the substrate necessary to effect activation of the IRE1α pathway, which was not seen. This may be due to the splicing of XBP1 mRNA preventing the annealing of primers. Whilst there was a significant increase in the expression of spliced XBP1 protein which was generated in L444P *GBA1* cells, the ratio of spliced to un-spliced XBP1 protein did not show a significant difference between wild type and L444P mutant *GBA1* cells, although a strong trend is evident. A possible explanation for this finding may be a general increase in XBP1 protein expression in L444P *GBA1* cells concurrent with the activation of the IRE1α pathway.

Since SH-SY5Y cells express low levels of endogenous α-synuclein and it is known that *GBA1* mutation is associated with increased expression of α-synuclein (Mazzulli et al., 2011), cells were transiently transfected with α-synuclein in order to better mimic biochemical conditions. Interestingly, the presence of accumulated α-synuclein caused a highly significant increase in XBP1 gene expression in wild type *GBA1* overexpressing cells but did not alter XBP1 gene expression in neither control SH-SHSY nor L444P *GBA1* SH-SY5Y cells **(Figure 26).** This increase in XBP1 gene expression in wild type *GBA1* overexpressing cells correlated with an increase in spliced XBP1 protein although not to a statistically significant level **(Figure 27).** Intriguingly, the expression of spliced XBP1 protein significantly reduces in L444P *GBA1* SH-

SY5Y cells transiently expressing α-synuclein, mirroring basal expression of spliced XBP1 in control and WT cells **(Figure 27).** This implies that the additional challenge of accumulated α-synuclein ceases activation of the IRE1α pathway and production of the downstream adaptive transcription factor, spliced XBP1. Since the responses elicited by the UPR exist in balance and there is extensive cross talk between the different pathways (Ron and Walter, 2007), perhaps it is not surprisingly that the IRE1α pathway is seemingly dampened under this condition of extreme ER stress which raises the question about the effect of mutant GCase and α-synuclein on the other UPR pathways, specifically those implicated in activating apoptosis. A caveat of this experimental design which needs to be considered when interpreting the IRE1α pathway response is the overexpression of α-synuclein to levels which are unlikely to be physiological. Furthermore, it is known that specifically α-synuclein oligomers are implicated with reduced GCase enzyme activity and the so called bi-directional loop which is considered to underlie pathology in the synucleinopathies. It is possible that transiently transfected α-synuclein does oligomerise within these cells although it would need to be confirmed. An alternative approach would be to test spliced XBP1 expression in cells treated with pre-formed α-synuclein fibrils (Volpicelli-Daley et al., 2014) or even oligomers (Hinault et al., 2010) although determining the exact species of α-synuclein and application of consistent concentrations between the cell lines would be challenging.

As alluded to, the demonstration of spliced XBP1 in L444P *GBA1* mutant cells and the dampening of response in the presence of α-synuclein uncovers the possibility of an alternative UPR response occurring. Since the levels of ER stress are increased with accumulating α-synuclein, investigating the PERK pathway and production of the pro-apoptotic effector CHOP is the logical progression of this work, discussed in the next chapter.

6. Investigating the Unfolded Protein Response (UPR) in wild type and L444P *GBA1* overexpressing SH-SY5Y cells – CHOP

6.1. Introduction

One of the most important adaptive responses of UPR activation is global repression of protein translation to minimise ER load and stress (Walter and Ron, 2011). This response is activated through the PERK pathway of the UPR and the effector eIF2α (Harding et al., 1999). PERK activation by ER stress is rapidly reversible and within minutes of restoring ER homeostasis, activated PERK is dephosphorylated (Bertolotti et al., 2000). Whilst a temporary halt in protein translation mediated by eIF2α phosphorylation is beneficial for cells, sustained ER stress causing a prolonged block in translation is detrimental to cell survival (Hetz et al., 2015). Furthermore, chronic ER stress is able to trigger cell death pathways initiated through the PERK pathway involving the upregulation of C/EBP homologous protein (CHOP) (McCullough et al., 2001).

6.1.1. PERK pathway

PERK superficially resembles IRE1α; both are ER localised type 1 transmembrane proteins with luminal stress sensing domains and cytoplasmic protein kinase domains which undergo trans-autophosphorylation by oligomerization and BiP dissociation in response to ER stress (Harding et al., 1999; Bertolotti et al., 2000). However, unlike IRE1α which has itself as the only known substrate, activated PERK phosphorylates the α subunit of eukaryotic translation initiation factor (eIF2) at serine residue 51 (Harding et al., 1999). Phosphorylation of eIF2α prevents GTP-GDP exchange by eIF2B, a pentameric complex which recycles eIF2 to its active GTP associated form (Hetz et al., 2015). eIF2α binds to both GTP and initiator methionyl-tRNA and is responsible for transferring methionyl-tRNA to the 40S ribosomal subunit (Rozpedek et al., 2015). After the initiation of translation, GTP is hydrolysed to GDP dependent upon the action of eIF2B facilitating the rebuild of new complexes of eIF2 to activate the next round of translation (Ron and Walter, 2007). Prevention of GTP-GDP exchange by eIF2α thereby results in global translation initiation repression and attenuation of protein synthesis thus reducing ER load and stress (Hetz et al., 2015).

Phosphorylation of eIF2α also allows for the preferential translation of UPR dependent genes such as activating transcriptional factor 4 (ATF4). Important targets for ATF4 are CHOP and GADD34 (Hetz et al., 2015).

6.1.2.CHOP

C/EBP homologous protein (CHOP) is a basic leucine domain transcription factor which is activated is response to persistent and unresolved ER stress causing activation and translation of ATF4 through the PERK pathway (Fawcett et al., 1999). Translated ATF4 protein binds to and activates the CHOP promoter (Fawcett et al., 1999) while CHOP protein is post-translationally activated by p38 kinase (Wang and Ron, 1996). Activation of CHOP causes reduced cell viability (McCullough et al., 2001) while cells which lack CHOP protein are significantly protected against ER stress mediated cell death (Zinszner et al., 1998).

CHOP promotes cell death through the repression of the anti-apoptotic protein BCL-2 (McCullough et al., 2001; Marciniak et al., 2004). The BCL-2 family of anti-apoptotic proteins govern the intrinsic mitochondrial apoptotic pathway by regulating the permeability of the mitochondrial membrane (Hockenbery et al., 1990). Dysregulation of BCL-2 due to the action of CHOP causes the upregulation and activation of the pro apoptotic BH3-only proteins which go on to further neutralise anti apoptotic BCL-2 proteins and directly engage the pro-apoptotic BAX and BAK proteins (Tait and Green, 2010; Shore et al., 2011). The result is permeabilization of the outer mitochondrial membrane (Tait and Green, 2010; Shore et al., 2011). Thus far it has been confirmed that this terminal arm of the UPR, the PERK pathway, activates at least 4 distinct BH3-only proteins: BID, BIM, NOXA and PUMA which ultimately signal mitochondrial apoptosis effected by the executioner protein, caspase 3 (Tait and Green, 2010; Shore et al., 2011) **(Figure 28).**

Additionally, CHOP is able to directly trans-activate the growth arrest and DNA inducible protein GADD34 (Marciniak et al., 2004; Han et al., 2013). GADD34 promotes de-phosphorylation of eIF2α to prevent the repression of protein translation, further increasing ER stress in affected cells causing the production of reactive oxygen species and the depletion of ATP (Marciniak et al., 2004; Han et al., 2013).

However, forced expression of CHOP does not cause significant transcription of previously identified apoptosis genes (Han et al., 2013). Furthermore, forced CHOP expression itself does not trigger cell death *in vitro* whereas forced expression of ATF4 does decrease cell survival (Han et al., 2013). This suggests that ATF4 may be the primary signal and CHOP the secondary signal required to trigger ER stress induced cell death (Han et al., 2013).

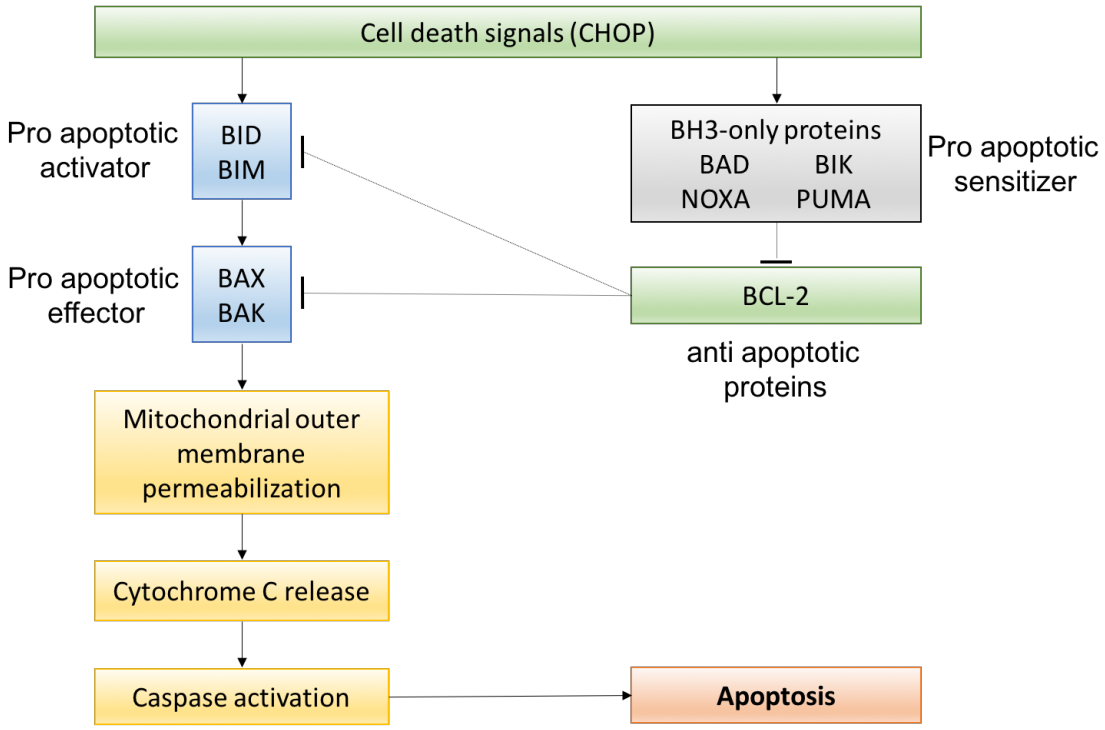

Figure 28 - Overview of mitochondrial associated apoptotic mechanisms. Cell death signals trigger BID and BIM to activate BAX and BAK, which in turn initiate mitochondrial outer membrane permeabilization leading to apoptosis. Cell death signals, in this case CHOP, can also inhibit the action of anti-apoptotic BCL-2 proteins resulting in the activation of pro apoptotic activates and effectors. Figure adapted from (Gibson and Davids, 2015)

6.1.3. Activation of the PERK pathway in association with *GBA1* mutation and synucleinopathy

Unlike the impact of *GBA1* mutation on BiP protein expression as discussed in chapter 5, activation of the PERK pathway causing upregulation of eIF2α and CHOP expression appears to be conclusive across different studies **(Table 17)**

Human post mortem tissue from sPD patients shows significant activation of PERK and eIF2α which is also observed in nigral dopaminergic neurons with α-synuclein inclusions (Hoozemans et al., 2007). Furthermore, immunohistochemistry has identified a significant increase in phosphorylated PERK in PDD and DLB human post mortem brain tissue from the prefrontal cortex when compared with controls (Baek et al., 2016).

Fibroblasts generated from N370S *GBA1* PD patients have significantly increased expression of PERK mRNA (Garcia-Sanz et al., 2017) while eIF2α phosphorylation is significantly increased in fibroblasts derived from both GD patients and *GBA1* heterozygous mutation carriers (Maor et al., 2013; Braunstein et al., 2018). Phosphorylation of eIF2α is also seen in *Drosophila* generated to mimic *GBA1* mutation carriers (Maor et al., 2013). Ubiquitous ectopic expression of human N370S or L444P mutant GCase in *Drosophila* also significantly increases phosphorylation of eIF2α (Maor et al., 2013). The use of a salubrinal, compound which is capable of phosphorylating eIF2α, preventing transduction of the signal cascade to activate CHOP, delays disease onset and improve motor defects in a rodent model of PD consistent with α-synuclein overexpression (Colla et al., 2012). However, this approach does not fully protect dopaminergic neurons despite reduced accumulation of α-synuclein in the ER (Colla et al., 2012).

ATF4 expression is significantly increased by 140% in the substantia nigra of a mouse model of α-synuclein overexpression targeted specifically to the nigrostriatal pathway (Bellucci et al., 2011). Specifically, ATF4 expression is induced within the cell nuclei of α-synuclein positive neurons reflecting the action of ATF4 as a transcription factor (Bellucci et al., 2011).

CHOP mRNA expression is significantly increased in the putamen of GBA-PD human post mortem brain tissue by 63% and in sPD by 89% (Gegg et al., 2012). Further evidence of increased

CHOP expression is seen in fibroblasts generated from GD patients homozygous for either N370S or L444P demonstrating significantly increased expression of both CHOP mRNA and protein (Maor et al., 2013; Braunstein et al., 2018). Furthermore, fibroblasts generated from L444P *GBA1* heterozygous PD patients exhibit a significant 280% increase in CHOP mRNA expression which is unaffected by treatment with the pharmacological chaperone Ambroxol (Maor et al., 2013; Sanchez-Martinez et al., 2016). Significant increase in CHOP mRNA expression is also seen in N370S *GBA1* PD heterozygous fibroblasts (Maor et al., 2013; Garcia-Sanz et al., 2017). Interestingly, deletion of CHOP in mouse models of PD protects dopaminergic neurons from 6-OHDA and MPTP induced dopaminergic cell death (Silva et al., 2005).

Activation of the PERK pathway in response to *GBA1* mutation and in PD appears to be conclusive from review of the literature. Most significantly, the upregulation of CHOP gene and protein expression in association with *GBA1* mutation suggests a plausible link between *GBA1* mutation and detrimental cellular effects, most prominently initiation of apoptosis. However, few studies have looked at the impact of upregulated CHOP by assessing associated apoptotic markers. Accordingly, the expression of CHOP and the initiation of apoptosis will be investigated in this chapter.

Model	Effector	Result	Reference
sPD striatal human tissue	PERK	↑	(Hoozemans et al., 2007)
sPD striatal human tissue	eIF2α	↑	(Hoozemans et al., 2007)
PDD prefrontal cortex human tissue	Phosphorylated PERK	↑	(Baek et al., 2016)
DLB prefrontal cortex human tissue	Phosphorylated PERK	↑	(Baek et al., 2016)
N370S GBA-PD fibroblasts	PERK mRNA	↑	(Garcia-Sanz et al., 2017)
GBA-PD fibroblasts	Phosphorylated eIF2α	↑	(Braunstein et al., 2018)
GD fibroblasts	Phosphorylated eIF2α	↑	(Maor et al., 2013)
Drosophila mimicking *GBA1* heterozygosity	Phosphorylated eIF2α	↑	(Maor et al., 2013)
Drosophila expressing human N370S or L444P	Phosphorylated eIF2α	↑	(Maor et al., 2013)
α-synuclein overexpressing mouse model	ATF4	↑ (140%)	(Bellucci et al., 2011)
GBA-PD putamen human tissue	CHOP mRNA	↑ (63%)	(Gegg et al., 2012)
sPD putamen human tissue	CHOP mRNA	↑ (89%)	(Gegg et al., 2012)
GD fibroblasts	CHOP mRNA	↑	(Maor et al., 2013)
GD fibroblasts	CHOP protein	↑	(Braunstein et al., 2018)
L444P GBA-PD fibroblasts	CHOP mRNA *L444P/WT only	↑ (280%)	(Sanchez-Martinez et al., 2016)

N370S GBA-PD fibroblasts	CHOP mRNA	↑	(Garcia-Sanz et al., 2017),
N370S GBA-PD fibroblasts	CHOP mRNA	↑	(Maor et al., 2013)

Table 17- Summary of PERK pathway activation in relation to *GBA1* mutation and synucleinopathies.

6.2. Aims and objectives

6.2.1.Aim

The aim of this chapter is to determine whether the PERK pathway of the UPR is activated in response to L444P mutation in the *GBA1* SH-SY5Y cell lines created in chapter 4. Specifically, the ability of L444P mutant GCase to evoke a response detrimental to cell survival through the enhanced expression of CHOP will be assessed. The relative contribution of accumulated α-synuclein on the expression of CHOP will also be investigated in these cells. Furthermore, the aim of this chapter is to also evaluate the expression of CHOP and linked effectors of the apoptotic cascade in human post mortem DLB tissue with and without *GBA1* mutation.

6.2.2.Objectives

- Establish whether CHOP protein expression is increased in L444P *GBA1* mutant SH-SY5Y cells by immunocytochemistry and western blot.
- Establish whether CHOP gene expression is increased in L444P *GBA1* mutant SH-SH5Y cells by quantitative PCR.
- Determine the effect of α-synuclein on CHOP gene expression in L444P *GBA1* mutant SH-SY5Y cell lines by quantitative PCR
- Determine the effects of α-synuclein on CHOP protein expression in L444P *GBA1* mutant SH-SY5Y cells by western blot.
- Assess CHOP protein expression in N370S *GBA1* and sporadic human DLB brain tissue by western blot.
- Assess BCL-2 protein expression in L444P *GBA1* mutant SY-SY5Y cells by western blot.
- Assess BCL-2 protein expression in N370S *GBA1* and sporadic human DLB brain tissue by western blot.
- Identify evidence of activated apoptosis through caspase 3 and caspase 12 protein expression in N370S *GBA1* and sporadic human DLB brain tissue by western blot.

6.3. Results

6.3.1.CHOP in SH-SY5Y *GBA1* cell lines

6.3.1.1. *CHOP* gene expression

The mRNA expression of *CHOP* was measured relative to the housekeeping gene *HPRT1*. There was no significant difference in *CHOP* gene expression between any of the cell groups tested. The degree of variance within each group, particularly the L444P *GBA1* overexpressing cells is extensive **(Figure 29).**

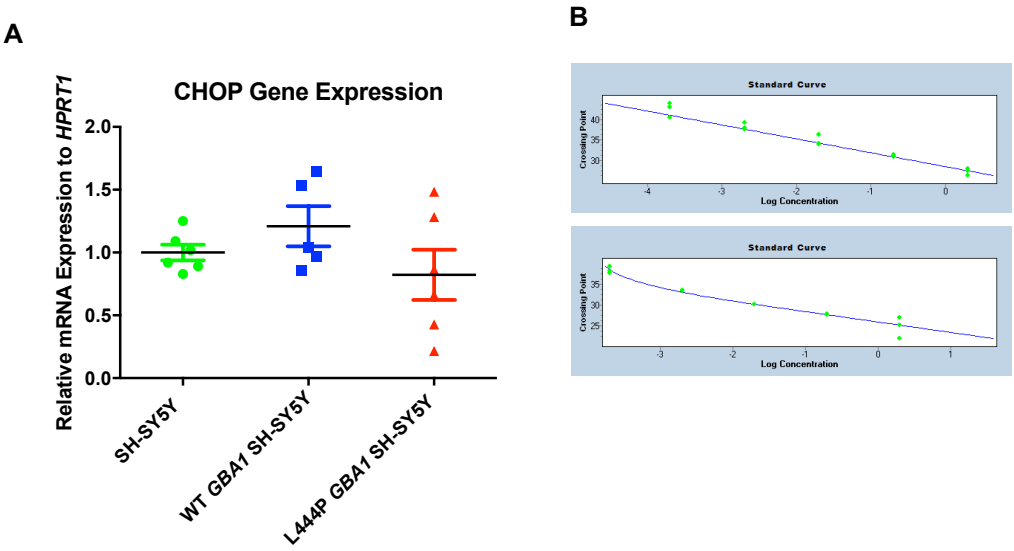

Figure 29 –Relative *CHOP* gene expression in overexpressing *GBA1* cell lines (a) Relative expression calculated by the $\Delta\Delta^{CT}$ method using *HPRT1* housekeeping gene. Data shown as mean +/- SEM, one-way ANOVA, p=0.2566, n=5-6. (b) Standard curves to measure primer efficiency. *CHOP* primer efficiency = 1.931, *HPRT1* primer efficiency = 2.091. Standard curves show primers successfully target the gene of interest resulting in exponential amplification of the mRNA of interest, validating the gene expression assay

6.3.1.2. CHOP protein expression in SH-SY5Y *GBA1* cell lines – Immunocytochemistry

Immunocytochemistry suggests there may be increased CHOP protein expression in wild type *GBA1* overexpressing cells compared with control SH-SH5Y cells, and more extensively in L444P *GBA1* overexpressing cells compared with both control SH-SY5Y and wild type *GBA1* overexpressing cells **(Figure 30).**

A

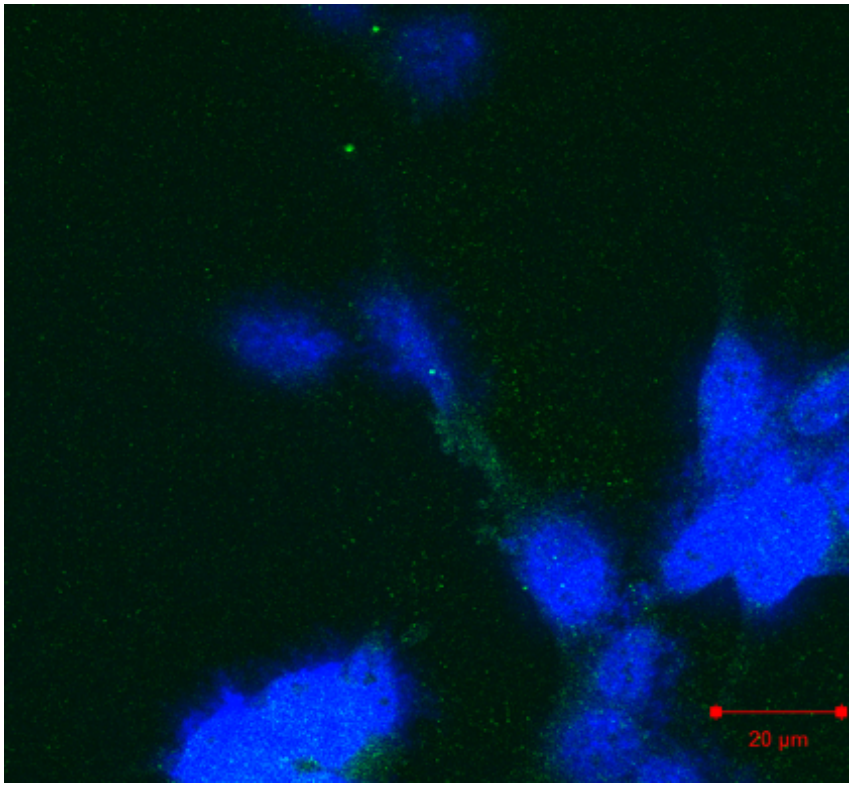

B

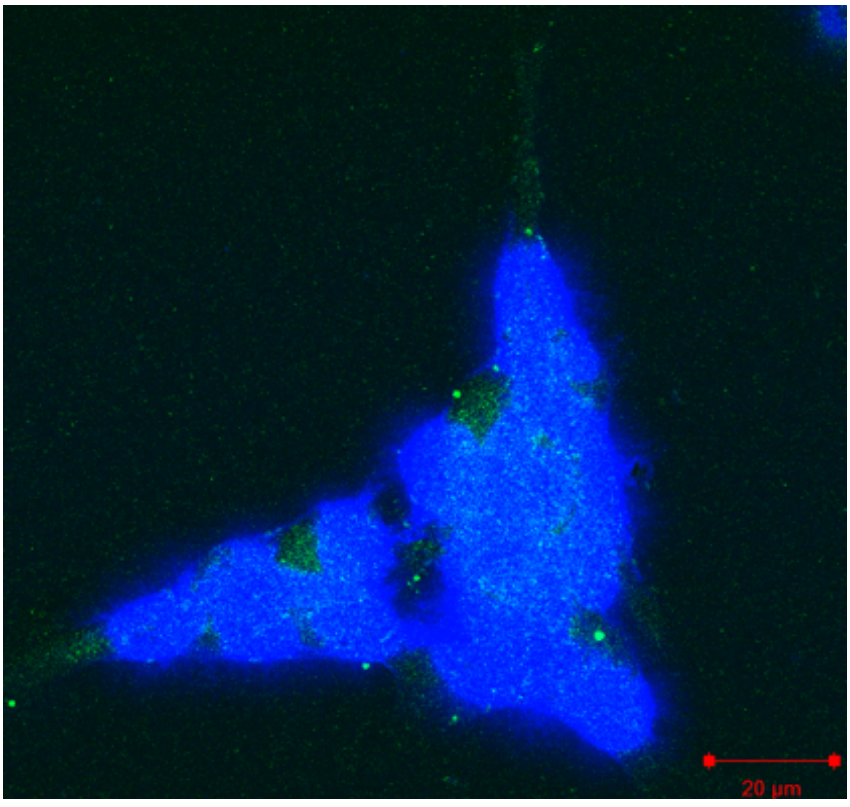

C

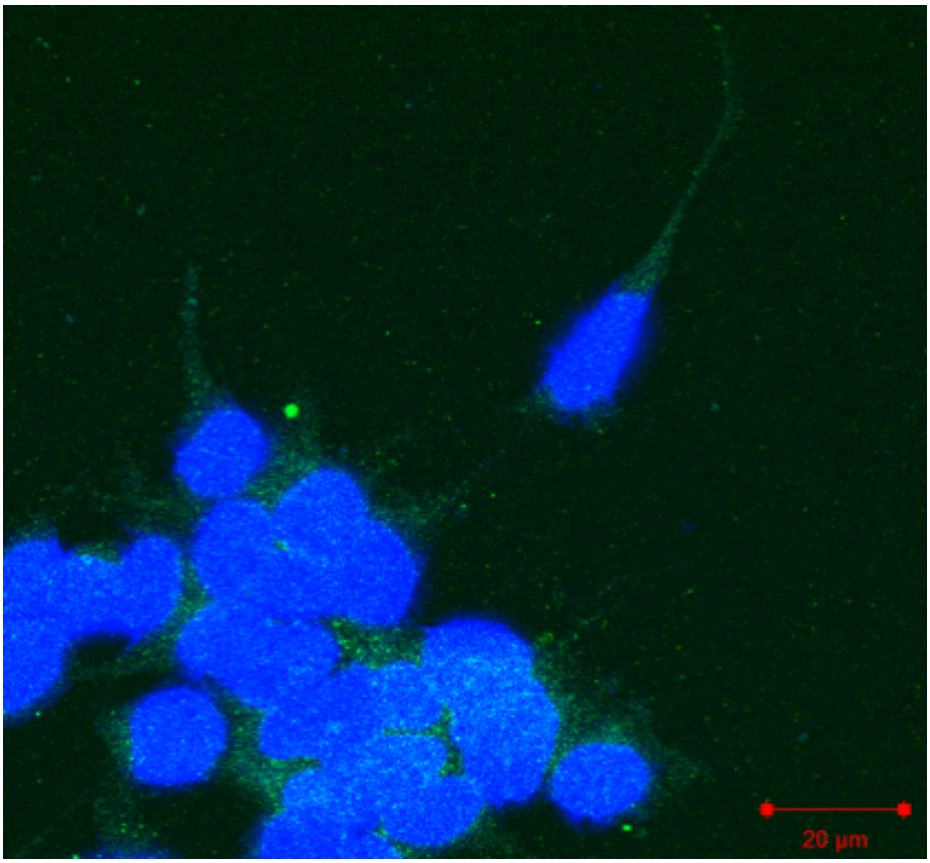

Figure 30 – Immunocytochemistry of (a) SH-SY5Y (b) WT *GBA1* SH-SY5Y (c) L444P *GBA1* SH-SY5Y cells. CHOP protein shown in green, DAPI in blue. Images were taken at x63 magnificantion with oil immersion. Scale bars shown at 20µM.

6.3.1.3. CHOP protein expression in SH-SY5Y *GBA1* cell lines – Western blot

L444P *GBA1* overexpressing cells show significantly more CHOP protein expression compared with control SH-SY5Y cells when semi-quantitatively assessed by western blot (one-way ANOVA, Tukey's HSD, p=0.011). CHOP protein expression does increase in wild type *GBA1* overexpressing cells, predominantly due to sample W1, but does not reach statistical significance **(Figure 31).**

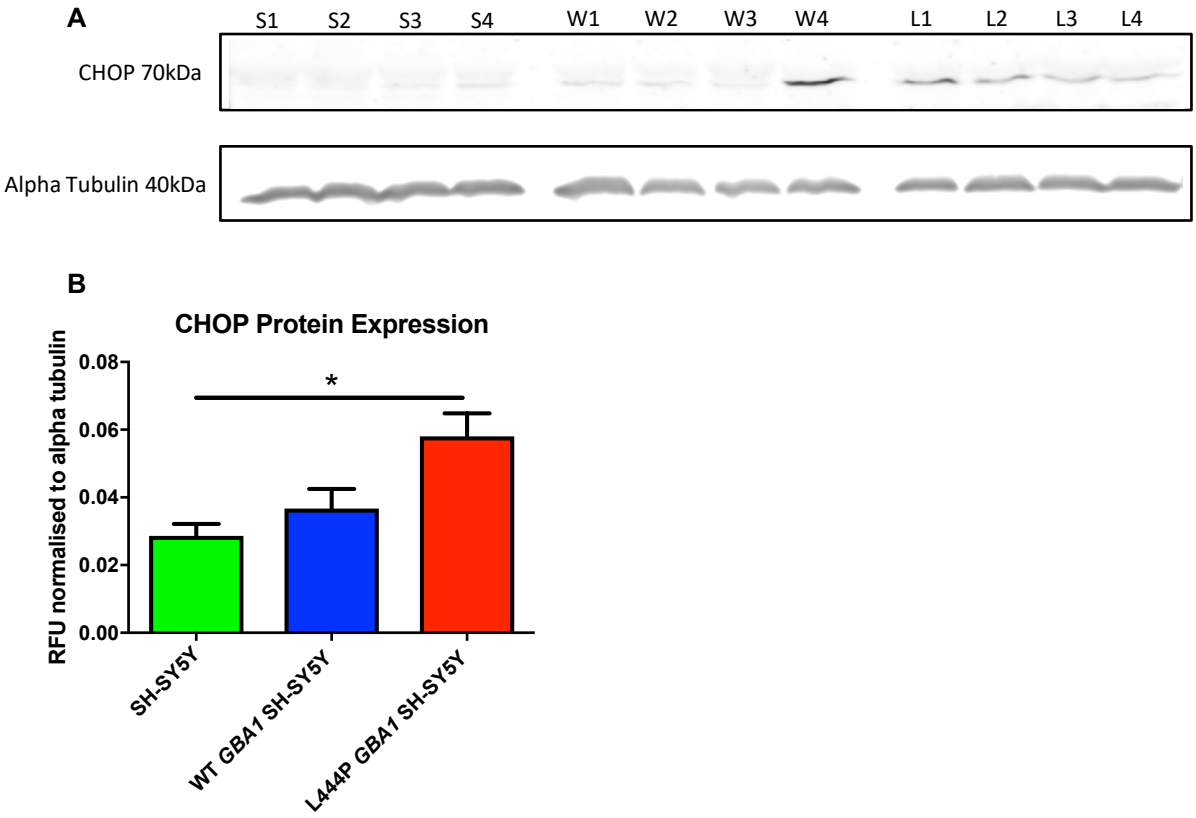

Figure 31 – CHOP protein expression in SH-SY5Y *GBA1* cell lines (a) Representative western blot of CHOP protein expression (b) Quantitation and statistical analysis of CHOP western blot. Bars are mean+/- SEM, one-way ANOVA, Tukey's HSD, n=4, *p=<0.05. S= SH-SY5Y, W= WT *GBA1* SH-SY5Y, L= L444P *GBA1* SH-SY5Y

6.3.2.CHOP in α-synuclein transiently transfected SH-SY5Y *GBA1* cells

6.3.2.1. *CHOP* gene expression

Transient transfection with α-synuclein does not affect *CHOP* gene expression in either controls or *GBA1* overexpressing cell lines; expression remains similar in both the empty vector and α-synuclein transfected cells. Interestingly, *CHOP* gene expression in the empty vector transfected cells, acting as an experimental control, does show an increase in both wild type and L444P *GBA1* gene expression compared to control SH-SY5Y cells, although this does not reach statistical significance **(Figure 32).**

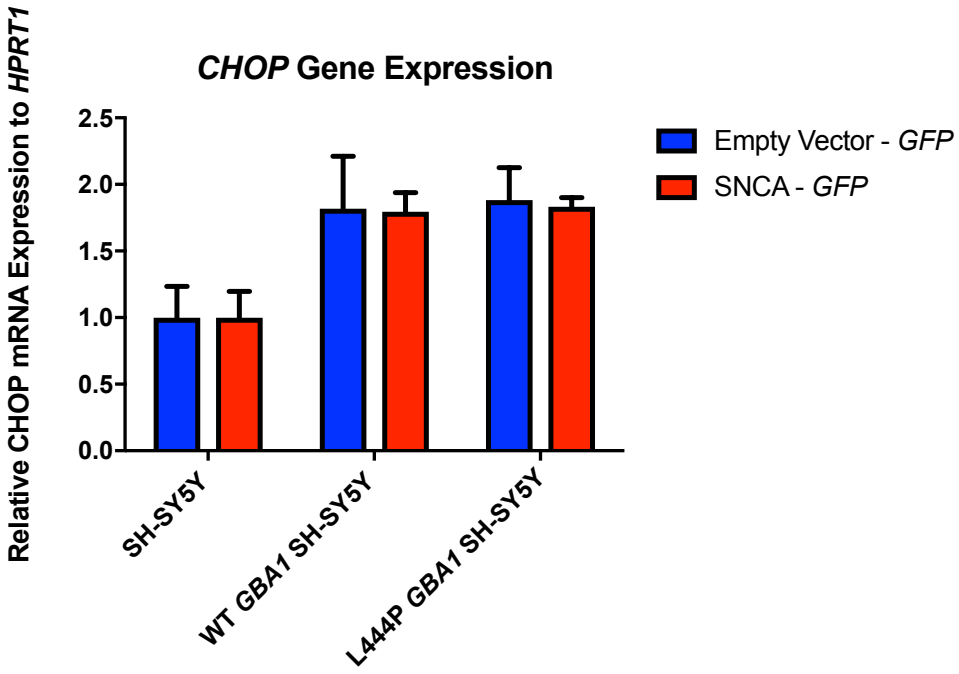

Figure 32 - Relative *CHOP* gene expression in cells transiently transfected with α-synuclein. Relative expression calculated by the $\Delta\Delta^{CT}$ method using *HPRT1* housekeeping gene. Data shown as mean +/- SEM, Two-Way ANOVA, n=3.

6.3.2.2. CHOP protein expression

CHOP protein expression is significantly increased in wild type *GBA1* overexpressing cells transiently transfected with α-synuclein compared with cells transfected with an empty vector (two-way ANOVA, Bonferroni post hoc, p=0.014). CHOP protein expression does not change in the presence of α-synuclein in either control SH-SY5Y or L444P *GBA1* overexpressing cells. CHOP protein expression in the experimental control empty vector transfections mirrors the pattern of expression seen in cells under normal conditions: increased CHOP protein expression in L444P *GBA1* overexpressing cells compared with SH-SY5Y control cells, validating the earlier result. Interestingly, the increase in CHOP protein expression seen in the wild type *GBA1*

overexpressing cell line upon transfection with *SNCA* does not far exceed that seen in the L444P *GBA1* overexpressing cells both transfected with α-synuclein and empty vector **(Figure 33).**

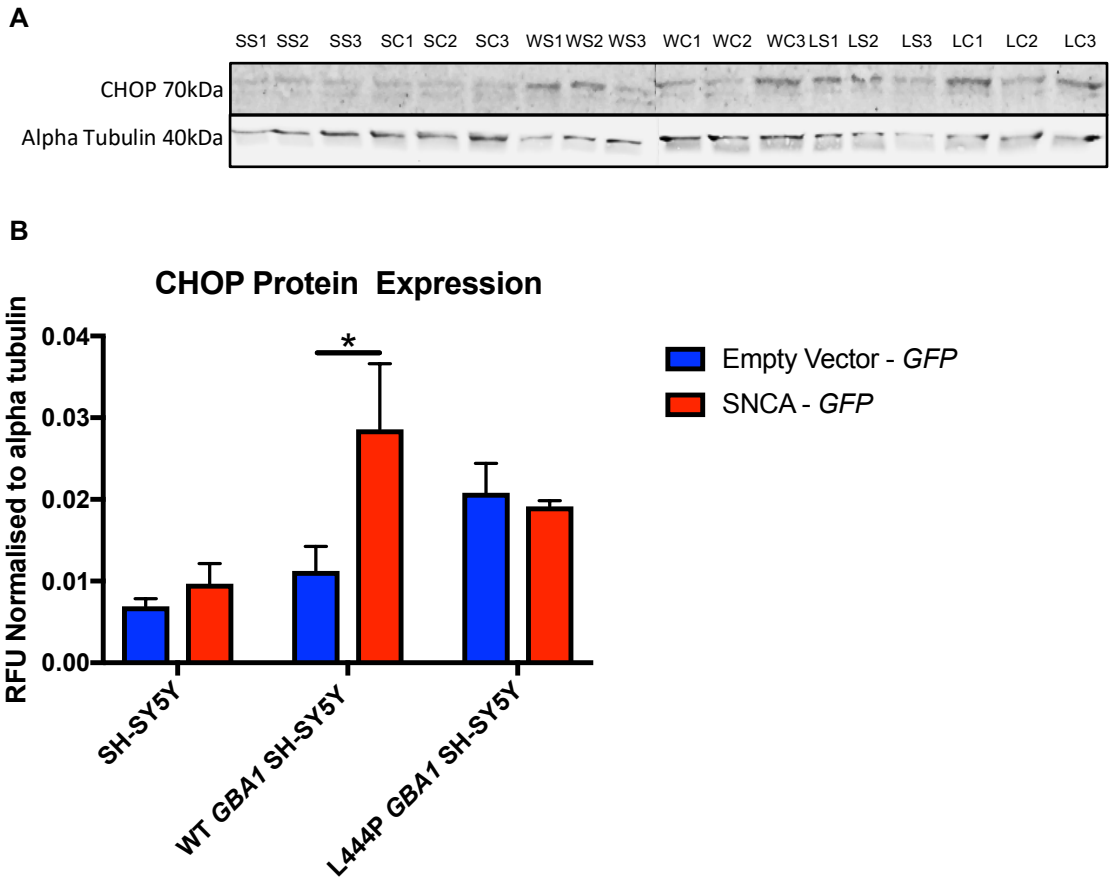

Figure 33 – CHOP protein expression in cells transiently transfected with α-synuclein (a) Representative western blot of CHOP protein expression (b) Quantitation and statistical analysis of CHOP western blot. Bars are mean+/- SEM, two-way ANOVA, Bonferroni post hoc, n=3, *p=<0.05. SS=SH-SY5Y + α-synuclein, SC=SH-SY5Y + empty vector, WS=WT *GBA1* SH-SY5Y + α-synuclein, WC= WT *GBA1* SH-SY5Y + emptor vector, LS=L444P *GBA1* SH-SY5Y + α-synuclein, LC= L444P *GBA1* SH-SY5Y + empty vector.

6.3.3. CHOP protein expression in human post mortem DLB brain tissue

CHOP protein expression remains constant relative to alpha tubulin between non-demented control, DLB and N370S-DLB cases when evaluating the dorsolateral prefrontal cortex (BA9) (one-way ANOVA, Bonferroni post hoc, p=0.616). However, there is a significant reduction in CHOP protein expression in N370S-DLB cases compared with DLB cases (one-way ANOVA, Bonferroni post hoc, p=0.0164) and non-demented controls (one-way ANOVA, Bonferroni post hoc, p=0.0064) respectively in the parietal cortex (BA40) **(Figure 34).** It should be noted that expression of α-tubulin remained constant amongst all groups and was tested by one-way ANOVA. α-tubulin is therefore a suitable loading control for all following investigations in human post mortem tissue.

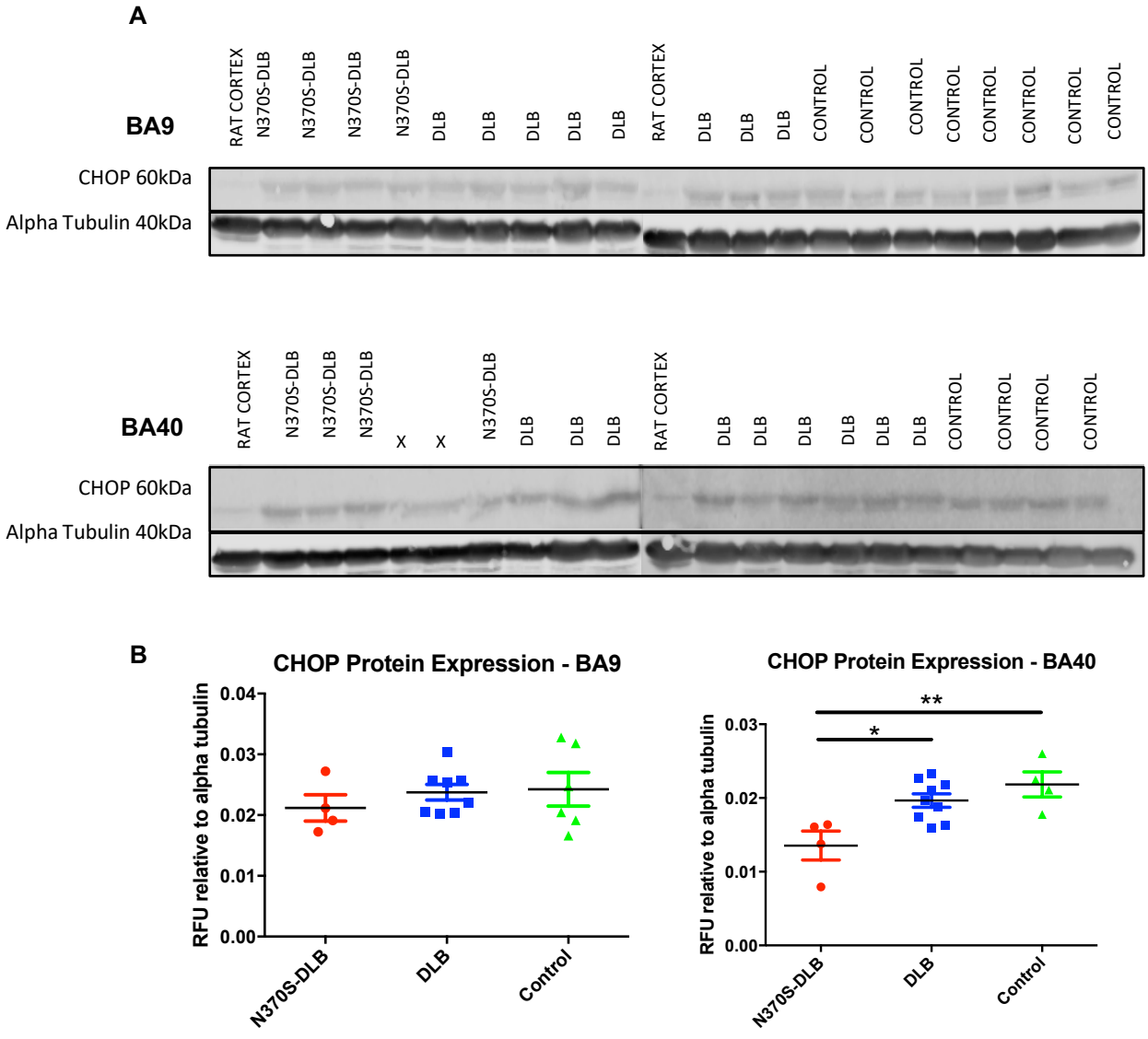

Figure 34 - Relative CHOP protein expression in human post mortem DLB brain tissue (a) Representative western blots of CHOP protein expression (b) Quantification and statistical analysis. Data are mean ± SEM, N370S-DLB n=4, DLB n = 8-9, control n=4-6, one-way ANOVA, Tukey's HSD, * p=<0.05, **p=<0.01.

6.3.4. BCL-2 protein expression in SH-SY5Y *GBA1* cell lines

BCL-2 protein expression relative to α-tubulin is not significantly different between control cells and those overexpressing either WT or L444P mutant *GBA1* (one-way ANOVA, p=0.9387) **(Figure 35).**

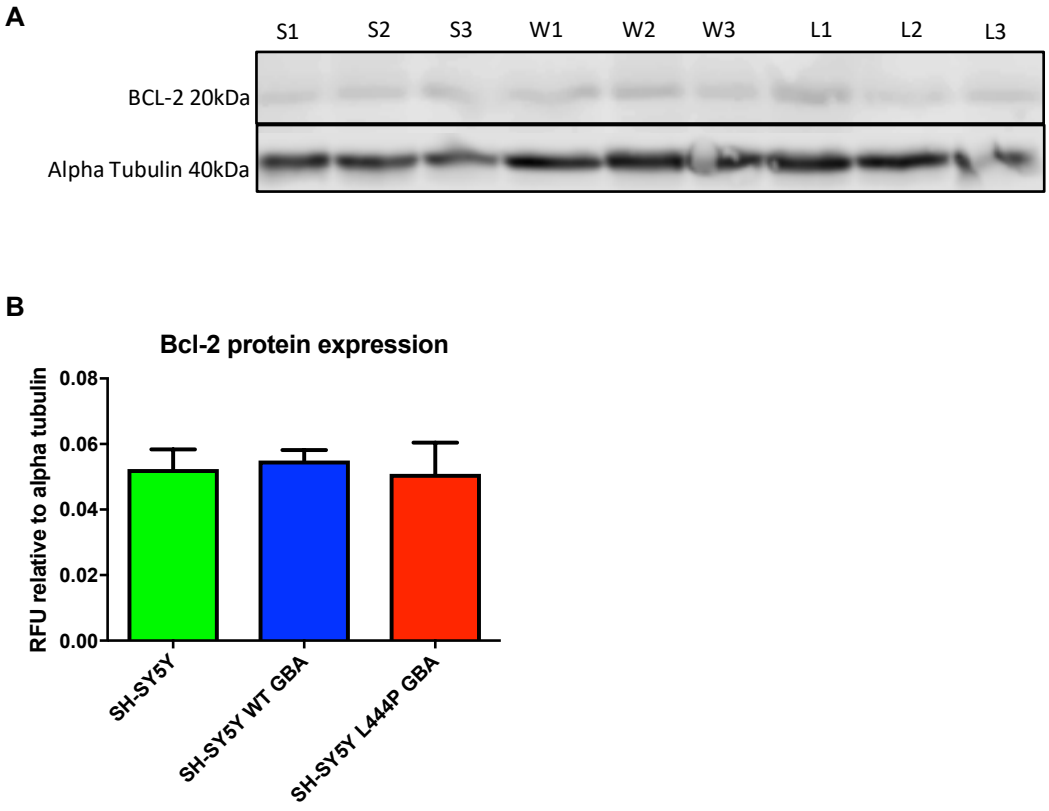

Figure 35 – BCL-2 protein expression in SH-SY5Y *GBA1* cell lines (a) Representative western blot of BCL-2 protein expression (b) Quantitation and statistical analysis of BCL-2 western blot. Bars are mean+/- SEM, one-way ANOVA, n=3. S= SH-SY5Y, W= WT *GBA1* SH-SY5Y, L= L444P *GBA1* SH-SY5Y

6.3.5. BCL-2 protein expression in human post mortem DLB brain tissue

BCL-2 protein expression remains constant between non-demented controls, DLB and N370S-DLB cases in the dorsolateral prefrontal cortex (one-way ANOVA, p=0.9735) and parietal cortex (one-way ANOVA, Tukey's HSD, p=0.7997). However, BCL-2 protein expression is significantly reduced in N370S *GBA1* mutant DLB cases compared with sporadic DLB in the temporal cortex (BA21) (one-way ANOVA, Tukey's HSD, p=0.0320) whilst BCL-2 protein expression is significantly increased in sporadic DLB cases compared with non-demented controls in the anterior cingulate gyrus (BA24) (one-way ANOVA, Tukey's HSD, p=0.0307) **(Figure 36).**

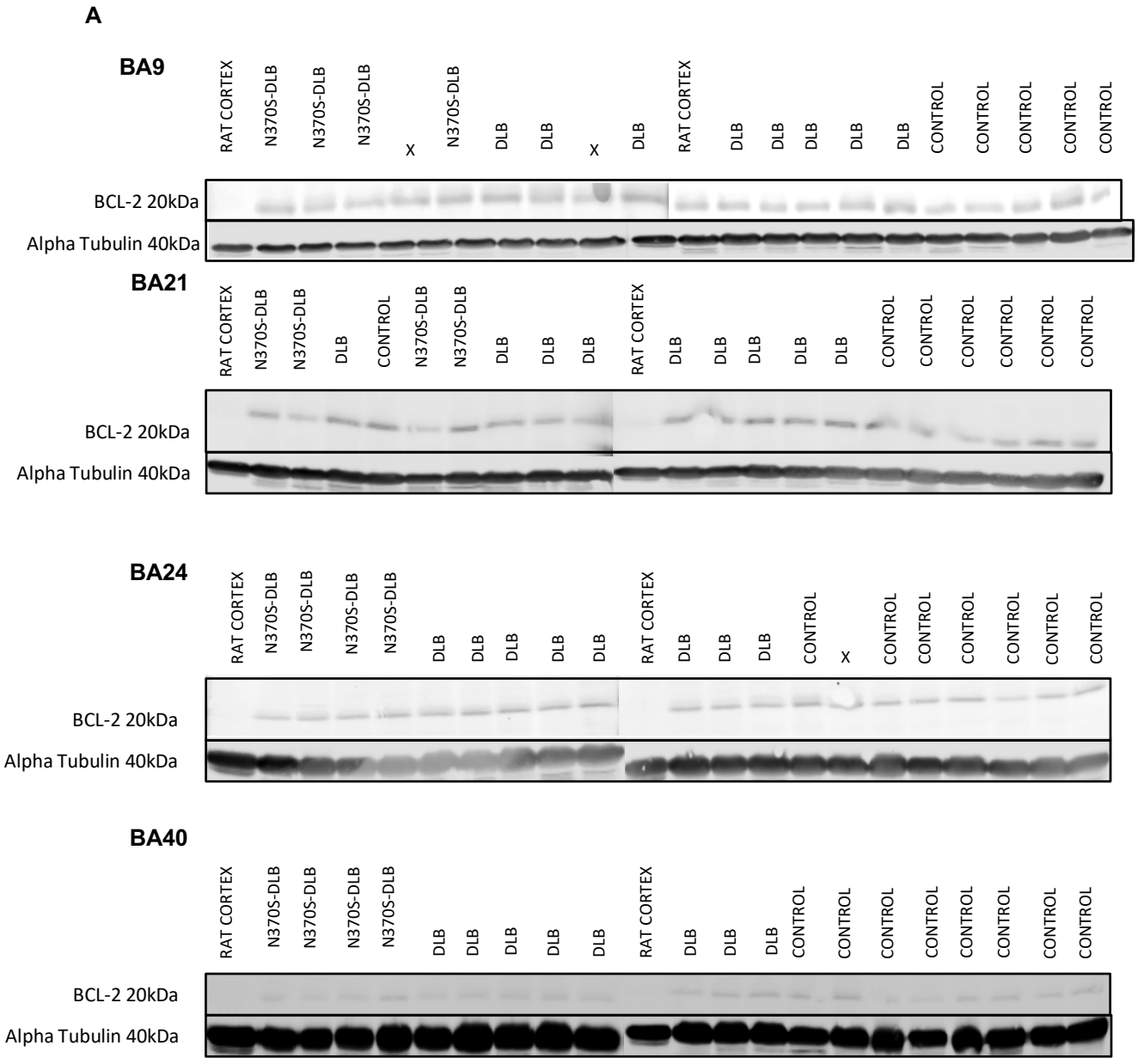

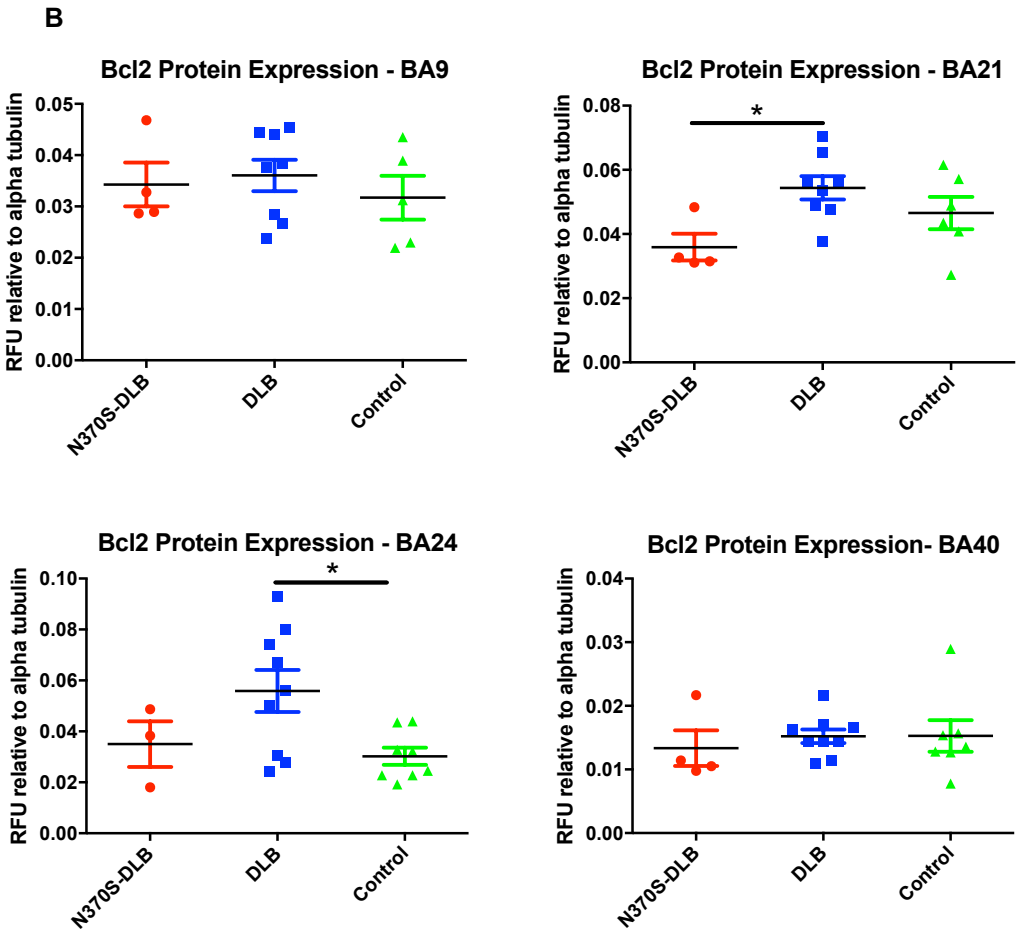

Figure 36 - BCL-2 protein expression in human post mortem DLB brain tissue (a) Representative western blots of BCL-2 protein expression (b) Quantification and statistical analysis of BCL-2 protein expression. Data are mean ± SEM, N370S-DLB n=3-4, DLB n = 8-9, control n=5-8, one-way ANOVA, Tukey's HSD, * p=<0.05

6.3.6.Caspase 3 protein expression in human post mortem DLB brain tissue

Caspase 3 protein expression remains constant between non-demented controls, sporadic DLB and N370S-DLB cases both in the temporal cortex (BA21) (one-way ANOVA, p=0.4458) and parietal cortex (BA40) (one-way ANOVA, p=0.1918) **(Figure 37).**

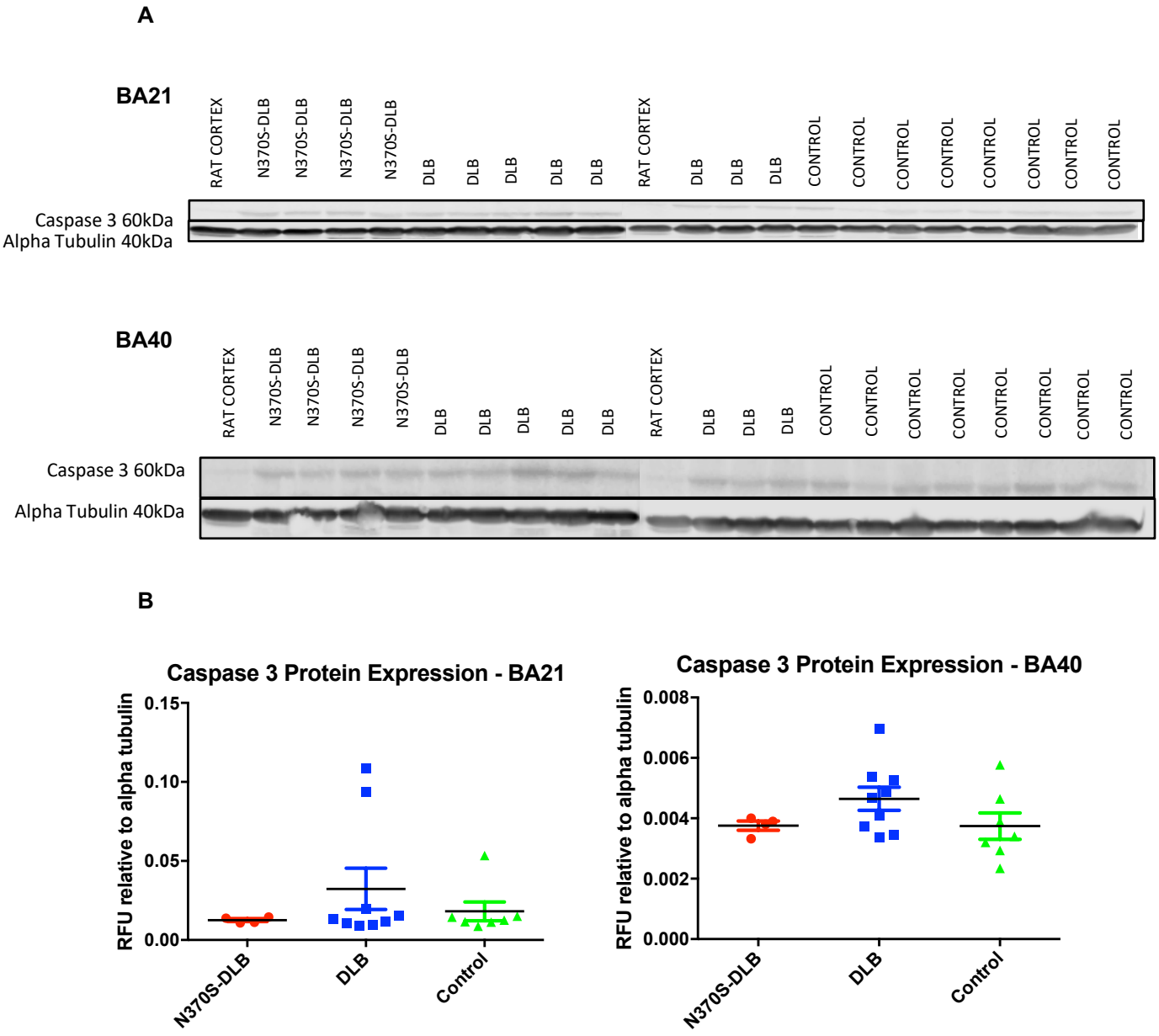

Figure 37 – Caspase 3 protein expression in human post mortem DLB brain tissue (a) Representative western blots of caspase 3 protein expression (b) Quantification and statistical analysis of caspase 3 protein expression. Data are mean ± SEM, N370S-DLB n=3-4, DLB n = 8-9, control n=5-8, one-way ANOVA, * p=<0.05

6.3.7.Caspase 12 protein expression in human post mortem DLB brain tissue

Caspase 12 protein expression does not differ between non-demented controls and either sporadic DLB or N370S *GBA1* heterozygous DLB cases in the temporal cortex (BA21), the parietal cortex (BA40) or the dorsolateral prefrontal cortex (BA9). However, the presence of N370S *GBA1* mutation in DLB cases causes a significant reduction in caspase 12 expression when compared with non-demented controls in the anterior cingulate gyrus (BA24) (one-way ANOVA, Tukey's HSD, p=0.0446) **(Figure 38).**

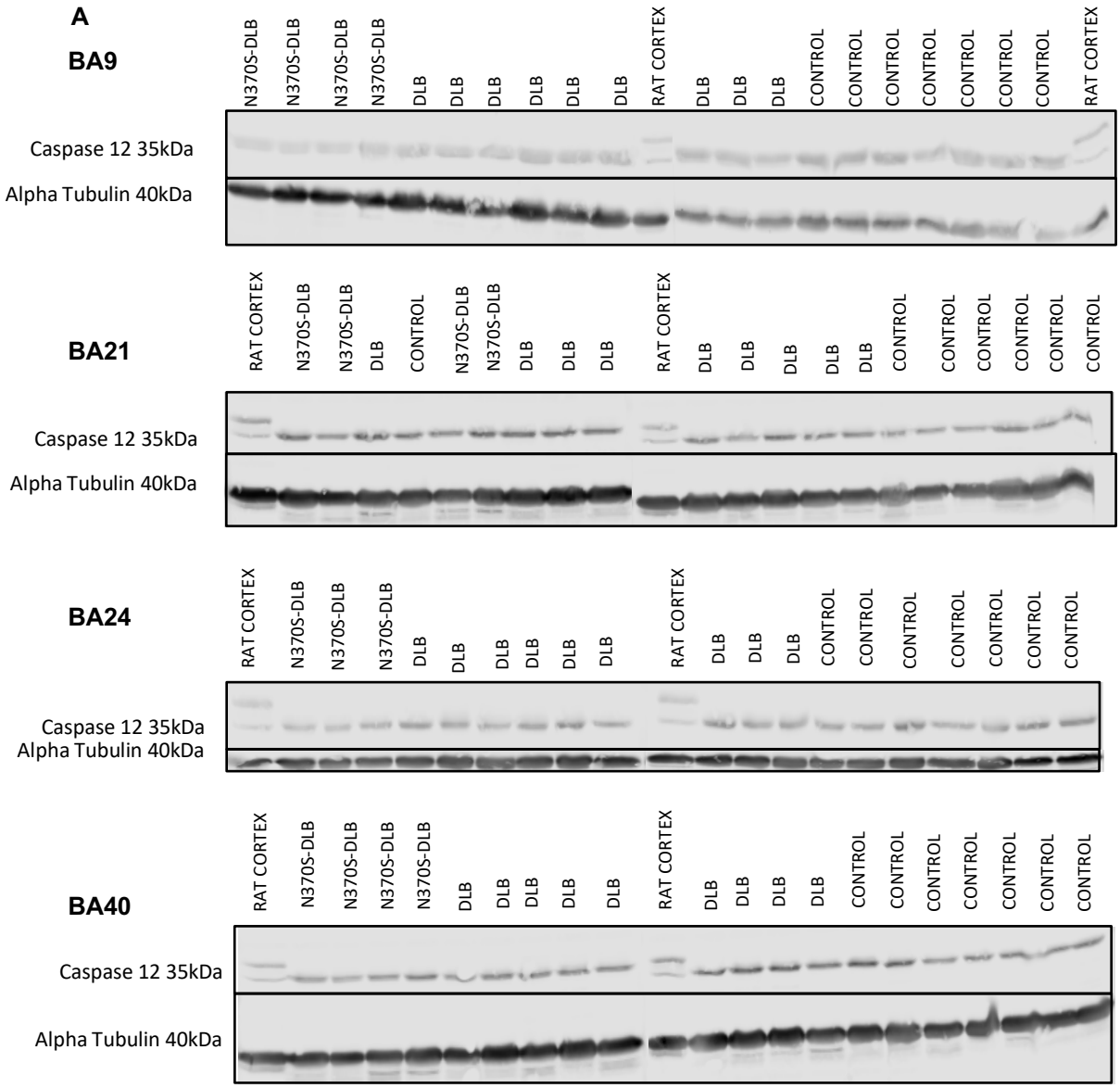

B

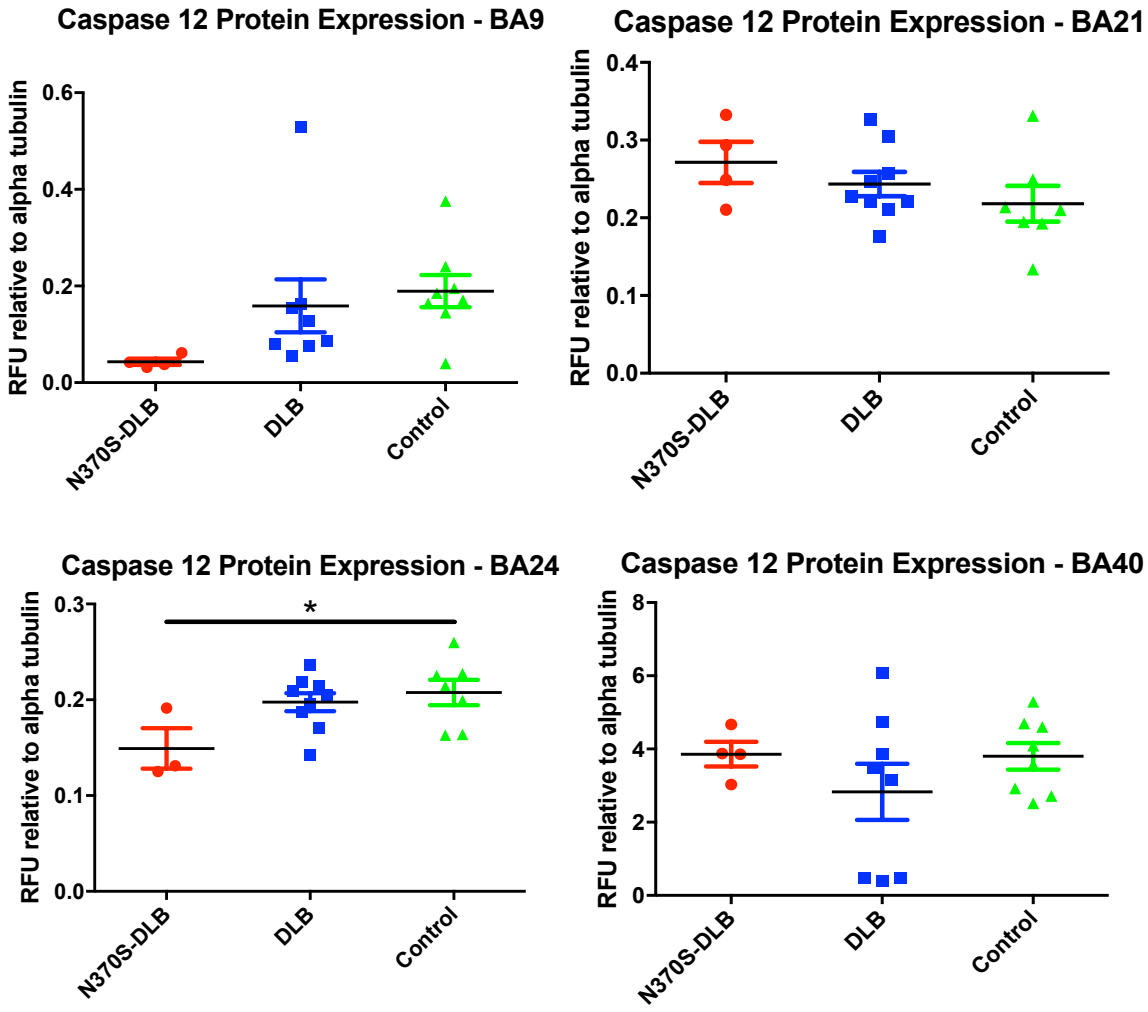

Figure 38 - Caspase 12 protein expression in human post mortem DLB brain tissue (a) Representative western blots of caspase 12 protein expression (b) Quantification and statistical analysis of caspase 12 protein expression. Data are mean ± SEM, N370S-DLB n=3-4, DLB n=8-9, control n=7, one-way ANOVA, Tukey's HSD, * p=<0.05.

6.4. Discussion

Overexpression of L444P *GBA1* in SH-SY5Y cells demonstrates upregulation of CHOP protein both by ICC **(Figure 30)** and western blot of cell lysates **(Figure 31, Figure 33).** Interestingly, a corresponding increase in CHOP gene expression was not seen **(Figure 29).** There is the possibility that variability within the qPCR results may have masked any significant change in gene expression although CHOP mRNA shows a similar expression profile in both qPCR performed on the untreated *GBA1* overexpressing SH-SY5Y cell lines and the same cell lines transfected with an empty vector GFP expressing plasmid used as a control for a later experiment **(Figure 29, Figure 32).** This indicates that it is likely that CHOP gene expression is not differentially regulated in conjunction with *GBA1* mutation. Consequently, increased CHOP protein expression seen in L444P *GBA1* cells cannot be explained simply by increased gene expression and must involve some other mechanism or pathway. Under normal cellular conditions, CHOP is expressed at very low levels in cells (Li et al., 2014). This is demonstrated by western blot in this study by the very feint bands corresponding to CHOP in control SH-SY5Y cells which makes the strong appearance of bands corresponding to CHOP in L444P *GBA1* cells more striking **(Figure 31).** However, the lack of a positive control in the experimental design prevents a comparison of the extent of CHOP protein expression in L444P *GBA1* cells against a known strong inducer of CHOP protein expression. Interestingly, one such known inducer of CHOP protein expression, tunicamycin, blocks protein glycosylation (Li et al., 2014). Glucose deprivation also induces CHOP protein expression due to inhibition of N-linked protein glycosylation (Li et al., 2014). It is known that a proportion of mutant GCase proteins are retained in the ER as identified through endoglycosidase H (EndoH) processing (Bendikov-Bar et al., 2011; Fernandes et al., 2016). EndoH is a highly specific endoglycosidase which cleaves asparagine-linked mannose oligosaccharides, but not highly processed oligosaccharides from glycoproteins (Maley et al., 1989). Many mutant GCase proteins are not endoH resistant indicating firstly that the protein is ER retained and has not traversed the Golgi. Secondly, the implication that glycosylation is deficient with mutant GCase protein, mirroring the effect of tunicamycin and glucose deprivation, provides a possible link with upregulation of CHOP protein. An increase in CHOP protein expression is consistent with previously reported findings in GD fibroblasts (Braunstein et al., 2018) although the upregulation of CHOP mRNA is more widely reported in GBA-PD fibroblasts (Maor et al., 2013; Sanchez-Martinez et al., 2016; Garcia-Sanz et al., 2017).

It could be hypothesised that the *GBA1* mutant cells are demonstrating a transient increase in CHOP protein expression due to alterations in the rapid degradation mechanisms for CHOP described earlier. This would cause a transient increase in CHOP protein expression in the absence of any change in CHOP mRNA levels.

Upon transient transfection of *GBA1* overexpressing cells with α-synuclein, CHOP gene expression was also unaffected **(Figure 32).** Interestingly, CHOP protein expression significantly increased in cells overexpressing wild type *GBA1* when transfected with α-synuclein whilst there was no difference in CHOP protein expression in L444P *GBA1* overexpressing cells treated with α-synuclein or empty vector **(Figure 33).** These results may suggest that CHOP protein expression cannot be further enhanced by the combination of accumulated α-synuclein and mutant GCase protein since maximal expression of CHOP protein has already been achieved in this model system. Furthermore, it may provide evidence for the gain of function effect of *GBA1* mutations since the presence of a *GBA1* mutation alone is sufficient to induce the expression of CHOP protein.

Whilst L444P *GBA1* overexpressing SH-SY5Y cells demonstrate a significant increase in the expression of CHOP protein, the opposite is seen in human post mortem brain tissue. CHOP protein expression is constant between N370S *GBA1*-DLB, sporadic DLB and non-demented controls in BA9. However, BA40 exhibits a significant reduction in CHOP protein expression in N370S *GBA1*-DLB cases when compared with both sporadic DLB and non-demented control cases, respectively **(Figure 34).** Consideration does need to be given to the different *GBA1* mutations studied between the cell lines and human tissue, especially since a dosage effect is well established with regard to the different *GBA1* mutations (sections 1.3.4 and 1.5.1.8). It may be that the mild N370S mutation is not capable of evoking a UPR response capable of resulting in the expression of CHOP. However, this would not satisfactorily explain why CHOP protein expression is significantly reduced in N370S *GBA1*-DLB cases when compared with sporadic DLB or non-demented controls. Although we did not investigate gene expression, our findings contradict reported increases in CHOP mRNA in the putamen of GBA-PD and sporadic PD human post mortem tissue (Gegg et al., 2012). Investigating CHOP gene expression in the post mortem cases used in this current study would be beneficial for comparison purposes although a

direct comparison between post mortem studies may not necessarily be the best approach due to the different brain regions used. Furthermore, data derived from human post mortem brain tissue is associated with the caveat of post mortem delay possibility affecting the expression of some proteins, which cannot be excluded when interpreting data. Whilst not significantly different, post mortem delay in sporadic DLB cases was lower (44.75 hours) compared with non-demented controls and N370S-DLB (56.19 hours and 56.04 hours). Considering these points, a possible explanation for a reduction in CHOP protein expression in N370S *GBA1*-DLB cases may involve a situation whereby enhanced CHOP protein expression has occurred earlier in the lifetime of the affected individuals and has already reached a maximal effect. To validate this hypothesis, further investigation of the clinical characteristics of the cases involved in the study needs to be performed to identify age on onset. As discussed in chapter 1.5, *GBA1* mutations are widely associated with earlier age of onset of dementia for both PDD and DLB, adding merit to this hypothesis. It may be that once transient CHOP protein expression has been enhanced and triggered apoptosis, levels of CHOP expression remain constant or return to basal levels.

To evaluate the impact of *GBA1* mutation on UPR induced apoptosis through the production of CHOP protein, BCL-2, caspase 3 and caspase 12 protein levels were evaluated in human post mortem tissue. A reduction of anti-apoptotic Bcl-2 protein expression, associated with the signal to induce apoptosis was identified in BA21 when comparing N370S *GBA1*-DLB cases with sporadic DLB **(Figure 36).** However, this does not correspond to increased expression of the active form of the executioner caspase, caspase 3 in the same brain region **(Figure 37).** Additionally, activated caspase 3 was not upregulated in either N370S *GBA1*-DLB or sporadic DLB cases in the other brain region tested, the parietal cortex. Perhaps this is not surprising since extensive atrophy is not necessarily associated with DLB pathology unless concurrent AD-like pathology is also present in which case greater atrophy is seen in the temporal and parietal cortices (Nedelska et al., 2015).

Caspase 12 is unusual since it has been suggested to be anchored in the ER and part of an independent apoptotic cascade specifically activated in response to ER stress (Nakagawa et al., 2000). When activated, caspase 12 translocates from the ER to the cytosol where it directly cleaves pro-caspase 9 which in turn activates the executioner caspase, caspase 3 (Szegezdi et al., 2003). However, to date functional caspase 12 has only been cloned from mouse and rat and

there is debate as to whether a human isoform of caspase 12 exists (Szegezdi et al., 2003). Despite this debate, activation of caspase 12 during apoptosis has been reported in human cells (Szegezdi et al., 2003). Cleaved caspase 12 was detected in all human post mortem tissues by western blot **(Figure 38).** While the level of cleaved caspase 12 was comparable between N370S *GBA1*-DLB, sporadic DLB and non-demented controls in the temporal cortex, parietal cortex and dorsolateral prefrontal cortex, the expression of activated caspase 12 was significantly lower in N370S *GBA1*-DLB cases compared with non-demented controls in anterior cingulate cortex **(Figure 38).** One interpretation of this result may be that *GBA1* mutation prevents apoptotic cell death through caspase 12 in the anterior cingulate gyrus. However, caspase 12 has also been designated as an inflammatory caspase (Shalini et al., 2015). Specifically, caspase 12 is a negative regulator of inflammation triggered by infection, inhibiting the production of the pro-inflammatory cytokines IL-1β and IL-18 (Garcia de la Cadena and Massieu, 2016). Conversely the human paralog to caspase 12, caspase 4, is a positive regulator of inflammation (Garcia de la Cadena and Massieu, 2016). It may be that caspase 12 down regulation as a result of *GBA1* mutation in DLB may be triggering the release of pro-inflammatory cytokines in response to accumulated and aggregated α-synuclein. Investigation of a potential link between caspase 12 and the established neuroinflammation associated with both DLB and PD (Lim et al., 2016) would be an interesting area of further study.

7. Behavioural characterisation of *GBA1* D427V/WT transgenic mice.

7.1. Introduction

In vivo models of *GBA1* deficiency have been developed for the study of GD. However, with the emergence of the link between *GBA1* mutations and synucleinopathy these models are increasingly being adapted to study pathological mechanisms and develop therapeutic compounds for LBD. Broadly, there are 3 main categories of GD mouse model: chemically induced, conditional knock down and point mutations.

7.1.1.Chemical models (CβE)

An *in vivo* model of GD was first developed in 1975 by Kanfer et al using the pharmacological GCase inhibitor CβE (Kanfer et al., 1975). This initial study established a dose of 100mg/Kg injected intraperitoneally was sufficient to cause an approximate 50% increase in GluCer in peripheral tissues and a 5-fold increase of GluCer in the brain of animals 3 months post-natal in the absence of any overt phenotypic consequence (Kanfer et al., 1975). However new born mice injected with CβE for 28 days exhibit profound symptoms indicating CNS involvement including: tail arching, tremor and a minimal startle response (Kanfer et al., 1975).

Neurological consequences associated with reduced GCase enzyme activity via the administration of CβE have since been replicated. Wild type mice injected intraperitoneally with CβE 100mg/Kg/day initiated at post-natal day 5 for 10 days display a neurological phenotype which is reversible with a 3-4 day latency following the last CβE injection (Xu et al., 2008). However post-natal day 15 mice injected with CβE developed a more severe neurological phenotype which results in death after 7-12 days contradicting the early reports by Kanfer et al (Kanfer et al., 1975; Xu et al., 2008).

More recently, a conclusive study demonstrated a correlation between the amount of CβE injected into mice and the levels of accumulated GluCer and GluSph in the brain which in turn correlates with survivability (Vardi et al., 2016). This study also confirmed that the age of the animal is an

important factor for severity of neurological symptoms and survival (Vardi et al., 2016). Mice injected with CβE of any concentration from post-natal day 15 display less severe symptoms and survive longer (Vardi et al., 2016). Of particular note is the report that CβE injected mice demonstrate very similar pathology and altered gene expression profiles to the genetic models K14-lnl and *GBA1*$^{flox/flox}$;nestin-cre described below, making CβE an attractive tool for modelling GD and potentially for studying the link between *GBA1* and synucleinopathies (Vardi et al., 2016).

7.1.2.Conditional knockdown

Initial attempts to create a *GBA1* knock down mouse model proved unsuccessful since ubiquitous knock down of *GBA1* caused neonatal lethality (Tybulewicz et al., 1992). Later, it was discovered that GCase activity is critical to dermal development with the cause of death of these mice being excessive water loss through the skin (Holleran et al., 1994).

A conditional type 1 GD mouse model has been generated using the *Mx1*-Cre-*loxP* system, allowing Cre mediated deletion of a floxed murine *GBA1* upon activation of the *Mx1* promoter with polyinosinic-polycytidylic acid (Enquist et al., 2006). *Mx1*-cre mediated deletion of *GBA1* occurs in haematopoietic stem cells and in all progeny including macrophages but only to a limited extent in the CNS (Enquist et al., 2006). These mice have significantly accumulated GluCer in bone marrow, spleen and liver but not the brain (Enquist et al., 2006). Phenotypically, these mice have a normal lifespan and do not show gross signs of bone disease or CNS abnormalities (Enquist et al., 2006). Similarly, mice have been generated whereby murine *GBA1* has been flanked by *loxP* sites and crossed with a Tie2Cre mouse line to enact knock down of *GBA1* in cells of haematopoietic and endothelial origin, resulting in similar visceral deficiencies of GCase enzyme activity and GluCer accumulation (Sinclair et al., 2007). A more recent adaptation of the *Mx1*-Cre-loxP system to conditionally knock down *GBA1* has proved to be more effective, causing over 95% reduction in GCase enzyme activity in cells of haematopoietic and mesenchymal stem cell lineages resulting in dramatic accumulation of GluCer and GluSph (Mistry et al., 2010). Furthermore, in addition to visceral and haematological pathologies, these mice also exhibited profound skeletal defects (Mistry et al., 2010). As such, the models described above may prove more useful for the investigation of GD, rather than PD-GD.

Conditional knockdown of *GBA1* has been performed to generate models of neuronopathic GD. Insertion of a *loxP*-neo-*loxP* (lnl) cassette into inton 8 of murine *GBA1* causes lnl homozygous mice to die within hours of birth, with a similar skin phenotype to ubiquitous *GBA1* knock down mice (Tybulewicz et al., 1992; Enquist et al., 2007). However, crossing *GBA1*$^{lnl/lnl}$ mice with K14-Cre transgenic mice allows for Cre-recombinase expression driven by the K14 promoter facilitating recombination of *GBA1*$^{lnl/lnl}$ within the skin (Enquist et al., 2007). The subsequent mice, K14-lnl/lnl, develop rapidly progressing neurological disease after an initial 10-day symptom free period (Enquist et al., 2007). Mice show symptoms of motor dysfunction including abnormal gait and seizures, ultimately requiring euthanasia 2 weeks following birth (Enquist et al., 2007). K14-lnl mice exhibit dramatically reduced GCase enzyme activity and accumulated levels of GluCer and GluSph in the brain, spleen and liver (Enquist et al., 2007). The same research group also developed the *GBA1*$^{flox/flox}$;nestin-cre transgenic mouse in which GCase enzyme deficiency is restricted to the progeny of neural and glial cell precursors but maintain normal GCase enzyme activity within microglia (Enquist et al., 2007). These mice also develop pathology and symptoms of neurogenic GD similar to those in K14-lnl mice although with a delayed onset of 2-3 weeks from birth (Enquist et al., 2007).

A different approach to creating a conditional neuronopathic model of GD has been the use of the K14 promoter to drive Cre recombination of D409H mutant *GBA1* allele in the skin, leaving all other tissues *GBA1* null (Xu et al., 2008). In this case, Kn-9H mice start to develop progressive neurological defects from post-natal day 10 including altered gait, tremor, myoclonus and seizures (Xu et al., 2008). However, the very early symptomatic onset reported in these models precludes them from modelling a late onset neurodegenerative condition such as GD-PD.

7.1.3.Point mutation

The introduction of point mutations into *GBA1* are considered to be the 'gold standard' for studying GD since this approach mirrors the molecular basis of the condition and involves factors other than solely reduced GCase enzyme activity. However, generation of these models has proved difficult. The first point mutations inserted into murine *GBA1* were RecNcil and L444P although in both cases the mice did not survive past 24 hours (Liu et al., 1998). A viable L444P mutant mouse has been engineered by crossing *GBA1*$^{+/L444P}$ mice with mice expressing heterozygous knockout of GluCer synthase (*Ugcg*$^{+/-}$) to generate the *GBA1*$^{+/L444P}$;*Ugcg*$^{+/-}$ mouse (Mizukami et al., 2002).

Through a series of cross breeding and inter-crossing, double mutant L444P mice were generated: *GBA1*$^{L444P/L444P}$;*Ugcg*$^{+/+}$ (*GBA1*$^{L444P/L444P}$).(Mizukami et al., 2002). *GBA1*$^{L444P/L444P}$ mice which survive weaning are generally fertile and have a lifespan of over 1 year (Mizukami et al., 2002). As expected there is a significant reduction in GCase enzyme activity in several organs, 15-20% of wild type levels, although the reduction in GCase enzyme activity does not result in GluCer accumulation making their utility for the study of GD debatable (Mizukami et al., 2002). Despite the lack of GluCer accumulation, these mice do display an interesting characteristic of extensive multi-organ inflammation (Mizukami et al., 2002)

Direct introduction of point mutations into the murine *GBA1* gene was first performed successfully by Xu et al (Xu et al., 2003). Homozygous V394L, D409H and D409V point mutations result in GCase enzyme activity between 4 and 25% of wild type in the major organs (Xu et al., 2003). However, GluCer accumulation is only present at modest levels and is absent in the brain (Xu et al., 2003). Additionally, there is no overt behavioural phenotype. Surprisingly, homozygous N370S mutation in murine *GBA1* caused neonatal lethality (Xu et al., 2003). The GD phenotype associated with V394L, D409H and D409V mutation has further been enhanced with concomitant intra-peritoneal injection of CβE to cause CNS involvement and death after 2 weeks (Xu et al., 2008). Neuronal degeneration is progressive and GluCer storage persists in D409V homozygous mice in the 2-5 months following CβE cessation; wild type and D409H mice have persistent neurological damage without progression (Xu et al., 2008). This suggests that a threshold of GCase enzyme activity is required to prevent progression to CNS involvement. Furthermore, neuronopathic GD phenotype has been enhanced in D409H and V384L homozygous mice by crossing with prosaposin-deficient mice containing hydromorphic *PSAP* (Xu et al., 2011).

Human wild type, N370S and L444P *GBA1* have been bred into mice with a *GBA1* null background, demonstrating progressive and early elevation of tissue GluCer and GluSph in the liver and spleen (Sanders et al., 2013). Specifically, human L444P causes dramatic elevation of GluCer particularly at older age. Unfortunately, CNS pathology or phenotype has not been investigated in this model (Sanders et al., 2013).

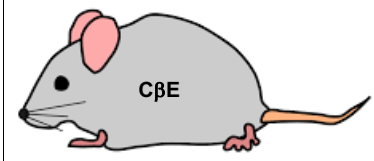	Intra peritoneal injection of GCase inhibitor CβE 100mg/Kg for 21-28 days	No evident behavioural difference at 3 months of age. Approx 50% increase in GluCer in peripheral tissues and 5 fold increase in brain tissue. New born mice injected with CβE demonstrate CNS involvement.	(Kanfer et al., 1975)
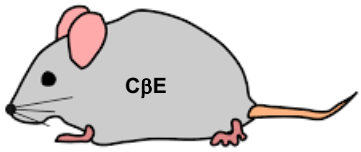	Intra peritoneal injection of GCase inhibitor CβE 100mg/Kg daily for 8-12 days	Post-natal day 5 mice injected with CβE for 10 days display a neurological phenotype which is reversible with a 3-4 day latency following the last CβE injection. Injection of post-natal day 15 mice causes a more severe phenotype and death after 7-12 days.	(Xu et al., 2008)
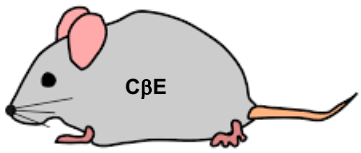	Intra peritoneal injection of GCase inhibitor CβE 100mg/Kg daily for 9 days into 8 week old mice	Motor impairment, Widespread activation of glia.	(Ginns et al., 2014)
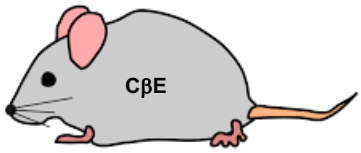	Intra peritoneal injection of GCase inhibitor CβE 100mg/Kg daily for 28 days into 8 week old mice	Widespread microglial activation in motor cortex, striatum and substantia nigra. Neuronal cell loss in motor and somatosensory cortices.	(Noelker et al., 2015)
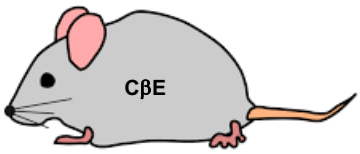	Intra peritoneal injection of GCase inhibitor CβE at different doses (25-100mg/Kg) for different durations and different post-natal age.	90-95% reduction in brain GCase activity regardless of CβE dose. Injection from post-natal day 15 causes less severe symptoms better survival. Similar pathology and altered gene expression profiles to the conditional knock down genetic models.	(Vardi et al., 2016)
	Ubiquitous *GBA1* knock out	Neonatal lethal. Die within 24 hours of birth due to GCase involvement in skin formation.	(Tybulewicz et al., 1992)
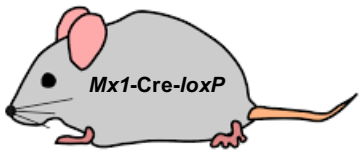	Conditional knockout. Mx1-cre mediated deletion of *GBA1* in haematopoietic stem cells and progeny	Normal lifespan. Accumulated GluCer in bone marrow, spleen and liver but NOT brain.	(Enquist et al., 2006)

	Conditional knock out. Hematopoietic and endothelial cell specific Tie2Cre strain	Progressive splenomegaly and GluCer storage by 26 weeks.	(Sinclair et al., 2007)
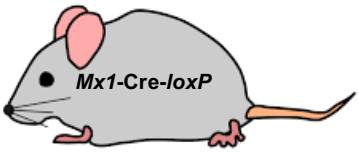	Conditional knockout. Mx1-cre mediated deletion of *GBA1* in haematopoietic and mesenchymal stem cell lineages	Dramatic visceral accumulation of GluCer and GluSph. Visceral, haematological and profound skeletal pathology.	(Mistry et al., 2010)
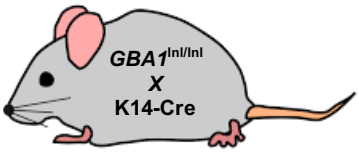	Conditional knockout. *GBA1*$^{Inl/Inl}$ crossed with K14-Cre transgenic mice to facilitate recombination of *GBA1*$^{Inl/Inl}$ within the skin.	Rapidly progressing neurological disease (nGD). Exhibit motor dysfunction and seizures. Die after 2 weeks. Reduced GCase enzyme activity and GluCer accumulation in visceral tissues and brain.	(Enquist et al., 2007)
	Conditional knockout. *GBA1*$^{flox/flox}$;nestin-cre. GCase deficiency restricted to progeny of neural and glial cell precursors. Normal GCase activity in microglia.	Similar pathology and development of neurological symptoms to *GBA1*$^{Inl/Inl}$ with delayed onset of 2-3 weeks	(Enquist et al., 2007)
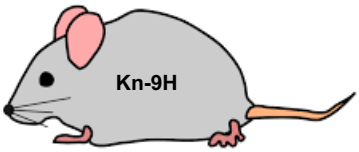	Conditional expression of D409H in the skin using the K14 promoter.	progressive neurological defects from post-natal day 10 including altered gait, tremor, myoclonus and seizures.	(Xu et al., 2008)
	Murine homozygous RecNcil and L444P *GBA1*	Neonatal lethal	(Liu et al., 1998)

	Murine L444P *GBA1* homozygous mice bred to be viable through cross breeding with *Ugcg*$^{-/+}$ mice.	Significant reduction in GCase enzyme activity but NO accumulation of GluCer.	(Mizukami et al., 2002)
	Murine homozygous D409V, D409H and V394L *GBA1* mutation. Murine homozygous N370S *GBA1* mutation.	GCase activity reduced to 4-25% in major organs. No GluCer accumulation in brain. Neonatal lethal	(Xu et al., 2003)
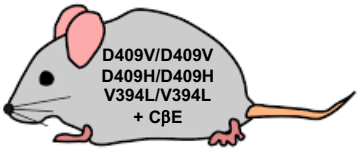	Murine homozygous D409V, D409H and V394L *GBA1* mutation + 100mg/Kg CβE i.p. for 8-12 days	CNS involvement and death after 2 weeks. Neuronal degeneration is progressive and GluCer storage persists in D409V homozygous mice in the 2-5 months following CβE cessation; wild type and D409H mice have persistent neurological damage without progression	(Xu et al., 2008)
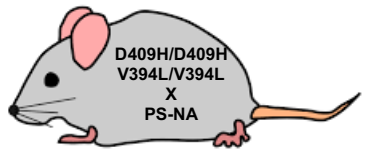	Murine homozygous, D409H or V394L *GBA1* mutation with hypomorphic prosaposin transgene	Progressive neurological manifestations and brain GluCer accumulation	(Xu et al., 2011)
	Human N370S or L444P homozygote bred into *GBA1*$^{-/-}$ background	Progressive and early elevation of tissue GluSph and GluCer in spleen and liver. L444P caused particularly enhanced elevation of GluCer at older age. CNS not assessed.	(Sanders et al., 2013)

Table 18 - Summary of GD mouse models

7.1.4.D427V/D427V *GBA1* mouse

The D427V *GBA1* homozygous mouse model is of particular interest for *GBA1* associated studies since it has been reported that these mice have a cognitive impairment phenotype (Sardi et al., 2011). Since these mice could be of particular value for studying the link between *GBA1* mutation and LBD, the characteristics of this model are described in detail below.

7.1.4.1. Biochemistry

GCase enzyme activity within the brain of D427V *GBA1* homozygous mice is less than 25% of wild type mice (Xu et al., 2003; Cullen et al., 2011; Sardi et al., 2011). Additionally, GCase enzyme activity is reduced to 2.5% compared with wild type in the liver, 6.2% in the spleen and 5.4% in the lungs (Xu et al., 2003).

D427V1 *GBA1* homozygous mice exhibit a 2-4 fold increase in GluCer in the liver, lung and spleen at 6 months of age, but not the brain (Xu et al., 2003). Accordingly, mass spectrometry analysis of glycosphingolipids in the hippocampus shows normal GluCer levels at 12 months but a marked and progressive accumulation of GluSph starting from 2 months (Sardi et al., 2011).

Total α-synuclein concentration in the forebrain measured by ELISA is not significantly different from wild type in D427V *GBA1* homozygous mice of 6 months of age however a significant increase in membrane bound α-synuclein is seen in mice at 12 months (Cullen et al., 2011). Similarly, a 125% increase in membrane bound α-synuclein is seen in the hippocampus of these animals concurrent with a trend for reduced soluble α-synuclein (Cullen et al., 2011). Importantly, these mice do not show a significant increase in the levels of insoluble α-synuclein characteristic of human PD and DLB brain (Cullen et al., 2011).

Whilst Cullen et al reported increased anti-ubiquitin staining by IHC in the cytoplasm of isolated neurons in the cortex and hippocampus from D427V *GBA1* homozygous mice at 12 months there was no consistent evidence of either neuronal or glial α-synuclein accumulation or cytoplasmic inclusions by standard IHC protocol using 2 antigen retrieval steps (Cullen et al., 2011). However, using an adapted IHC technique and including treatment with proteinase K, Sardi et al. revealed the presence of α-synuclein aggregates containing ubiquitin in the hippocampus of the same

animals in a progressive manner starting from 6 months of age, mirroring pathology seen in human DLB or advanced PD (Sardi et al., 2011). These α-synuclein/ubiquitin aggregates are also present in the cerebral cortex and cerebellum but to a lesser extent and primarily occur within neurites (Sardi et al., 2011).

D427V *GBA1* homozygous mice also exhibit progressive accumulation of tau aggregates from 6 months predominantly in the hippocampus but also in the cortex and cerebellum (Sardi et al., 2013). A modest but significant increase in hyper-phosphorylated tau detected by AT8 staining in hippocampal lysates from 18 months D427V *GBA1* homozygous mice hints at the presence of neurofibrillary tangles, a contributor to the mixed pathology of human LBD (Sardi et al., 2013).

D427V *GBA1* homozygous mice at 12 months show no evidence of inflammation in hippocampal sections through the absence of significant Iba1 or GFAP staining (Sardi et al., 2011). Furthermore, Fluoro-Jade C staining revealed no significant neuronal cell death in the hippocampus (Sardi et al., 2011). Tyrosine hydroxylase staining shows no overt nigrostriatal cell loss (Sardi et al., 2011).

7.1.4.2. Phenotype

D427V *GBA1* homozygous mice have a normal lifespan and display no overt signs of neurological dysfunction (Xu et al., 2003; Cullen et al., 2011). However, at 6 months D427V *GBA1* homozygous mice exhibit impaired cognitive function demonstrated through a significant lack of novelty discrimination assed through the novel object recognition test (Sardi et al., 2011). Confounding factors such as loss of ambulatory activity or anxiety were excluded due to similar performance to wild type mice in the open field behavioural test (Sardi et al., 2011). Memory impairment in the same mice has been confirmed with the fear conditioning paradigm whereby D427V *GBA1* homozygous mice at 6 months exhibit significant deficits in both contextual and cued fear tasks (Sardi et al., 2011).

7.1.4.3. D427V/WT *GBA1* mouse

Since heterozygous mutations in *GBA1* are associated with PD and DLB, a heterozygous D427V *GBA1* mouse may more accurately reflect GCase enzyme activity and be a more translational

model for LBD. Unfortunately, very few characteristics of heterozygous mice are reported in the literature.

D427V/WT *GBA1* mice exhibit 59% brain GCase enzyme activity compared with wild type mice and do not show accumulation of GluSph as seen in homozygous mice, suggesting that one wild type allele is sufficient to prevent toxic substrate accumulation (Sardi et al., 2011). However, α-synuclein-ubiquitin aggregates are detected in the hippocampus but the number of aggregates is only approximately 50% of those seen in the homozygous D427V *GBA1* mouse (Sardi et al., 2011). Interestingly, α-synuclein-ubiquitin aggregates are not seen in *GBA1* +/- mice (Sardi et al., 2011). D427V/WT mice aged to 12 months have been reported to show a non-significant trend towards increased α-synuclein in the hippocampus (+6%) and brainstem (+2%) by ELISA (Cullen et al., 2011).

D427V/WT *GBA1* mice have a normal lifespan and display no overt signs of neurological dysfunction (Xu et al., 2003; Cullen et al., 2011). Unlike D427V *GBA1* homozygous mice, heterozygotes do not exhibit any hippocampal memory deficit at 6 months of age (Sardi et al., 2011). The authors suggest that hippocampal α-synuclein-ubiquitin aggregates to the extent seen in this model are not sufficient to causes a loss in memory recognisable by novel object recognition or contextual fear conditioning; loss of more than 75% GCase activity appears to be the additional requirement (Sardi et al., 2011).

Since heterozygous *GBA1* mutant mice would be a more translational model for LBD, it appears the lack of studies extensively characterising the behavioural phenotype of these mice is an unmet area of research. Accordingly, the final chapter of this thesis investigates cognitive impairment in the D427V/WT *GBA1* mouse.

	D427V/D427V *GBA1*	D427V/WT *GBA1*
GCase enzyme activity	25%	59%
α-synuclein-ubiquitin aggregates in hippocampus	Progressive accumulation from 6 months	Evidence of aggregates at 12 months. 50% of homozygous aggregates
GluCer accumulation in hippocampus	No accumulation	No accumulation
GluSph accumulation in hippocampus	Progressive accumulation from 2 months	No accumulation
Tau aggregates in hippocampus	Progressive accumulation from 6 months	Not tested
Neurofibrillary tangles in hippocampus	Potentially – moderate but significant increase in AT8 staining	Not tested
Inflammation in hippocampus (Iba1 and GFAP staining)	None at 12 months	Not tested
Neuronal cell death in hippocampus (Fluoro-jade staining)	None at 12 months	Not tested
Nigrostriatal cell loss (Tyrsoine hydroxylase staining)	None at 12 months	Not tested
Novel object recognition	Cognitive impairment from 6 months	No cognitive impairment evident at 6 months
Contextual fear conditioning	Cognitive impairment from 6 months	Not tested
Anxiety (open field)	Not evident at 12 months	Not tested
Locomotion (open field)	No impairment at 12 months	Not tested

Table 19 - Summary of characteristics of D427V *GBA1* mouse model

7.2. Aims and objectives

7.2.1. Aims

The aim of this chapter is to characterise the behavioural phenotype of D427V/WT *GBA1* mice over a 12-month period to establish whether D427V/WT mice are a suitable translational model for the study of LBD. Previously, heterozygous mice had only been tested until the age of 6 months.

7.2.2. Objectives

- Establish whether D427V/WT mice have a motor impairment by performing open field analysis at 3, 6, 9 and 12 months of age
- Establish whether D427V/WT mice display symptoms of anxiety evident in open field analysis
- Establish whether D427V/WT mice have a cognitive impairment phenotype as assessed by Morris water maze and Y-maze at 3, 6, 9 and 12 months of age

7.3. Results

7.3.1.Open field

7.3.1.1. Distance moved

At 3 months of age, D427V/WT mice appeared to move a greater distance (35211 ± 9268cm) compared with WT (25057 ± 6262cm) although not to a statistically significant degree (repeated measured ANOVA, F(3,39)=10.49, p=0.3624). From 6 months of age, D427V/WT and WT mice cover shorter distances (5196.723 ± 324.019cm and 9055.017 ± 486.868cm, respectively) which are not statistically different dependent upon genotype (repeated measures ANOVA, F(3,39)=10.49, p=0.3624). From this age point onwards, D427V/WT and WT mice perform similarly for the parameter of distance moved **(Figure 39).**

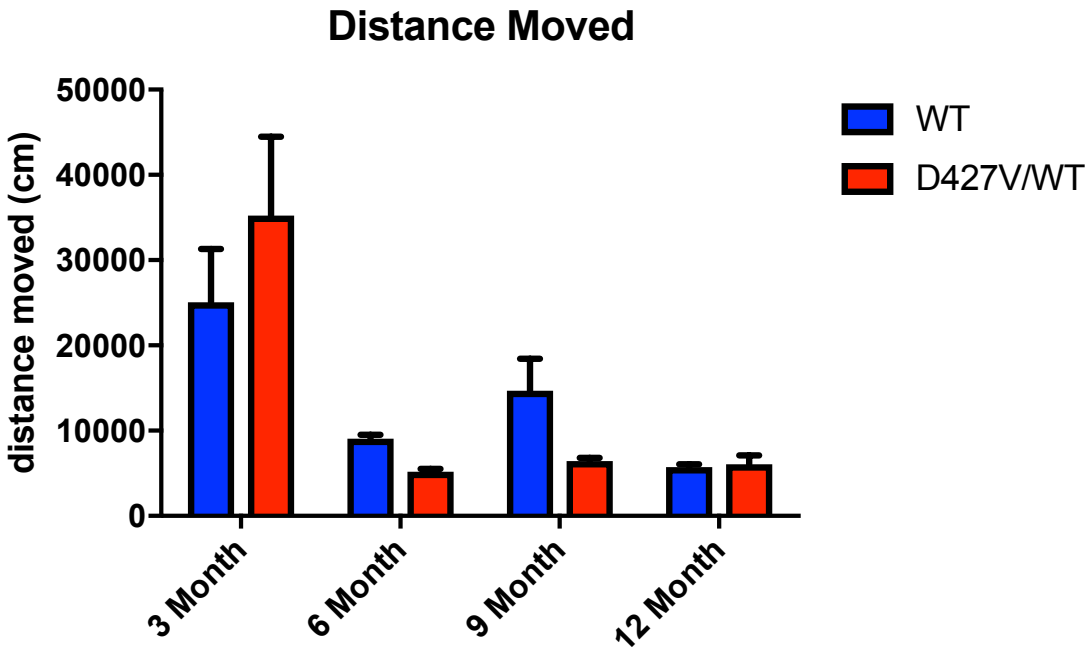

Figure 39 –Distance moved in open field. Distance moved measured in cm by WT (blue) and D427V/WT(red) mice at 3,6,9 and 12 months of age. Data are represented as mean ± SEM, n=8-10 per group, repeated measures ANOVA, F(3,39)=10.49, p=0.3624). No significant differences were observed between groups at any age tested.

7.3.1.2. Velocity

The speed each animal moved in the open field was measured and recorded as cm/s. At 3 months of age D427V/WT mice moved faster than WT mice of the same age although not to a statistically significant degree (31.35 ± 6.006 cm/s and 24.41 ± 8.257 cm/s respectively, repeated measures ANOVA, Sidak 's post hoc, F(3,39)=11.17, p=0.4713). At 6 months of age D427V/WT and WT mice move at similar speeds (4.334 ± 0.271 cm/s and 7.702 ± 0.412 cm/s respectively) although the speed is much slower than the performance of 3-month-old mice. From 6 months of age onwards, D427V/WT and WT mice exhibit similar velocity without any impact of genotype on performance **(Figure 40).**

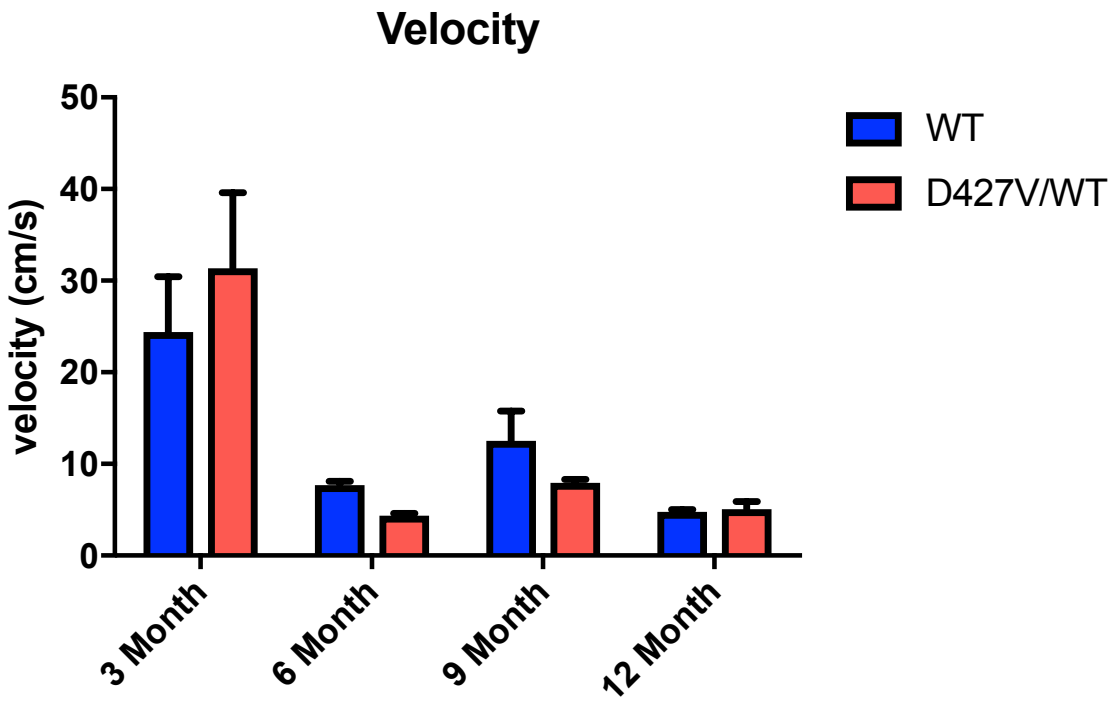

Figure 40 – Velocity of mice in the open field. Velocity measured as cm/s in WT (blue) and D427V/WT (red) mice at 3,6,9 and 12 months of age. Data are represented as mean ± SEM, n=8-10 per group. Repeated measures ANOVA, Sidak's post hoc, F(3,39)=11.17, p=<0.001. No significant differences were observed between groups at any age tested after correcting for multiple comparison using Sidak's post hoc test.

7.3.1.3. Anxiety - % time in perimeter

The amount of time each mouse spent within a 11.25cm^2 perimeter of the open field arena was calculated and expressed as a percentage of the 20-minute trial. Between genotype and across all time points, there was no difference in % time spent in the perimeter, indicating the absence of an anxiety phenotype **(Figure 41).**

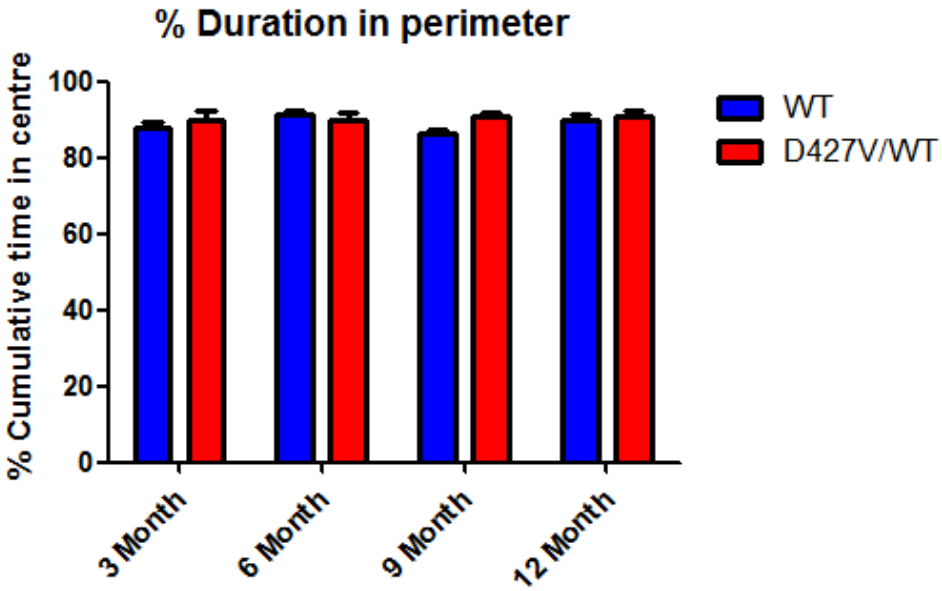

Figure 41 - Anxiety measured in open field. Anxiety measured indirectly through % cumulative time spent in the perimeter of the open field arena of WT (blue) and D427V/WT (red) mice at 3,6,9 and 12 months of age. Data are represented as mean ± SEM, n=8-10 per group. Repeated measured ANOVA, F(3,39)=0.0513, p=0.6759. No significant differences were seen between groups at any age tested.

7.3.2.Y-Maze

7.3.2.1. Spontaneous alternation performance (SAP)

The number of spontaneous alternating arm entries in a Y-maze were recorded and presented in the graph below as a percentage of the total number of triad arm entries attempted during the trial period.

The %SAP was very similar between D427V/WT and WT mice in 3,6 and 9-month cohorts indicating similar cognitive performance in executing the test. However, by 12 months of age there is a significant decrease in %SAP indicative of cognitive impairment in D427V/WT mice compared with WT mice of the same age (Repeated measures ANOVA, Sidak's post hoc test, F(3,42)=4.591, p=0.0189) **(Figure 42).**

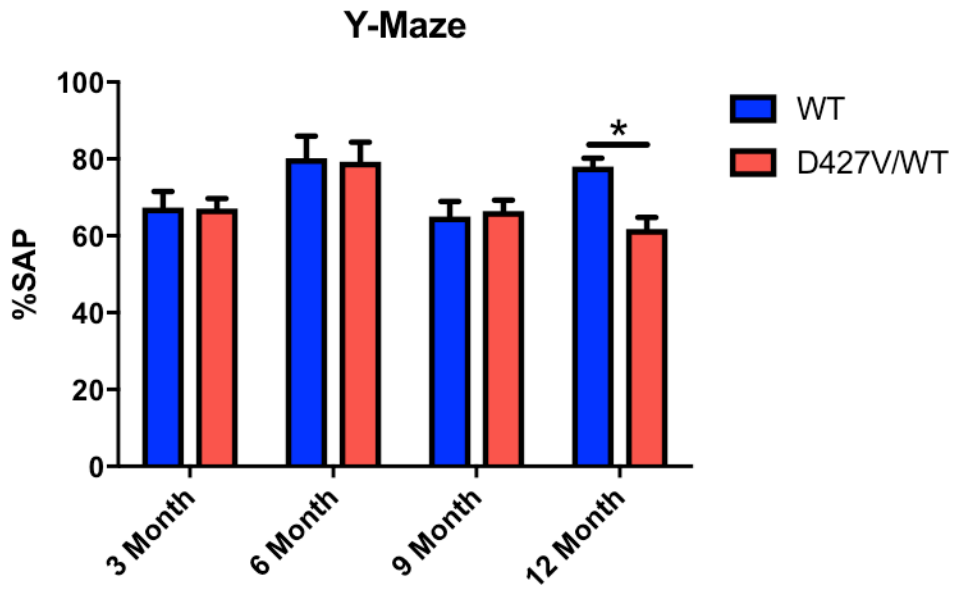

Figure 42 - Spontaneous alternation performance measured in the Y-maze. SAP measured as a percentage of the total number of attempts within 8 minutes. %SAP measured in WT (blue) and D427V/WT (red) mice at 3,6,9 and 12 months of age. Data are represented as mean +/- SEM, n=8-10 per group, repeated measures ANOVA, Sidak's post hoc test, F(3,42)=4.591, p=0.0189 between D427V and WT at 12 months of age, *p=<0.05

7.3.3.Morris water maze

7.3.3.1. Trial duration

The time taken for mice to reach a submerged platform was recorded and averaged over 4 trials from different starting locations in the maze. This was repeated for 5 consecutive days to generate learning curves for both WT and D427V/WT mice.

Testing at 3 months of age, both D427V/WT and WT mice exhibit learning as seen by the reduction in trial duration over time. Surprisingly, D427V/WT mice performed better than WT, finding the platform significantly faster by day 5 (19.11 ± 1.949s compared with 43.55 ± 8.872s, two-way ANOVA with Bonferroni correction, F(1,16)=8.466, p=0.0383) **(Figure 43).**

At 6 months of age, both groups show reduction in trial duration over the consecutive 5 days of testing indicating learning had taken place. There was no significant difference in the time taken to find the platform between WT and D427V/WT mice at any day during the test **(Figure 43).** Mice at 9 months of age once again demonstrate learning; reduction in trial duration over time. However, in contrast to 3 months old mice, D427V/WT consistently perform worse than WT; taking longer to find the platform throughout the test. However, the difference between the groups fails to reach statistical significance on any specific day following Bonferroni correction, despite overall significance seen by two-way ANOVA (two-way ANOVA with Bonferroni correction, F(1,16)=7.208, p=>0.05) **(Figure 43)**.

By 12 months of age, learning continues to be exhibited in WT animals but appears to plateau in D427V/WT; trail duration remains relatively constant over the time of the test. Consequently, there are statistically significant increases in trial duration by D427V/WT mice when compared to WT at day 2 (56.79 ± 4.847s compared with 34.82 ± 4.089s, Two-way ANOVA with Bonferroni correction, F(1,16)=17.27, p=0.0423) and more prominently at day 5 (45.57 ± 8.123s compared with 17.79 ± 2.657s, two-way ANOVA with Bonferroni correction, F(1,16)-17.27, p=0.0051) **(Figure 43)**.

Findings were validated by performing a probe trial in which the platform was removed, and the time mice spent in the quadrant previously containing the platform recorded. There was a statistically significance decrease in the amount of time D427V/WT mice spent in the correct

quadrant (11.57 ± 2.293s) when compared with WT mice at 12 months of age (17.87 ± 2.293s)(Repeated measures ANOVA, F(1,16)=0.0397, p=0.0397), although significance was lost after correction for multiple comparison using Sidak's post hoc test. Exploratory analyses using student's t-test used also describes a statistically significance between WT and D427V/WT at 12 months (p=0.0445) **(Figure 44).**

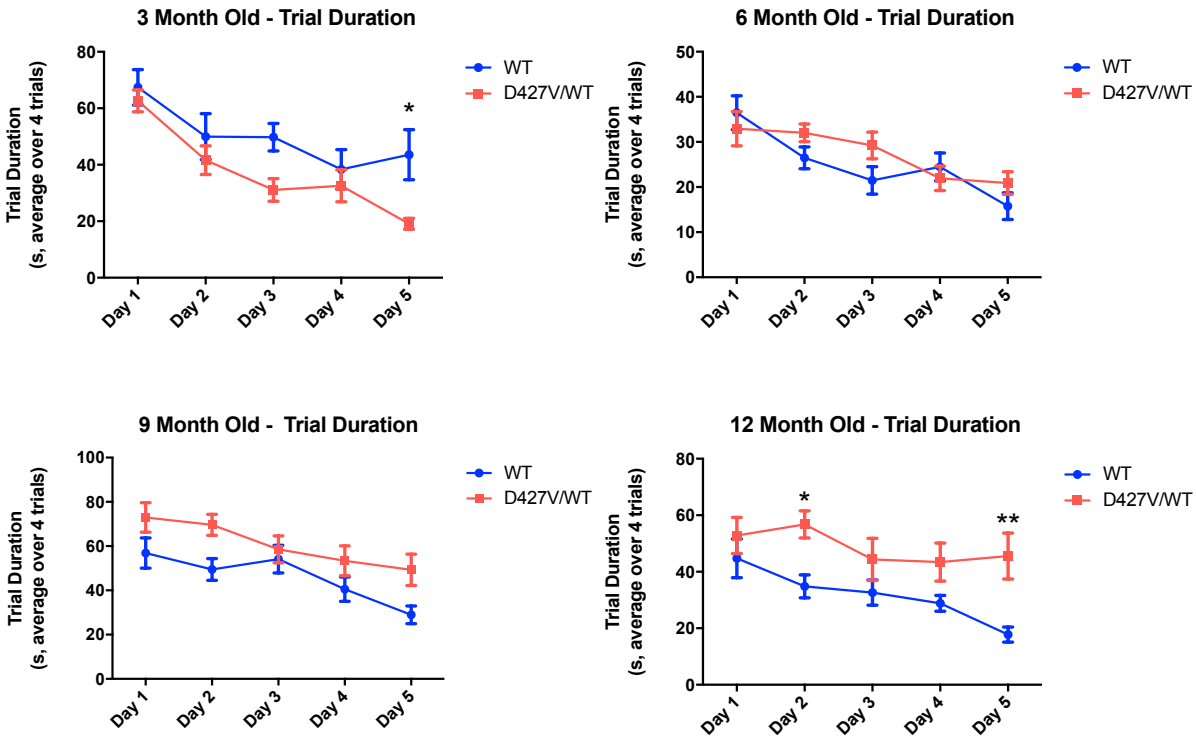

Figure 43 – Trial duration in Morris water maze. Trial duration measured in seconds, averaged over 4 trials in D427V/WT (red) and WT (blue) mice at 3,6,9 and 12 months of age. Data are represented as mean ±SEM, n=8-10 per group. Two-way ANOVA with Bonferroni correction, 3 months old F(1,16)=8.4688, p=0.0383, 12 months old F(1,16)=17.27, p = 0.0051, *p=<0.05, **p=<0.01

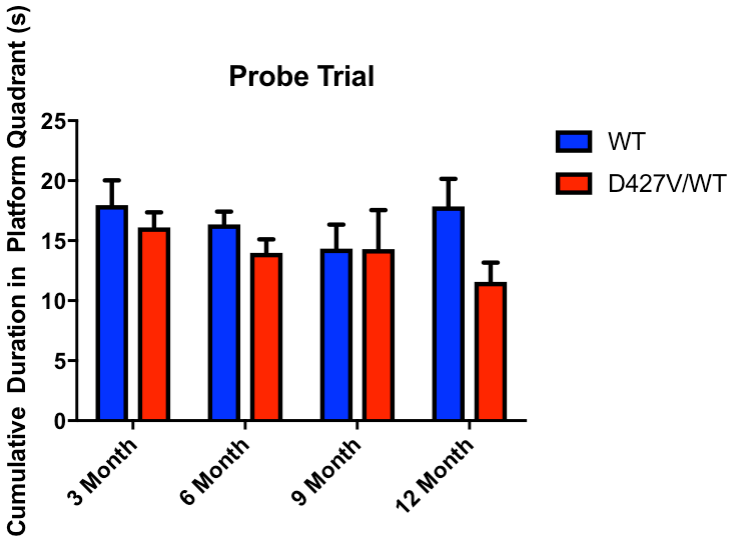

Figure 44 – Morris water maze probe trial. Cumulative time in the correct quadrant measured in seconds in D427V/WT (red) and WT (blue) mice at 3,6,9 and 12 months of age. Data are represented as mean ±SEM, n=8-10 per group, repeated measures ANOVA, Sidak's post hoc test. No significant differences were observed between groups at any age tested.

7.3.3.2. Trial distance covered

The distance each mouse travelled whilst searching for the platform was recorded to account for any possible motor impairments which may confound trial duration as a readout for learning and memory.

Total distance to platform reduced over time indicating learning was observed in both WT and D427V/WT mice in the 3,6 and 9 months age groups. Furthermore, there was no significant difference in performance between D427V/WT and WT mice at any of these age groups. However, by 12 months of age D427V/WT mice take a significantly longer distance to find the platform compared with WT mice at day 2 (903.507 ± 87.867cm compared with 493.973 ± 63.860cm, Two-way ANOVA with Bonferroni correction, F(1,16)=19.67, p=0.0059) and day 5 (651.068 ± 121.832cm compared with 257.069 ± 46.378cm, Two-way ANOVA with Bonferroni correction, F(1,16)=19.67, p=0.0088) **(Figure 45).**

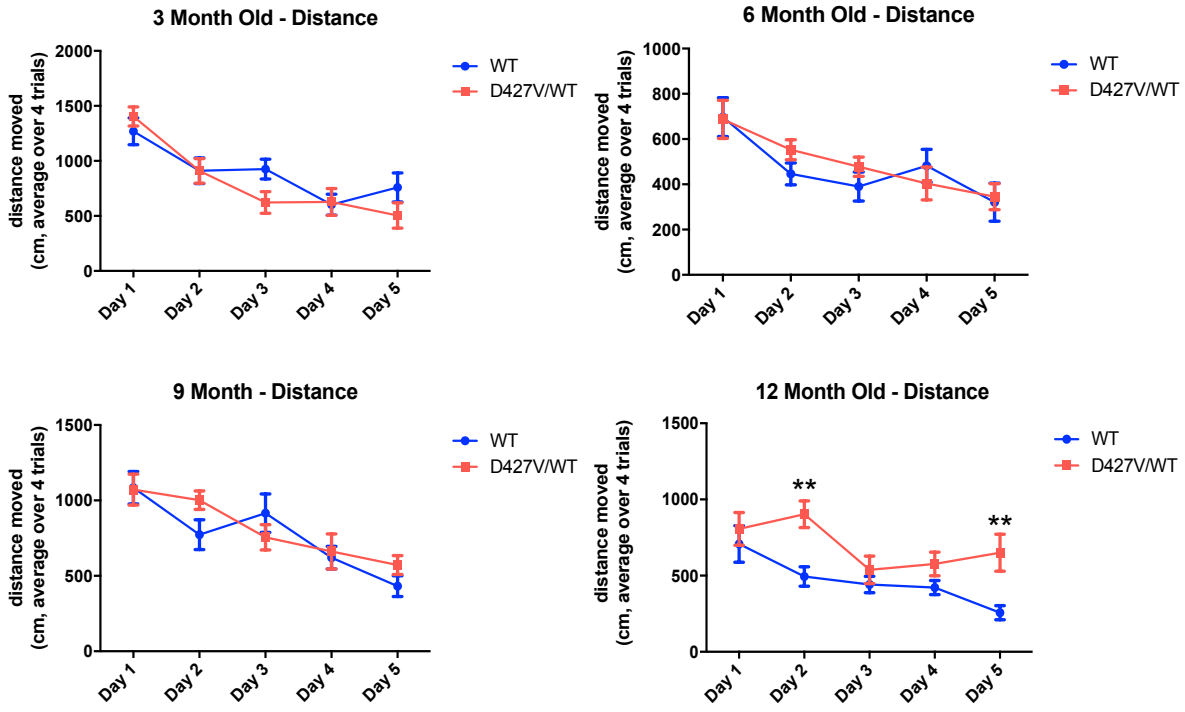

Figure 45 – Distance to platform in Morris water maze. Total distance measured in cm, averaged over 4 trials in D427V/WT (red) and WT (blue) mice at 3,6,9 and 12 months of age. Data are represented as mean ±SEM, n=8-10 per group. 12 months old, Two way ANOVA with Bonferroni correction, F(1,16)=19.67, *p=<0.05,**p=<0.01

7.3.3.3. Velocity

The velocity of mice whilst swimming was recorded to identify any potential motor impairment which could confound conclusions based upon time taken to platform results. Velocity measurements indicate there was no statistically significant difference between D427V/WT and WT mice at any age. However, at 3 months of age, there is a trend for increased velocity in D427V/WT mice at day 5, with statistical significance by two-way ANOVA (two-way ANOVA, $F(1,16)=5.155$, $p=0.0373$) which is lost upon Bonferroni correction **(Figure 46).**

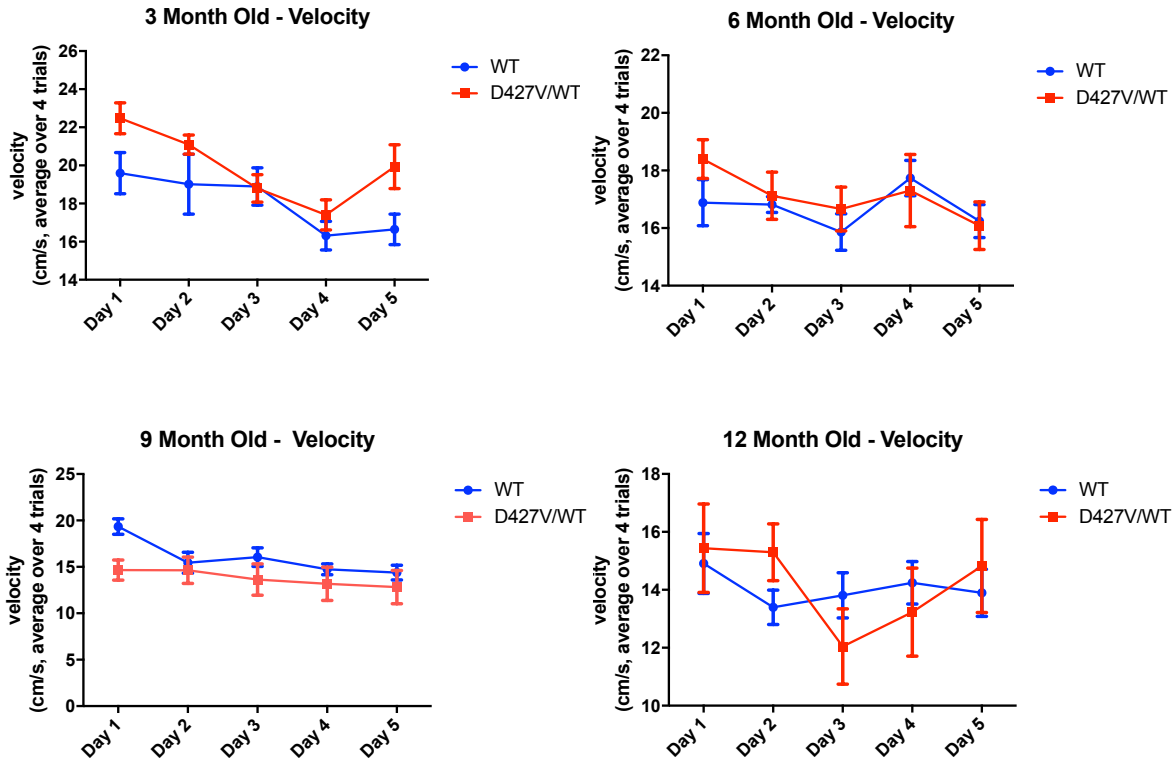

Figure 46 - Swimming velocity of mice in Morris water maze. Velocity measured in cm/s, averaged over 4 trials in D427V/WT (red) and WT (blue) mice at 3,6,9 and 12 months of age. Data are represented as mean ±SEM, n=8-10 per group. Two-way ANOVA followed by Bonferroni correction. No significant differences were observed between groups at any age tested.

7.4. Discussion

Behavioural testing has identified a progressive cognitive impairment phenotype in D427V/WT mice which is significantly evident by 12 months of age. The existence of cognitive impairment in these mice can be reported due to deficits identified by two independent behavioural tests: Morris water maze and Y-maze **(Figure 44, Figure 42).**

The Morris water maze has historically been used as a test of spatial learning and memory mediated predominantly by the hippocampus (Morris, 1984; Vorhees and Williams, 2006). Accordingly, deficits in Morris water maze performance identified in this study implicate the hippocampus as a potential area of pathological interest in association with a heterozygous *GBA1* mutation. Correspondingly, pathological accumulation of α-synuclein and tau have previously been reported in the hippocampus of D427V *GBA1* homozygous mice alongside a cognitive deficit at the earlier age of 6 months (Sardi et al., 2011; Sardi et al., 2013). It may be that heterozygous mice require an additional age-related decline in GCase enzyme activity in order to manifest a cognitive impairment phenotype potentially involving the accumulation of tau and α-synuclein; a hypothesis requiring further investigation. It is now established that in addition to the hippocampus, the cholinergic basal forebrain is necessary for Morris water maze assessed spatial learning and memory since rats with lesions in medial septum or nucleus basalis of Meynert display overt deficits (D'Hooge and De Deyn, 2001). Accordingly, the highest proportion of GCase expression has recently been identified in the cholinergic neurons of the nucleus basalis of Meynert in non-human primate brain (Dopeso-Reyes et al., 2017). Reduced activity of GCase enzyme activity in this particularly GCase dependent subset of neurons may therefore contribute to cognitive impairment demonstrated in the Morris water maze.

Deficits were also observed in the cognitive function of 12-month D427V/WT mice which had undergone Y-maze testing **(Figure 42)**. Spontaneous alternation performance (SAP) is a controversial measure of working memory implicating involvement of the hippocampus (Deacon and Rawlins, 2006). SAP involves responsiveness to novelty that relies on the need to remember which two maze arms were recently visited so as to enable selection of the novel alternative (Hughes, 2004). However, the choice made does not necessarily reflect memory of the previously entered arms and may involves sensory and attentional factors in addition to motivationally

related novelty preferences (Hughes, 2004). Despite these concerns, when taken into consideration with other tests of cognition, deficits in Y-maze SAP performance can strengthen the case for cognitive impairment, which is the case with this study.

The cognitive impairment phenotype in D427V/WT mice described by this study appears to be independent from the effect of locomotor deficits or anxiety as measured by performance in the open field arena **(Figure 39, Figure 40, Figure 41).** Heterozygous D427V mutation did not affect the distance or speed mice moved. This finding is significant since locomotor deficit could have confounded the interpretation of Morris water maze results. Further evidence for the lack of motor impairment can be derived from the constant swim speeds in the Morris water maze when comparing D427V/WT and WT mice. Perhaps it is surprising that there was no motor impairment in D427V/WT mice of any age given the link between *GBA1* and PD (Sidransky et al., 2009b). However, motor impairment has not been reported in the D427V homozygous mouse either (Sardi et al., 2011). In order to confidently exclude the presence of motor impairment, it is important to perform specifically designed motor behaviour tasks such as rotarod which have not been reported in the literature as yet.

Interestingly, young D427V/WT mice appear to display some degree of hyperactivity. Whilst not statistically significant, D427V/WT mice at 3 months of age move faster and further than WT mice in the open field. This same phenomenon can also be seen in the Morris water maze to a significant degree. D427V/WT mice at 3 months of age find the platform significantly faster than WT mice. It is unlikely this is a reflection of cognitive ability, but more accordingly hyperactivity since the distance travelled to the platform remained constant. Furthermore, although not statistically significant, there was a trend for D427V/WT mice to have a faster swim speed than WT at this key age. Hyperactivity has been widely reported in A53T mutant α-synuclein mouse models (Unger et al., 2006; Graham and Sidhu, 2010) and in a model of cognitive impairment caused by knockout out vesicular acetylcholine transferase (vAChT) (Martyn et al., 2012). Hyperactivity as an early symptom may therefore prove to be an interesting candidate as an early diagnostic marker at which point interventions could be made to prevent irreversible progression to cognitive impairment associated with LBD.

This study represents the first report of a progressive decline in cognitive impairment phenotype associated with heterozygous *GBA1* mutation. Moreover, cognitive decline is evidenced by two independent behavioural tests providing a strong evidence base for the phenotype. Therefore, the main aim of this chapter has been achieved. It would be interesting to test mice of an older age to more accurately mirror the age of onset associated with LBD and further investigate the impact of age. Considering the impact of age upon phenotype, testing for motor deficits at later time points would be of relevance since the development of a motor impairment following the presentation of cognitive deficits would provide more evidence that the D427V/WT mouse is an appropriate translational model for DLB in particular.

Overall, the novel phenotypes described in this *GBA1* D427V/WT mouse could prove to be a helpful translational model of LBD with implications for drug discovery and testing.

8. General discussion

GBA1 cell lines were successfully created demonstrating the fundamental characteristic associated with GCase: reduced GCase enzyme activity in L444P mutant cells and enhanced GCase enzyme activity in wild type overexpressing cells (chapter 4.3.5.3) (McNeill et al., 2014; Schondorf et al., 2014; Sanchez-Martinez et al., 2016). The creation of monoclonal *GBA1* cell lines for comparison has permitted several experiments to be performed on what can be considered equivalent cells, therefore a more accurate picture of changes within the unfolded protein response can be assessed and considered in the context of other results. Whilst successful insertion of the *GBA1* ORF into the TOPO-GFP plasmid and L444P site directed mutagenesis was demonstrated by sanger sequencing **(Figure 8, Figure 10)**, sanger sequencing of the monoclonal cells themselves should also be performed to validate that the cells do in fact express GFP tagged wild type / L444P *GBA1*. This would also help address the uncertainty around the expression of GFP protein as an indirect measure of overexpressed GCase protein **(Figure 14).** Furthermore, relative expression of GFP mRNA could be assessed between naïve SH-SHSY cells and those overexpressing *GBA1*-GFP. Despite these additional validation steps which could be performed, alterations to GCase enzyme activity are robustly demonstrated, indicating expression of the plasmid constructs. With this is mind and the validation steps already performed, the aim of chapter 4 was successfully achieved: Monoclonal *GBA1* overexpressing SH-SY5Y cell lines were created.

An interesting finding from chapter 4 is the impact of overexpressed WT and L444P mutant *GBA1* on SH-SY5Y cell viability **(Figure 18, Figure 19)**. Whilst the results from the two different measures of cell viability (PrestoBlue® and MTT assay) do not replicate each other, both do show a significant reduction in cell viability in L444P *GBA1* overexpressing cells, indicating that L444P *GBA1* mutation is detrimental to cell health. However, the impact of overexpressed WT *GBA1* on cell viability is unclear. It would be beneficial to investigate the viability of the cell lines created with alternative measures of cell viability and cell death such as the lacto dehydrogenase and TUNEL assays.

As discussed in chapter 4, further investigation is required to confirm ER retention of L444P mutant *GBA1* in the cell model created, complementing the literature (Ron and Horowitz, 2005; Bendikov-Bar et al., 2011; Fernandes et al., 2016), in order to consolidate the evidence for ER stress and subsequent activation of the UPR which is reported in this thesis. Accompanying ER retention, alterations to the trafficking of GCase to lysosomes as a consequence of *GBA1* mutation is considered a pathway to reduced GCase enzyme activity since GCase is only functional in the acidic environment of the lysosome. Furthermore, the success of chaperones, particularly Ambroxol in stabilising mutant GCase protein and assisting trafficking to the lysosome thereby enhancing GCase activity (McNeill et al., 2014; Ambrosi et al., 2015; Migdalska-Richards et al., 2016), highlights the importance of trafficking as a pathogenic mechanism involved in PD and DLB. Nevertheless, deficient trafficking of solely mutant GCase cannot underlie PD/DLB since GCase enzyme activity is also significantly reduced in the brain of sporadic PD and DLB patients (Gegg et al., 2012; Chiasserini et al., 2015; Rocha et al., 2015a). However, Ambroxol is also able to improve lysosomal delivery of non-mutant GCase in the brain (Migdalska-Richards et al., 2016; Migdalska-Richards et al., 2017). It may be possible that pathogenic substrates associated with PD and DLB, primarily aggregated α-synuclein, may invoke ER stress, preventing the maturation of GCase within the ER thereby causing ER retention and subsequently ER stress. Alternatively, α-synuclein may affect ER resident chaperones associated with trafficking. α-synuclein has been reported to interact with the GCase specific receptor required for trafficking to lysosomes, LIMP 2. Since GCase binds LIMP 2 in the late ER/early Golgi, the impact of α-synuclein interacting with LIMP 2 may cause accumulation of GCase in the ER and subsequent ER stress. Since enhanced trafficking of GCase to lysosomes boosts GCase activity and is associated with improved phenotypes in a Drosophila model of heterozygous *GBA1* mutation (Sanchez-Martinez et al., 2016), ER stress mechanisms appear to play a critical part in the pathogenesis of PD/DLB. Accordingly, the expression of key UPR effector molecules described in this thesis, particularly those associated with adverse outcomes, is significant and complements current hypotheses.

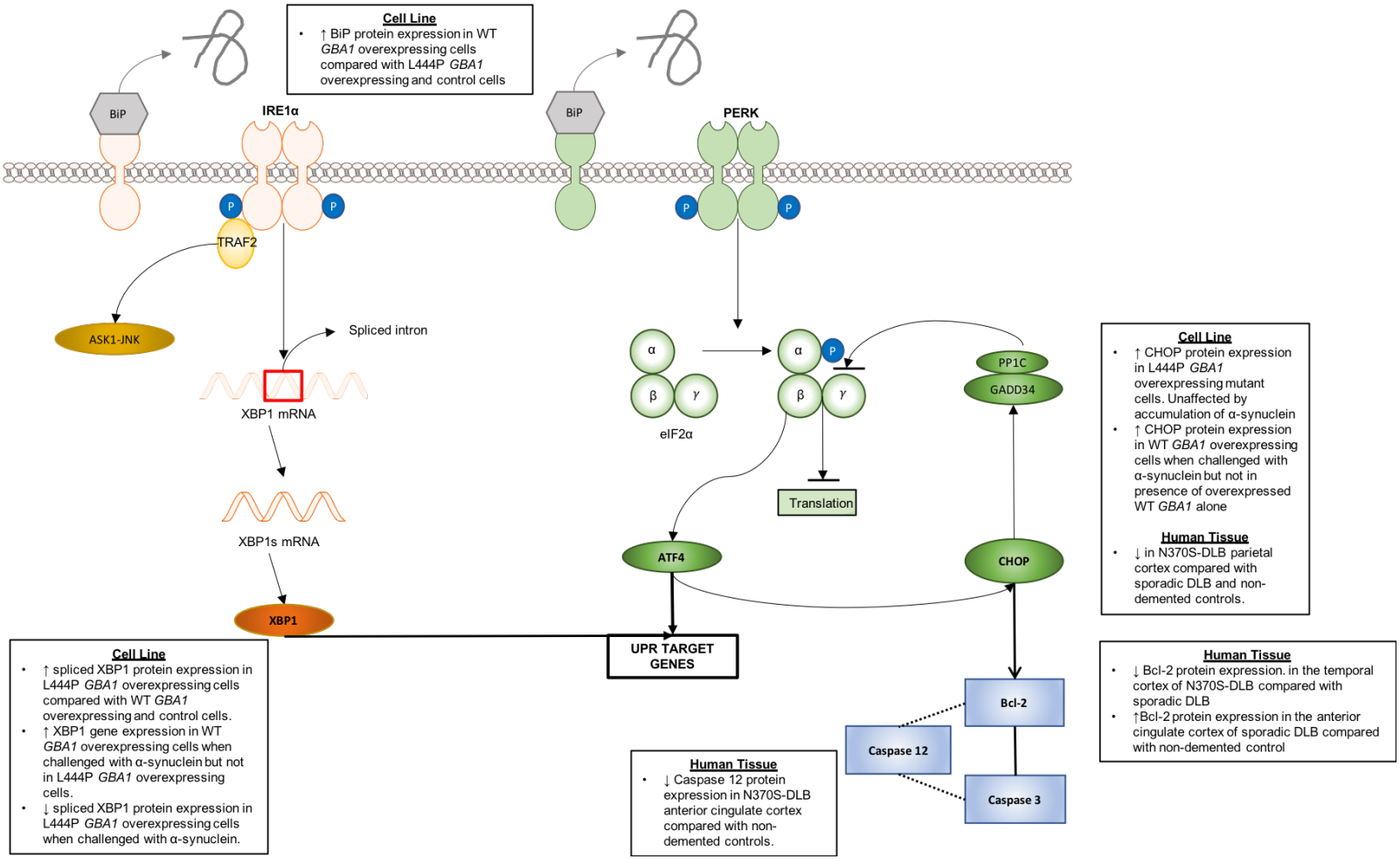

Figure 47 - Summary of UPR changes included in this thesis

The aim of chapters 5 and 6 was to establish whether the UPR is activated in response to L444P *GBA1* mutation in SH-SH5Y cells, more specifically whether the PERK pathway is preferentially activated (findings summarised in **Figure 47**). This thesis reports that the L444P mutation causes a significant increase in spliced XBP1 protein expression compared with wild type *GBA1* **(Figure 24) (Figure 25)** which is subsequently significantly reduced in the presence of excess α-synuclein **(Figure 27).** Accordingly, excess α-synuclein does not alter XBP1 transcript levels in L444P cells but does cause a significant increase in wild type *GBA1* cells **(Figure 26)**. These findings suggest that IRE1α pathway activation initially serves the protective function reported in literature (chapter 5.1.2). However, as the pathological impact of *GBA1* mutation progresses, represented by α-synuclein accumulation, and is compounded by age related decline in GCase activity, expression of the protective spliced XBP1 ceases and returns to basal levels. The relationship described supports the general hypothesis of this thesis: UPR responses adapt from being protective to being detrimental. Furthermore, significantly increased CHOP protein expression is only seen in L444P mutant cells **(Figure 31)** which does not change in the presence of excess α-synuclein, whereas CHOP protein expression is induced in wild type *GBA1* cells in the presence of α-synuclein **(Figure 33).** CHOP, an effector with detrimental effects to cells, is seemingly expressed when IRE1α responses of the UPR are insufficient to resolve stress, demonstrated in this thesis by the presence of L444P mutation or accumulation of α-synuclein.

Novel interpretation of UPR activation as a balance between protective and detrimental responses contributes to the field since it widens interpretation of previous reports pertaining to the expression of UPR effectors, which tend to be considered in isolation. The UPR comprises of 3 arms which are known to exhibit extensive cross reactivity (Chan et al., 2015), therefore a hypothesis which involves a balance between the pathways which is perturbed in the presence of *GBA1* mutation is more feasible.

The aim to identify UPR linked initiation of mitochondrial apoptosis through the action of CHOP has been less conclusive. While downregulation of the anti-apoptotic protein Bcl-2 was not identified in L444P mutant cells **(Figure 35)**, significant downregulation was seen in N370S *GBA1* DLB human post mortem tissue from the temporal cortex **(Figure 36)**. Since the cells were not tested in the presence of excess α-synuclein, it may be that the cells are not stressed to a high

enough degree to initiate apoptosis. The impact of enhanced CHOP expression and possible links to apoptosis requires further investigation and could be performed in the *GBA1* D427V/WT mouse phenotypically characterised as part of this thesis (chapter 7). Unfortunately, time did not permit UPR investigations in the *GBA1* D427V/WT mouse for this thesis.

The role of the UPR in neurodegenerative diseases has been of increasing interest with confirmed reports of PERK pathway activation in AD, PD and frontotemporal dementia (FTD) (Smith and Mallucci, 2016). The results from the cell line experiments evaluating CHOP expression in this thesis appear to contribute to these reports. Furthermore, therapeutics have been developed, inhibiting phosphorylation of PERK or enacting de-phosphorylation of eIF2α (Smith and Mallucci, 2016). Amelioration of memory impairments and reduction of phosphorylated tau has been reported in a mouse model of FTD treated with an inhibitor of PERK phosphorylation (Radford et al., 2015). These therapeutic adjustments to UPR responses in neurodegenerative conditions could therefore be of value in LBD once UPR response and the impact of *GBA1* have been fully characterised and explored.

Behavioural characterisation of the D427V/WT *GBA1* mouse has revealed an important and previously unreported phenotype which may prove to have a translational purpose for the study of LBD – cognitive impairment. Hitherto, cognitive impairment has only been reported in the D427V *GBA1* homozygous mouse, which by definition is a model of Gaucher's disease (Sardi et al., 2011). However, Sardi et al report the absence of cognitive impairment measured by novel object recognition, in heterozygous mice (Sardi et al., 2011). Sardi et al tested heterozygous mice at 6 months of age, whereas we identified a progressive decline in cognition which reached significance by 12 months of age, albeit with a different tests of cognitive function – the Morris water maze and Y-maze **(Figure 42, Figure 43, Figure 44, Figure 45).** Since heterozygous mice have a subtler decline in GCase enzyme activity, approximately 69% of wild type activity (Sardi et al., 2011), age related factors must contribute to cause the progressive decline in cognitive function we report. Nominally, we postulate that an age-related decline in GCase enzyme activity (Rocha et al., 2015a; Supriya et al., 2017) contributes to deficiencies conferred by the single D427V mutant allele, crossing a biochemical threshold for presentation of a cognitive impairment phenotype. In order to confirm this, brain GCase enzyme activity will need to be measured in wild type mice over a range of ages in order definitively establish the contribution of reduced

endogenous GCase enzyme activity. Furthermore, to consolidate these findings, brain GCase enzyme activity should be measured in the D427V/WT mice at different ages. A limitation of the behavioural characterisation of D427V/WT mice is ageing of the mice. Since aging mice is time consuming and costly, the final time point for this study was 12 months of age. It would be beneficial to study mice of an older age which is more translational to the age of onset of LBD. Accordingly, mice aged between 18-24 months are considered old with the human age equivalence of 56-69 years (https://www.jax.org/research-and-faculty/research-labs/the-harrison-lab/gerontology/life-span-as-a-biomarker)

MWM is a behavioural test historically used to investigate spatial learning and memory mediated predominantly by the hippocampus (Morris, 1984; Vorhees and Williams, 2006). Since the homozygous D427V *GBA1* mouse displays significant accumulation of ubiquitin positive α-synuclein aggregates in the hippocampus (Sardi et al., 2011) this was considered an appropriate test of cognitive function to investigate the heterozygous D427V/WT *GBA1* mouse. Furthermore, at 6 months of age D427V/WT *GBA1* heterozygous mice but not *GBA1*$^{+/-}$ despite having similar residual GCase enzyme activity, have been reported to show ubiquitin positive α-synuclein aggregates in the hippocampus, although not to a significant level (Sardi et al., 2011). We suggest that the findings we report in the MWM may be explained by a progressive accumulation of α-synuclein in relation to a progressive decline in GCase enzyme activity. Staining for α-synuclein aggregates should be performed in D427V/WT *GBA1* mice at 12 months of age and beyond to validate this hypothesis. Furthermore, since LBD is associated with mixed pathology and not solely aggregation of α-synuclein (chapter 1.1.5), staining for the associated pathological proteins amyloid beta and phosphorylated tau should be performed to assess whether the D427V/WT *GBA1* mouse is translational for LBD research.

Evaluating the activity of non-lysosomal GCase transcribed from *GBA2* would be an interesting addition to the characterisation both the D427V/WT *GBA1* mice and *GBA1* cell lines generated. A compensatory increase in *GBA2* GCase enzyme activity has been reported to occur in response to *GBA1* mutation (Aureli et al., 2012; Burke et al., 2013).Furthermore, in addition to hydrolysing excess cytoplasmic GluCer, *GBA2* transcribed GCase hydrolyses GluSph in the

cytoplasm forming sphingosine and consequently the toxic metabolite sphingosine-1-phosphate (Dekker et al., 2011b; Ferraz et al., 2016a). Enhanced action of *GBA2* transcribed GCase may therefore contribute to pathology and needs to be considered.

A growing school of thought regarding the pathological links between *GBA1* mutation and synucleinopathies postulates that phenotypes and pathology described in the literature are not *GBA1* specific. It is suggested that a wider dysfunction of lysosomes underlies changes traditionally attributed to *GBA1* mutations (Moors et al., 2016). Furthermore, it is suggested that the genetic link between *GBA1* mutation and synucleinopathies are a reflection of GD being the most common lysosomal storage disorder and as such more easily identifiable. Indeed, the activity of other lysosomal enzymes are reported to be altered in Parkinson's disease (Moors et al., 2016) and a recent genetic study identified an excessive burden of lysosomal storage disorder gene variants in Parkinson's disease including *CTSD*, *SLC17A5*, and *ASAH1* (Robak et al., 2017).

9. Concluding remarks

The work presented in this thesis presents a novel interpretation of UPR activation as a consequence of *GBA1* mutation. Whilst enhanced expression of both spliced XBP1 and CHOP in L444P *GBA1* mutant cells **(Figure 25, Figure 31)** complements findings in the field **(Table 15, Table 16, Table 17),** this thesis demonstrates that L444P mutant cells illustrate a switch in UPR response upon experiencing further stress in the form of overexpressed α-synuclein. The return of spliced XBP1 to basal levels upon overexpression of α-synuclein **(Figure 27)** suggests that L444P *GBA1* cells have reached a level of stress which has surpassed the ability of IRE1α signalling to resolve and therefore UPR signalling continues through PERK signalling and detrimental CHOP expression **(Figure 33)**. Although this finding requires further investigation, the implications for drug development are promising. The identification of compounds which are able to readdress the balance between expression of protective un-spliced XBP1 and detrimental CHOP would be an interesting next step, particularly investigation into whether said compounds could ameliorate behavioural phenotypes in the D427V/WT mouse model.

This thesis also presents the previously unreported finding of progressive cognitive decline in D427V/WT *GBA1* mice **(Figure 42, Figure 43, Figure 44, Figure 45)**. This is a significant discovery since cognitive impairment was only previously only reported in homozygous D427V *GBA1* mice (Sardi et al., 2011). This finding consolidates previous reports of an age-related decline in brain GCase enzyme activity (Rocha et al., 2015a; Supriya et al., 2017) as a contributing factor towards the development of synucleinopathies through the illustration of a progressive decline in cognitive impairment whereby a statistically significant decline in cognition was only seen at 12 months of age. The implications for the field are that we suggest study of cognitive decline in heterozygous *GBA1* mutant mice should be performed from the age of 12 months to better represent endogenous GCase enzyme activity. Furthermore, D427V/WT mice may prove to be a good translational model for the study of LBD and subsequent development of novel therapies. However, biochemical investigation of the D427V/WT mouse is required to be carried out initally, which unfortunately time did not permit for inclusion in this thesis.

10. References

Aarsland D (2016) Cognitive impairment in Parkinson's disease and dementia with Lewy bodies. Parkinsonism & related disorders 22 Suppl 1:S144-148.

Aarsland D, Kurz MW (2010) The epidemiology of dementia associated with Parkinson disease. Journal of the neurological sciences 289:18-22.

Aarsland D, Ballard CG, Halliday G (2004) Are Parkinson's disease with dementia and dementia with Lewy bodies the same entity? Journal of geriatric psychiatry and neurology 17:137-145.

Aarsland D, Zaccai J, Brayne C (2005a) A systematic review of prevalence studies of dementia in Parkinson's disease. Movement disorders : official journal of the Movement Disorder Society 20:1255-1263.

Aarsland D, Andersen K, Larsen JP, Lolk A, Kragh-Sorensen P (2003) Prevalence and characteristics of dementia in Parkinson disease: an 8-year prospective study. Archives of neurology 60:387-392.

Aarsland D, Perry R, Larsen JP, McKeith IG, O'Brien JT, Perry EK, Burn D, Ballard CG (2005b) Neuroleptic sensitivity in Parkinson's disease and parkinsonian dementias. The Journal of clinical psychiatry 66:633-637.

Abbasi M, Ghalandari N, Farzanefar S, Aghamollaii V, Ahmadi M, Ganji M, Afarideh M, Loloee S, Naseri M, Tafakhori A (2017) Potential diagnostic value of (131)I-MIBG myocardial scintigraphy in discrimination between Alzheimer disease and dementia with Lewy bodies. Clinical neurology and neurosurgery 163:163-166.

Abbott SK, Li H, Munoz SS, Knoch B, Batterham M, Murphy KE, Halliday GM, Garner B (2014) Altered ceramide acyl chain length and ceramide synthase gene expression in Parkinson's disease. Movement disorders : official journal of the Movement Disorder Society 29:518-526.

Acosta-Alvear D, Zhou Y, Blais A, Tsikitis M, Lents NH, Arias C, Lennon CJ, Kluger Y, Dynlacht BD (2007) XBP1 controls diverse cell type- and condition-specific transcriptional regulatory networks. Molecular cell 27:53-66.

Adamowicz DH, Roy S, Salmon DP, Galasko DR, Hansen LA, Masliah E, Gage FH (2017) Hippocampal alpha-Synuclein in Dementia with Lewy Bodies Contributes to Memory Impairment and Is Consistent with Spread of Pathology. The Journal of neuroscience : the official journal of the Society for Neuroscience 37:1675-1684.

Aerts JM, Hollak CE, Boot RG, Groener JE, Maas M (2006) Substrate reduction therapy of glycosphingolipid storage disorders. Journal of inherited metabolic disease 29:449-456.

Aerts JM, van Breemen MJ, Bussink AP, Ghauharali K, Sprenger R, Boot RG, Groener JE, Hollak CE, Maas M, Smit S, Hoefsloot HC, Smilde AK, Vissers JP, de Jong S, Speijer D, de Koster CG (2008) Biomarkers for lysosomal storage disorders: identification and application as exemplified by chitotriosidase in Gaucher disease. Acta paediatrica (Oslo, Norway : 1992) 97:7-14.

Agosta F, Kostic VS, Davidovic K, Kresojevic N, Sarro L, Svetel M, Stankovic I, Comi G, Klein C, Filippi M (2013) White matter abnormalities in Parkinson's disease patients with glucocerebrosidase gene mutations. Movement disorders : official journal of the Movement Disorder Society 28:772-778.

Aharon-Peretz J, Rosenbaum H, Gershoni-Baruch R (2004) Mutations in the glucocerebrosidase gene and Parkinson's disease in Ashkenazi Jews. The New England journal of medicine 351:1972-1977.

Alattia JR, Shaw JE, Yip CM, Prive GG (2007) Molecular imaging of membrane interfaces reveals mode of beta-glucosidase activation by saposin C. Proceedings of the National Academy of Sciences of the United States of America 104:17394-17399.

Alcalay RN, Dinur T, Quinn T, Sakanaka K, Levy O, Waters C, Fahn S, Dorovski T, Chung WK, Pauciulo M, Nichols W, Rana HQ, Balwani M, Bier L, Elstein D, Zimran A (2014) Comparison of Parkinson risk in Ashkenazi Jewish patients with Gaucher disease and GBA heterozygotes. JAMA neurology 71:752-757.

Alcalay RN, Levy OA, Waters CC, Fahn S, Ford B, Kuo SH, Mazzoni P, Pauciulo MW, Nichols WC, Gan-Or Z, Rouleau GA, Chung WK, Wolf P, Oliva P, Keutzer J, Marder K, Zhang X (2015) Glucocerebrosidase activity in Parkinson's disease with and without GBA mutations. Brain : a journal of neurology 138:2648-2658.

Altarescu G, Hill S, Wiggs E, Jeffries N, Kreps C, Parker CC, Brady RO, Barton NW, Schiffmann R (2001) The efficacy of enzyme replacement therapy in patients with chronic neuronopathic Gaucher's disease. The Journal of pediatrics 138:539-547.

Ambrosi G, Ghezzi C, Zangaglia R, Levandis G, Pacchetti C, Blandini F (2015) Ambroxol-induced rescue of defective glucocerebrosidase is associated with increased LIMP-2 and saposin C levels in GBA1 mutant Parkinson's disease cells. Neurobiology of disease 82:235-242.

Anheim M, Elbaz A, Lesage S, Durr A, Condroyer C, Viallet F, Pollak P, Bonaiti B, Bonaiti-Pellie C, Brice A, French Parkinson Disease Genetic G (2012) Penetrance of Parkinson disease in glucocerebrosidase gene mutation carriers. Neurology 78:417-420.

Armstrong RA, Cairns NJ (2015) Comparative quantitative study of 'signature' pathological lesions in the hippocampus and adjacent gyri of 12 neurodegenerative disorders. Journal of neural transmission (Vienna, Austria : 1996) 122:1355-1367.

Asselta R, Rimoldi V, Siri C, Cilia R, Guella I, Tesei S, Solda G, Pezzoli G, Duga S, Goldwurm S (2014) Glucocerebrosidase mutations in primary parkinsonism. Parkinsonism & related disorders 20:1215-1220.

Astudillo L, Therville N, Colacios C, Segui B, Andrieu-Abadie N, Levade T (2016) Glucosylceramidases and malignancies in mammals. Biochimie 125:267-280.

Auburger G, Klinkenberg M, Drost J, Marcus K, Morales-Gordo B, Kunz WS, Brandt U, Broccoli V, Reichmann H, Gispert S, Jendrach M (2012) Primary skin fibroblasts as a model of Parkinson's disease. Molecular neurobiology 46:20-27.

Aureli M, Loberto N, Chigorno V, Prinetti A, Sonnino S (2011) Remodeling of sphingolipids by plasma membrane associated enzymes. Neurochemical research 36:1636-1644.

Aureli M, Bassi R, Loberto N, Regis S, Prinetti A, Chigorno V, Aerts JM, Boot RG, Filocamo M, Sonnino S (2012) Cell surface associated glycohydrolases in normal and Gaucher disease fibroblasts. Journal of inherited metabolic disease 35:1081-1091.

Bae EJ, Yang NY, Lee C, Lee HJ, Kim S, Sardi SP, Lee SJ (2015) Loss of glucocerebrosidase 1 activity causes lysosomal dysfunction and alpha-synuclein aggregation. Experimental & molecular medicine 47:e153.

Bae EJ, Yang NY, Song M, Lee CS, Lee JS, Jung BC, Lee HJ, Kim S, Masliah E, Sardi SP, Lee SJ (2014) Glucocerebrosidase depletion enhances cell-to-cell transmission of alpha-synuclein. Nature communications 5:4755.

Baek JH, Whitfield D, Howlett D, Francis P, Bereczki E, Ballard C, Hortobagyi T, Attems J, Aarsland D (2016) Unfolded protein response is activated in Lewy body dementias. Neuropathology and applied neurobiology 42:352-365.

Balducci C, Pierguidi L, Persichetti E, Parnetti L, Sbaragli M, Tassi C, Orlacchio A, Calabresi P, Beccari T, Rossi A (2007) Lysosomal hydrolases in cerebrospinal fluid from subjects with Parkinson's disease. Movement disorders : official journal of the Movement Disorder Society 22:1481-1484.

Ballard C, Grace J, McKeith I, Holmes C (1998) Neuroleptic sensitivity in dementia with Lewy bodies and Alzheimer's disease. Lancet 351:1032-1033.

Ballard C, Aarsland D, Francis P, Corbett A (2013) Neuropsychiatric symptoms in patients with dementias associated with cortical Lewy bodies: pathophysiology, clinical features, and pharmacological management. Drugs & aging 30:603-611.

Ballard C, Ziabreva I, Perry R, Larsen JP, O'Brien J, McKeith I, Perry E, Aarsland D (2006) Differences in neuropathologic characteristics across the Lewy body dementia spectrum. Neurology 67:1931-1934.

Barrett MJ, Hagenah J, Dhawan V, Peng S, Stanley K, Raymond D, Deik A, Gross SJ, Schreiber-Agus N, Mirelman A, Marder K, Ozelius LJ, Eidelberg D, Bressman SB, Saunders-Pullman R, Consortium LAJ (2013) Transcranial sonography and functional imaging in glucocerebrosidase mutation Parkinson disease. Parkinsonism & related disorders 19:186-191.

Barton NW, Brady RO, Dambrosia JM, Di Bisceglie AM, Doppelt SH, Hill SC, Mankin HJ, Murray GJ, Parker RI, Argoff CE, et al. (1991) Replacement therapy for inherited enzyme deficiency--macrophage-targeted glucocerebrosidase for Gaucher's disease. The New England journal of medicine 324:1464-1470.

Bassetti CL, Bargiotas P (2018) REM Sleep Behavior Disorder. Frontiers of neurology and neuroscience 41:104-116.

Beavan M, McNeill A, Proukakis C, Hughes DA, Mehta A, Schapira AH (2015) Evolution of prodromal clinical markers of Parkinson disease in a GBA mutation-positive cohort. JAMA neurology 72:201-208.

Bellucci A, Navarria L, Zaltieri M, Falarti E, Bodei S, Sigala S, Battistin L, Spillantini M, Missale C, Spano P (2011) Induction of the unfolded protein response by alpha-synuclein in experimental models of Parkinson's disease. Journal of neurochemistry 116:588-605.

Bembi B, Zanatta M, Carrozzi M, Baralle F, Gornati R, Berra B, Agosti E (1994) Enzyme replacement treatment in type 1 and type 3 Gaucher's disease. Lancet 344:1679-1682.
Bembi B, Zambito Marsala S, Sidransky E, Ciana G, Carrozzi M, Zorzon M, Martini C, Gioulis M, Pittis MG, Capus L (2003) Gaucher's disease with Parkinson's disease: clinical and pathological aspects. Neurology 61:99-101.
Bendikov-Bar I, Horowitz M (2012) Gaucher disease paradigm: from ERAD to comorbidity. Human mutation 33:1398-1407.
Bendikov-Bar I, Ron I, Filocamo M, Horowitz M (2011) Characterization of the ERAD process of the L444P mutant glucocerebrosidase variant. Blood cells, molecules & diseases 46:4-10.
Bertolotti A, Zhang Y, Hendershot LM, Harding HP, Ron D (2000) Dynamic interaction of BiP and ER stress transducers in the unfolded-protein response. Nature cell biology 2:326-332.
Biundo R, Weis L, Antonini A (2016) Cognitive decline in Parkinson's disease: the complex picture. NPJ Parkinson's disease 2:16018.
Blanc F, Verny M (2017) Prodromal stage of disease (dementia) with Lewy bodies, how to diagnose in practice? Geriatrie et psychologie neuropsychiatrie du vieillissement 15:196-204.
Blanz J, Saftig P (2016) Parkinson's disease: acid-glucocerebrosidase activity and alpha-synuclein clearance. Journal of neurochemistry 139 Suppl 1:198-215.
Boeve BF et al. (2013) Clinicopathologic correlations in 172 cases of rapid eye movement sleep behavior disorder with or without a coexisting neurologic disorder. Sleep medicine 14:754-762.
Boven LA, van Meurs M, Boot RG, Mehta A, Boon L, Aerts JM, Laman JD (2004) Gaucher cells demonstrate a distinct macrophage phenotype and resemble alternatively activated macrophages. American journal of clinical pathology 122:359-369.
Braak H, Del Tredici K, Rub U, de Vos RA, Jansen Steur EN, Braak E (2003) Staging of brain pathology related to sporadic Parkinson's disease. Neurobiology of aging 24:197-211.
Bradford MM (1976) A rapid and sensitive method for the quantitation of microgram quantities of protein utilizing the principle of protein-dye binding. Analytical biochemistry 72:248-254.
Brady RO, Kanfer JN, Shapiro D (1965) Metabolism of Glucocerebrosides. Ii. Evidence of an Enzymatic Deficiency in Gaucher's Disease. Biochemical and biophysical research communications 18:221-225.
Bras J, Paisan-Ruiz C, Guerreiro R, Ribeiro MH, Morgadinho A, Januario C, Sidransky E, Oliveira C, Singleton A (2009) Complete screening for glucocerebrosidase mutations in Parkinson disease patients from Portugal. Neurobiology of aging 30:1515-1517.
Bras J et al. (2014) Genetic analysis implicates APOE, SNCA and suggests lysosomal dysfunction in the etiology of dementia with Lewy bodies. Human molecular genetics 23:6139-6146.
Braunstein H, Maor G, Chicco G, Filocamo M, Zimran A, Horowitz M (2018) UPR activation and CHOP mediated induction of GBA1 transcription in Gaucher disease. Blood cells, molecules & diseases 68:21-29.
Brigo F, Turri G, Tinazzi M (2015) 123I-FP-CIT SPECT in the differential diagnosis between dementia with Lewy bodies and other dementias. Journal of the neurological sciences 359:161-171.
Broadstock M, Lewinsky R, Jones EL, Mitchelmore C, Howlett DR, Francis PT (2012) Synaptic protein expression is regulated by a pro-oxidant diet in APPxPS1 mice. Journal of neural transmission (Vienna, Austria : 1996) 119:493-496.
Brockmann K, Srulijes K, Hauser AK, Schulte C, Csoti I, Gasser T, Berg D (2011) GBA-associated PD presents with nonmotor characteristics. Neurology 77:276-280.
Brockmann K, Hilker R, Pilatus U, Baudrexel S, Srulijes K, Magerkurth J, Hauser AK, Schulte C, Csoti I, Merten CD, Gasser T, Berg D, Hattingen E (2012) GBA-associated PD. Neurodegeneration, altered membrane metabolism, and lack of energy failure. Neurology 79:213-220.
Brodaty H, Connors MH, Xu J, Woodward M, Ames D, group Ps (2015) The course of neuropsychiatric symptoms in dementia: a 3-year longitudinal study. Journal of the American Medical Directors Association 16:380-387.
Bultron G, Kacena K, Pearson D, Boxer M, Yang R, Sathe S, Pastores G, Mistry PK (2010) The risk of Parkinson's disease in type 1 Gaucher disease. Journal of inherited metabolic disease 33:167-173.
Burke D (2017) Interplay between Glucocerebrosidase 1 and Glucocerebrosidase 2; potential implications for the pathogenesis of Gaucher and Parkinson’s diseases. In: UCL Great Ormond Street Institute of Child Health, p 236: University College London.

Burke DG, Rahim AA, Waddington SN, Karlsson S, Enquist I, Bhatia K, Mehta A, Vellodi A, Heales S (2013) Increased glucocerebrosidase (GBA) 2 activity in GBA1 deficient mice brains and in Gaucher leucocytes. Journal of inherited metabolic disease 36:869-872.

Burn DJ, Rowan EN, Allan LM, Molloy S, O'Brien JT, McKeith IG (2006) Motor subtype and cognitive decline in Parkinson's disease, Parkinson's disease with dementia, and dementia with Lewy bodies. Journal of neurology, neurosurgery, and psychiatry 77:585-589.

Burre J (2015) The Synaptic Function of alpha-Synuclein. Journal of Parkinson's disease 5:699-713.

Burton EJ, McKeith IG, Burn DJ, Williams ED, O'Brien JT (2004) Cerebral atrophy in Parkinson's disease with and without dementia: a comparison with Alzheimer's disease, dementia with Lewy bodies and controls. Brain : a journal of neurology 127:791-800.

Butters TD, Dwek RA, Platt FM (2005) Imino sugar inhibitors for treating the lysosomal glycosphingolipidoses. Glycobiology 15:43R-52R.

Calfon M, Zeng H, Urano F, Till JH, Hubbard SR, Harding HP, Clark SG, Ron D (2002) IRE1 couples endoplasmic reticulum load to secretory capacity by processing the XBP-1 mRNA. Nature 415:92-96.

Chahine LM, Qiang J, Ashbridge E, Minger J, Yearout D, Horn S, Colcher A, Hurtig HI, Lee VM, Van Deerlin VM, Leverenz JB, Siderowf AD, Trojanowski JQ, Zabetian CP, Chen-Plotkin A (2013) Clinical and biochemical differences in patients having Parkinson disease with vs without GBA mutations. JAMA neurology 70:852-858.

Chan JY, Luzuriaga J, Maxwell EL, West PK, Bensellam M, Laybutt DR (2015) The balance between adaptive and apoptotic unfolded protein responses regulates beta-cell death under ER stress conditions through XBP1, CHOP and JNK. Molecular and cellular endocrinology 413:189-201.

Chan RB, Perotte AJ, Zhou B, Liong C, Shorr EJ, Marder KS, Kang UJ, Waters CH, Levy OA, Xu Y, Shim HB, Pe'er I, Di Paolo G, Alcalay RN (2017) Elevated GM3 plasma concentration in idiopathic Parkinson's disease: A lipidomic analysis. PloS one 12:e0172348.

Chen Y, Brandizzi F (2013) IRE1: ER stress sensor and cell fate executor. Trends in cell biology 23:547-555.

Chiasserini D, Paciotti S, Eusebi P, Persichetti E, Tasegian A, Kurzawa-Akanbi M, Chinnery PF, Morris CM, Calabresi P, Parnetti L, Beccari T (2015) Selective loss of glucocerebrosidase activity in sporadic Parkinson's disease and dementia with Lewy bodies. Molecular neurodegeneration 10:15.

Choi JM, Kim WC, Lyoo CH, Kang SY, Lee PH, Baik JS, Koh SB, Ma HI, Sohn YH, Lee MS, Kim YJ (2012) Association of mutations in the glucocerebrosidase gene with Parkinson disease in a Korean population. Neuroscience letters 514:12-15.

Chung CY et al. (2013) Identification and rescue of alpha-synuclein toxicity in Parkinson patient-derived neurons. Science 342:983-987.

Cilia R et al. (2016) Survival and dementia in GBA-associated Parkinson's disease: The mutation matters. Annals of neurology 80:662-673.

Clark LN, Ross BM, Wang Y, Mejia-Santana H, Harris J, Louis ED, Cote LJ, Andrews H, Fahn S, Waters C, Ford B, Frucht S, Ottman R, Marder K (2007) Mutations in the glucocerebrosidase gene are associated with early-onset Parkinson disease. Neurology 69:1270-1277.

Clark LN, Kartsaklis LA, Wolf Gilbert R, Dorado B, Ross BM, Kisselev S, Verbitsky M, Mejia-Santana H, Cote LJ, Andrews H, Vonsattel JP, Fahn S, Mayeux R, Honig LS, Marder K (2009) Association of glucocerebrosidase mutations with dementia with lewy bodies. Archives of neurology 66:578-583.

Clark LN, Chan R, Cheng R, Liu X, Park N, Parmalee N, Kisselev S, Cortes E, Torres PA, Pastores GM, Vonsattel JP, Alcalay R, Marder K, Honig LL, Fahn S, Mayeux R, Shelanski M, Di Paolo G, Lee JH (2015) Gene-wise association of variants in four lysosomal storage disorder genes in neuropathologically confirmed Lewy body disease. PloS one 10:e0125204.

Cleeter MW, Chau KY, Gluck C, Mehta A, Hughes DA, Duchen M, Wood NW, Hardy J, Mark Cooper J, Schapira AH (2013) Glucocerebrosidase inhibition causes mitochondrial dysfunction and free radical damage. Neurochemistry international 62:1-7.

Colla E, Coune P, Liu Y, Pletnikova O, Troncoso JC, Iwatsubo T, Schneider BL, Lee MK (2012) Endoplasmic reticulum stress is important for the manifestations of alpha-synucleinopathy in vivo. The Journal of neuroscience : the official journal of the Society for Neuroscience 32:3306-3320.

Colom-Cadena M, Gelpi E, Marti MJ, Charif S, Dols-Icardo O, Blesa R, Clarimon J, Lleo A (2013) MAPT H1 haplotype is associated with enhanced alpha-synuclein deposition in dementia with Lewy bodies. Neurobiology of aging 34:936-942.

Colom-Cadena M, Grau-Rivera O, Planellas L, Cerquera C, Morenas E, Helgueta S, Munoz L, Kulisevsky J, Marti MJ, Tolosa E, Clarimon J, Lleo A, Gelpi E (2017) Regional Overlap of Pathologies in Lewy Body Disorders. Journal of neuropathology and experimental neurology 76:216-224.

Compta Y, Parkkinen L, O'Sullivan SS, Vandrovcova J, Holton JL, Collins C, Lashley T, Kallis C, Williams DR, de Silva R, Lees AJ, Revesz T (2011) Lewy- and Alzheimer-type pathologies in Parkinson's disease dementia: which is more important? Brain : a journal of neurology 134:1493-1505.

Costa A, Bak T, Caffarra P, Caltagirone C, Ceccaldi M, Collette F, Crutch S, Della Sala S, Demonet JF, Dubois B, Duzel E, Nestor P, Papageorgiou SG, Salmon E, Sikkes S, Tiraboschi P, van der Flier WM, Visser PJ, Cappa SF (2017) The need for harmonisation and innovation of neuropsychological assessment in neurodegenerative dementias in Europe: consensus document of the Joint Program for Neurodegenerative Diseases Working Group. Alzheimer's research & therapy 9:27.

Coutinho MF, Santos JI, Alves S (2016) Less Is More: Substrate Reduction Therapy for Lysosomal Storage Disorders. International journal of molecular sciences 17.

Cox TM, Drelichman G, Cravo R, Balwani M, Burrow TA, Martins AM, Lukina E, Rosenbloom B, Ross L, Angell J, Puga AC (2015) Eliglustat compared with imiglucerase in patients with Gaucher's disease type 1 stabilised on enzyme replacement therapy: a phase 3, randomised, open-label, non-inferiority trial. Lancet 385:2355-2362.

Credle JJ, Finer-Moore JS, Papa FR, Stroud RM, Walter P (2005) On the mechanism of sensing unfolded protein in the endoplasmic reticulum. Proceedings of the National Academy of Sciences of the United States of America 102:18773-18784.

Cullen V, Sardi SP, Ng J, Xu YH, Sun Y, Tomlinson JJ, Kolodziej P, Kahn I, Saftig P, Woulfe J, Rochet JC, Glicksman MA, Cheng SH, Grabowski GA, Shihabuddin LS, Schlossmacher MG (2011) Acid beta-glucosidase mutants linked to Gaucher disease, Parkinson disease, and Lewy body dementia alter alpha-synuclein processing. Annals of neurology 69:940-953.

Cummings J, Isaacson S, Mills R, Williams H, Chi-Burris K, Corbett A, Dhall R, Ballard C (2014) Pimavanserin for patients with Parkinson's disease psychosis: a randomised, placebo-controlled phase 3 trial. Lancet 383:533-540.

D'Angelo G, Capasso S, Sticco L, Russo D (2013) Glycosphingolipids: synthesis and functions. The FEBS journal 280:6338-6353.

D'Hooge R, De Deyn PP (2001) Applications of the Morris water maze in the study of learning and memory. Brain research Brain research reviews 36:60-90.

Dai M, Liou B, Swope B, Wang X, Zhang W, Inskeep V, Grabowski GA, Sun Y, Pan D (2016) Progression of Behavioral and CNS Deficits in a Viable Murine Model of Chronic Neuronopathic Gaucher Disease. PloS one 11:e0162367.

Davis AA, Andruska KM, Benitez BA, Racette BA, Perlmutter JS, Cruchaga C (2016a) Variants in GBA, SNCA, and MAPT influence Parkinson disease risk, age at onset, and progression. Neurobiology of aging 37:209 e201-209 e207.

Davis MY et al. (2016b) Association of GBA Mutations and the E326K Polymorphism With Motor and Cognitive Progression in Parkinson Disease. JAMA neurology 73:1217-1224.

De Marco EV, Annesi G, Tarantino P, Rocca FE, Provenzano G, Civitelli D, Ciro Candiano IC, Annesi F, Carrideo S, Condino F, Nicoletti G, Messina D, Novellino F, Morelli M, Quattrone A (2008) Glucocerebrosidase gene mutations are associated with Parkinson's disease in southern Italy. Movement disorders : official journal of the Movement Disorder Society 23:460-463.

Deacon RM, Rawlins JN (2006) T-maze alternation in the rodent. Nature protocols 1:7-12.

Dekker N, Voorn-Brouwer T, Verhoek M, Wennekes T, Narayan RS, Speijer D, Hollak CE, Overkleeft HS, Boot RG, Aerts JM (2011a) The cytosolic beta-glucosidase GBA3 does not influence type 1 Gaucher disease manifestation. Blood cells, molecules & diseases 46:19-26.

Dekker N, van Dussen L, Hollak CE, Overkleeft H, Scheij S, Ghauharali K, van Breemen MJ, Ferraz MJ, Groener JE, Maas M, Wijburg FA, Speijer D, Tylki-Szymanska A, Mistry PK, Boot RG, Aerts JM (2011b) Elevated plasma glucosylsphingosine in Gaucher disease: relation to phenotype, storage cell markers, and therapeutic response. Blood 118:e118-127.

Deramecourt V, Bombois S, Maurage CA, Ghestem A, Drobecq H, Vanmechelen E, Lebert F, Pasquier F, Delacourte A (2006) Biochemical staging of synucleinopathy and amyloid

deposition in dementia with Lewy bodies. Journal of neuropathology and experimental neurology 65:278-288.
Dermentzaki G, Dimitriou E, Xilouri M, Michelakakis H, Stefanis L (2013) Loss of beta-glucocerebrosidase activity does not affect alpha-synuclein levels or lysosomal function in neuronal cells. PloS one 8:e60674.
Do CB, Tung JY, Dorfman E, Kiefer AK, Drabant EM, Francke U, Mountain JL, Goldman SM, Tanner CM, Langston JW, Wojcicki A, Eriksson N (2011) Web-based genome-wide association study identifies two novel loci and a substantial genetic component for Parkinson's disease. PLoS genetics 7:e1002141.
Dopeso-Reyes IG, Sucunza D, Rico AJ, Pignataro D, Marin-Ramos D, Roda E, Rodriguez-Perez AI, Labandeira-Garcia JL, Lanciego JL (2017) Glucocerebrosidase expression patterns in the non-human primate brain. Brain structure & function.
Dos Santos AV, Pestana CP, Diniz KR, Campos M, Abdalla-Carvalho CB, de Rosso AL, Pereira JS, Nicaretta DH, de Carvalho WL, Dos Santos JM, Santos-Reboucas CB, Pimentel MM (2010) Mutational analysis of GIGYF2, ATP13A2 and GBA genes in Brazilian patients with early-onset Parkinson's disease. Neuroscience letters 485:121-124.
Eblan MJ, Walker JM, Sidransky E (2005) The glucocerebrosidase gene and Parkinson's disease in Ashkenazi Jews. The New England journal of medicine 352:728-731; author reply 728-731.
Emre M, Ford PJ, Bilgic B, Uc EY (2014) Cognitive impairment and dementia in Parkinson's disease: practical issues and management. Movement disorders : official journal of the Movement Disorder Society 29:663-672.
Emre M et al. (2007) Clinical diagnostic criteria for dementia associated with Parkinson's disease. Movement disorders : official journal of the Movement Disorder Society 22:1689-1707; quiz 1837.
Enquist IB, Nilsson E, Ooka A, Mansson JE, Olsson K, Ehinger M, Brady RO, Richter J, Karlsson S (2006) Effective cell and gene therapy in a murine model of Gaucher disease. Proceedings of the National Academy of Sciences of the United States of America 103:13819-13824.
Enquist IB, Lo Bianco C, Ooka A, Nilsson E, Mansson JE, Ehinger M, Richter J, Brady RO, Kirik D, Karlsson S (2007) Murine models of acute neuronopathic Gaucher disease. Proceedings of the National Academy of Sciences of the United States of America 104:17483-17488.
Erickson AH, Ginns EI, Barranger JA (1985) Biosynthesis of the lysosomal enzyme glucocerebrosidase. The Journal of biological chemistry 260:14319-14324.
Farfel-Becker T, Vitner E, Dekel H, Leshem N, Enquist IB, Karlsson S, Futerman AH (2009) No evidence for activation of the unfolded protein response in neuronopathic models of Gaucher disease. Human molecular genetics 18:1482-1488.
Fawcett TW, Martindale JL, Guyton KZ, Hai T, Holbrook NJ (1999) Complexes containing activating transcription factor (ATF)/cAMP-responsive-element-binding protein (CREB) interact with the CCAAT/enhancer-binding protein (C/EBP)-ATF composite site to regulate Gadd153 expression during the stress response. The Biochemical journal 339 (Pt 1):135-141.
Ferman TJ, Smith GE, Boeve BF, Ivnik RJ, Petersen RC, Knopman D, Graff-Radford N, Parisi J, Dickson DW (2004) DLB fluctuations: specific features that reliably differentiate DLB from AD and normal aging. Neurology 62:181-187.
Ferman TJ, Boeve BF, Smith GE, Lin SC, Silber MH, Pedraza O, Wszolek Z, Graff-Radford NR, Uitti R, Van Gerpen J, Pao W, Knopman D, Pankratz VS, Kantarci K, Boot B, Parisi JE, Dugger BN, Fujishiro H, Petersen RC, Dickson DW (2011) Inclusion of RBD improves the diagnostic classification of dementia with Lewy bodies. Neurology 77:875-882.
Fernandes HJ, Hartfield EM, Christian HC, Emmanoulidou E, Zheng Y, Booth H, Bogetofte H, Lang C, Ryan BJ, Sardi SP, Badger J, Vowles J, Evetts S, Tofaris GK, Vekrellis K, Talbot K, Hu MT, James W, Cowley SA, Wade-Martins R (2016) ER Stress and Autophagic Perturbations Lead to Elevated Extracellular alpha-Synuclein in GBA-N370S Parkinson's iPSC-Derived Dopamine Neurons. Stem cell reports 6:342-356.
Ferraz MJ, Kallemeijn WW, Mirzaian M, Herrera Moro D, Marques A, Wisse P, Boot RG, Willems LI, Overkleeft HS, Aerts JM (2014) Gaucher disease and Fabry disease: new markers and insights in pathophysiology for two distinct glycosphingolipidoses. Biochimica et biophysica acta 1841:811-825.
Ferraz MJ, Marques AR, Appelman MD, Verhoek M, Strijland A, Mirzaian M, Scheij S, Ouairy CM, Lahav D, Wisse P, Overkleeft HS, Boot RG, Aerts JM (2016a) Lysosomal glycosphingolipid catabolism by acid ceramidase: formation of glycosphingoid bases during deficiency of glycosidases. FEBS letters 590:716-725.

Ferraz MJ, Marques AR, Gaspar P, Mirzaian M, van Roomen C, Ottenhoff R, Alfonso P, Irun P, Giraldo P, Wisse P, Sa Miranda C, Overkleeft HS, Aerts JM (2016b) Lyso-glycosphingolipid abnormalities in different murine models of lysosomal storage disorders. Molecular genetics and metabolism 117:186-193.
Fishbein I, Kuo YM, Giasson BI, Nussbaum RL (2014) Augmentation of phenotype in a transgenic Parkinson mouse heterozygous for a Gaucher mutation. Brain : a journal of neurology 137:3235-3247.
Foo LC (2013) Purification of astrocytes from transgenic rodents by fluorescence-activated cell sorting. Cold Spring Harbor protocols 2013:551-560.
Francis PT, Perry EK (2007) Cholinergic and other neurotransmitter mechanisms in Parkinson's disease, Parkinson's disease dementia, and dementia with Lewy bodies. Movement disorders : official journal of the Movement Disorder Society 22 Suppl 17:S351-357.
Fujishiro H, Ferman TJ, Boeve BF, Smith GE, Graff-Radford NR, Uitti RJ, Wszolek ZK, Knopman DS, Petersen RC, Parisi JE, Dickson DW (2008) Validation of the neuropathologic criteria of the third consortium for dementia with Lewy bodies for prospectively diagnosed cases. Journal of neuropathology and experimental neurology 67:649-656.
Fujiwara H, Hasegawa M, Dohmae N, Kawashima A, Masliah E, Goldberg MS, Shen J, Takio K, Iwatsubo T (2002) alpha-Synuclein is phosphorylated in synucleinopathy lesions. Nature cell biology 4:160-164.
Futerman AH, Platt FM (2017) The metabolism of glucocerebrosides - From 1965 to the present. Molecular genetics and metabolism 120:22-26.
Galasko D (2017) Lewy Body Disorders. Neurologic clinics 35:325-338.
Galvagnion C (2017) The Role of Lipids Interacting with alpha-Synuclein in the Pathogenesis of Parkinson's Disease. Journal of Parkinson's disease 7:433-450.
Gamez-Valero A, Prada-Dacasa P, Santos C, Adame-Castillo C, Campdelacreu J, Rene R, Gascon-Bayarri J, Ispierto L, Alvarez R, Ariza A, Beyer K (2016) GBA Mutations Are Associated With Earlier Onset and Male Sex in Dementia With Lewy Bodies. Movement disorders : official journal of the Movement Disorder Society 31:1066-1070.
Gan-Or Z, Giladi N, Rozovski U, Shifrin C, Rosner S, Gurevich T, Bar-Shira A, Orr-Urtreger A (2008) Genotype-phenotype correlations between GBA mutations and Parkinson disease risk and onset. Neurology 70:2277-2283.
Garcia de la Cadena S, Massieu L (2016) Caspases and their role in inflammation and ischemic neuronal death. Focus on caspase-12. Apoptosis : an international journal on programmed cell death 21:763-777.
Garcia-Sanz P, Orgaz L, Bueno-Gil G, Espadas I, Rodriguez-Traver E, Kulisevsky J, Gutierrez A, Davila JC, Gonzalez-Polo RA, Fuentes JM, Mir P, Vicario C, Moratalla R (2017) N370S-GBA1 mutation causes lysosomal cholesterol accumulation in Parkinson's disease. Movement disorders : official journal of the Movement Disorder Society 32:1409-1422.
Gault CR, Obeid LM, Hannun YA (2010) An overview of sphingolipid metabolism: from synthesis to breakdown. Advances in experimental medicine and biology 688:1-23.
Gegg ME, Sweet L, Wang BH, Shihabuddin LS, Sardi SP, Schapira AH (2015) No evidence for substrate accumulation in Parkinson brains with GBA mutations. Movement disorders : official journal of the Movement Disorder Society 30:1085-1089.
Gegg ME, Burke D, Heales SJ, Cooper JM, Hardy J, Wood NW, Schapira AH (2012) Glucocerebrosidase deficiency in substantia nigra of parkinson disease brains. Annals of neurology 72:455-463.
Geiger JT, Ding J, Crain B, Pletnikova O, Letson C, Dawson TM, Rosenthal LS, Pantelyat A, Gibbs JR, Albert MS, Hernandez DG, Hillis AE, Stone DJ, Singleton AB, North American Brain Expression C, Hardy JA, Troncoso JC, Scholz SW (2016) Next-generation sequencing reveals substantial genetic contribution to dementia with Lewy bodies. Neurobiology of disease 94:55-62.
Ghosh R et al. (2014) Allosteric inhibition of the IRE1alpha RNase preserves cell viability and function during endoplasmic reticulum stress. Cell 158:534-548.
Gibson CJ, Davids MS (2015) BCL-2 Antagonism to Target the Intrinsic Mitochondrial Pathway of Apoptosis. Clinical cancer research : an official journal of the American Association for Cancer Research 21:5021-5029.
Ginns EI, Choudary PV, Tsuji S, Martin B, Stubblefield B, Sawyer J, Hozier J, Barranger JA (1985) Gene mapping and leader polypeptide sequence of human glucocerebrosidase: implications for Gaucher disease. Proceedings of the National Academy of Sciences of the United States of America 82:7101-7105.
Ginns EI, Mak SK, Ko N, Karlgren J, Akbarian S, Chou VP, Guo Y, Lim A, Samuelsson S, LaMarca ML, Vazquez-DeRose J, Manning-Bog AB (2014) Neuroinflammation and

alpha-synuclein accumulation in response to glucocerebrosidase deficiency are accompanied by synaptic dysfunction. Molecular genetics and metabolism 111:152-162.
Goedert M, Spillantini MG, Del Tredici K, Braak H (2013) 100 years of Lewy pathology. Nature reviews Neurology 9:13-24.
Goker-Alpan O, Stubblefield BK, Giasson BI, Sidransky E (2010) Glucocerebrosidase is present in alpha-synuclein inclusions in Lewy body disorders. Acta neuropathologica 120:641-649.
Goker-Alpan O, Schiffmann R, LaMarca ME, Nussbaum RL, McInerney-Leo A, Sidransky E (2004) Parkinsonism among Gaucher disease carriers. Journal of medical genetics 41:937-940.
Goker-Alpan O, Lopez G, Vithayathil J, Davis J, Hallett M, Sidransky E (2008) The spectrum of parkinsonian manifestations associated with glucocerebrosidase mutations. Archives of neurology 65:1353-1357.
Goker-Alpan O, Masdeu JC, Kohn PD, Ianni A, Lopez G, Groden C, Chapman MC, Cropp B, Eisenberg DP, Maniwang ED, Davis J, Wiggs E, Sidransky E, Berman KF (2012) The neurobiology of glucocerebrosidase-associated parkinsonism: a positron emission tomography study of dopamine synthesis and regional cerebral blood flow. Brain : a journal of neurology 135:2440-2448.
Goldman JG, Williams-Gray C, Barker RA, Duda JE, Galvin JE (2014) The spectrum of cognitive impairment in Lewy body diseases. Movement disorders : official journal of the Movement Disorder Society 29:608-621.
Gomperts SN (2014) Imaging the role of amyloid in PD dementia and dementia with Lewy bodies. Current neurology and neuroscience reports 14:472.
Gomperts SN (2016) Lewy Body Dementias: Dementia With Lewy Bodies and Parkinson Disease Dementia. Continuum (Minneapolis, Minn) 22:435-463.
Gorbatyuk MS, Shabashvili A, Chen W, Meyers C, Sullivan LF, Salganik M, Lin JH, Lewin AS, Muzyczka N, Gorbatyuk OS (2012) Glucose regulated protein 78 diminishes alpha-synuclein neurotoxicity in a rat model of Parkinson disease. Molecular therapy : the journal of the American Society of Gene Therapy 20:1327-1337.
Goris A, Williams-Gray CH, Clark GR, Foltynie T, Lewis SJ, Brown J, Ban M, Spillantini MG, Compston A, Burn DJ, Chinnery PF, Barker RA, Sawcer SJ (2007) Tau and alpha-synuclein in susceptibility to, and dementia in, Parkinson's disease. Annals of neurology 62:145-153.
Grabowski GA (2008) Phenotype, diagnosis, and treatment of Gaucher's disease. Lancet 372:1263-1271.
Grabowski GA, Gatt S, Horowitz M (1990) Acid beta-glucosidase: enzymology and molecular biology of Gaucher disease. Critical reviews in biochemistry and molecular biology 25:385-414.
Grabowski GA, Zimran A, Ida H (2015) Gaucher disease types 1 and 3: Phenotypic characterization of large populations from the ICGG Gaucher Registry. American journal of hematology 90 Suppl 1:S12-18.
Grabowski GA, Osiecki-Newman K, Dinur T, Fabbro D, Legler G, Gatt S, Desnick RJ (1986) Human acid beta-glucosidase. Use of conduritol B epoxide derivatives to investigate the catalytically active normal and Gaucher disease enzymes. The Journal of biological chemistry 261:8263-8269.
Graham DR, Sidhu A (2010) Mice expressing the A53T mutant form of human alpha-synuclein exhibit hyperactivity and reduced anxiety-like behavior. Journal of neuroscience research 88:1777-1783.
Gregory SG et al. (2006) The DNA sequence and biological annotation of human chromosome 1. Nature 441:315-321.
Gruschus JM, Jiang Z, Yap TL, Hill SA, Grishaev A, Piszczek G, Sidransky E, Lee JC (2015) Dissociation of glucocerebrosidase dimer in solution by its co-factor, saposin C. Biochemical and biophysical research communications 457:561-566.
Guedes LC, Chan RB, Gomes MA, Conceicao VA, Machado RB, Soares T, Xu Y, Gaspar P, Carrico JA, Alcalay RN, Ferreira JJ, Outeiro TF, Miltenberger-Miltenyi G (2017) Serum lipid alterations in GBA-associated Parkinson's disease. Parkinsonism & related disorders 44:58-65.
Guo JL, Covell DJ, Daniels JP, Iba M, Stieber A, Zhang B, Riddle DM, Kwong LK, Xu Y, Trojanowski JQ, Lee VM (2013) Distinct alpha-synuclein strains differentially promote tau inclusions in neurons. Cell 154:103-117.
Halliday GM, Leverenz JB, Schneider JS, Adler CH (2014) The neurobiological basis of cognitive impairment in Parkinson's disease. Movement disorders : official journal of the Movement Disorder Society 29:634-650.

Halperin A, Elstein D, Zimran A (2006) Increased incidence of Parkinson disease among relatives of patients with Gaucher disease. Blood cells, molecules & diseases 36:426-428.
Han D, Lerner AG, Vande Walle L, Upton JP, Xu W, Hagen A, Backes BJ, Oakes SA, Papa FR (2009) IRE1alpha kinase activation modes control alternate endoribonuclease outputs to determine divergent cell fates. Cell 138:562-575.
Han F, Grimes DA, Li F, Wang T, Yu Z, Song N, Wu S, Racacho L, Bulman DE (2016) Mutations in the glucocerebrosidase gene are common in patients with Parkinson's disease from Eastern Canada. The International journal of neuroscience 126:415-421.
Han J, Back SH, Hur J, Lin YH, Gildersleeve R, Shan J, Yuan CL, Krokowski D, Wang S, Hatzoglou M, Kilberg MS, Sartor MA, Kaufman RJ (2013) ER-stress-induced transcriptional regulation increases protein synthesis leading to cell death. Nature cell biology 15:481-490.
Harding AJ, Halliday GM (2001) Cortical Lewy body pathology in the diagnosis of dementia. Acta neuropathologica 102:355-363.
Harding HP, Zhang Y, Ron D (1999) Protein translation and folding are coupled by an endoplasmic-reticulum-resident kinase. Nature 397:271-274.
Hely MA, Reid WG, Adena MA, Halliday GM, Morris JG (2008) The Sydney multicenter study of Parkinson's disease: the inevitability of dementia at 20 years. Movement disorders : official journal of the Movement Disorder Society 23:837-844.
Hepp DH, Ruiter AM, Galis Y, Voorn P, Rozemuller AJ, Berendse HW, Foncke EM, van de Berg WD (2013) Pedunculopontine cholinergic cell loss in hallucinating Parkinson disease patients but not in dementia with Lewy bodies patients. Journal of neuropathology and experimental neurology 72:1162-1170.
Hetz C, Chevet E, Harding HP (2013) Targeting the unfolded protein response in disease. Nature reviews Drug discovery 12:703-719.
Hetz C, Chevet E, Oakes SA (2015) Proteostasis control by the unfolded protein response. Nature cell biology 17:829-838.
Hinault MP, Cuendet AF, Mattoo RU, Mensi M, Dietler G, Lashuel HA, Goloubinoff P (2010) Stable alpha-synuclein oligomers strongly inhibit chaperone activity of the Hsp70 system by weak interactions with J-domain co-chaperones. The Journal of biological chemistry 285:38173-38182.
Hindle JV (2010) Ageing, neurodegeneration and Parkinson's disease. Age and ageing 39:156-161.
Hockenbery D, Nunez G, Milliman C, Schreiber RD, Korsmeyer SJ (1990) Bcl-2 is an inner mitochondrial membrane protein that blocks programmed cell death. Nature 348:334-336.
Hogan DB, Fiest KM, Roberts JI, Maxwell CJ, Dykeman J, Pringsheim T, Steeves T, Smith EE, Pearson D, Jette N (2016) The Prevalence and Incidence of Dementia with Lewy Bodies: a Systematic Review. The Canadian journal of neurological sciences Le journal canadien des sciences neurologiques 43 Suppl 1:S83-95.
Hogl B, Stefani A, Videnovic A (2018) Idiopathic REM sleep behaviour disorder and neurodegeneration - an update. Nature reviews Neurology 14:40-55.
Holleran WM, Ginns EI, Menon GK, Grundmann JU, Fartasch M, McKinney CE, Elias PM, Sidransky E (1994) Consequences of beta-glucocerebrosidase deficiency in epidermis. Ultrastructure and permeability barrier alterations in Gaucher disease. The Journal of clinical investigation 93:1756-1764.
Hollien J, Weissman JS (2006) Decay of endoplasmic reticulum-localized mRNAs during the unfolded protein response. Science 313:104-107.
Hoozemans JJ, van Haastert ES, Eikelenboom P, de Vos RA, Rozemuller JM, Scheper W (2007) Activation of the unfolded protein response in Parkinson's disease. Biochemical and biophysical research communications 354:707-711.
Hopfner F, Schulte EC, Mollenhauer B, Bereznai B, Knauf F, Lichtner P, Zimprich A, Haubenberger D, Pirker W, Brucke T, Peters A, Gieger C, Kuhlenbaumer G, Trenkwalder C, Winkelmann J (2013) The role of SCARB2 as susceptibility factor in Parkinson's disease. Movement disorders : official journal of the Movement Disorder Society 28:538-540.
Horowitz M, Wilder S, Horowitz Z, Reiner O, Gelbart T, Beutler E (1989) The human glucocerebrosidase gene and pseudogene: structure and evolution. Genomics 4:87-96.
Howlett DR, Whitfield D, Johnson M, Attems J, O'Brien JT, Aarsland D, Lai MK, Lee JH, Chen C, Ballard C, Hortobagyi T, Francis PT (2015) Regional Multiple Pathology Scores Are Associated with Cognitive Decline in Lewy Body Dementias. Brain pathology (Zurich, Switzerland) 25:401-408.

Hruska KS, LaMarca ME, Scott CR, Sidransky E (2008) Gaucher disease: mutation and polymorphism spectrum in the glucocerebrosidase gene (GBA). Human mutation 29:567-583.
Hu FY, Xi J, Guo J, Yu LH, Liu L, He XH, Liu ZL, Zou XY, Xu YM (2010) Association of the glucocerebrosidase N370S allele with Parkinson's disease in two separate Chinese Han populations of mainland China. European journal of neurology 17:1476-1478.
Huang WJ, Zhang X, Chen WW (2015) Gaucher disease: a lysosomal neurodegenerative disorder. European review for medical and pharmacological sciences 19:1219-1226.
Hughes RN (2004) The value of spontaneous alternation behavior (SAB) as a test of retention in pharmacological investigations of memory. Neuroscience and biobehavioral reviews 28:497-505.
Hunya A, Foldi I, Szegedi V, Soos K, Zarandi M, Szabo A, Zadori D, Penke B, Datki ZL (2008) Differences between normal and alpha-synuclein overexpressing SH-SY5Y neuroblastoma cells after Abeta(1-42) and NAC treatment. Brain research bulletin 75:648-654.
Hurtig HI, Trojanowski JQ, Galvin J, Ewbank D, Schmidt ML, Lee VM, Clark CM, Glosser G, Stern MB, Gollomp SM, Arnold SE (2000) Alpha-synuclein cortical Lewy bodies correlate with dementia in Parkinson's disease. Neurology 54:1916-1921.
Irwin DJ, Lee VM, Trojanowski JQ (2013) Parkinson's disease dementia: convergence of alpha-synuclein, tau and amyloid-beta pathologies. Nature reviews Neuroscience 14:626-636.
Irwin DJ, White MT, Toledo JB, Xie SX, Robinson JL, Van Deerlin V, Lee VM, Leverenz JB, Montine TJ, Duda JE, Hurtig HI, Trojanowski JQ (2012) Neuropathologic substrates of Parkinson disease dementia. Annals of neurology 72:587-598.
Irwin DJ et al. (2017) Neuropathological and genetic correlates of survival and dementia onset in synucleinopathies: a retrospective analysis. The Lancet Neurology 16:55-65.
Jakes R, Spillantini MG, Goedert M (1994) Identification of two distinct synucleins from human brain. FEBS letters 345:27-32.
Jellinger KA (2008) Re: In dementia with Lewy bodies, Braak stage determines phenotype, not Lewy body distribution. Neurology 70:407-408.
Jellinger KA (2017) Dementia with Lewy bodies and Parkinson's disease-dementia: current concepts and controversies. Journal of neural transmission (Vienna, Austria : 1996).
Jesus S, Huertas I, Bernal-Bernal I, Bonilla-Toribio M, Caceres-Redondo MT, Vargas-Gonzalez L, Gomez-Llamas M, Carrillo F, Calderon E, Carballo M, Gomez-Garre P, Mir P (2016) GBA Variants Influence Motor and Non-Motor Features of Parkinson's Disease. PloS one 11:e0167749.
Kacher Y, Brumshtein B, Boldin-Adamsky S, Toker L, Shainskaya A, Silman I, Sussman JL, Futerman AH (2008) Acid beta-glucosidase: insights from structural analysis and relevance to Gaucher disease therapy. Biological chemistry 389:1361-1369.
Kalaitzakis ME, Walls AJ, Pearce RK, Gentleman SM (2011) Striatal Abeta peptide deposition mirrors dementia and differentiates DLB and PDD from other parkinsonian syndromes. Neurobiology of disease 41:377-384.
Kanfer JN, Legler G, Sullivan J, Raghavan SS, Mumford RA (1975) The Gaucher mouse. Biochemical and biophysical research communications 67:85-90.
Kang L, Zhan X, Ye J, Han L, Qiu W, Gu X, Zhang H (2018) A rare form of Gaucher disease resulting from saposin C deficiency. Blood cells, molecules & diseases 68:60-65.
Kempster PA, O'Sullivan SS, Holton JL, Revesz T, Lees AJ (2010) Relationships between age and late progression of Parkinson's disease: a clinico-pathological study. Brain : a journal of neurology 133:1755-1762.
Kleene R, Schachner M (2004) Glycans and neural cell interactions. Nature reviews Neuroscience 5:195-208.
Klein JC, Eggers C, Kalbe E, Weisenbach S, Hohmann C, Vollmar S, Baudrexel S, Diederich NJ, Heiss WD, Hilker R (2010) Neurotransmitter changes in dementia with Lewy bodies and Parkinson disease dementia in vivo. Neurology 74:885-892.
Koide N, Muramatsu T (1974) Endo-beta-N-acetylglucosaminidase acting on carbohydrate moieties of glycoproteins. Purification and properties of the enzyme from Diplococcus pneumoniae. The Journal of biological chemistry 249:4897-4904.
Kolter T, Sandhoff K (2006) Sphingolipid metabolism diseases. Biochimica et biophysica acta 1758:2057-2079.
Kolter T, Sandhoff K (2010) Lysosomal degradation of membrane lipids. FEBS letters 584:1700-1712.
Kong B, Yang T, Gu JW, Kuang YQ, Cheng L, Yang WT, Yang XK, Xia X, Cheng JM, Ma Y, Zhang JH, Yu SX (2013) The association between lysosomal protein glucocerebrosidase

and Parkinson's disease. European review for medical and pharmacological sciences 17:143-151.
Kono S, Ouchi Y, Terada T, Ida H, Suzuki M, Miyajima H (2010) Functional brain imaging in glucocerebrosidase mutation carriers with and without parkinsonism. Movement disorders : official journal of the Movement Disorder Society 25:1823-1829.
Korennykh AV, Egea PF, Korostelev AA, Finer-Moore J, Zhang C, Shokat KM, Stroud RM, Walter P (2009) The unfolded protein response signals through high-order assembly of Ire1. Nature 457:687-693.
Kosaka K (2014) Lewy body disease and dementia with Lewy bodies. Proceedings of the Japan Academy Series B, Physical and biological sciences 90:301-306.
Kosaka K, Oyanagi S, Matsushita M, Hori A (1976) Presenile dementia with Alzheimer-, Pick- and Lewy-body changes. Acta neuropathologica 36:221-233.
Kotzbauer PT, Cairns NJ, Campbell MC, Willis AW, Racette BA, Tabbal SD, Perlmutter JS (2012) Pathologic accumulation of alpha-synuclein and Abeta in Parkinson disease patients with dementia. Archives of neurology 69:1326-1331.
Kurzawa-Akanbi M, Hanson PS, Blain PG, Lett DJ, McKeith IG, Chinnery PF, Morris CM (2012) Glucocerebrosidase mutations alter the endoplasmic reticulum and lysosomes in Lewy body disease. Journal of neurochemistry 123:298-309.
Labbe C et al. (2016) MAPT haplotype H1G is associated with increased risk of dementia with Lewy bodies. Alzheimer's & dementia : the journal of the Alzheimer's Association 12:1297-1304.
Lall N, Henley-Smith CJ, De Canha MN, Oosthuizen CB, Berrington D (2013) Viability Reagent, PrestoBlue, in Comparison with Other Available Reagents, Utilized in Cytotoxicity and Antimicrobial Assays. International journal of microbiology 2013:420601.
Lee AH, Iwakoshi NN, Glimcher LH (2003) XBP-1 regulates a subset of endoplasmic reticulum resident chaperone genes in the unfolded protein response. Molecular and cellular biology 23:7448-7459.
Lerche S, Schulte C, Srulijes K, Pilotto A, Rattay TW, Hauser AK, Stransky E, Deuschle C, Csoti I, Lachmann I, Zetterberg H, Liepelt-Scarfone I, Gasser T, Maetzler W, Berg D, Brockmann K (2017) Cognitive impairment in Glucocerebrosidase (GBA)-associated PD: Not primarily associated with cerebrospinal fluid Abeta and Tau profiles. Movement disorders : official journal of the Movement Disorder Society 32:1780-1783.
Li Y, Guo Y, Tang J, Jiang J, Chen Z (2014) New insights into the roles of CHOP-induced apoptosis in ER stress. Acta biochimica et biophysica Sinica 46:629-640.
Lim S, Chun Y, Lee JS, Lee SJ (2016) Neuroinflammation in Synucleinopathies. Brain pathology (Zurich, Switzerland) 26:404-409.
Liu Y, Suzuki K, Reed JD, Grinberg A, Westphal H, Hoffmann A, Doring T, Sandhoff K, Proia RL (1998) Mice with type 2 and 3 Gaucher disease point mutations generated by a single insertion mutagenesis procedure. Proceedings of the National Academy of Sciences of the United States of America 95:2503-2508.
Livak KJ, Schmittgen TD (2001) Analysis of relative gene expression data using real-time quantitative PCR and the 2(-Delta Delta C(T)) Method. Methods (San Diego, Calif) 25:402-408.
Lonser RR, Schiffman R, Robison RA, Butman JA, Quezado Z, Walker ML, Morrison PF, Walbridge S, Murray GJ, Park DM, Brady RO, Oldfield EH (2007) Image-guided, direct convective delivery of glucocerebrosidase for neuronopathic Gaucher disease. Neurology 68:254-261.
Lwin A, Orvisky E, Goker-Alpan O, LaMarca ME, Sidransky E (2004) Glucocerebrosidase mutations in subjects with parkinsonism. Molecular genetics and metabolism 81:70-73.
Lynes EM, Simmen T (2011) Urban planning of the endoplasmic reticulum (ER): how diverse mechanisms segregate the many functions of the ER. Biochimica et biophysica acta 1813:1893-1905.
Maegawa GH, Tropak MB, Buttner JD, Rigat BA, Fuller M, Pandit D, Tang L, Kornhaber GJ, Hamuro Y, Clarke JT, Mahuran DJ (2009) Identification and characterization of ambroxol as an enzyme enhancement agent for Gaucher disease. The Journal of biological chemistry 284:23502-23516.
Malec-Litwinowicz M, Rudzinska M, Szubiga M, Michalski M, Tomaszewski T, Szczudlik A (2014) Cognitive impairment in carriers of glucocerebrosidase gene mutation in Parkinson disease patients. Neurologia i neurochirurgia polska 48:258-261.
Maley F, Trimble RB, Tarentino AL, Plummer TH, Jr. (1989) Characterization of glycoproteins and their associated oligosaccharides through the use of endoglycosidases. Analytical biochemistry 180:195-204.

Maniwang E, Tayebi N, Sidransky E (2013) Is Parkinson disease associated with lysosomal integral membrane protein type-2?: challenges in interpreting association data. Molecular genetics and metabolism 108:269-271.
Manning-Bog AB, Schule B, Langston JW (2009) Alpha-synuclein-glucocerebrosidase interactions in pharmacological Gaucher models: a biological link between Gaucher disease and parkinsonism. Neurotoxicology 30:1127-1132.
Mao XY, Burgunder JM, Zhang ZJ, An XK, Zhang JH, Yang Y, Li T, Wang YC, Chang XL, Peng R (2010) Association between GBA L444P mutation and sporadic Parkinson's disease from Mainland China. Neuroscience letters 469:256-259.
Maor G, Rencus-Lazar S, Filocamo M, Steller H, Segal D, Horowitz M (2013) Unfolded protein response in Gaucher disease: from human to Drosophila. Orphanet journal of rare diseases 8:140.
Marciniak SJ, Yun CY, Oyadomari S, Novoa I, Zhang Y, Jungreis R, Nagata K, Harding HP, Ron D (2004) CHOP induces death by promoting protein synthesis and oxidation in the stressed endoplasmic reticulum. Genes & development 18:3066-3077.
Martin-Montanez E, Lopez-Tellez JF, Acevedo MJ, Pavia J, Khan ZU (2010) Efficiency of gene transfection reagents in NG108-15, SH-SY5Y and CHO-K1 cell lines. Methods and findings in experimental and clinical pharmacology 32:291-297.
Martyn AC, De Jaeger X, Magalhaes AC, Kesarwani R, Goncalves DF, Raulic S, Guzman MS, Jackson MF, Izquierdo I, Macdonald JF, Prado MA, Prado VF (2012) Elimination of the vesicular acetylcholine transporter in the forebrain causes hyperactivity and deficits in spatial memory and long-term potentiation. Proceedings of the National Academy of Sciences of the United States of America 109:17651-17656.
Masliah E, Rockenstein E, Veinbergs I, Sagara Y, Mallory M, Hashimoto M, Mucke L (2001) beta-amyloid peptides enhance alpha-synuclein accumulation and neuronal deficits in a transgenic mouse model linking Alzheimer's disease and Parkinson's disease. Proceedings of the National Academy of Sciences of the United States of America 98:12245-12250.
Massimo A, Maura S, Nicoletta L, Giulia M, Valentina M, Elena C, Alessandro P, Rosaria B, Sandro S (2016) Current and Novel Aspects on the Non-lysosomal beta-Glucosylceramidase GBA2. Neurochemical research 41:210-220.
Mata IF, Samii A, Schneer SH, Roberts JW, Griffith A, Leis BC, Schellenberg GD, Sidransky E, Bird TD, Leverenz JB, Tsuang D, Zabetian CP (2008) Glucocerebrosidase gene mutations: a risk factor for Lewy body disorders. Archives of neurology 65:379-382.
Mata IF et al. (2017) Large-scale exploratory genetic analysis of cognitive impairment in Parkinson's disease. Neurobiology of aging 56:211 e211-211 e217.
Mata IF et al. (2014) APOE, MAPT, and SNCA genes and cognitive performance in Parkinson disease. JAMA neurology 71:1405-1412.
Mata IF et al. (2016) GBA Variants are associated with a distinct pattern of cognitive deficits in Parkinson's disease. Movement disorders : official journal of the Movement Disorder Society 31:95-102.
Mattila PM, Rinne JO, Helenius H, Roytta M (1999) Neuritic degeneration in the hippocampus and amygdala in Parkinson's disease in relation to Alzheimer pathology. Acta neuropathologica 98:157-164.
Maurel M, Chevet E, Tavernier J, Gerlo S (2014) Getting RIDD of RNA: IRE1 in cell fate regulation. Trends in biochemical sciences 39:245-254.
Mazzulli JR, Zunke F, Isacson O, Studer L, Krainc D (2016a) alpha-Synuclein-induced lysosomal dysfunction occurs through disruptions in protein trafficking in human midbrain synucleinopathy models. Proceedings of the National Academy of Sciences of the United States of America 113:1931-1936.
Mazzulli JR, Xu YH, Sun Y, Knight AL, McLean PJ, Caldwell GA, Sidransky E, Grabowski GA, Krainc D (2011) Gaucher disease glucocerebrosidase and alpha-synuclein form a bidirectional pathogenic loop in synucleinopathies. Cell 146:37-52.
Mazzulli JR, Zunke F, Tsunemi T, Toker NJ, Jeon S, Burbulla LF, Patnaik S, Sidransky E, Marugan JJ, Sue CM, Krainc D (2016b) Activation of beta-Glucocerebrosidase Reduces Pathological alpha-Synuclein and Restores Lysosomal Function in Parkinson's Patient Midbrain Neurons. The Journal of neuroscience : the official journal of the Society for Neuroscience 36:7693-7706.
McCullough KD, Martindale JL, Klotz LO, Aw TY, Holbrook NJ (2001) Gadd153 sensitizes cells to endoplasmic reticulum stress by down-regulating Bcl2 and perturbing the cellular redox state. Molecular and cellular biology 21:1249-1259.

McKeith IG et al. (1996) Consensus guidelines for the clinical and pathologic diagnosis of dementia with Lewy bodies (DLB): report of the consortium on DLB international workshop. Neurology 47:1113-1124.
McKeith IG et al. (2005) Diagnosis and management of dementia with Lewy bodies: third report of the DLB Consortium. Neurology 65:1863-1872.
McKeith IG et al. (2017) Diagnosis and management of dementia with Lewy bodies: Fourth consensus report of the DLB Consortium. Neurology 89:88-100.
McNeill A, Duran R, Hughes DA, Mehta A, Schapira AH (2012) A clinical and family history study of Parkinson's disease in heterozygous glucocerebrosidase mutation carriers. Journal of neurology, neurosurgery, and psychiatry 83:853-854.
McNeill A, Roberti G, Lascaratos G, Hughes D, Mehta A, Garway-Heath DF, Schapira AH (2013) Retinal thinning in Gaucher disease patients and carriers: results of a pilot study. Molecular genetics and metabolism 109:221-223.
McNeill A, Magalhaes J, Shen C, Chau KY, Hughes D, Mehta A, Foltynie T, Cooper JM, Abramov AY, Gegg M, Schapira AH (2014) Ambroxol improves lysosomal biochemistry in glucocerebrosidase mutation-linked Parkinson disease cells. Brain : a journal of neurology 137:1481-1495.
Medhurst AD, Harrison DC, Read SJ, Campbell CA, Robbins MJ, Pangalos MN (2000) The use of TaqMan RT-PCR assays for semiquantitative analysis of gene expression in CNS tissues and disease models. Journal of neuroscience methods 98:9-20.
Meissner WG, Frasier M, Gasser T, Goetz CG, Lozano A, Piccini P, Obeso JA, Rascol O, Schapira A, Voon V, Weiner DM, Tison F, Bezard E (2011) Priorities in Parkinson's disease research. Nature reviews Drug discovery 10:377-393.
Mercado G, Castillo V, Soto P, Sidhu A (2016) ER stress and Parkinson's disease: Pathological inputs that converge into the secretory pathway. Brain research 1648:626-632.
Michelakakis H, Xiromerisiou G, Dardiotis E, Bozi M, Vassilatis D, Kountra PM, Patramani G, Moraitou M, Papadimitriou D, Stamboulis E, Stefanis L, Zintzaras E, Hadjigeorgiou GM (2012) Evidence of an association between the scavenger receptor class B member 2 gene and Parkinson's disease. Movement disorders : official journal of the Movement Disorder Society 27:400-405.
Mielke MM, Maetzler W, Haughey NJ, Bandaru VV, Savica R, Deuschle C, Gasser T, Hauser AK, Graber-Sultan S, Schleicher E, Berg D, Liepelt-Scarfone I (2013) Plasma ceramide and glucosylceramide metabolism is altered in sporadic Parkinson's disease and associated with cognitive impairment: a pilot study. PloS one 8:e73094.
Migdalska-Richards A, Schapira AH (2016) The relationship between glucocerebrosidase mutations and Parkinson disease. Journal of neurochemistry 139 Suppl 1:77-90.
Migdalska-Richards A, Daly L, Bezard E, Schapira AH (2016) Ambroxol effects in glucocerebrosidase and alpha-synuclein transgenic mice. Annals of neurology 80:766-775.
Migdalska-Richards A, Ko WKD, Li Q, Bezard E, Schapira AHV (2017) Oral ambroxol increases brain glucocerebrosidase activity in a nonhuman primate. Synapse (New York, NY) 71.
Mistry PK, Lopez G, Schiffmann R, Barton NW, Weinreb NJ, Sidransky E (2017) Gaucher disease: Progress and ongoing challenges. Molecular genetics and metabolism 120:8-21.
Mistry PK, Liu J, Sun L, Chuang WL, Yuen T, Yang R, Lu P, Zhang K, Li J, Keutzer J, Stachnik A, Mennone A, Boyer JL, Jain D, Brady RO, New MI, Zaidi M (2014) Glucocerebrosidase 2 gene deletion rescues type 1 Gaucher disease. Proceedings of the National Academy of Sciences of the United States of America 111:4934-4939.
Mistry PK et al. (2010) Glucocerebrosidase gene-deficient mouse recapitulates Gaucher disease displaying cellular and molecular dysregulation beyond the macrophage. Proceedings of the National Academy of Sciences of the United States of America 107:19473-19478.
Mizukami H, Mi Y, Wada R, Kono M, Yamashita T, Liu Y, Werth N, Sandhoff R, Sandhoff K, Proia RL (2002) Systemic inflammation in glucocerebrosidase-deficient mice with minimal glucosylceramide storage. The Journal of clinical investigation 109:1215-1221.
Montfort M, Chabas A, Vilageliu L, Grinberg D (2004) Functional analysis of 13 GBA mutant alleles identified in Gaucher disease patients: Pathogenic changes and "modifier" polymorphisms. Human mutation 23:567-575.
Moors T, Paciotti S, Chiasserini D, Calabresi P, Parnetti L, Beccari T, van de Berg WD (2016) Lysosomal Dysfunction and alpha-Synuclein Aggregation in Parkinson's Disease: Diagnostic Links. Movement disorders : official journal of the Movement Disorder Society 31:791-801.
Morad SA, Cabot MC (2013) Ceramide-orchestrated signalling in cancer cells. Nature reviews Cancer 13:51-65.

Moraitou M, Hadjigeorgiou G, Monopolis I, Dardiotis E, Bozi M, Vassilatis D, Vilageliu L, Grinberg D, Xiromerisiou G, Stefanis L, Michelakakis H (2011) beta-Glucocerebrosidase gene mutations in two cohorts of Greek patients with sporadic Parkinson's disease. Molecular genetics and metabolism 104:149-152.
Morris R (1984) Developments of a water-maze procedure for studying spatial learning in the rat. Journal of neuroscience methods 11:47-60.
Mosimann UP, Mather G, Wesnes KA, O'Brien JT, Burn DJ, McKeith IG (2004) Visual perception in Parkinson disease dementia and dementia with Lewy bodies. Neurology 63:2091-2096.
Mosmann T (1983) Rapid colorimetric assay for cellular growth and survival: application to proliferation and cytotoxicity assays. Journal of immunological methods 65:55-63.
Murphy KE, Halliday GM (2014) Glucocerebrosidase deficits in sporadic Parkinson disease. Autophagy 10:1350-1351.
Murphy KE, Gysbers AM, Abbott SK, Tayebi N, Kim WS, Sidransky E, Cooper A, Garner B, Halliday GM (2014) Reduced glucocerebrosidase is associated with increased alpha-synuclein in sporadic Parkinson's disease. Brain : a journal of neurology 137:834-848.
Murugesan V, Chuang WL, Liu J, Lischuk A, Kacena K, Lin H, Pastores GM, Yang R, Keutzer J, Zhang K, Mistry PK (2016) Glucosylsphingosine is a key biomarker of Gaucher disease. American journal of hematology 91:1082-1089.
Myhill N, Lynes EM, Nanji JA, Blagoveshchenskaya AD, Fei H, Carmine Simmen K, Cooper TJ, Thomas G, Simmen T (2008) The subcellular distribution of calnexin is mediated by PACS-2. Molecular biology of the cell 19:2777-2788.
Nakagawa T, Zhu H, Morishima N, Li E, Xu J, Yankner BA, Yuan J (2000) Caspase-12 mediates endoplasmic-reticulum-specific apoptosis and cytotoxicity by amyloid-beta. Nature 403:98-103.
Nalls MA et al. (2013) A multicenter study of glucocerebrosidase mutations in dementia with Lewy bodies. JAMA neurology 70:727-735.
Nalls MA et al. (2014) Large-scale meta-analysis of genome-wide association data identifies six new risk loci for Parkinson's disease. Nature genetics 46:989-993.
Nedelska Z, Ferman TJ, Boeve BF, Przybelski SA, Lesnick TG, Murray ME, Gunter JL, Senjem ML, Vemuri P, Smith GE, Geda YE, Graff-Radford J, Knopman DS, Petersen RC, Parisi JE, Dickson DW, Jack CR, Jr., Kantarci K (2015) Pattern of brain atrophy rates in autopsy-confirmed dementia with Lewy bodies. Neurobiology of aging 36:452-461.
Neudorfer O, Giladi N, Elstein D, Abrahamov A, Turezkite T, Aghai E, Reches A, Bembi B, Zimran A (1996) Occurrence of Parkinson's syndrome in type I Gaucher disease. QJM : monthly journal of the Association of Physicians 89:691-694.
Neumann J, Bras J, Deas E, O'Sullivan SS, Parkkinen L, Lachmann RH, Li A, Holton J, Guerreiro R, Paudel R, Segarane B, Singleton A, Lees A, Hardy J, Houlden H, Revesz T, Wood NW (2009) Glucocerebrosidase mutations in clinical and pathologically proven Parkinson's disease. Brain : a journal of neurology 132:1783-1794.
Nichols WC, Pankratz N, Marek DK, Pauciulo MW, Elsaesser VE, Halter CA, Rudolph A, Wojcieszek J, Pfeiffer RF, Foroud T, Parkinson Study Group PI (2009) Mutations in GBA are associated with familial Parkinson disease susceptibility and age at onset. Neurology 72:310-316.
Nilsson O, Svennerholm L (1982) Accumulation of glucosylceramide and glucosylsphingosine (psychosine) in cerebrum and cerebellum in infantile and juvenile Gaucher disease. Journal of neurochemistry 39:709-718.
Noelker C, Lu L, Hollerhage M, Vulinovic F, Sturn A, Roscher R, Hoglinger GU, Hirsch EC, Oertel WH, Alvarez-Fischer D, Andreas H (2015) Glucocerebrosidase deficiency and mitochondrial impairment in experimental Parkinson disease. Journal of the neurological sciences 356:129-136.
Nutt JG, Carter JH, Sexton GJ (2004) The dopamine transporter: importance in Parkinson's disease. Annals of neurology 55:766-773.
Orvisky E, Park JK, LaMarca ME, Ginns EI, Martin BM, Tayebi N, Sidransky E (2002) Glucosylsphingosine accumulation in tissues from patients with Gaucher disease: correlation with phenotype and genotype. Molecular genetics and metabolism 76:262-270.
Osellame LD, Rahim AA, Hargreaves IP, Gegg ME, Richard-Londt A, Brandner S, Waddington SN, Schapira AH, Duchen MR (2013) Mitochondria and quality control defects in a mouse model of Gaucher disease--links to Parkinson's disease. Cell metabolism 17:941-953.
Pagano G, Rengo G, Pasqualetti G, Femminella GD, Monzani F, Ferrara N, Tagliati M (2015) Cholinesterase inhibitors for Parkinson's disease: a systematic review and meta-analysis. Journal of neurology, neurosurgery, and psychiatry 86:767-773.

Pao WC, Boeve BF, Ferman TJ, Lin SC, Smith GE, Knopman DS, Graff-Radford NR, Petersen RC, Parisi JE, Dickson DW, Silber MH (2013) Polysomnographic findings in dementia with Lewy bodies. The neurologist 19:1-6.
Parkin JL, Brunning RD (1982) Pathology of the Gaucher cell. Progress in clinical and biological research 95:151-175.
Parkkinen L, Pirttila T, Alafuzoff I (2008) Applicability of current staging/categorization of alpha-synuclein pathology and their clinical relevance. Acta neuropathologica 115:399-407.
Parkkinen L, Neumann J, O'Sullivan SS, Holton JL, Revesz T, Hardy J, Lees AJ (2011) Glucocerebrosidase mutations do not cause increased Lewy body pathology in Parkinson's disease. Molecular genetics and metabolism 103:410-412.
Parnetti L, Paciotti S, Eusebi P, Dardis A, Zampieri S, Chiasserini D, Tasegian A, Tambasco N, Bembi B, Calabresi P, Beccari T (2017) Cerebrospinal fluid beta-glucocerebrosidase activity is reduced in parkinson's disease patients. Movement disorders : official journal of the Movement Disorder Society 32:1423-1431.
Parnetti L, Balducci C, Pierguidi L, De Carlo C, Peducci M, D'Amore C, Padiglioni C, Mastrocola S, Persichetti E, Paciotti S, Bellomo G, Tambasco N, Rossi A, Beccari T, Calabresi P (2009) Cerebrospinal fluid beta-glucocerebrosidase activity is reduced in Dementia with Lewy Bodies. Neurobiology of disease 34:484-486.
Parnetti L, Chiasserini D, Persichetti E, Eusebi P, Varghese S, Qureshi MM, Dardis A, Deganuto M, De Carlo C, Castrioto A, Balducci C, Paciotti S, Tambasco N, Bembi B, Bonanni L, Onofrj M, Rossi A, Beccari T, El-Agnaf O, Calabresi P (2014) Cerebrospinal fluid lysosomal enzymes and alpha-synuclein in Parkinson's disease. Movement disorders : official journal of the Movement Disorder Society 29:1019-1027.
Peters SP, Coyle P, Glew RH (1976) Differentiation of beta-glucocerebrosidase from beta-glucosidase in human tissues using sodium taurocholate. Archives of biochemistry and biophysics 175:569-582.
Petrou M, Dwamena BA, Foerster BR, MacEachern MP, Bohnen NI, Muller ML, Albin RL, Frey KA (2015) Amyloid deposition in Parkinson's disease and cognitive impairment: a systematic review. Movement disorders : official journal of the Movement Disorder Society 30:928-935.
Postuma RB, Berg D, Stern M, Poewe W, Olanow CW, Oertel W, Obeso J, Marek K, Litvan I, Lang AE, Halliday G, Goetz CG, Gasser T, Dubois B, Chan P, Bloem BR, Adler CH, Deuschl G (2015) MDS clinical diagnostic criteria for Parkinson's disease. Movement disorders : official journal of the Movement Disorder Society 30:1591-1601.
Poulopoulos M, Levy OA, Alcalay RN (2012) The neuropathology of genetic Parkinson's disease. Movement disorders : official journal of the Movement Disorder Society 27:831-842.
Pozzi D, Ban J, Iseppon F, Torre V (2017) An improved method for growing neurons: Comparison with standard protocols. Journal of neuroscience methods 280:1-10.
Puangmalai N, Somani A, Thangnipon W, Ballard C, Broadstock M (2015) A genetically immortalized human stem cell line: a promising new tool for Alzheimer's disease therapy. EXCLI journal 14:1135-1114.
Pulkes T, Choubtum L, Chitphuk S, Thakkinstian A, Pongpakdee S, Kulkantrakorn K, Hanchaiphiboolkul S, Tiamkao S, Boonkongchuen P (2014) Glucocerebrosidase mutations in Thai patients with Parkinson's disease. Parkinsonism & related disorders 20:986-991.
Radford H, Moreno JA, Verity N, Halliday M, Mallucci GR (2015) PERK inhibition prevents tau-mediated neurodegeneration in a mouse model of frontotemporal dementia. Acta neuropathologica 130:633-642.
Rana HQ, Balwani M, Bier L, Alcalay RN (2013) Age-specific Parkinson disease risk in GBA mutation carriers: information for genetic counseling. Genetics in medicine : official journal of the American College of Medical Genetics 15:146-149.
Reczek D, Schwake M, Schroder J, Hughes H, Blanz J, Jin X, Brondyk W, Van Patten S, Edmunds T, Saftig P (2007) LIMP-2 is a receptor for lysosomal mannose-6-phosphate-independent targeting of beta-glucocerebrosidase. Cell 131:770-783.
Ridley CM, Thur KE, Shanahan J, Thillaiappan NB, Shen A, Uhl K, Walden CM, Rahim AA, Waddington SN, Platt FM, van der Spoel AC (2013) beta-Glucosidase 2 (GBA2) activity and imino sugar pharmacology. The Journal of biological chemistry 288:26052-26066.
Robak LA, Jansen IE, van Rooij J, Uitterlinden AG, Kraaij R, Jankovic J, Heutink P, Shulman JM (2017) Excessive burden of lysosomal storage disorder gene variants in Parkinson's disease. Brain : a journal of neurology 140:3191-3203.
Rocha EM, Smith GA, Park E, Cao H, Brown E, Hallett P, Isacson O (2015a) Progressive decline of glucocerebrosidase in aging and Parkinson's disease. Annals of clinical and translational neurology 2:433-438.

Rocha EM, Smith GA, Park E, Cao H, Graham AR, Brown E, McLean JR, Hayes MA, Beagan J, Izen SC, Perez-Torres E, Hallett PJ, Isacson O (2015b) Sustained Systemic Glucocerebrosidase Inhibition Induces Brain alpha-Synuclein Aggregation, Microglia and Complement C1q Activation in Mice. Antioxidants & redox signaling 23:550-564.

Rolinski M, Fox C, Maidment I, McShane R (2012) Cholinesterase inhibitors for dementia with Lewy bodies, Parkinson's disease dementia and cognitive impairment in Parkinson's disease. The Cochrane database of systematic reviews:CD006504.

Ron D, Walter P (2007) Signal integration in the endoplasmic reticulum unfolded protein response. Nature reviews Molecular cell biology 8:519-529.

Ron I, Horowitz M (2005) ER retention and degradation as the molecular basis underlying Gaucher disease heterogeneity. Human molecular genetics 14:2387-2398.

Rothaug M, Zunke F, Mazzulli JR, Schweizer M, Altmeppen H, Lullmann-Rauch R, Kallemeijn WW, Gaspar P, Aerts JM, Glatzel M, Saftig P, Krainc D, Schwake M, Blanz J (2014) LIMP-2 expression is critical for beta-glucocerebrosidase activity and alpha-synuclein clearance. Proceedings of the National Academy of Sciences of the United States of America 111:15573-15578.

Rozpedek W, Markiewicz L, Diehl JA, Pytel D, Majsterek I (2015) Unfolded Protein Response and PERK Kinase as a New Therapeutic Target in the Pathogenesis of Alzheimer's Disease. Current medicinal chemistry 22:3169-3184.

Salganik M, Sergeyev VG, Shinde V, Meyers CA, Gorbatyuk MS, Lin JH, Zolotukhin S, Gorbatyuk OS (2015) The loss of glucose-regulated protein 78 (GRP78) during normal aging or from siRNA knockdown augments human alpha-synuclein (alpha-syn) toxicity to rat nigral neurons. Neurobiology of aging 36:2213-2223.

Sanchez-Martinez A, Beavan M, Gegg ME, Chau KY, Whitworth AJ, Schapira AH (2016) Parkinson disease-linked GBA mutation effects reversed by molecular chaperones in human cell and fly models. Scientific reports 6:31380.

Sanders A, Hemmelgarn H, Melrose HL, Hein L, Fuller M, Clarke LA (2013) Transgenic mice expressing human glucocerebrosidase variants: utility for the study of Gaucher disease. Blood cells, molecules & diseases 51:109-115.

Sandhoff K, Harzer K (2013) Gangliosides and gangliosidoses: principles of molecular and metabolic pathogenesis. The Journal of neuroscience : the official journal of the Society for Neuroscience 33:10195-10208.

Sardi SP, Clarke J, Kinnecom C, Tamsett TJ, Li L, Stanek LM, Passini MA, Grabowski GA, Schlossmacher MG, Sidman RL, Cheng SH, Shihabuddin LS (2011) CNS expression of glucocerebrosidase corrects alpha-synuclein pathology and memory in a mouse model of Gaucher-related synucleinopathy. Proceedings of the National Academy of Sciences of the United States of America 108:12101-12106.

Sardi SP, Clarke J, Viel C, Chan M, Tamsett TJ, Treleaven CM, Bu J, Sweet L, Passini MA, Dodge JC, Yu WH, Sidman RL, Cheng SH, Shihabuddin LS (2013) Augmenting CNS glucocerebrosidase activity as a therapeutic strategy for parkinsonism and other Gaucher-related synucleinopathies. Proceedings of the National Academy of Sciences of the United States of America 110:3537-3542.

Schneider JA, Arvanitakis Z, Yu L, Boyle PA, Leurgans SE, Bennett DA (2012) Cognitive impairment, decline and fluctuations in older community-dwelling subjects with Lewy bodies. Brain : a journal of neurology 135:3005-3014.

Schonauer S, Korschen HG, Penno A, Rennhack A, Breiden B, Sandhoff K, Gutbrod K, Dormann P, Raju DN, Haberkant P, Gerl MJ, Brugger B, Zigdon H, Vardi A, Futerman AH, Thiele C, Wachten D (2017) Identification of a feedback loop involving beta-glucosidase 2 and its product sphingosine sheds light on the molecular mechanisms in Gaucher disease. The Journal of biological chemistry 292:6177-6189.

Schondorf DC, Aureli M, McAllister FE, Hindley CJ, Mayer F, Schmid B, Sardi SP, Valsecchi M, Hoffmann S, Schwarz LK, Hedrich U, Berg D, Shihabuddin LS, Hu J, Pruszak J, Gygi SP, Sonnino S, Gasser T, Deleidi M (2014) iPSC-derived neurons from GBA1-associated Parkinson's disease patients show autophagic defects and impaired calcium homeostasis. Nature communications 5:4028.

Schubert U, Anton LC, Gibbs J, Norbury CC, Yewdell JW, Bennink JR (2000) Rapid degradation of a large fraction of newly synthesized proteins by proteasomes. Nature 404:770-774.

Sechi A, Dardis A, Bembi B (2016) Profile of eliglustat tartrate in the management of Gaucher disease. Therapeutics and clinical risk management 12:53-58.

Seibenhener ML, Wooten MC (2015) Use of the Open Field Maze to measure locomotor and anxiety-like behavior in mice. Journal of visualized experiments : JoVE:e52434.

Serratrice C, Carballo S, Serratrice J, Stirnemann J (2016) Imiglucerase in the management of Gaucher disease type 1: an evidence-based review of its place in therapy. Core evidence 11:37-47.
Seto-Salvia N, Pagonabarraga J, Houlden H, Pascual-Sedano B, Dols-Icardo O, Tucci A, Paisan-Ruiz C, Campolongo A, Anton-Aguirre S, Martin I, Munoz L, Bufill E, Vilageliu L, Grinberg D, Cozar M, Blesa R, Lleo A, Hardy J, Kulisevsky J, Clarimon J (2012) Glucocerebrosidase mutations confer a greater risk of dementia during Parkinson's disease course. Movement disorders : official journal of the Movement Disorder Society 27:393-399.
Shalini S, Dorstyn L, Dawar S, Kumar S (2015) Old, new and emerging functions of caspases. Cell death and differentiation 22:526-539.
Shea YF, Ha J, Chu LW (2015) Comparisons of clinical symptoms in biomarker-confirmed Alzheimer's disease, dementia with Lewy bodies, and frontotemporal dementia patients in a local memory clinic. Psychogeriatrics : the official journal of the Japanese Psychogeriatric Society 15:235-241.
Shemesh E, Deroma L, Bembi B, Deegan P, Hollak C, Weinreb NJ, Cox TM (2015) Enzyme replacement and substrate reduction therapy for Gaucher disease. The Cochrane database of systematic reviews:CD010324.
Sheth JJ, Sheth FJ, Oza NJ, Gambhir PS, Dave UP, Shah RC (2010) Plasma chitotriosidase activity in children with lysosomal storage disorders. Indian journal of pediatrics 77:203-205.
Shimizu S, Hirao K, Kanetaka H, Namioka N, Hatanaka H, Hirose D, Fukasawa R, Umahara T, Sakurai H, Hanyu H (2016) Utility of the combination of DAT SPECT and MIBG myocardial scintigraphy in differentiating dementia with Lewy bodies from Alzheimer's disease. European journal of nuclear medicine and molecular imaging 43:184-192.
Shiner T, Mirelman A, Gana Weisz M, Bar-Shira A, Ash E, Cialic R, Nevler N, Gurevich T, Bregman N, Orr-Urtreger A, Giladi N (2016) High Frequency of GBA Gene Mutations in Dementia With Lewy Bodies Among Ashkenazi Jews. JAMA neurology 73:1448-1453.
Shore GC, Papa FR, Oakes SA (2011) Signaling cell death from the endoplasmic reticulum stress response. Current opinion in cell biology 23:143-149.
Sidransky E (2004) Gaucher disease: complexity in a "simple" disorder. Molecular genetics and metabolism 83:6-15.
Sidransky E, Samaddar T, Tayebi N (2009a) Mutations in GBA are associated with familial Parkinson disease susceptibility and age at onset. Neurology 73:1424-1425, author reply 1425-1426.
Sidransky E et al. (2009b) Multicenter analysis of glucocerebrosidase mutations in Parkinson's disease. The New England journal of medicine 361:1651-1661.
Silva RM, Ries V, Oo TF, Yarygina O, Jackson-Lewis V, Ryu EJ, Lu PD, Marciniak SJ, Ron D, Przedborski S, Kholodilov N, Greene LA, Burke RE (2005) CHOP/GADD153 is a mediator of apoptotic death in substantia nigra dopamine neurons in an in vivo neurotoxin model of parkinsonism. Journal of neurochemistry 95:974-986.
Sinclair GB, Jevon G, Colobong KE, Randall DR, Choy FY, Clarke LA (2007) Generation of a conditional knockout of murine glucocerebrosidase: utility for the study of Gaucher disease. Molecular genetics and metabolism 90:148-156.
Smith HL, Mallucci GR (2016) The unfolded protein response: mechanisms and therapy of neurodegeneration. Brain : a journal of neurology 139:2113-2121.
Sorge J, West C, Westwood B, Beutler E (1985) Molecular cloning and nucleotide sequence of human glucocerebrosidase cDNA. Proceedings of the National Academy of Sciences of the United States of America 82:7289-7293.
Sorge J, Gross E, West C, Beutler E (1990) High level transcription of the glucocerebrosidase pseudogene in normal subjects and patients with Gaucher disease. The Journal of clinical investigation 86:1137-1141.
Sorge JA, West C, Kuhl W, Treger L, Beutler E (1987) The human glucocerebrosidase gene has two functional ATG initiator codons. American journal of human genetics 41:1016-1024.
Spillantini MG, Goedert M (2017) Neurodegeneration and the ordered assembly of alpha-synuclein. Cell and tissue research.
Spillantini MG, Crowther RA, Jakes R, Hasegawa M, Goedert M (1998) alpha-Synuclein in filamentous inclusions of Lewy bodies from Parkinson's disease and dementia with lewy bodies. Proceedings of the National Academy of Sciences of the United States of America 95:6469-6473.
Spillantini MG, Schmidt ML, Lee VM, Trojanowski JQ, Jakes R, Goedert M (1997) Alpha-synuclein in Lewy bodies. Nature 388:839-840.

Spitz M, Rozenberg R, Pereira Lda V, Reis Barbosa E (2008) Association between Parkinson's disease and glucocerebrosidase mutations in Brazil. Parkinsonism & related disorders 14:58-62.
Sriburi R, Jackowski S, Mori K, Brewer JW (2004) XBP1: a link between the unfolded protein response, lipid biosynthesis, and biogenesis of the endoplasmic reticulum. The Journal of cell biology 167:35-41.
Stinton C, McKeith I, Taylor JP, Lafortune L, Mioshi E, Mak E, Cambridge V, Mason J, Thomas A, O'Brien JT (2015) Pharmacological Management of Lewy Body Dementia: A Systematic Review and Meta-Analysis. The American journal of psychiatry 172:731-742.
Stirnemann J, Belmatoug N, Camou F, Serratrice C, Froissart R, Caillaud C, Levade T, Astudillo L, Serratrice J, Brassier A, Rose C, Billette de Villemeur T, Berger MG (2017) A Review of Gaucher Disease Pathophysiology, Clinical Presentation and Treatments. International journal of molecular sciences 18.
Stirnemann J et al. (2012) The French Gaucher's disease registry: clinical characteristics, complications and treatment of 562 patients. Orphanet journal of rare diseases 7:77.
Stojkovska I, Krainc D, Mazzulli JR (2017) Molecular mechanisms of alpha-synuclein and GBA1 in Parkinson's disease. Cell and tissue research.
Sun QY, Guo JF, Wang L, Yu RH, Zuo X, Yao LY, Pan Q, Xia K, Tang BS (2010) Glucocerebrosidase gene L444P mutation is a risk factor for Parkinson's disease in Chinese population. Movement disorders : official journal of the Movement Disorder Society 25:1005-1011.
Sun Y, Qi X, Grabowski GA (2003) Saposin C is required for normal resistance of acid beta-glucosidase to proteolytic degradation. The Journal of biological chemistry 278:31918-31923.
Supriya M, De T, Christopher R (2017) Age and gender-specific reference intervals for lysosomal enzymes in dried blood spot samples: A study in Indian population. Clinical biochemistry 50:858-863.
Svennerholm L, Bostrom K, Fredman P, Mansson JE, Rosengren B, Rynmark BM (1989) Human brain gangliosides: developmental changes from early fetal stage to advanced age. Biochimica et biophysica acta 1005:109-117.
Szegezdi E, Fitzgerald U, Samali A (2003) Caspase-12 and ER-stress-mediated apoptosis: the story so far. Annals of the New York Academy of Sciences 1010:186-194.
Tabas I, Ron D (2011) Integrating the mechanisms of apoptosis induced by endoplasmic reticulum stress. Nature cell biology 13:184-190.
Taguchi YV, Liu J, Ruan J, Pacheco J, Zhang X, Abbasi J, Keutzer J, Mistry PK, Chandra SS (2017) Glucosylsphingosine Promotes alpha-Synuclein Pathology in Mutant GBA-Associated Parkinson's Disease. The Journal of neuroscience : the official journal of the Society for Neuroscience 37:9617-9631.
Tait SW, Green DR (2010) Mitochondria and cell death: outer membrane permeabilization and beyond. Nature reviews Molecular cell biology 11:621-632.
Takahashi K, Yamanaka S (2016) A decade of transcription factor-mediated reprogramming to pluripotency. Nature reviews Molecular cell biology 17:183-193.
Takemoto M, Sato K, Hatanaka N, Yamashita T, Ohta Y, Hishikawa N, Abe K (2016) Different Clinical and Neuroimaging Characteristics in Early Stage Parkinson's Disease with Dementia and Dementia with Lewy Bodies. Journal of Alzheimer's disease : JAD 52:205-211.
Tamargo RJ, Velayati A, Goldin E, Sidransky E (2012) The role of saposin C in Gaucher disease. Molecular genetics and metabolism 106:257-263.
Tan EK, Tong J, Fook-Chong S, Yih Y, Wong MC, Pavanni R, Zhao Y (2007) Glucocerebrosidase mutations and risk of Parkinson disease in Chinese patients. Archives of neurology 64:1056-1058.
Tayebi N (2003) Gaucher disease with parkinsonian manifestations: does glucocerebrosidase deficiency contribute to a vulnerability to parkinsonism? Molecular genetics and metabolism 79:104-109.
Thaipisuttikul P, Lobach I, Zweig Y, Gurnani A, Galvin JE (2013) Capgras syndrome in Dementia with Lewy Bodies. International psychogeriatrics 25:843-849.
Tiraboschi P, Attems J, Thomas A, Brown A, Jaros E, Lett DJ, Ossola M, Perry RH, Ramsay L, Walker L, McKeith IG (2015) Clinicians' ability to diagnose dementia with Lewy bodies is not affected by beta-amyloid load. Neurology 84:496-499.
Toft M, Pielsticker L, Ross OA, Aasly JO, Farrer MJ (2006) Glucocerebrosidase gene mutations and Parkinson disease in the Norwegian population. Neurology 66:415-417.

Torok R, Zadori D, Torok N, Csility E, Vecsei L, Klivenyi P (2016) An assessment of the frequency of mutations in the GBA and VPS35 genes in Hungarian patients with sporadic Parkinson's disease. Neuroscience letters 610:135-138.
Tsuang D et al. (2012) GBA mutations increase risk for Lewy body disease with and without Alzheimer disease pathology. Neurology 79:1944-1950.
Tsuboi Y, Dickson DW (2005) Dementia with Lewy bodies and Parkinson's disease with dementia: are they different? Parkinsonism & related disorders 11 Suppl 1:S47-51.
Tybulewicz VL, Tremblay ML, LaMarca ME, Willemsen R, Stubblefield BK, Winfield S, Zablocka B, Sidransky E, Martin BM, Huang SP, et al. (1992) Animal model of Gaucher's disease from targeted disruption of the mouse glucocerebrosidase gene. Nature 357:407-410.
Tylki-Szymanska A, Vellodi A, El-Beshlawy A, Cole JA, Kolodny E (2010) Neuronopathic Gaucher disease: demographic and clinical features of 131 patients enrolled in the International Collaborative Gaucher Group Neurological Outcomes Subregistry. Journal of inherited metabolic disease 33:339-346.
Uemura N, Koike M, Ansai S, Kinoshita M, Ishikawa-Fujiwara T, Matsui H, Naruse K, Sakamoto N, Uchiyama Y, Todo T, Takeda S, Yamakado H, Takahashi R (2015) Viable neuronopathic Gaucher disease model in Medaka (Oryzias latipes) displays axonal accumulation of alpha-synuclein. PLoS genetics 11:e1005065.
Unger EL, Eve DJ, Perez XA, Reichenbach DK, Xu Y, Lee MK, Andrews AM (2006) Locomotor hyperactivity and alterations in dopamine neurotransmission are associated with overexpression of A53T mutant human alpha-synuclein in mice. Neurobiology of disease 21:431-443.
Urwyler P, Nef T, Muri R, Archibald N, Makin SM, Collerton D, Taylor JP, Burn D, McKeith I, Mosimann UP (2016) Visual Hallucinations in Eye Disease and Lewy Body Disease. The American journal of geriatric psychiatry : official journal of the American Association for Geriatric Psychiatry 24:350-358.
Vaccaro AM, Motta M, Tatti M, Scarpa S, Masuelli L, Bhat M, Vanier MT, Tylki-Szymanska A, Salvioli R (2010) Saposin C mutations in Gaucher disease patients resulting in lysosomal lipid accumulation, saposin C deficiency, but normal prosaposin processing and sorting. Human molecular genetics 19:2987-2997.
Valdes P, Mercado G, Vidal RL, Molina C, Parsons G, Court FA, Martinez A, Galleguillos D, Armentano D, Schneider BL, Hetz C (2014) Control of dopaminergic neuron survival by the unfolded protein response transcription factor XBP1. Proceedings of the National Academy of Sciences of the United States of America 111:6804-6809.
Van Rossum A, Holsopple M (2016) Enzyme Replacement or Substrate Reduction? A Review of Gaucher Disease Treatment Options. Hospital pharmacy 51:553-563.
van Weely S, Brandsma M, Strijland A, Tager JM, Aerts JM (1993) Demonstration of the existence of a second, non-lysosomal glucocerebrosidase that is not deficient in Gaucher disease. Biochimica et biophysica acta 1181:55-62.
Vann Jones SA, O'Brien JT (2014) The prevalence and incidence of dementia with Lewy bodies: a systematic review of population and clinical studies. Psychological medicine 44:673-683.
Vardi A, Zigdon H, Meshcheriakova A, Klein AD, Yaacobi C, Eilam R, Kenwood BM, Rahim AA, Massaro G, Merrill AH, Jr., Vitner EB, Futerman AH (2016) Delineating pathological pathways in a chemically induced mouse model of Gaucher disease. The Journal of pathology 239:496-509.
Velayudhan L, Ffytche D, Ballard C, Aarsland D (2017) New Therapeutic Strategies for Lewy Body Dementias. Current neurology and neuroscience reports 17:68.
Vembar SS, Brodsky JL (2008) One step at a time: endoplasmic reticulum-associated degradation. Nature reviews Molecular cell biology 9:944-957.
Vergouw LJM, van Steenoven I, van de Berg WDJ, Teunissen CE, van Swieten JC, Bonifati V, Lemstra AW, de Jong FJ (2017) An update on the genetics of dementia with Lewy bodies. Parkinsonism & related disorders 43:1-8.
Vitner EB, Dekel H, Zigdon H, Shachar T, Farfel-Becker T, Eilam R, Karlsson S, Futerman AH (2010) Altered expression and distribution of cathepsins in neuronopathic forms of Gaucher disease and in other sphingolipidoses. Human molecular genetics 19:3583-3590.
Volpicelli-Daley LA, Luk KC, Lee VM (2014) Addition of exogenous alpha-synuclein preformed fibrils to primary neuronal cultures to seed recruitment of endogenous alpha-synuclein to Lewy body and Lewy neurite-like aggregates. Nature protocols 9:2135-2146.
Vorhees CV, Williams MT (2006) Morris water maze: procedures for assessing spatial and related forms of learning and memory. Nature protocols 1:848-858.

Walker Z, Possin KL, Boeve BF, Aarsland D (2015) Lewy body dementias. Lancet 386:1683-1697.
Walter P, Ron D (2011) The unfolded protein response: from stress pathway to homeostatic regulation. Science 334:1081-1086.
Wang HF, Yu JT, Tang SW, Jiang T, Tan CC, Meng XF, Wang C, Tan MS, Tan L (2015) Efficacy and safety of cholinesterase inhibitors and memantine in cognitive impairment in Parkinson's disease, Parkinson's disease dementia, and dementia with Lewy bodies: systematic review with meta-analysis and trial sequential analysis. Journal of neurology, neurosurgery, and psychiatry 86:135-143.
Wang P, Li X, Li X, Yang W, Yu S (2016) Blood Plasma of Patients with Parkinson's Disease Increases Alpha-Synuclein Aggregation and Neurotoxicity. Parkinson's disease 2016:7596482.
Wang XZ, Ron D (1996) Stress-induced phosphorylation and activation of the transcription factor CHOP (GADD153) by p38 MAP Kinase. Science 272:1347-1349.
Wang Y, Liu L, Xiong J, Zhang X, Chen Z, Yu L, Chen C, Huang J, Zhang Z, Mohmed AA, Lin Z, Xiong N, Wang T (2012) Glucocerebrosidase L444P mutation confers genetic risk for Parkinson's disease in central China. Behavioral and brain functions : BBF 8:57.
Weisman D, Cho M, Taylor C, Adame A, Thal LJ, Hansen LA (2007) In dementia with Lewy bodies, Braak stage determines phenotype, not Lewy body distribution. Neurology 69:356-359.
Westbroek W, Gustafson AM, Sidransky E (2011) Exploring the link between glucocerebrosidase mutations and parkinsonism. Trends in molecular medicine 17:485-493.
Whitfield DR, Vallortigara J, Alghamdi A, Howlett D, Hortobagyi T, Johnson M, Attems J, Newhouse S, Ballard C, Thomas AJ, O'Brien JT, Aarsland D, Francis PT (2014) Assessment of ZnT3 and PSD95 protein levels in Lewy body dementias and Alzheimer's disease: association with cognitive impairment. Neurobiology of aging 35:2836-2844.
Williams-Gray CH, Foltynie T, Brayne CE, Robbins TW, Barker RA (2007) Evolution of cognitive dysfunction in an incident Parkinson's disease cohort. Brain : a journal of neurology 130:1787-1798.
Winder-Rhodes SE, Evans JR, Ban M, Mason SL, Williams-Gray CH, Foltynie T, Duran R, Mencacci NE, Sawcer SJ, Barker RA (2013) Glucocerebrosidase mutations influence the natural history of Parkinson's disease in a community-based incident cohort. Brain : a journal of neurology 136:392-399.
Wong K, Sidransky E, Verma A, Mixon T, Sandberg GD, Wakefield LK, Morrison A, Lwin A, Colegial C, Allman JM, Schiffmann R (2004) Neuropathology provides clues to the pathophysiology of Gaucher disease. Molecular genetics and metabolism 82:192-207.
Woodard CM et al. (2014) iPSC-derived dopamine neurons reveal differences between monozygotic twins discordant for Parkinson's disease. Cell reports 9:1173-1182.
Wu YR, Chen CM, Chao CY, Ro LS, Lyu RK, Chang KH, Lee-Chen GJ (2007) Glucocerebrosidase gene mutation is a risk factor for early onset of Parkinson disease among Taiwanese. Journal of neurology, neurosurgery, and psychiatry 78:977-979.
Xu YH, Quinn B, Witte D, Grabowski GA (2003) Viable mouse models of acid beta-glucosidase deficiency: the defect in Gaucher disease. The American journal of pathology 163:2093-2101.
Xu YH, Reboulet R, Quinn B, Huelsken J, Witte D, Grabowski GA (2008) Dependence of reversibility and progression of mouse neuronopathic Gaucher disease on acid beta-glucosidase residual activity levels. Molecular genetics and metabolism 94:190-203.
Xu YH, Sun Y, Ran H, Quinn B, Witte D, Grabowski GA (2011) Accumulation and distribution of alpha-synuclein and ubiquitin in the CNS of Gaucher disease mouse models. Molecular genetics and metabolism 102:436-447.
Xu YH, Xu K, Sun Y, Liou B, Quinn B, Li RH, Xue L, Zhang W, Setchell KD, Witte D, Grabowski GA (2014) Multiple pathogenic proteins implicated in neuronopathic Gaucher disease mice. Human molecular genetics 23:3943-3957.
Yanagitani K, Kimata Y, Kadokura H, Kohno K (2011) Translational pausing ensures membrane targeting and cytoplasmic splicing of XBP1u mRNA. Science 331:586-589.
Yang J, Hertz E, Zhang X, Leinartaite L, Lundius EG, Li J, Svenningsson P (2016) Overexpression of alpha-synuclein simultaneously increases glutamate NMDA receptor phosphorylation and reduces glucocerebrosidase activity. Neuroscience letters 611:51-58.
Yap TL, Velayati A, Sidransky E, Lee JC (2013a) Membrane-bound alpha-synuclein interacts with glucocerebrosidase and inhibits enzyme activity. Molecular genetics and metabolism 108:56-64.

Yap TL, Gruschus JM, Velayati A, Sidransky E, Lee JC (2013b) Saposin C protects glucocerebrosidase against alpha-synuclein inhibition. Biochemistry 52:7161-7163.
Yap TL, Gruschus JM, Velayati A, Westbroek W, Goldin E, Moaven N, Sidransky E, Lee JC (2011) Alpha-synuclein interacts with Glucocerebrosidase providing a molecular link between Parkinson and Gaucher diseases. The Journal of biological chemistry 286:28080-28088.
Yap TL, Jiang Z, Heinrich F, Gruschus JM, Pfefferkorn CM, Barros M, Curtis JE, Sidransky E, Lee JC (2015) Structural features of membrane-bound glucocerebrosidase and alpha-synuclein probed by neutron reflectometry and fluorescence spectroscopy. The Journal of biological chemistry 290:744-754.
Yildiz Y, Matern H, Thompson B, Allegood JC, Warren RL, Ramirez DM, Hammer RE, Hamra FK, Matern S, Russell DW (2006) Mutation of beta-glucosidase 2 causes glycolipid storage disease and impaired male fertility. The Journal of clinical investigation 116:2985-2994.
Yoshida H, Uemura A, Mori K (2009) pXBP1(U), a negative regulator of the unfolded protein response activator pXBP1(S), targets ATF6 but not ATF4 in proteasome-mediated degradation. Cell structure and function 34:1-10.
Yoshita M, Taki J, Yokoyama K, Noguchi-Shinohara M, Matsumoto Y, Nakajima K, Yamada M (2006) Value of 123I-MIBG radioactivity in the differential diagnosis of DLB from AD. Neurology 66:1850-1854.
Yu Z, Wang T, Xu J, Wang W, Wang G, Chen C, Zheng L, Pan L, Gong D, Li X, Qu H, Li F, Zhang B, Le W, Han F (2015) Mutations in the glucocerebrosidase gene are responsible for Chinese patients with Parkinson's disease. Journal of human genetics 60:85-90.
Zaccai J, McCracken C, Brayne C (2005) A systematic review of prevalence and incidence studies of dementia with Lewy bodies. Age and ageing 34:561-566.
Zhang J, Zhang X, Wang L, Yang C (2017) High Performance Liquid Chromatography-Mass Spectrometry (LC-MS) Based Quantitative Lipidomics Study of Ganglioside-NANA-3 Plasma to Establish Its Association with Parkinson's Disease Patients. Medical science monitor : international medical journal of experimental and clinical research 23:5345-5353.
Zhao P, Luo Z, Tian W, Yang J, Ibanez DP, Huang Z, Tortorella MD, Esteban MA, Fan W (2014) Solving the puzzle of Parkinson's disease using induced pluripotent stem cells. Experimental biology and medicine (Maywood, NJ) 239:1421-1432.
Ziegler SG, Eblan MJ, Gutti U, Hruska KS, Stubblefield BK, Goker-Alpan O, LaMarca ME, Sidransky E (2007) Glucocerebrosidase mutations in Chinese subjects from Taiwan with sporadic Parkinson disease. Molecular genetics and metabolism 91:195-200.
Zinszner H, Kuroda M, Wang X, Batchvarova N, Lightfoot RT, Remotti H, Stevens JL, Ron D (1998) CHOP is implicated in programmed cell death in response to impaired function of the endoplasmic reticulum. Genes & development 12:982-995.
Zunke F, Moise AC, Belur NR, Gelyana E, Stojkovska I, Dzaferbegovic H, Toker NJ, Jeon S, Fredriksen K, Mazzulli JR (2017) Reversible Conformational Conversion of alpha-Synuclein into Toxic Assemblies by Glucosylceramide. Neuron.